

**Design and development of a novel, self-contained, and field-portable biosensor platform
for the detection and identification of microbial pathogens in near-real time.**

A thesis submitted in partial fulfilment of the requirements of
Manchester Metropolitan University for the degree of Doctor of Philosophy

James Hall

Department of Engineering

2019

ABSTRACT

The interactions of microorganisms are considered fundamental to all life, and plants and animals are increasingly viewed in the context of their associated microbiomes. However, there are significant health and economic costs associated with microbial pathogen contamination in farming, food processing, and the supply of potable water. While contemporary microbiology techniques play a valuable role in pathogen surveillance, they are predominantly laboratory-based, time-consuming, and are reliant on skilled personnel. To both ensure safety and productivity in increasingly intensive food production and to meet the challenge of antimicrobial resistance, there is a requirement for portable, real-time microbiology tools and a broader role for rapid diagnostics. This thesis outlines the development of a unique, self-contained, and field-portable biosensor system for the detection of microbial DNA sequences in food, water, and environmental samples.

The novel design utilises a 'macro-fluidic' model as basis for sample processing, reagent introduction, and analytical functionality and takes advantage of low-cost materials and electronics. Based on DNA hybridisation, the platform benefits from extensive resources accumulated in phylogenetic classification and the development of technologies such as gene sequencing and polymerase chain reaction (PCR). Other than sample loading, the biosensor system is totally automated and simple to use. An Arduino microprocessor controls all process control and electrochemical analysis, while user input and data display are handled by a smartphone app. The ground-up design makes use of modular design principles and off-the-shelf electronic components.

The platform cell lysis unit demonstrates DNA extraction performance comparable to that of bench-top mini-prep kits, with high elution efficiency and repeatability. The macro-fluidic design is entirely novel and is unique in delivering high quality nucleic acid purification in a portable unit. The DNA amplification and hybridisation-based biosensor module demonstrates highly sensitive (pico-molar) nucleic acid detection and a lower limit of approximately 500 bacteria in the detection and identification of *Campylobacter jejuni*. The platform can generate samples for comparative analysis or for analysis using technologies such as the Minion portable gene sequencer.

Using innovative design to bring self-contained molecular analysis into the field, the developed biosensor platform has potential applications in detection and identification of microbial species in areas from pathogen surveillance and microbial population characterisation to antibiotic resistance tracking and clinical diagnostics.

Dedicated to Sarah and Molly

ACKNOWLEDGEMENTS

The sincerest thanks to Dr Viji Velusamy for giving me this opportunity and for her ceaseless encouragement.

Many thanks to Professor Jo Verran, Dr Selva Palanisamy, Dr Bamidele Adebisi, Dr Rupak Kharel, Dr Kirstie Shaw, Dr Andrew Plunket, and Dr Daniel Anang for all help and advice.

A very special thanks to all MMU staff and in particular –

Pamela Flint
Kathy Lees
Clare Holdcroft
Megan Paines
Kristina Ganchenko
Francesca Robinson
Aly Goncherova
Phoebe Apeagyei
Hayley Andrews
Roya Alamzad
Nilima Arora
Shelley Winterbottom
Vincent Bear
Robert Bamford
Mike Green
Steven Moyles
Glenn Ferris
Lee Harman
Bill Ellison
Chris Kearney

TABLE OF CONTENTS

Abstract	i
Acknowledgements	iii
Table of Contents	iv
List of tables	xi
List of figures	xii
Scope of the thesis	xxv
Chapter 1	
The Microbiome	
1.1. Microbial pathogens - how much do we know?	1
1.2. Microbes and pathogens	2
1.2.1 Microbial communities	2
1.3 Pathogenicity and virulence	5
1.3.1 Virulence factors	5
1.3.2 Antimicrobial resistance (AMR)	5
1.4 Food and waterborne pathogens	7
Chapter 2	
<i>Campylobacter spp.</i> as a model organism	
2.1 The <i>Campylobacter</i> genus	10
2.1.1 <i>Campylobacter spp.</i> classification – conventional methods	10
2.1.2 Molecular techniques in <i>Campylobacter</i> classification	11
2.1.3 Comparative genomic phylogeny	11
2.2 The influence of niche habitat on bacterial evolution	13
2.2.1 <i>Campylobacter spp.</i> reservoirs and environmental distribution	14
2.2.2 Pathogenic <i>Campylobacter</i> reservoirs	14
2.2.3 Limits of contemporary <i>Campylobacter spp.</i> characterisation	15
2.3 Validated techniques and media for recovery of <i>Campylobacter spp.</i>	16

2.3.1	Enrichment incubation	19
2.3.2	Viable but non-culturable conformations	20
2.4	<i>Campylobacter spp.</i> persistence in the environment.	21
2.4.1	Environmental dissemination from campylobacteriosis outbreak data	22
2.4.2	Poultry as a <i>Campylobacter</i> reservoir	24
2.5	<i>Campylobacter spp.</i> contamination of poultry products	24
2.5.1	Vertical transmission of <i>Campylobacter</i>	25
2.5.2	Horizontal bacterial transmission	26
2.5.3	Prevention of bird and flock colonisation	26
2.6	Waterborne <i>Campylobacter spp.</i>	27
2.6.1	<i>Campylobacter</i> circulation in wastewater treatment	28
2.6.2	Seasonal variation in campylobacteriosis	29
2.7	Campylobacteriosis	30
2.7.1	Epidemiology	30
2.7.2	Infection Pathology	30
2.7.3	Cell surface structure, and immuno-modulation	31
2.7.4	Symptoms and sequelae	32
2.7.5	Guillain-Barré Syndrome (GBS) and <i>Campylobacter spp.</i> hypervariability	33
2.8	In summary	34

Chapter 3

Contemporary analytical techniques for pathogen detection

3.1	Molecular microbiology tools as first-generation biosensors	35
3.2	Enzyme-linked immunosorbent assay (ELISA)	35
3.3	API-bioMérieux	37
3.4	Polymerase chain reaction (PCR)	39
3.5	Data acquisition and sampling rate	43
3.6	Biosensors	44
3.6.1	Biosensor sample DNA preparation	47
3.6.2	Biosensor probe oligonucleotide immobilisation	47
3.7	Biosensor platform design criteria	48
3.7.1	DNA extraction	48

3.7.2	DNA conformation	48
3.7.3	Probe oligonucleotide immobilisation	49
3.7.4	Potentiostat	49
3.8	Summary	49

Chapter 4

Experimental Procedures

4.1	Introduction	50
4.2	Materials	50
4.2.1	Analytical reagents	50
4.2.2	Bio-molecules	50
4.2.3	Solutions	51
4.2.4	Consumables	51
4.2.5	Apparatus and instrumentation	51
4.2.6	Software	51
4.3	Culture based bacterial enumeration	51
4.3.1	Microscopy	51
4.3.2	Selective media inoculation	51
4.3.3	Colony counting	52
4.4	Nucleic acid extraction and purification	52
4.4.1	CONGEN spin filter kit	52
4.4.2	Spectrophotometric DNA quantification	53
4.5	Real-time polymerase chain reaction (RT-PCR)	53
4.5.1	Sample formulation	53
4.5.2	PCR cycle parameters	53
4.6	Gel electrophoresis	54
4.6.1	Sample buffer formulation	54
4.6.2	Electrophoresis parameters	54
4.6.3	Visualisation	54
4.7	Electrochemical characterisation and analysis	54
4.7.1	Electrochemical cell	54
4.7.2	Working electrode	55

4.7.2.1	Glassy carbon electrode preparation	55
4.7.2.2	Screen printed carbon electrode activation	55
4.7.2.3	Electrode modification by surface adsorption	55
4.7.2.4	Electrode surface silanisation	56
4.7.3	Counter and reference electrodes	56
4.7.4	Electrolytes	56
4.7.5	Cyclic voltammetry	56
4.7.6	Chronoamperometry	56
4.7.7	Differential pulse voltammetry	56
4.8	DNA immobilisation and hybridisation	57
4.8.1	DNA immobilisation by UV crosslinking	57
4.8.2	DNA immobilisation by electrochemical adsorption	57
4.8.3	DNA hybridisation incubation	57
4.9	Surface analysis	57
4.9.1	Scanning electron microscopy	57
4.10	Statistical analysis	60

Chapter 5

Design of the field portable analysis platform

5.1	Introduction	59
5.2	Sample transport - mobile phase	60
5.2.1	Reciprocating pumps vs syringe pumps	62
5.2.2	Pressure driven syringe pump design	65
5.2.3	Multichannel pressure driven reagent reservoir	65
5.2.4	Integrated multichannel reagent reservoir and distributor	67
5.2.5	Reagent air pressure reservoir	69
5.2.6	Stepper motor reagent selection	69
5.2.7	Stepper motor process control	70
5.2.8	Interrupter valves and actuators	71
5.3	Sample Introduction	72
5.3.1	Sample volume	72
5.3.2	Sample receiver design	72

5.3.3	Sample loading protocol	73
5.3.4	Sample parameters	74
5.3.5	Self-cleaning cycle	75
5.4	Cell lysis unit	76
5.4.1	Lysis buffer	76
5.4.2	Temperature driven cell lysis	77
5.4.3	Electromagnetic agitation/bead mill	77
5.4.4	Pressure driven cell lysis	81
5.5	DNA purification module	81
5.5.1	Chaotropic agent-based DNA purification	82
5.5.1	Spin filter silica membrane	85
5.5.2	DNA purification matrix	86
5.5.3	Temperature mediated DNA elution	87
5.5.4	Deoxyribonucleases and ribonucleases	88
5.5.5	Sample separation for analytical validation	88
5.6	Polymerase chain reaction (PCR) amplification module	89
5.6.1	'Hotplate' protocol	89
5.6.2	Peltier cell temperature modulation	90
5.6.3	Injection system for primers and master mix	90
5.6.4	Vortex <i>cold snap</i> DNA strand denaturation	91
5.7	Power supply, microprocessor, and electrochemical analysis	92
5.7.1	Power supply	92
5.7.2	Arduino micro-controller	92
5.7.3	Three-electrode electrochemical cell	93
5.7.4	Potentiostat design	95
5.7.5	Optimisation of electrode characteristics by surface modification	96
5.7.6	Multiplex analysis model	99
5.7.7	Software	100
5.7.7.1	Process control	100
5.7.7.2	Analytical graphic user interface	101
5.8	Materials	102

Chapter 6

Results and discussion

6.1	Introduction	104
6.2	Microbial cell lysis module	104
6.2.1	Robustness in cell lysis and nucleic acid extraction	106
6.2.2	Lysis buffer	107
6.2.3	Temperature and pressure	107
6.2.4	Electromagnetic sample agitation	109
6.3	DNA purification module	114
6.3.1	Silica gel DNA extraction	114
6.3.2	Borosilicate glass DNA extraction	117
6.3.3	Nucleic acid purity	118
6.3.3.1	Retention of lysis chemistry and cell debris	119
6.3.3.2	Ethanol elimination	122
6.3.4	DNA elution efficiency	123
6.3.5	Stationary phase purge and recycle	124
6.3.6	Extraction module flow rate regulation	124
6.4	DNA amplification results	125
6.5	Electrochemical characterisation of electrode modification	128
6.5.1	Glassy carbon electrode (GCE), characteristics	129
6.5.2	Graphene oxide (GO)	131
6.5.3	Reduced graphene oxide (rGO)	133
6.5.4	Graphene oxide and cellulose microfibres	134
6.5.5	Graphene oxide, cellulose microfibres, and Nafion	136
6.5.6	Poly(3,4-ethylenedioxythiophene)- polystyrene sulfonate (PEDOT:PSS)	137
6.5.7	PEDOT- (3-Aminopropyl)triethoxysilane (APTES) 1%	138
6.5.8	Activated screen-printed carbon electrode (SPCE)	138
6.5.9	α SPCE and PEDOT	142
6.5.10	Silanised α SPCE	143
6.6	PEDOT:PSS- α SPCE detection of guanine	144
6.7	PEDOT:PSS- α SPCE detection of single-stranded DNA	145

6.8	α SPCE characterisation	147
6.9	Single-stranded DNA probe immobilisation	148
6.9.1	UV-crosslinking	148
6.9.2	Electrochemical immobilisation	148
6.10	Co-factor detection of DNA hybridisation using Methylene blue	149
6.11	Bovine serum albumin (BSA) – blocking non-specific binding	150
6.12	Electrochemical detection of DNA hybridisation	152
6.13	Statistical analysis of cyclic voltammetry data	155

Chapter 7

Conclusions and future direction

7.1	Introduction	155
7.2	Equivalent portable technologies	155
7.3	Laboratory-based applications	160
7.4	Suggested further research	160
7.4.1	The development of user specific interface ‘apps’	162
7.6	In summary	162

References	164
-------------------	------------

Appendix A – Acronyms	194
------------------------------	------------

Appendix B - List of publication and conferences	196
---	------------

List of tables

- Table 2.1.* Detailing the wide-ranging distribution of *Campylobacter* spp. across areas of highly variable temperature and relative humidity and sharing a common basis in waterborne transmission. **23**
- Table 4.1.* Detailing the PCR parameters applied to *C. Jejuni* 16s amplification using the Roche LightCycler 96. **53**
- Table 5.1.* Table 5.1. Reagent formulations for DNA extraction and purification (Medina-Acosta and Cross, 1993; Boom et al., 1990; F. Yang et al., 1997) **85**
- Table 5.2.* Arduino Uno specifications, highlighting the operating voltage and maximum current draw. 2KB static random-access memory (SRAM) and 1KB electrically erasable programmable read-only memory (EEPROM) allow for process control, potentiostat operation, and Bluetooth data transmission to a smartphone for analysis and presentation. **86**

List of figures

- Figure 1.1.* Outlining potential dissemination routes for waterborne pathogenic bacteria and facilitating the transfer of virulence and antibiotic resistance gene cassettes in soil, multispecies aquatic biofilms, and as part of the commensal microbiota in humans, livestock, and wild animals such as insects and birds. **7**
- Figure 2.1.* The *Campylobacter* genus, highlighting those species considered as primary (orange) and emerging (yellow) human pathogens (Kamei et al., 2014). The reclassification of species initially identified as *Campylobacter* spp. (blue), reflects the revision of bacterial genera with the integration of data generated by techniques such as comparative 16s sequencing. (Compiled using data from bacterio.net) **10**
- Figure 2.2.* Figure 2.2. Summation of the International Standards Organisation (ISO) guidelines for employment of enrichment incubation in the recovery of *Campylobacter* spp. from food, water, and environmental samples. (mCCDA – modified charcoal-cefoperazone-deoxycholate agar, API® Bacterial identification strips – Biomerieux, France). **18**
- Figure 3.1.* Detailing the fluorescence visualisation of reference standard (top, increasing in concentration left to right) and sample inoculations plated in triplicate. **36**
- Figure 3.2.* Chromogenic medium for *Coli* differentiation. The bacterial colonies are coloured according to the cleavage of chromogenic substrates. Bacterial production of the enzyme galactosidase (produced by coliforms) results in pink cultures, while glucuronidase production (*E. coli*) cleaves the second substrate and generates teal cultures. Pink and teal gives purple. **38**

- Figure 3.3.* Typical API® strip, using colorimetric and binary test results to identify microbial species based on largely on their metabolic capacity. The colour indicator system makes API© strips ideal for high throughput automatic analysis. **38**
- Figure 3.4.* PCR multiplication is exponential in nature, following a temperature mediated cycle of DNA synthesis – raised temperature to separate the strands and lowered to allow the primers to bind, engage the DNA polymerase, and replicate the template strand. **40**
- Figure 3.5.* Typical mini-prep, or column-based DNA extraction and purification process based on chaotropic salts. DNA is adsorbed to the silica matrix allowing flow-through of cell debris. A low ionic strength buffer allows the DNA to disassociate and be eluted for analysis. **42**
- Figure 3.6.* Figure 3.6. Outlining the typical biosensor system architecture and the processing of signals generated by analyte/bioreceptor interaction (Velusamy et al., 2010). **44**
- Figure 3.7.* Depicts the typical electrochemical DNA hybridisation-based biosensor paradigm: Synthetic ssDNA probe oligonucleotides are immobilised on the modified electrode surface via the amino groups to linker molecules such as thiols, aldehydes, and epoxides, or through biotin-avidin binding (a) and hybridise with complementary ssDNA target sequences (b). Electrochemically Immobilised DNA strands are likely to lie flat on the sensor surface (c). **46**
- Figure 4.1.* Cuvette based three-electrode cell using a standard reference and counter electrode with an SPCE, and facilitating the analysis of 1000µl volumes, representative of the biosensor platform analytical cell. **55**

- Figure 5.1.* Schematic outline of the steps necessary for the extraction and purification of microbial DNA prior to electrochemical analysis of probe-target hybridisation. **60**
- Figure 5.2.* Outlining the minimum necessary macro-fluidic architecture to facilitate an entire automation of sample loading, cell lysis, DNA extraction and purification, sample division for confirmatory analysis, electrochemical sample analysis, containment of all used reagents, and utilisation of a self-cleaning cycle for subsequent re-use. **61**
- Figure 5.3.* Illustrating the operating principle of the reciprocating piston pump typically used to drive the mobile phase in liquid chromatography. Check valves (highlighted orange) act to maintain the liquid flow in one direction though intake (i) and expulsion (ii). **63**
- Figure 5.4.* Typical twin-channel syringe pump for research applications; rotation of the screw thread causes the drawbar to move along the guide bars and depress the syringe plunger. **64**
- Figure 5.5.* Initial drawings for a pressure driven multichannel syringe pump powered by CO₂ cartridges. The high-pressure block (a), reagent reservoirs (b), and outlet block (c), are assembled using threaded 4mm bar in 4.5mm channels and secured with nuts at each end. The outlet block is machined to use standard 10 32 HPLC fittings and 1mm PEEK tubing. **66**
- Figure 5.6.* Revised drawings for an air pressure driven carousel type multichannel syringe pump. The pressurised air reservoir (a), reagent carousel (b), and stepper motor-controlled rotational disc-valve distributor (c), are again assembled using a through bar system. Reagents from the carousel are supplied to downstream processes by a single 10 32 HPLC fitting. **68**

- Figure 5.7.* Withdrawal/infusion syringe pump design, switchable between the regulation of reagent flow and the expulsion of used reagents to the secondary waste reservoir. Drive screw rotation (a) draws plunger (b) from the primary waste reagent reservoir (c) and regulates carousel reagent outflow, through the microfluidic system to the HPLC port (d). **70**
- Figure 5.8.* Two-way switchable valve to direct reagent flow, waste expulsion, and sterilisation cycle. Paired housings (a) contain the valve cam and fit directly into neighbouring modules (b). Actuation by servo motor allows 30mm travel, with flow closed at 15mm travel (c). **71**
- Figure 5.9.* The sample receiver consists of a receiver well of base area of 1cm², and a screw down sealed lid. The receiver is connected to the reagent carousel using PEEK tubing and standard HPLC fittings, while the sample well base is attached directly to the cell lysis unit. **73**
- Figure 5.10.* The screw down action of the lid (a) expels the excess sample via the overflow vent (b) and delivers 1ml sample to the cell lysis unit (c). Sample overflow is cleared to the secondary waste reagent chamber and the upper screw-lid decontaminated from reagent reservoir 2 (d). Reagents from the carousel are introduced to the receiver via 1mm PEEK tubing and 10 32 HPLC connections, acting as a mobile phase to transfer sample through lysis (e) and DNA purification. **74**
- Figure 5.11.* Electromagnetic bead mill prototype, detailing the lysis chamber and neodymium chromed ball bearings (a), assembly (b), and heater element (c). 1mm id PEEK tubing and 10 32 HPLC fittings connect the unit for sample/reagent flow through and pressurisation. **78**

- Figure 5.12.* Showing the solenoid model actuation bead mill with windings around the top of the lysis chamber (a), acrylic scaffold wound with ~800 windings of 0.2mm/35 SWG (standard wire gauge) poly vinyl acetal coated copper wire, connecting pins, and protective paper wrapping (b), and the electromagnetic scaffolds fitted to the cell lysis unit (c). **79**
- Figure 5.13.* Figure 5.13. Guanidine (Gu) (a), a strong base, and guanidine hydrochloride salt (GuHCl) (b). At high concentrations in solutions, the NH (cation) and Cl (ion) hydrogen bonding interactions with macromolecule hydrogen bonding species and with dipolar water molecules (c and d) disrupt protein hydrophobic regions and the hydration shells of nucleic acid chains. **84**
- Figure 5.14.* (a) Spin filters for bacterial DNA extraction and purification (Congen, Germany). Electron microscopy shows the spun silica matrix (b) – combining a high surface area for nucleic acid adsorption with a relative pore size appropriate to the clearance of cell debris by high speed centrifugation. **86**
- Figure 5.15.* Flow-through DNA purification matrix testbed (a), with 0.45µm membrane filters acting to retain the chromatography grade silica gel as shown in electron micrograph (b). **87**
- Figure 5.16.* Inert acrylic and stainless-steel plunger pump. Injection of PCR components is actuated by an off-the-shelf micro-servo and the pump volume is automatically refilled from the master mix reservoir on return of the spring-loaded plunger. **90**
- Figure 5.17.* 130mm Ranque-Hilsch vortex tube. Integrated within the biosensor platform, the vortex tube provides rapid cooling for temperature mediated DNA denaturation and balances the action of the Peltier cell in cyclic temperature ramping **91**

- Figure 5.18.* A typical research/analytical three-electrode cell comprising reference (a), counter (b), and working (c) electrodes, supported by electrolyte (d). Top view (e) shows the electrode support lid with venting ports to facilitate electrolyte degassing as required (f). **94**
- Figure 5.19.* Triangular waveform potential as applied in cyclic voltammetry – in this instance diverging from equilibrium by ± 1 Volt with a periodicity of 40 seconds. **94**
- Figure 5.20.* Typical cyclic voltammetry traces through a sweep of ± 0.8 V and showing surface capacitance before (a) and after DNA oligonucleotide immobilisation (b). The REDOX couples (c) and (d) relate to a fixed concentration of the indicator dye methylene blue. **95**
- Figure 5.21.* Schematic showing the operational-amplifier-based analogue potentiostat circuitry integrated with the Arduino Uno micro-controller through the on-board analogue to digital convertor. The USB interface may be adapted for wireless connection to a smartphone. **96**
- Figure 5.22.* Cyclic voltammetry analysis representing the increase in GCE surface capacitance (a) modified by drop-coating $8\mu\text{l}$ of 20% graphene platelets in DD water and dried in a nitrogen atmosphere at 40°C (b). **98**
- Figure 5.23.* Arduino-potentiostat data as a comma separated value monitor output (a) for wireless transmission to the paired smartphone app for statistical analysis, and as a plotter output charting voltage (b) against current (c). **101**
- Figure 5.24.* Electron microscopy of acrylic surfaces treated with a solution of adsorption buffer and wash buffer at pH4.2, from time (t)=0 (a), t=10 days (b), t=20 days (c), t=30 days (d), t=40 days (e) and t=60 days (f). Salt accumulation is obvious from t=30 days (circled). **103**

- Figure 6.1.* Prototype pressure driven syringe pump employed in experimental reagent delivery; with syringe and PEEK flow line (a), sealed valve body (b), seal (c) and piston (d). **105**
- Figure 6.2.* Regulator (a) controls the gas pressure from a high-pressure reservoir, via a Presta valve fitting (b) to the syringe, driving travel of the piston (c) to displace the reagent. **105**
- Figure 6.3.* Showing the effect of cell lysis temperature on subsequent DNA extraction yield as determined by spectrophotometry for planktonic *C. jejuni* lysis (~10⁶ cfu/ml) at a pressure of approximately 300kPa. Control sample denotes the DNA yield extracted using a standard protocol. Error bars represent experimental variation as a percentage of the yield value, n=6. **108**
- Figure 6.4.* Relative size-based separation of *C. jejuni* genomic DNA by SDS page electrophoresis, showing DNA fragmentation from SDS/GuHCl-based *C. jejuni* cell lysis. Lanes 5, 6 & 7 contain samples lysed at 100oC and 300kPa. Control (lane 9) was lysed at 99oC at ambient pressure. No sample agitation was applied during cell lysis. Standard ladder (SeeBlue™ Pre-stained Standard, Invitrogen, USA) relates molecular weight. **111**
- Figure 6.5.* Gel electrophoresis separation of *C. jejuni* DNA by standard shaker-plate method at 900 rpm and 99oC (lanes 3, 4 & 5) and utilising the cell lysis unit at 100oC and 300pKa: single 9mm bead - 60 rpm (lane 2), 3 x 9mm beads - 300rpm (lane 1), 4 x 5mm beads - 300rpm (lane 6) and 2 x 5mm beads with 15 x 1mm beads- 300rpm (lane 7). Significant banding patterns are labelled (a) through (g). Standard ladder (SeeBlue™ Pre-stained Standard, Invitrogen, USA) relates molecular weight. **113**

- Figure 6.6.* Modified 10mm stainless-steel HPLC column, detailing PEEK tubing connected via 10 32 fitting (a) acrylic volume adjustment spacer, pressure fittings, and frits (b); and inlet pressure fitting removed for frit fitment following pump filling of the stationary phase (c). **115**
- Figure 6.7.* Showing DNA recovery over the DNA purification protocol development utilising a ‘Fluka’ silica gel stationary phase matrix of particle size 63µm to 200µm with 200µl free volume relative to Congen miniprep yield. Error bars indicate variation based on control samples and miniprep extraction protocol, n=5. **116**
- Figure 6.8.* Figure 6.8. Scanning electron microscopy detailing the characteristics of the borosilicate glass stationary phase matrix Endecott filtered to a particle size of to 0.01mm 0.125mm. **117**
- Figure 6.9* Showing DNA recovery over the DNA purification protocol development utilising a borosilicate glass-based stationary phase matrix with 200µl free volume and particle size 0.01mm to 0.125mm and. Error bars indicate DNA recovery variation in protocol 13, n=3. **118**
- Figure 6.10.* Showing DNA purity as determined by the ratio of sample absorbance at 260nm divided by absorbance at 280nm. Values of 2 and above – protocols 8 through to 11b – indicate contamination by cell lysis debris and components of the lysis buffer chemistry. **119**
- Figure 6.11.* UV Spectrum for protocol 9 sample [0.25] showing absorbance of 14.2 absorbance units (AU) at 230nm and 15.6AU at 233nm (b), indicative of GuHCl contamination, and a 3.0AU peak at 260nm associated with nucleic acid absorbance. **120**
- Figure 6.12.* UV Spectrum for protocol 11 sample [0.5] showing absorbance of 2.8AU at 230nm (a), peak absorbance of 16.5AU peak at 241.5nm (b), and a ‘shoulder’ absorbance peak of 5.8AU at 260nm (c) attributable to sample DNA content. **121**

- Figure 6.13.* UV Spectrum for protocol 11b sample [0.25] with absorbance of 3.2AU at 230nm, a peak absorbance of 2.95 AU at 260nm and absorbance at 280nm of 1.54AU (c). Inset is a corresponding spectrum for the Congen control sample with absorbance values of 1.75AU, 3.6AU, and 2.25AU at 230nm (d), 260nm (e), and 280nm (f) respectively. **123**
- Figure 6.14.* Outlining the relationship between reservoir pressure and reagent flow through the 200µl free space within the borosilicate glass solid phase extraction matrix of grain size 10µm to 125µm. Error bars indicate experimental variation, n=10. **124**
- Figure 6.15.* Final amplicon concentrations for sample replicates for serial dilutions from 1:1 to 1:2048 following 50 PCR cycles (95oC for 15secs and 62oC for 30secs). Projected control values are presented for comparison. **127**
- Figure 6.16.* Showing the absolute quantification from the C. jejuni 1:2 serial dilution with slope -3.5582, efficiency -3.5582, error 1.91, and Y-Intercept 61.25. R2=0.63. **128**
- Figure 6.17.* Cyclic voltammetry characterisation of a GCE through a 3-cycle sweep of -1V to 1V and the corresponding current range of 0.175mA (-0.085mA to +0.09mA). The variability described over the course of 3 identical voltage scans suggests an instability or reconstruction at the electrode surface. This baseline variation directly limits the sensitivity of the sensor setup regardless of the target affinity of the bioreceptor molecule employed. **130**
- Figure 6.18.* Cyclic voltammetry showing forward and reverse scans from -1V to 1V and the corresponding current range for a GCE. The peak at -0.72V denotes the presence of dissolved oxygen in the electrolyte solution and decreases in magnitude as the gas is oxidised by each successive reverse scan. **131**

- Figure 6.19.* Voltammetry depiction of Graphene oxide (GO) modified GCE through a voltage sweep of -1V to 1V. The progressive fall in peak current at maximum voltage application relates the cumulative reduction/oxidation of oxygen containing groups on the GO surface. **132**
- Figure 6.20.* Differential pulse voltammetry (DPV) scans showing the oxidation of guanine (a), adenine (b), and thymine (c) at 100 μ M concentrations employing a reduced Graphene oxide modified GCE. **134**
- Figure 6.21.* Highlights the change in cyclic voltammetry response sensitivity for the detection of a 10 μ M dopamine concentration using a bare (a), graphite (b), cellulose microfiber (CMF) (c), CMF coated graphite (d), and graphite-CMF composite (e) modified screen printed electrode. **135**
- Figure 6.22.* Cyclic voltammetry REDOX stabilisation of a Graphene oxide (GO)-cellulose microfiber modified electrode (2 sets of 3 scans). The abundant oxygen functional groups associated with the GO require prolonged oxidation and reduction cycling to acquire levels of electronic stability suited to analytical electrochemistry techniques. **135**
- Figure 6.23.* Describes the relationship between the volume of graphite-CMF used to drop-coat the electrode surface and the resulting levels of dopamine oxidation. The peak height increases significantly with an increase in volume from 1 μ l to 6 μ l and indicates an optimal electrode modification volume between layer thickness at 6 μ l and 9 μ l. **135**
- Figure 6.24.* Consecutive cyclic voltammetry scans highlighting the current range of a GO-CMF-Nafion™ modified electrode surface in the region of 1 μ A. **137**
- Figure 6.25.* Scanning electron microscopy (500X) detailing the SPCE surface morphology prior to electrochemical activation. In comparison to the smooth and relatively uniform surface of the GCE (a) inset, the SPCE surface exhibits minor surface undulation and granularity, along with a high degree of porosity. **139**

- Figure 6.26.* Chronoamperometry scan the effect on current flow on the activation of an SPCE at 2.0V for 300s. The decrease in current corresponds with an increase in SPCE surface area during electrochemical 'etching'. The observed variability may be attributed to gas bubble formation on the electrode surface and to localised temperature fluctuation **140**
- Figure 6.27.* Figure 6.27. Scanning electron microscopy (500X) detailing the activated screen-printed carbon electrode (α SPCE) surface morphology and fractured edge flake morphology, inset (a). **141**
- Figure 6.28.* Cyclic voltammetry for the SPCE (a) and α SPCE (b) showing a significant increase in surface capacitance, and a characteristic REDOX pair at 0.3V and 0.22V on the forward and reverse scans respectively. **141**
- Figure 6.29.* Describing the change in surface capacitance and peak REDOX current for an 'as printed' SPCE (a), and the α SPCE (b) pre and post electrochemical PEDOT:PSS deposition (c). **142**
- Figure 6.30.* Scanning electron microscopy showing the morphology of a PEDOT:PSS:APTES modified α SPCE. Inset shows fracturing of the modification layer during curing (a) and surface fragmenting as a result of DPV electrochemical analysis (b). **143**
- Figure 6.31.* DPV oxidisation of 2.5 to 25 picomolar concentrations of guanine. In comparative DPV analysis, the analyte concentration present in the electrolyte is directly proportional to the area under the corresponding oxidation curve. **145**
- Figure 6.32.* DPV quantification of 1 to 5 pM concentrations of *C. jejuni* single-stranded DNA (ssDNA) showing significant peak volume over the analytical baseline (a) at [5pM]. **146**

- Figure 6.33.* DPV nucleobase oxidation detection for *C. jejuni* ssDNA concentrations from 5pM to 25pM as an increase in peak size at 1.2V to 1.5V. **146**
- Figure 6.34.* Cyclic voltammetry characterisation of α SPCE stability highlighting the characteristic peak at 0.3V (a) and oxygen group REDOX activity between 0V and -0.8V. **147**
- Figure 6.37.* Cyclic voltammetry showing activated electrode (a), 2 μ g DNA immobilisation (b), and associated increase in surface negativity (c). **149**
- Figure 6.36.* Cyclic voltammetry characterisation of immobilised DNA (a) and electrode/DNA with associated oxidation (b) and reduction (c) peaks for 10 mM methylene blue (MB) **150**
- Figure 6.37.* Voltammogram demonstrating the blocking effect of BSA in restricting methylene blue oxidation and reduction (a) via the immobilised ssDNA sequences only (b). **151**
- Figure 6.38.* Highlighting the stability of the immobilised DNA/BSA blocking protein combination through 5 voltammetry scans -0.8V to 0.8V. **151**
- Figure 6.39.* Cyclic voltammetry showing the MB REDOX couple before (red) and after (green) electrode incubation with 2 μ g/ml non-complementary target sequences for 15 minutes. **152**
- Figure 6.40.* Cyclic voltammetry showing the MB REDOX couple before (blue) and after (red) electrode incubation with 2 μ g/ml complementary target sequences for 15 minutes. **153**
- Figure 6.41.* Cyclic voltammetry data outlining the decrease in MB REDOX couple activity resulting from the cumulative addition of PCR amplicon aliquots of 0.5 μ g of target DNA. **154**

- Figure 6.42.* Detailing the cyclic voltammetry data range selected -0.2V (a) to 0V (b) to test the hypothesis: cumulative addition of 0.5ug of target sequence DNA has no statistically significant effect on MB REDOX electron transfer levels. **155**
- Figure 6.43.* Summary of the statistical evaluation of changes in DNA MB REDOX activity levels resulting from cumulative additions of 0.5ug aliquots of target sequence. Treatments 1 to 5 refer to for current values generated by voltages between -0.2V and 0V and corresponding to the incremental addition of 0, 0.5µg, 1µg, 1.5µg and 2µg of target DNA. **156**
- Figure 6.44.* Describes the linear relationship between peak methylene blue oxidation current and the cumulative hybridisation of 0.5µg to 2.0µg target with immobilised probe DNA. **156**
- Figure 6.45.* Summary of the statistical evaluation of DNA immobilised and BSA blacked αSPCE prior to incremental hybridisation with target sequence aliquots. Treatments 1 to 5 refer to cyclic voltammetry generated current data for the voltage range -0.2V and 0V. **157**
- Figure 7.1.* Biosensor array design, facilitating the detection of multiple DNA sequences simultaneously with applications in the characterisation of microbial population dynamics, for clinical genotyping, or in antibiotic resistance characterisation. **161**

Scope of the thesis

Chapter 1 - Highlights the role of pathogens in relation to the delivery of safe food and water, but also stresses their position as a relatively tiny fraction of a highly complex, numerous, interconnected community. This first chapter also considers the requirement for development of novel technologies for the characterisation of microbial populations in the environment. Broad characterisation of such reservoirs is likely to be fundamental to mitigating the impact of factors such as antibiotic resistance, pollutants, and climate change of microbial populations fundamental to ecosystem stability.

Chapter 2 - A focus on *Campylobacter* as the primary cause of bacterial enterocolitis and discusses how the development of analytical techniques has shaped our understanding of individual microbial species and the nature of microbial communities. This chapter also highlights how the use of analytical techniques designed for use in pathogen surveillance may act to introduce error and bias when applied as research tools.

Chapter 3 - Examines contemporary molecular microbiology assays routinely applied to confirmatory identification of microbial species. As analytical tools, the advantages and disadvantages of ELISA, PCR, and enzymatic substrate-based assays are evaluated, in the context of the validation challenges that relegate these techniques to a predominantly corroborative analytical role.

Chapter 4 – Details the experimental methods, equipment, and reagents used. The techniques used to validate the performance of the biosensor platform are outlined in addition to those used to provide analytical control and reference.

Chapter 5 - Outlines the initial design and development of the component parts of the field-portable biosensor platform in the context of performance, practicality, and production design. This chapter covers all aspects of reagent storage, delivery and disposal; sample loading and processing; electronic process control and analysis; reusability; and potential interface models.

Chapter 6 - Presents the experimental validation of the techniques and principles outlined in the development section in the order of sample processing by the biosensor platform. The data presented is divided into three segments – microbial cell lysis, DNA extraction and purification, and electrochemical analysis of probe-target DNA

hybridisation. Novel, task-specific electronic and engineering solutions developed over the course of the research are described in the context of their application.

Chapter 7 – Reviews the functionality of the biosensor platform and considers areas which might be enhanced to improve analytical performance. Future objectives are considered in relation to multiplex analysis and parallel sample handling. Customisable ‘Apps’ are discussed as a means to deliver user specific controls and data presentation and enhance usability. Lastly the capacity to be used in conjunction with existing analytical and sequencing platforms in-the-field is considered.

Chapter 1

The microbiome

1.1 Microbial populations - how much do we know?

Among the most significant developments in the discipline of life sciences has been the *re-tasking* of bacterial proteins as components of a molecular tool-kit and establishment of the twin disciplines of biotechnology and bio-informatics. The impact of such tools on research areas from molecular and evolutionary biology to clinical diagnostics and plant sciences cannot be overstated. However, despite advances in methodologies and significant cost reductions in molecular analysis and data processing, the characterisation of microbial metagenomics across environments key to human health is comparatively limited (Lok, 2015; Logue et al., 2016; Pedrós-Alió and Manrubia, 2016; Salmonová and Bunešová, 2017). Accordingly, our understanding of such microbiomes tends to be drawn from meta-analysis of surveillance and clinical data gathered using conventional, culture-based techniques.

The main challenge to the characterisation of microbial dissemination in the environment is simply the complexity of the microbiome. Contemporary estimates set the number of bacterial species between 10 million and 1 billion, with less than 1% characterised (Glick, 2015). Similarly, there are an estimated 3-5 million species of fungi (Wong, 2017), of which around 170,000 have been identified, while viral strains are thought to outnumber all other microbial species by a factor of 10. In contrast, the analytical techniques currently available to the microbiologist are limited by the capacity to detect, identify, and enumerate only a small part of this diverse, complex microbial population. Furthermore, given their impact it is unsurprising that the great majority of validated methods and protocols applied to microbial recovery are specific to those species posing the greatest threat to human health. Because of their exceptional reliability and robustness, contemporary clinical and pathogen surveillance assays are predominantly culture-based.

Considered the gold standard in pathogen surveillance, culture-based microbiology techniques have a basis in the recovery of microbial species from food, water, and clinical sample matrices. Consequently, they are not designed for the characterisation

of microbial populations outside human/animal biomes, nor are they specific to many of the cellular conformations existing as components of multispecies biofilms or within surface, drainage or wastewater. Conversely, molecular techniques, and particularly sequencing technologies, represent a tool-kit ideally suited to the characterisation of ecological microbiomes. However, such techniques are limited by a dependence on laboratory-based equipment and techniques, complex protocols, and a dependency on skilled personnel. Accordingly, a user-friendly, field-portable system with the capacity to detect, identify, and quantify key microbial species has the potential to make a significant contribution to our understanding of environmental microbial communities. At present, no such system exists.

1.2. Microbes and pathogens

The term pathogen is broadly used to define a microorganism that causes disease in its host. However, while they may have significant and far-reaching implications, pathogenic microbes represent a fraction of all known microorganisms. In outlining the challenges inherent to their detection and identification, it is most practical to consider pathogenic microorganisms as a tiny subset of a much broader community. The enormously diverse microbiome population consists of archaea, bacteria, and members of the eukaryota. It also includes many viruses - autonomous biological agents with the capacity to hijack the genetic replication functionality of a host cell.

1.2.1 Microbial communities

The first microorganisms are thought to have originated in the primordial chemistry of Earth around 3.8 billion years ago and they have gone on to exploit every available habitat. They are the archetypal life of Earth; they shape the natural world and are fundamental to the maintenance of environmental stability. Microbial populations are highly social and may be best considered as multi-species, multi-domain population: acting co-operatively and forming highly complex symbiotic and/or parasitic relationships. The interactions of microorganisms are fundamental to life as we recognise it today, and in the context of agriculture or medicine, multicellular lifeforms such as plants and animals are increasingly viewed in the context of their associated microbiomes.

Among the most important of such interactions are those between plants and fungi, and the exchange of nutrients and sugars through mycorrhizal associations. Believed to have been fundamental to colonisation of the landmasses by plants during the Ordovician period some 485 to 445 million years ago, mycorrhizal associations are equally important to the success of wild plants and agricultural crops today. Relationships between plants and fungi are ubiquitous. Endophytes and epiphytes, fungi that live within plant tissue or on its surface, are shown to confer protection from insect predation and grazing, and to limit the effects of environmental stressors (Verma et al., 2017; Rowan and Popay, 2017). Likewise, for wild rice (*Oryza officinalis*), nitrogen fixation by bacterial species is of such importance to seedling success that rice seed husks are effectively pre-packed with endophytic bacterial species such as *Herbaspirillum spp.* (Hoseinzade et al., 2016). The contemporary understanding of such relationships is at best limited.

The average gram of soil contains as many as 50,000 bacterial species in addition to fungi and protists. Yet without characterising such populations and identifying trends relating to seasonal factors such as humidity or temperature, we have neither a reference against which to judge the impact of agrichemicals or environmental contaminants on biome structure, nor a foundation on which to base remediation strategies. Our limited understanding of such populations is highlighted by programs which have effectively reversed desertification by mimicking the activities of prehistoric grazing ruminants using very large herds of cattle. Mixing of the surface soil and the dispersal of nutrients and seeds in the animal waste is thought to promote water retention and encourage the growth of flora and fauna, with the additional benefit of sequestering atmospheric carbon dioxide (Savory and Duncan, 2016). The success of such strategies is likely to have a basis in the co-evolution of animal, soil, and plant microbiomes over long periods of prehistory, but how we analyse, interpret and model such interactions and identify key relationships represents a significant challenge. Yet without such an understanding, it may not be possible to determine the effects of environmental contaminants from agrichemicals (Chernov et al., 2015) and heavy metals (Frossard et al., 2018) to phthalates (Kong et al., 2018), polychlorinated biphenyls (Vergani et al., 2017), or antibiotics (C. Pal et al., 2016; Berendonk et al., 2015).

One of the research interests being human pathogenic microorganisms, it is little surprise that we too share a complex relationship with our co-evolved microbiome (Lloyd-Price et al., 2016; Vogtmann and Goedert, 2016; Ursell et al., 2012). The human body is host to between 10 and 100 trillion symbiotic microbes including archaea, eukaryota, and viruses, of which the great majority are bacteria. Interestingly, while human genomic content is around 99.9% identical between individuals, genetic overlap in the gastrointestinal tract (GIT) microbiome may be as low as 10%. Whether this reflects natural variation or the result of contemporary factors such as dietary habits, food processing, or widespread antibiotic use is unclear. The consumption of dietary probiotics to select for bacterial species such as *Lactobacilli* and *Bifidobacteria* (Gomes and Malcata, 1999) is demonstrated to have positive effects on immune function, inflammatory responses, and glucose homeostasis. However, such benefits may be negated by other ways in which we have exploited microbial activity: in brewing, baking, and wine and cheese making (Boulton and Quain, 2008; Donalies et al., 2008; Parker et al., 1998).

1.3 Pathogenicity and virulence

Taken together, the *Pathosystems Resource Integration Centre database* (PATRIC), *Virulence Factor Database* (VFDB) and the *Comprehensive Antibiotic Resistance Database* (CARD) list those bacterial species classified as human pathogens and their associated virulence factors and/or antibiotic resistance genes. At present, this bioinformatics resource lists 307 bacterial species and provides genomic, proteomic, and metabolic pathway data to aid the development of treatments, vaccines, and diagnostics (Snyder et al., 2006; L. Chen et al., 2005; McArthur et al., 2013).

Infective disease describes a proliferation of pathogenic microorganisms within the host organism and can range from mild localised infection to systemic life-threatening illness. Pathogenic bacteria are most important in animals while fungal disease is more usual in plants. In describing the pathology of infection related disease, pathogenicity and virulence are often applied interchangeably. However, their different intended meanings are useful in highlighting the role the host immune response may play in the pathology of infective disease.

Pathogenicity is broadly defined as the *capacity* of a microorganism to cause damage to cells of the host organism and describes processes such as host cell invasion and lysis by bacterial pathogens or the appropriation of cellular functionality during viral replication. It is not unusual for pathogenic microorganisms to exist benignly as a constituent of the commensal microbiota or in a state of dormancy within host tissue (L. Li et al., 2014; Oliver, 2005c). Where pathogenicity is expressed by a microbial species in response to factors such as host/site-specific signal molecules or interactions with the host immune system, virulence describes the *extent* of the subsequent tissue damage (SacristAN and GARCÍA-ARENAL, 2008; Casadevall and Pirofski, 1999).

1.3.1 Virulence factors

While it might be more accurate to describe them as pathogenicity factors, microbial features expressed in host colonisation are termed virulence factors. These include adherence and host cell invasion mechanisms, exotoxins and endotoxins. Structural elements such as S layer proteins, encapsulation coats, and flagella may also act as virulence factors which, although not inherently damaging to the host cells, prompt an immune response (P. Y. Ong and Leung, 2016). Tissue damage in this instance results from the resulting immune system cascade and may be aggravated by the lysis of bacterial cells in a chain reaction feedback loop akin to immune hypersensitivity in asthma or nut allergy.

1.3.2 Antimicrobial resistance (AMR)

Much of our understanding of the transmission and dissemination of microbial species in the environment is based on conventional culture-based microbiology methods, and on molecular techniques with an equivalent focus on identification and relative quantification. Contemporary phylogenetic classification of bacterial species is based on the comparison of genomic regions coding for the highly conserved 16s rRNA subunit, extensive database records make it relatively straightforward to identify microbes within a sample matrix by way of polymerase chain reaction analysis (PCR). The amplification of sequences other than those coding for conserved genomic regions may be appropriate to applications such as the characterisation of environmental reservoirs and transmission vectors of genes coding for virulence factors or antibiotic resistant. A

portable device with the capacity to detect such sequences has many potential applications in research and diagnostic roles.

With little development of new compounds since the 1970s, antibiotic resistance is among the most significant challenges to human health in the modern era. Treatment resistant infections have already led to more frequent and longer hospital admissions, increased medical costs, and a growth in associated fatalities. Reviewing the contemporary and potential impact of antimicrobial resistance in 2016, the O'Neill report (Resistance, 2016) estimates that around 700,000 people currently die each year due to treatment resistant infection. If not addressed, this will rise to 10 million lives annually by 2050, with an associated cost to productivity in the region of 100 trillion US dollars. The loss of effective antibiotics would also render procedures such as heart by-pass surgery, organ replacement, caesarean section birth, and chemotherapy-based cancer treatment simply too hazardous to be practicable.

A range of measures have been implemented to reduce the unnecessary use of antibiotics. However, the characterisation of resistance gene distribution in the environment may be key to the identification of control points and the implementation of strategies to minimise their propagation. As antibiotic resistance gene cassettes, termed resistomes, are carried and exchanged by both pathogenic and non-pathogenic species, it may be best to consider them as discrete entities; independent of their host microbe.

From this perspective, parallels with information processing may be drawn, with vectors for bacterial environmental dissemination viewed as a distribution network. By extension, environmental reservoirs such as multi-species aquatic biofilms may be considered as redistribution nodes in the dissemination of genetic information within bacterial communities. Furthermore, given that resistomes are essentially data packets, those processing techniques applicable to data analysis and transmission within digital networks may be equally applicable to epidemiological research and the prevention of antibiotic resistance proliferation.

1.4 Food and waterborne pathogens

The World Health Organisation estimates that 2.2 million people die each year from infection by food and waterborne pathogens (Kirk et al., 2015). While there is a tendency to associate such diseases with the developing world, food and waterborne diseases have a significant health and social impact across Europe and the United Kingdom. Contamination of foods may occur at any point in the food processing and supply chain or may be the result of inadequate cooking or poor hygiene. Foodborne illness is most commonly associated with seafood, poultry, and meats. Symptoms include nausea, stomach cramps, vomiting and diarrhoea, and may lead to life-threatening conditions and sequela.

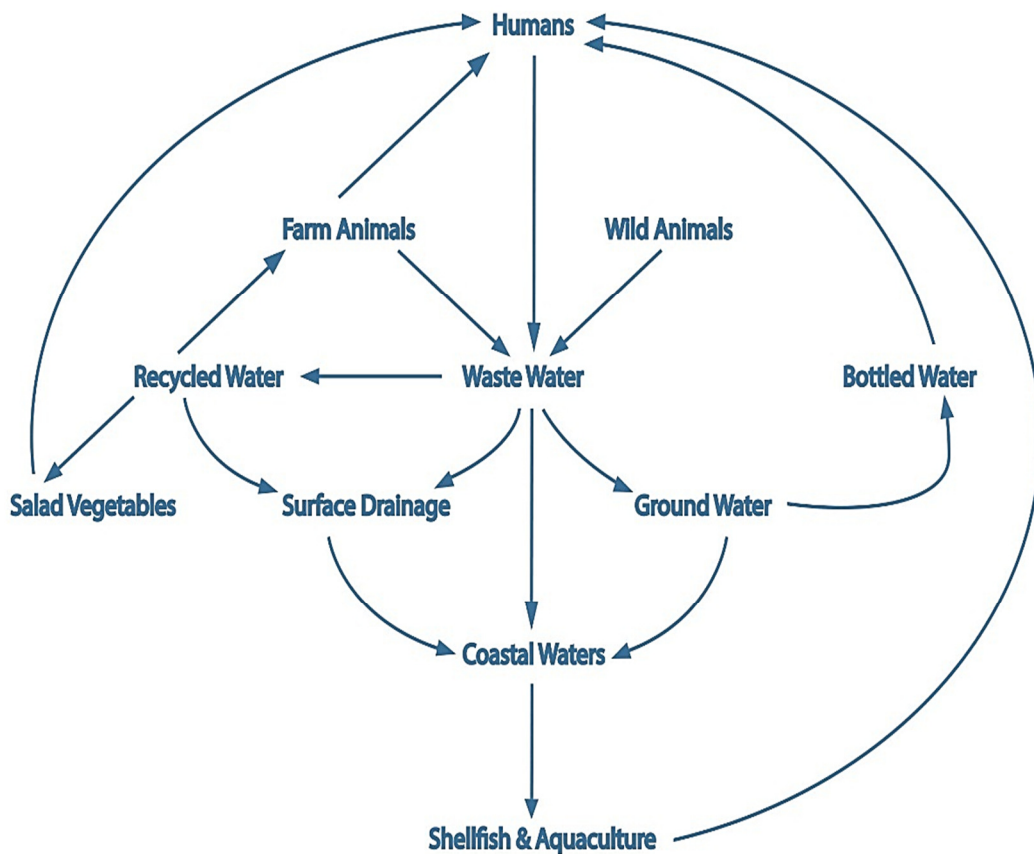


Figure 1.1. Outlining potential dissemination routes for waterborne pathogenic bacteria and facilitating the transfer of virulence and antibiotic resistance gene cassettes in soil, multispecies aquatic biofilms, and as part of the commensal microbiota in humans, livestock, and wild animals such as insects and birds.

Vibrio, *Cryptosporidium*, *Campylobacter*, *norovirus*, and *Salmonella* are responsible for the great majority of food and waterborne infective disease in humans. The characterisation of colonisation vectors, transmission routes, and environmental reservoirs has aided in hazard analysis and critical control point identification. Figure 1.1 highlights how pathogenic species may circulate through waste, runoff, recycled, and coastal waters and re-enter the food chain. Furthermore, in the current era of jet aircraft and the transport of fresh and frozen foods from around the globe, the international circulation of bacterial species and gene cassettes such as those coding for antibiotic resistance must be considered the norm (Findlater and Bogoch, 2018; Roca et al., 2015; Berendonk et al., 2015).

The incidence and impact of disease and outbreaks caused by food and waterborne pathogens are comprehensively documented by the World Health Organisation (WHO), the European Centre for Disease Prevention and Control (ECDC), and the European Food Safety Authority (EFSA). The data presented indicates an increased incidence of vibriosis and salmonella associated with both hotter and wetter weather (Baker-Austin et al., 2017; Hernroth and Baden, 2018), while incidence of norovirus and cryptosporidiosis is associated with heavy rainfall and the contamination of watercourses with wastewater overflow (Sterk et al., 2016; P. Wang et al., 2018). Accordingly, the warmer summers and wetter winters predicted as a result of climate change is likely to have a significant effect on the prevalence and incidence characteristics of food and waterborne diseases such as salmonella and campylobacteriosis (I. R. Lake et al., 2012; I. Lake et al., 2009).

Of around half a million cases of food poisoning in the UK annually where the cause can be attributed to a characterised pathogen, approximately 280,000 are caused by *Campylobacter*, against 80,000 *Clostridium perfringens* infections and 74,000 cases of norovirus (FSA, 2015). While most commonly attributed to contaminated poultry products, an increase in clinically notified *Campylobacter spp.* incidence is also associated with patterns of heavy rainfall and increasing temperatures in springtime, suggesting a waterborne component (Djennad et al., 2017; I. Lake et al., 2009). However, relatively little research has focused on the role of environmental dissemination vectors

or that of aquatic biofilms, and *Campylobacter* are characterised as reproducing only within the gut of an animal host.

This limited understanding of *Campylobacter spp.* reflects the limitations inherent to contemporary microbiological analysis and the influence such shortcomings have in the subsequent characterisation of microbial species. Accordingly, Chapter 2 examines the current understanding of *Campylobacter spp.* from the perspective of how the data contributing to this representation has been gathered and suggests areas which may warrant further consideration in the identification of transmission vectors and potential control points.

Chapter 2

***Campylobacter spp.* as a model organism**

A focus on *Campylobacter* as the primary cause of bacterial enterocolitis and how the development of analytical techniques has shaped our understanding of individual microbial species and the nature of microbial communities. This chapter also highlights how the use of analytical techniques designed for use in pathogen surveillance may act to introduce error and bias when applied as research tools.

2.1 The *Campylobacter* genus

Campylobacter spp. are a Gram-negative proteobacteria between 1.5µm and 8µm long, and are curved, spiral, or gull-winged in appearance. With single or bi-polar flagellum, they are highly motile, moving in a characteristic corkscrew fashion. *Campylobacter* are typically associated with the gastrointestinal microbiota of cattle, poultry, and wild birds, and are microaerophilic and capnophilic - suited to the low oxygen and increased carbon dioxide atmosphere of the digestive tract.

Given their similarities in appearance, prevalence, and virulence in humans, *Campylobacter spp.* were first categorised as a member of the *Vibrio* genus. In expanding the aims of the introduction, this chapter charts the subsequent classification of *Campylobacter* and considers the relationship between the phylogeny of bacterial species and the characterisation of their interactions, transmission, and distribution in the environment.

2.1.1 *Campylobacter spp.* classification – conventional methods

The initial categorisation of *Campylobacter* as a member of the *Vibrio* genus was based on the description of cellular features, a characteristic morphology of isolated cultures, and on the capacity of the bacteria to metabolise specific substrates. Given that bacterial species sharing an evolutionary niche are highly likely to share environment specific structural and functional adaptations, it is hardly surprising that they can be difficult to differentiate by conventional microbiology techniques.

The capacity to discriminate between otherwise similar pathogenic and non-pathogenic bacterial species or strains may be fundamental to effective pathogen surveillance in

food and water supply. Similarly, the capacity to identify microbial populations containing treatment resistance gene cassettes may be essential to the delivery of appropriate treatment in a clinical context. The attainment of higher levels of analytical resolution in the identification and classification of microbial species such as *Campylobacter spp.* has led to an increasingly important role for molecular techniques in augmenting culture-based methods.

2.1.2 Molecular techniques in *Campylobacter* classification

Among the earliest molecular techniques applied to bacterial phylogeny was G:C analysis. A measure of the genomic percentage consisting of guanine-cytosine base-pairing, G:C ratios are determined using spectrophotometry during temperature driven denaturation of genomic DNA (Marmur and Doty, 1962). In the case of the *Vibrio* genus, G:C analysis highlighted a group of subspecies maintaining a G:C content of around 30% - significantly lower than 42% in the remaining species.

Accordingly, the *Campylobacter* (curved bacteria) nomenclature was proposed by Sebald and Véron in 1963 (Véron and Chatelain, 1973) and classified as a separate genus. While genomic G:C content is suggested to relate to evolutionary development within a low nitrogen environment (Luo et al., 2015; Giovannoni et al., 2005), it does not appear to correlate to specific microbial activities or interactions. Similarly, while they differ significantly in genomic composition, the form, function, and environmental interactions of enteric *Vibrio* and *Campylobacter spp.* are essentially indistinguishable.

2.1.3 Comparative genomic phylogeny

The current phylogeny of *Campylobacter spp.* is outlined in *Figure 2.1*, with species judged as primary and emerging pathogens highlighted. Interestingly, although sharing significant genomic similarities, *Campylobacter* subspecies vary greatly in terms of niche habitat, proliferation characteristics and host specificity. Also highlighted in *Figure 2.1* are *Arcobacter* and *Helicobacter spp.* initially considered to be *Campylobacters* and sharing habitat and pathogenicity characteristics, but identified as separate species in 1982 (Marshall and Warren, 1984). Conventional culture-based microbiology techniques cannot differentiate these bacteria from *Campylobacter spp.* based on cell structure and colony morphology. Likewise, G:C analysis shows a similar genomic base-pair ratio.

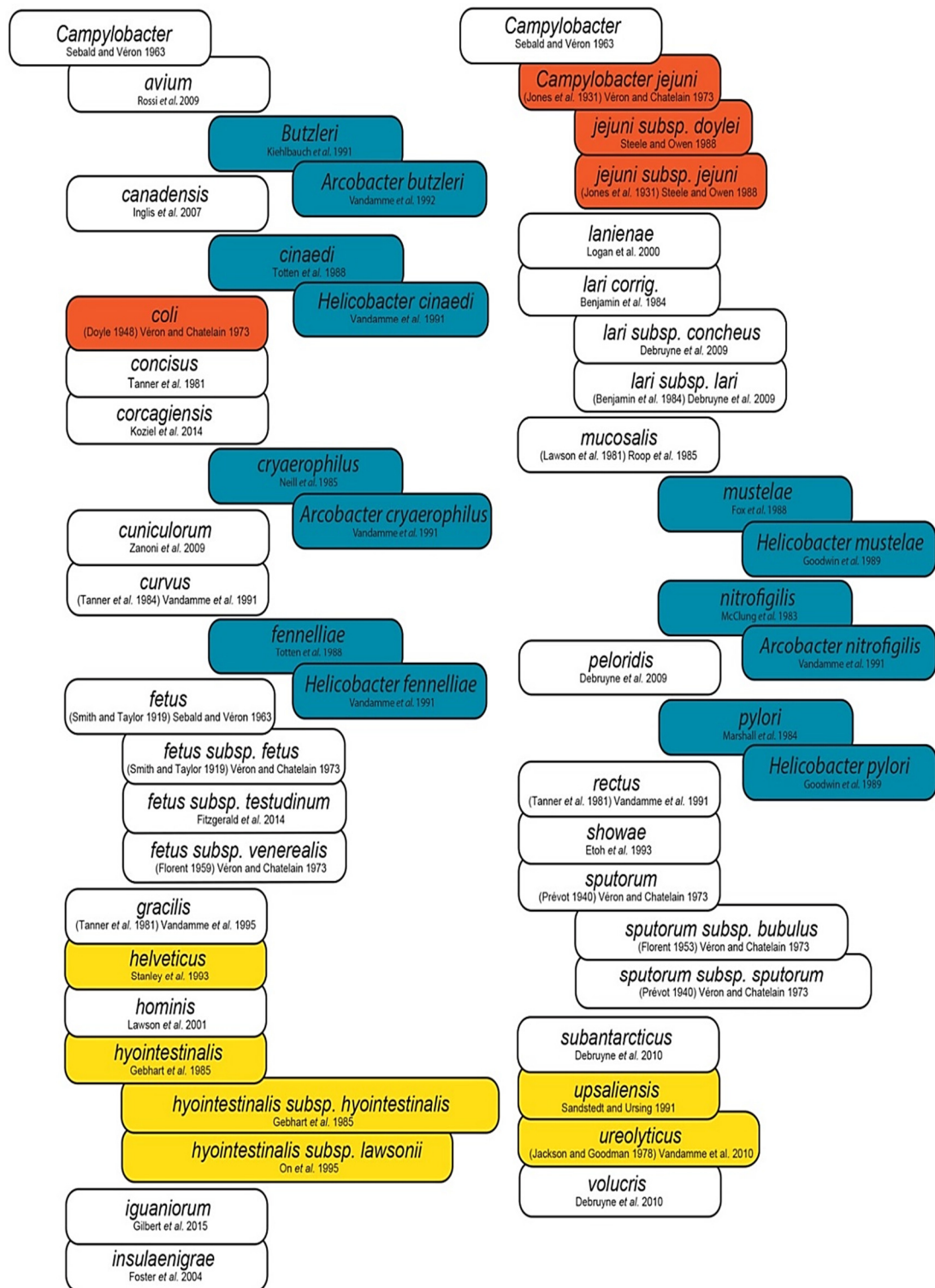


Figure 2.1. The *Campylobacter* genus, highlighting those species considered as primary (orange) and emerging (yellow) human pathogens (Kamei et al., 2014). The reclassification of species initially identified as *Campylobacter* spp. (blue), reflects the revision of bacterial genera with the integration of data generated by techniques such as comparative 16s sequencing. (Compiled using data from bacterio.net)

Accordingly, their reclassification was a direct result of the introduction of bacterial phylogeny based on the comparison of evolutionarily conserved regions in the bacterial genome in the early 1980's. Proposed by Woese and Fox in the 1970's (Woese and Fox, 1977) and building on contemporary advances in computing, bio-informatics, and gene sequencing, the comparison of conserved regions of the genome has remained the basis of prokaryotic taxonomy to the present day. In the classification of *Helicobacter*, comparison of genes coding for the 16s ribosomal subunit in *C. pylori* were compared with those from other members of the *Campylobacter* genus and with equivalent sequences from the wider bacterial genera. When no sequence homolog was found, this newly differentiated genus was named *Helicobacter* (describing its helical shape) and *H. pylori* and *H. mustelae* were reclassified (Goodwin et al., 1989).

2.2 The influence of niche habitat on bacterial evolution

DNA sequencing technologies have since had an enormous influence with all disciplines of the life sciences. However, while such techniques are fundamental to mapping the relatedness of microbial species based on evolutionary relatedness, bacterial characterisation employing alternative methods of categorisation may have a greater practical relevance. For example, a comparative analysis of *Campylobacter spp.* and *Vibrio spp.* based on structure, colony morphology, and metabolic capacity is insufficient to differentiate between these species. However, should the same characteristics be determined for an unknown bacterium, it could be proposed with a relatively high degree of confidence that the unidentified species is likely to share a similar lifecycle or niche habitat.

Comparative genomic analysis of *Campylobacter* has identified sequence homology and similarities which have enabled it to be placed within the wider bacterial phylogeny. Interestingly, in terms of genomic organisation, *Campylobacter spp.* show a high similarity to *Pelagibacter ubique*, an alpha-proteobacteria accounting for around 25% of all microbial cells in the ocean (Giovannoni et al., 2005). The small genome of *Campylobacter* (1.6 mega base-pairs or Mbp) is notable for an almost

complete lack of repeat, insertion or phage associated sequences, while that of *P. ubique* is the smallest genome of any free-living organism at 1.3Mbp and is similarly streamlined with no pseudogenes, introns, transposons, extrachromosomal elements, or inteins.

Considering the characterisation of *Campylobacter spp.* as enteric bacteria, any such similarities could easily be deemed coincidental. However, when considered in relation to the bacteria's adoption of a viable but non-culturable (VBNC) conformation in response to sustained planktonic suspension, such characterisation does not seem so unrealistic. With the genomic G:C content of *P. ubique* (29.7%) attributed to the selective influence of the low nitrogen ocean surface environment (Luo et al., 2015; Giovannoni et al., 2005), the relatively low *C. jejuni* genome G:C content (29.6%) suggests a requirement to consider waterborne persistence as a factor in *Campylobacter spp.* evolution, or as an element of the bacteria's lifecycle.

2.2.1 *Campylobacter spp.* reservoirs and environmental distribution

Currently characterised as enteric bacteria, *Campylobacter spp.* are considered to exist primarily as commensal gut microbiota in poultry, cattle, and other animals (Hendrixson and DiRita, 2004; Guévremont et al., 2014; Humphrey et al., 2007). However, they may also be isolated from surface runoff and drainage water, rivers, and estuarine and coastal waters (Khan et al., 2014; Pitkänen, 2013b; Vereen et al., 2013; Keener et al., 2004). *Campylobacter* exhibit a broadly overlapping host specificity and demonstrate routine zoonosis between avian and mammalian species, highlighting a high degree of adaptability on the part of the bacteria and supporting a hypothesis of transmission via a faecal-water-oral route. From a phylogeny comprising three separate clades, or branches, the genetic comparison of related species indicates the evolution of the most common pathogenic species, *C. jejuni*, to have occurred within the last 12,000 years (Wilson et al., 2009).

2.2.2 Pathogenic *Campylobacter* reservoirs

All *Campylobacter spp.* strains known to cause disease in humans, and the majority of those found in farm animals, belong to a single clade with origins in a branching

event around 2,500 years ago. This colonisation of different animals by similar *Campylobacter* strains is considered to indicate the adoption of a newly available niche by a specifically adapted lineage rather than a bacterium sharing a common gene pool with a pre-existing natural reservoir (Sheppard et al., 2010). On the other hand, the widespread application of broad-spectrum antibiotics in both animal feed and in agricultural animal husbandry in the last 50 years are likely to have acted to reduce genetic variation within the population. Applied as a means to increase growth rates and to reduce the energetic demands associated with microbial infection of the host (Brüssow, 2015), antibiotic compounds are likely to represent a selective influence on animal commensal microbiota diversity; on the population dynamics of the host animal commensal microbiota as a whole; and on the composition of water run-off and soil contaminated by animal waste (McCrackin et al., 2016).

2.2.3 Limits of contemporary *Campylobacter* spp. characterisation

Food animals are considered to represent both a primary reservoir for human pathogenic *Campylobacter* strains and the main source of zoonotic transmission. Consequently, a great deal of the pertinent data relating to bacterial distribution has been gathered through mandatory pathogen monitoring in food processing and water supply, and from the clinical reporting of campylobacteriosis in communicable disease surveillance. However, as such data represents a comprehensive resource readily suited to meta-analysis in the characterisation *Campylobacter* spp. for review publications (Sockett et al., 1993; Schielke et al., 2014b; Lindmark et al., 2009; Lund et al., 2003) this appears to generate something of a self-perpetuating research cycle.

Essentially, a focus on *Campylobacter* as an enteric organism with primary reservoirs in food animals largely overlooks the ways in which these bacteria persist in the environment between hosts. Compounding this, those culture-based microbiology methods validated for pathogen surveillance are not suited to the detection and identification of cellular conformations adopted by *Campylobacter* spp. for survival in surface water or on surfaces. Without such a contribution to the characterisation

of human pathogenic campylobacter reservoirs, the impression presented in the literature is, at best, incomplete. Unfortunately, research resources are then directed to the discovery of missing elements within the established and accepted bacterial distribution model rather than in consideration of the broader possibilities. Once established, such perceived wisdoms can, through the review process, engender bias in both journal article publication and research grant allocation.

In contrast, the development of molecular techniques and bioinformatics resources has greatly increased the contemporary understanding of microbial functionality at a cellular and molecular level. However, relating specific patterns of gene expression, surface receptors, or protein synthesis to the activities of microbial cells or populations remains problematic. The importance of interactions within multi-species microbial communities appears fundamental to population dynamics and behaviour, but the highly complex nature of such interactions renders them problematic to characterise.

Accordingly, the great majority of what is understood in relation to the cellular and molecular biology of microbial species has been gleaned through laboratory-based study of comparatively unrepresentative mono-cultures. Expansion or revision of the contemporary characterisation of *Campylobacter spp.* therefore may depend on the development of new approaches, and on new analytical techniques suited to the characterisation of microbial populations in-the-field. To get an idea of the kind of data or analytical scope such novel techniques should address requires an examination of the advantages and shortcomings inherent to contemporary microbiological analytical methodologies.

2.3 Validated techniques and media for recovery of *Campylobacter spp.*

In public health monitoring, validated protocols for the recovery of *Campylobacter spp.* from food, water, and stool sample matrices are contingent on culture-based microbiological techniques for primary detection and enumeration. In part a result of the challenges inherent to their validation, the application of molecular techniques such as ELISA and PCR is limited to confirmatory analysis. Both the formulation of

commercially available culture media and the method protocols applied in mandatory pathogen monitoring are specified by regulatory bodies such as Public Health England (PHE) and the International Standards Organisation (ISO). Such protocols are designed for the recovery, detection, and identification of *Campylobacter spp.* from specific sample matrices such as food produce or clinical samples. However, and despite often carrying labels advising to the contrary, the consistency and reliability of such tests has given rise to their widespread use in a plethora of microbiology research settings. As a potential source of experimental bias therefore, the limitations of validated *Campylobacter* recovery techniques merit further consideration.

ISO standards 10272:2006³/2006⁴ (E. ISO, 2006) define the validated techniques and media formulations for the identification and enumeration of *Campylobacter spp.* in food and water samples, and from rinses and surface sampling within food processing or preparation areas. While the isolation and identification of *Campylobacter* strains is relatively straightforward, precise enumeration of bacterial populations can present a significant challenge.

Plating and incubation of serial dilutions from a homogenised sample matrix represents a simple means to determine the bacterial loading of the original sample. However, both food processing and the inclusion of preservatives can damage a percentage of the bacterial cells present in the sample matrix. These injured bacterial cells may continue to represent a risk to health, but as they cannot be cultured, they are neither detected nor quantified. To ensure the safety of consumer produce, pathogen surveillance in the food industry employs an enrichment step to promote the resuscitation of injured cells and to increase the number of bacterial cells available for analysis. The ISO guidelines for this process, as summarised in figure 2.2, highlight the fundamental role of enrichment plays in ensuring the detection of food and waterborne *Campylobacter spp.*

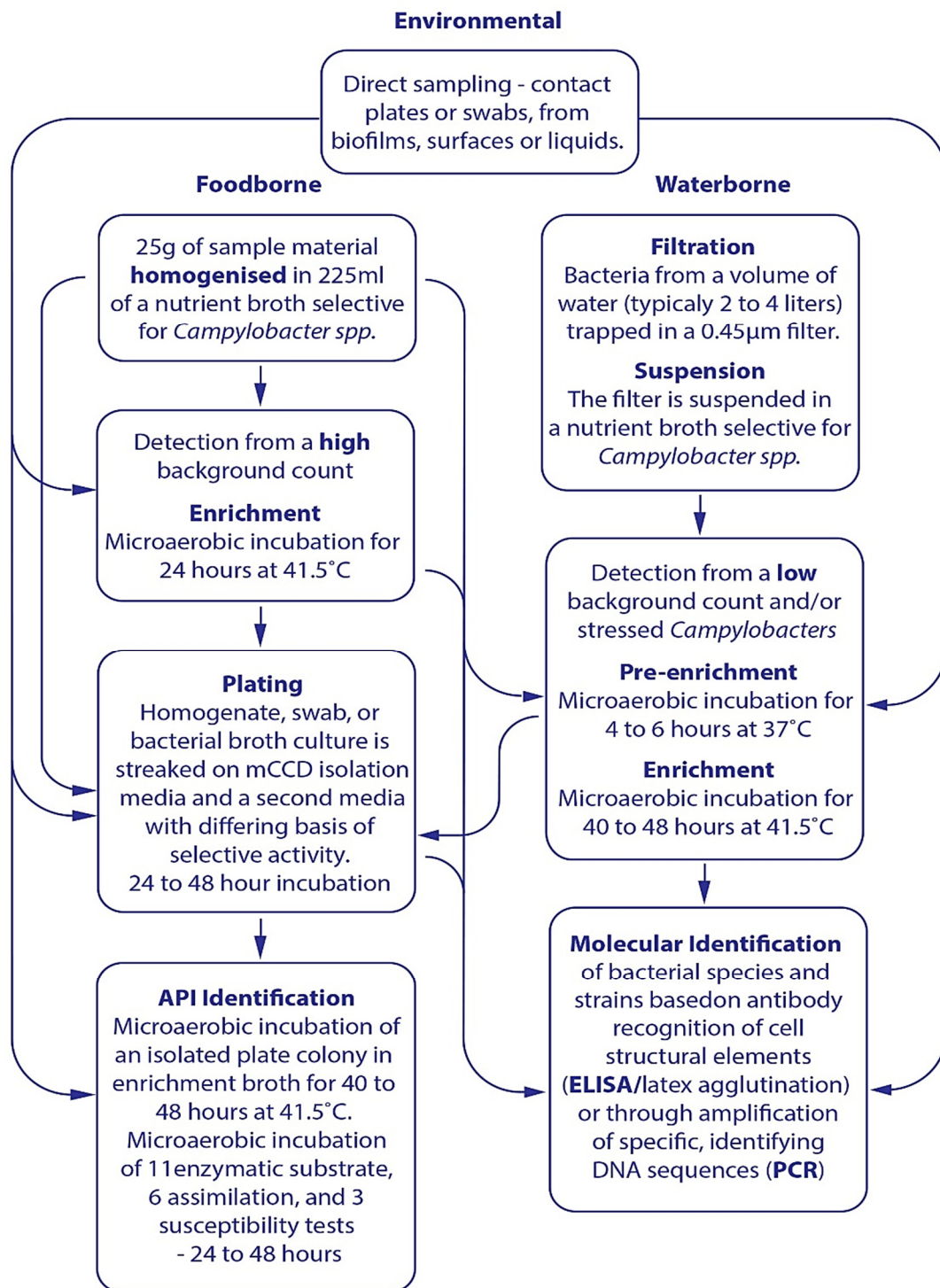


Figure 2.2. Summation of the International Standards Organisation (ISO) guidelines for employment of enrichment incubation in the recovery of *Campylobacter* spp. from food, water, and environmental samples. (mCCDA – modified charcoal-cefoperazone-deoxycholate agar, API® Bacterial identification strips – Biomerieux, France).

2.3.1 Enrichment incubation

Enrichment incubation therefore is considered essential to prevent the reporting of false-negatives. However, factors inherent to the process, such as media formulation, incubation temperature, and dissolved gas composition, select for the proliferation of specific bacterial sub-groups over others. As a surveillance tool, *Campylobacter* enrichment media is formulated to isolate the primary human pathogenic species - thermotolerant *Campylobacter jejuni*, *C. coli*, *C. lari*, and *C. upsaliensis* (Seliwiorstow et al., 2016; Bolton and Robertson, 1982; Habib et al., 2011) – from the microbial background present in the sample matrix. Although advantageous to detection of microbial contamination of food and water, the use of commercial enrichment media in a research context gives rise to similar bias in the recovery of *Campylobacter spp.* An observed bias toward the recovery of *C. jejuni* and *C. coli* in culture-based research (Man, 2011; On, 2013; Bojanić et al., 2016a) suggests that tools such as microbial enrichment are at times applied without a complete understanding of their downstream influence on analytical deductions.

Considered experimental design can negate or make allowances for the influence of bias arising from use of specific media formulations or enrichment methodologies. Furthermore, such bias can also be present in data generated by molecular techniques such as PCR or multi-locus sequence typing, when enrichment incubation or isolation media are employed in sample preparation. Again, while this may have little or no relevance to the detection of target species for pathogen monitoring, such bias effectively precludes the modelling of *Campylobacter spp.* environmental distribution or population dynamics based on data derived from enriched sample matrices. As they are likely to include data, or the meta-analysis of data, in which such sources of experimental bias are un-considered, contemporary characterisations of *Campylobacter* distribution and environmental transmission may frustrate the identification of effective control strategies.

In short, the utility of culture-based methods and enrichment incubation as a basis for *Campylobacter spp.* detection in pathogen surveillance has a basis in their specificity and focus on the task for which they have been developed. Both the media

formulation and incubation temperatures employed are specific to the recovery of *Campylobacter* expressing a cellular conformation specific to their endurance as a component of the mammalian or avian digestive tract commensal microbiota. However, as previously outlined, *Campylobacter spp.* may also be recovered from surface drainage, rivers and coastal waters and demonstrate a capacity to survive through a wide gamut of environmental conditions over considerable periods. In this setting, the *Campylobacter* cellular conformation differs greatly to that of those persisting in the enteric environment and cannot be recovered by conventional culture-based media or techniques.

2.3.2 Viable but non-culturable conformations

Relatively little is known in relation to viable but non-culturable (VBNC) *Campylobacter* conformations and, possibly due to the challenges inherent to their detection and characterisation, they do not represent a significant area of research. Nonetheless, understanding the distribution, prevalence and transmission of VBNC *Campylobacter spp.* conformations may be fundamental to mitigating the significant health and social costs associated with campylobacteriosis. Given the analytical challenges inherent to detection and recovery of VBNC cells (K. L. Hiett, 2017; Chaveerach et al., 2003; Cox et al., 2015), such investigation is likely to necessitate development of novel analytical approaches to bacterial detection, identification, and enumeration. As a target for such analytical techniques the contemporary understanding of VBNC conformations in *Campylobacter* and other bacterial species merits examination.

The VBNC cellular conformation was first described for *Escherichia Coli* and *Vibrio Cholera* in 1982 (Xu et al., 1982), prompting much debate and suggesting a significantly broader range of bacterial diversity than previously recognised. The VBNC conformation is described as ‘a situation where exposure to environmental stressors causes bacterial cells to lose culturability while retaining viability and potential to revert to an active state’ (Oliver, 2005b). Adoption of a VBNC conformation has been characterised for a range of bacterial species, including a number of significant human pathogens (Oliver, 2005a; Ramamurthy et al., 2014) and

has been observed in response to challenges such as nutrient stress, temperature, and planktonic suspension (Du et al., 2007; Ducret et al., 2014; Besnard et al., 2002b). VBNC conformations appear comparable to microbial dormancy, observed in disease pathology and antibiotic resistance (Ayrapetyan et al., 2015), and may indicate a proportion of bacteria to have the capacity to express specific non-culturable conformations according to particular environmental cues or stressors.

Adoption of a VBNC conformation in *Campylobacter spp.* corresponds to the progressive adoption of a coccoidal shape comparable to that of the bacteria in lag phase. The cell conformation remains metabolically active, albeit at a much-reduced level, and is observed to remain viable for long periods under conditions of planktonic suspension in water at low temperatures (Besnard et al., 2002a; Thomas et al., 2002; Cook and Bolster, 2007). While little is known in relation to the VBNC confirmation in *Campylobacter*, a study of VBNC conformations in *Escherichia coli* indicates the structure of the outer membrane to vary according to environmental cues such as light intensity, temperature, and salinity (Muela et al., 2008). Environment specific membrane structures expressed by VBNC bacteria are likely to influence factors from virulence and host colonisation potential to adhesion properties and antibiotic resistance (S.-H. Li et al., 2014). The role of VBNC bacterial transmission warrants investigation in the context of those strategies facilitating bacterial dissemination in the environment.

2.4 *Campylobacter spp.* persistence in the environment.

Between hosts, *Campylobacter spp.* demonstrate a capacity to survive through a wide variety of environmental conditions, and adaptations such as VBNC expression enable them to endure planktonic suspension, low temperatures, and prolonged freezing with limited loss of viability (Membré et al., 2013). In response to challenges such as oxygen tension, pH variation, heat shock, or nutrient stress, *Campylobacter spp.* colonies may also form biofilms (Turonova et al., 2015; Bronowski et al., 2014). Conferring protection from ultraviolet radiation, desiccation, anti-microbial agents, and predation, biofilms can effectively double the viable duration of *Campylobacter* on surfaces or in drainage waters (Reuter et al., 2010).

Campylobacter are shown to form mono-species biofilms, but with limited biosynthesis capability are more suited to a secondary coloniser role, catalysing the metabolites of other bacterial species (Hanning et al., 2008; Teh et al., 2010; Ica et al., 2012). Both the formation and the dispersal of such multispecies biofilm structures are thought to be mediated by bacterial quorum sensing, and the release of bacterial DNA into the extra-cellular matrix by cell autolysis (Svensson et al., 2014).

Interestingly, gene knockout analysis in *Campylobacter spp.* indicates a pivotal role for functional flagella in both biofilm formation and host colonisation (Kalmokoff et al., 2006; Hermans et al., 2011).

2.4.1 Environmental dissemination from campylobacteriosis outbreak data

As discussed previously, the characterisation of *Campylobacter* distribution in the environment effectively precludes use of contemporary culture-based methods and of molecular analytical techniques that require sample enrichment. However, while campylobacteriosis outbreaks are relatively rare (Pitkänen, 2013a; E. V. Taylor et al., 2013b; J. Silva and Teixeira, 2015), their incidence merits discussion as it indicates a blurring in the distinction between a bacterial species employing limited survival strategies and one exploiting multiple adaptative strategies to persist across a wide range of environments and colonise a variety of physiologically differing hosts.

Table 2.1 highlights the variation present in campylobacteriosis transmission and clearly demonstrates the capacity of *Campylobacter spp.* capacity to make use of a wide range of vectors, in environmental dissemination and between hosts. The link between campylobacteriosis and chicken produce is acknowledged (FSA, 2015), but despite representing an ideal transmission medium with buffering of both temperature and pH, water as a primary vector in the transmission of *Campylobacter* remains relatively unexplored. Accordingly, it is fitting to review the published literature relating to *Campylobacter spp.* in the poultry industry and examining the role of water as a medium for bacterial dissemination.

Table 2.1. Detailing the wide-ranging distribution of *Campylobacter* spp. across areas of highly variable temperature and relative humidity and sharing a common basis in waterborne transmission.

Place and Year	Numbers	Transmission vector	Epidemiology	Reference
Ohio, Oregon, and Washington, USA. 2013/2014	6 cases campylobacteriosis	Chicken livers, prepared as pâté, and as an ingredient in a naturopathic treatment	Both outbreaks attributed to a common distributor of contaminated chicken liver	153
England 2011	49 cases campylobacteriosis	Chicken liver pâté	Identified as undercooked chicken liver pâté, with <i>Campylobacter</i> infection correlating to the amount consumed.	154
San Luis Río Colorado, Sonora, Mexico and Yuma County, Arizona. 2011	26 cases Guillain–Barré syndrome	Washed fruit and vegetables	Linked to a large outbreak of campylobacteriosis resulting from inadequately disinfected tap water in San Luis Río Colorado.	155
Køge, Denmark. 2010	50 cases campylobacteriosis	Drinking of supply water and the use of tap water in food preparation.	Point source contamination of a community water supply by a single <i>Campylobacter</i> clone.	156
Chania, Crete. 2009	37 cases campylobacteriosis	Drinking of supply water and the use of tap water in food preparation.	Attributed to a single point source contamination of tap water exacerbated by inadequate supply chlorination.	157
South Central Alaska. 2008	43 cases campylobacteriosis	Consumption of raw peas	Epidemiologic link to raw peas contaminated by Sandhill cranes.	158
British Columbia, Canada. 2007	225 cases campylobacteriosis	Ingestion of mud by competitors of a mountain bike racing event.	Outbreak attributed to agricultural <i>Campylobacter</i> spp. in surface water drainage.	159
California, USA. 2006	1,644 cases campylobacteriosis	Pasteurised dairy milk.	Epidemiologically linked to milk and related products supplied by an on-site dairy.	160
Kansas, USA. 1998	27 cases campylobacteriosis	Consumption of prepared pineapple dishes, and those meals served with gravy.	Poor hygiene of an infected cafeteria worker identified as likely source of contamination.	137

2.4.2 Poultry as a *Campylobacter* reservoir

With 50% to 80% of campylobacteriosis attributed to the consumption of chicken produce, the poultry industry is considered the front line in reducing the health and social impact. It is therefore unrealistic to overlook the measures taken to prevent the dissemination of *Campylobacter spp.* in this context. The rearing and processing of broiler birds in the UK and Europe is subject to mandatory pathogen monitoring according to ISO guidelines, and employs validated microbiology techniques specific to thermotolerant pathogenic *Campylobacter spp.* strains (E. ISO, 2006). These techniques relate to the extent to which broiler flocks are colonised by *C. jejuni* and *C. coli*, and the consequent levels of these bacterial species present on poultry meat after processing. However, they offer no insight as to the distribution of non-thermotolerant *Campylobacter spp.* or VBNC conformations in the environment.

Patterns of on-farm distribution have been characterised by RT-PCR for the purpose of identifying sites suited to 'early warning' pathogen detection for targeting biosecurity measures, and again suggest a need to further categorise the role of non-culturable bacterial conformations (Battersby et al., 2016b; Agunos et al., 2014). As in the characterisation of *Campylobacter spp.* across the greater environment, identification of bias inherent to the analytical techniques applied may be fundamental to constructing an accurate representation. Furthermore, limitations inherent to the relative enumeration of microbial populations, such as the efficiency of DNA extraction in sample preparation to bacterial enumeration from 16s copy numbers (often present as multiples in the bacterial genome), highlight a need for a refinement or revision of current molecular methodologies.

2.5 *Campylobacter spp.* contamination of poultry products

Given the mandatory monitoring of *Campylobacter*, bacterial contamination of the chicken carcass during processing is relatively well characterised. Other than systemic infection of a bird due to stressors such as ill health, thinning, or prolonged confinement, *Campylobacter* contamination of chicken flesh is a consequence of GIT microflora spillage during processing of broiler birds (Berrang et al., 2001; Rosenquist et al., 2006; V. Allen et al., 2007). High levels of bacterial contamination are shown to

occur during mechanical evisceration, in waterborne contamination during scalding tank feather loosening; and in aerosol diffusion during de-feathering. The extent to which the bacteria are able to colonise and persist in the processing plant environment is highlighted by *Campylobacter spp.* present on portioned chicken meat at higher numbers than on the whole bird carcass (Corry and Atabay, 2001). As in determining environmental distribution, challenges inherent to detection of non-culturable and biofilm bacteria represent an obstacle in the characterisation of bacterial distribution in the poultry processing environment and, by extension the implementation of effective surveillance-based biosecurity measures.

2.5.1 Vertical transmission of *Campylobacter*

Eradication of *Campylobacter spp.* from the GIT microbiota of broiler birds is considered the most practical approach to reducing the incidence of human campylobacteriosis. Accordingly, the transmission mechanisms leading to the initial bacterial colonisation of broiler birds must be identified, and strategies implemented for their elimination. Vertical transmission, where *Campylobacter* populations present in the brood bird pass infection on to the egg, represents the most obvious vector for flock colonisation and PCR analysis indicates the presence of *Campylobacter spp.* DNA in the GIT of developing broiler bird embryos and hatchling chicks (K. Hiett et al., 2013; Marin et al., 2015). However, the detection of *Campylobacter* DNA does not necessarily signify the presence of viable bacterial, and culture-based analysis shows hatchling birds *Campylobacter spp.* free with no detectable colonisation until 2 to 3 weeks of age (Shoaf-Sweeney et al., 2008; Sahin et al., 2001).

Interestingly, bacterial associations with the eggs of fish are shown to influence embryonic development, with the host regulating the recruitment of specific bacterial species (Wilkins et al., 2016; Wilkins et al., 2015). Accordingly, co-development of the bird embryo and GIT microbiome in avian hosts may confer a specific advantage. Chicken eggs are shown to contain polyclonal antibodies that provide defence against vertical transmission of *Salmonella enteritidis* (Herrera et al., 2013), and suggest an innate immune protection against systemic bacterial infection.

Genomic analysis of DNA from the chicken embryo GIT may advance current understating of chicken commensal microbiota formation, But the evidence to date neither confirms the presence of viable bacteria, nor proves the colonisation of broiler birds by vertical transmission.

2.5.2 Horizontal bacterial transmission

Irrespective of vertical *Campylobacter spp.* transmission, broiler houses provide an ideal environment for faecal-oral bacterial carriage between birds, and an entire flock may be colonised within a few days from first infection (Mifflin et al., 2001). Culture-based detection of *Campylobacter* colonisation in hatchling flocks usually tests positive from 2 to 3 weeks and may reflect a protection afforded by maternal antibodies during development of the chick immune system. Colonisation of the entire flock usually occurs within a further 24 to 48 hours. Site surveys using RT-PCR have identified on-farm sites suited to 'early warning' *Campylobacter spp.* reservoirs and vectors specific to flock rearing houses and the external farm environment (Battersby et al., 2016c; Agunos et al., 2014). Accordingly, biosecurity measures such as segregation of specific areas and practices during rearing and processing are proposed to lower the incidence or extent of broiler flock colonisation. In turn, a reduction of *Campylobacter spp.* contamination in chilled chicken products during processing (Smith et al., 2016; Battersby et al., 2016a; Dale et al., 2015) would translate to a lower incidence of human campylobacteriosis.

2.5.3 Prevention of bird and flock colonisation

Implementing such measures has resulted in a reduction in the proportion of retail chilled chicken produce carrying the highest levels of *Campylobacter spp.* contamination, but achieving further reduction remains a significant challenge (FSA, 2015). Consequently, a number of approaches aimed at preventing colonisation by horizontal transmission are currently under consideration. The vaccination of broiler flocks has been widely considered, but the identification of novel, non-cross reactive antigen targets that reliably generate a rapid and potent immune response remains a significant challenge (de Zoete et al., 2007; Meunier et al., 2016).

By way of an alternative, passive immunisation of laying hens with whole cell lysate and hydrophobic protein fraction of *C. jejuni* is demonstrated to significantly reduce both bacterial colonisation and bird-to-bird transmission (Hermans et al., 2014). Mucosal exclusion measures are also demonstrated to produce a significant decrease in relative *Salmonella enteritidis* and *Campylobacter spp.* populations in commensal microbiota (Stern et al., 2001; Schneitz and Hakkinen, 2016).

The reduction of GIT *Campylobacter* in broiler birds is proposed as the most effective way to lower contamination in poultry produce during processing. The manipulation of commensal populations may represent a cost-effective means to reduce campylobacteriosis incidence. However, as in the manipulation of any multi-factorial system, any action to reduce or eliminate *Campylobacter spp.* must maintain the balance of the remaining microbial population and prevent the dominance of an, as-yet, uncharacterised bacterial pathogen.

2.6 Waterborne *Campylobacter spp.*

As discussed, a focus on foodborne carriage of *Campylobacter spp.* as the primary route for campylobacteriosis may reflect a research bias stemming from the use of detection techniques with specificity for bacteria of an 'enteric' conformation. Conversely, the utilisation of DNA sequencing, relatively cost effective and ideally suited to the characterisation of waterborne microbial population dynamics, is limited by a dependence on expensive laboratory-based processes. Given its capacity to provide a relatively stable environment in terms of temperature, pH, and dissolved gases it seems short-sighted to discount a potential role for water as a reservoir and transmission medium. It is appropriate therefore to review the published literature relating to waterborne bacterial carriage and to *Campylobacter spp.* in particular.

Detection of *Campylobacter spp.* in surface water (Battersby et al., 2016c; Agunos et al., 2014), rivers, estuarine and coastal waters (Khan et al., 2014; Pitkänen, 2013b; Vereen et al., 2013; Keener et al., 2004), suggests the existence of a bacterial reservoir complementary to that of commensal microbiota in animals. As mentioned, outbreak data indicates that such bacterial conformations retain both colonisation potential and virulence. Furthermore, many *Campylobacters* isolated from

environmental samples are indistinguishable from human pathogenic serotypes (Bolton et al., 1987; Devane et al., 2005).

Such bacterial distribution indicates a cyclic element to human campylobacteriosis similar to transmission by the faecal-oral route in broiler flocks, and a possible human infection vector by way of contaminated potable water supplies (Koenraad et al., 1997). Given that the protocols and media validated for mandatory pathogen surveillance lack the capacity to detect planktonic VBNC *Campylobacter*, it is not possible to discount potable or recycled agricultural water supplies as a vector for sporadic human campylobacteriosis and the colonisation of poultry flocks.

2.6.1 *Campylobacter* circulation in wastewater treatment

Interestingly, the incidence of *Campylobacter spp.* infection in Scandinavian broiler flocks appears to support a cyclic carriage of bacterial pathogens in wastewater treatment. Sweden particularly demonstrates a low level of colonisation, with the routine delivery of *Campylobacter*-free flocks for processing (Hansson et al., 2010). Geographical separation of farms, climatic conditions, and predominance of modern facilities are all proposed as possible mitigating factors accounting for this disparity with UK farms where broiler flock infection is endemic (Newell and Fearnley, 2003). However, significant differences in waste-water treatment are largely overlooked, with Sweden applying among the most far-reaching standards in the world, particularly in the antimicrobial treatment of residual sludge (Sweden-EPA, 2006).

Conversely, residual solid waste from sewage plants that treat domestic and urban wastewater in the UK is untreated, and supports a plethora of pathogenic bacteria that are subsequently spread on set-aside agricultural land (Bondarczuk et al., 2016; Q. Chen et al., 2016). The dissemination of *Campylobacter* and other bacterial species has potential to contaminate downstream rivers, estuarine and coastal waters by of surface water, flooding, and run-off. With insects, wild animals and agricultural livestock acting as additional transmission vectors, the scope for bacterial dissemination is potentially unlimited, and may have significant implications for the exchange of virulence and antibiotic resistance gene cassettes (Stiborova et al., 2015; Rahube et al., 2014) in soil or multispecies aquatic biofilms.

2.6.2 Seasonal variation in campylobacteriosis

Interestingly, both the levels of broiler chicken flock colonisation by *Campylobacter*, and the incidence of human campylobacteriosis are seen to increase in late spring each year. Coinciding with an increase in ambient temperatures and longer daylight hours, this increase in *Campylobacter spp.* related food poisoning is suggested to relate to beginning of barbeque season (Meldrum et al., 2005a). However, the observed peak in human campylobacteriosis occurs before the associated increase in bacterial colonisation of housed broiler chickens and suggesting a factor common to both infection pathologies rather than a transmission from chilled chicken products to humans (Meldrum et al., 2005b; Patrick et al., 2004). In addition, *Campylobacter* host colonisation demonstrates a geographical variability, peaking during week 22 in Wales, week 26 in Scotland and week 32 in Denmark, with human behaviour, bacterial prevalence, or both suggested as possible explanations (Nylen et al., 2002). As a common transmission vector, the case for water is clearly stated above, and the geographic data can be interpreted to fit with this hypothesis. At a lower Latitude, the temperatures in Welsh water reservoirs are likely to increase before similar reservoirs in Scotland. While Denmark is at roughly the same latitude as Scotland, factors such as the North Atlantic Oscillation and land mass effect may account for slower temperature rise in spring in Denmark (D'Odorico et al., 2002).

Of course, correlation does not constitute causation. But it is equally unrealistic to discount waterborne *Campylobacter spp.* carriage, or a scenario of aquatic multi-species biofilm persistence where bacterial dissociation is triggered by increasing spring temperatures. The published literature leaves no doubt as to the capacity of *Campylobacter* and other pathogenic bacterial species to persist in aquatic environments and to utilise water in the colonisation of host animals.

In the context of mitigating transmission of pathogenicity or resistomes such as antibiotic resistance, characterisation of bacterial reservoirs, interactions, and dissemination vectors may be fundamental to future public health. Doing so is dependent on an informed interpretation of the available data, and the development and utilisation of analytical tools with specificity and detection capabilities equal to

the task. To view campylobacteriosis only in the context of transmission from the poultry industry may be to overlook elements that could be key to reducing the impact on consumer health. The pathology of campylobacteriosis warrants discussion from this perspective.

2.7 Campylobacteriosis

An estimated 9 million cases of campylobacteriosis are thought to occur across the EU every year, with an associated cost to the economy of 2.4 billion euros. In the UK, around 210,000 cases are reported annually, but the great majority, the self-resolving cases, are thought to go unrecorded. From 1981 to 2012, UK Food Safety Authority (FSA) clinical surveillance records show an increase in *Campylobacter spp.* infection cases from 10,000 to 72,000. Evaluating the significance of this increase in incidence must consider the optimisation and dissemination of detection techniques and an increased level of clinical awareness over the same period. An annual cost to UK productivity estimated by the FSA at around £900 million ensures a continued focus on strategies to reduce incidence of human campylobacteriosis (FSA, 2015).

2.7.1 Epidemiology

Campylobacter spp. may be transmitted through raw milk, bottled water, and salad vegetables (Evans et al., 2003), but between 50% and 80% of campylobacteriosis is attributed to chicken produce (FSA, 2015). *Campylobacter* related enterocolitis is associated with the consumption of undercooked chicken or of ready-to-eat foods that have been in contact with raw chicken, directly or through shared utensils and work surfaces. The condition is normally non-communicable, and incidence is usually sporadic. Outbreak type campylobacteriosis may occur through the infection of multiple individuals from a single point source, and the epidemiology of chronicled outbreaks indicate significant bacterial reservoirs in untreated water (E. V. Taylor et al., 2013a; Whiley et al., 2013; Pitkänen, 2013b).

2.7.2 Infection Pathology

The biomolecular mechanisms employed by *Campylobacter* in eukaryotic cell invasion are relatively well characterised (Elmi et al., 2015; Lugert et al., 2015; Le et

al., 2012). However, the largely asymptomatic colonisation of animal hosts by *Campylobacter spp.* suggests an extracellular colonisation of the GIT when the bacteria is part of the commensal microbiota. While host cell invasion and epithelial inflammation is observed in campylobacteriosis, it may equally represent a survival or opportunistic response to combinations of environmental cues from host upregulated stress hormones or impaired immune function. In broiler chickens, *Campylobacter* establish asymptotically in the gastrointestinal tract, but again the processes underlying colonisation are not clearly understood (Hermans et al., 2012).

Electron microscopy identifies *Campylobacter* localisation in the ceca, large intestine and the cloaca of the birds, and colonisation of the mucus lining in numbers of the order $\log 10^7$ to $\log 10^9$, but without attachment to crypt microvilli (Beery et al., 1988). *Campylobacter spp.* exhibit a chemotactic response to mucin, and, as in biofilm formation, flagellar motility appears essential to successful colonisation of the gastrointestinal tract (Lertsethtakarn et al., 2011). Equally, sustained flagellar motility is likely to be critical to the sustained occupation of this niche. Isogenic *Campylobacter* strains are shown to exhibit variable and unpredictable population structures *in vivo*, which suggests that hypervariable gene expression may play a role in niche colonisation. Similarly, factors such as founder effect (the genetic influence of the founding bacterial population), are thought to play a fundamental role in the subsequent organisation of commensal bacterial populations (Coward et al., 2008).

2.7.3 Cell surface structure, and immuno-modulation

Comparative genomic analysis of *C. jejuni* shows hypervariable homo-polymeric repeat sequences within genes coding for the synthesis and modification of surface and flagellar proteins (Parkhill et al., 2000); potentially facilitating a complex modification of the bacterial S layer through the recombination of a relatively small number of gene sequences. Relatively uncommon in Gram-negative bacteria, *Campylobacter spp.* employ both N-linked and O-linked glycosylation in post-translational protein modification, with biosynthetic precursors and respective molecular pathways similar to those found in eukaryotic cells (Szymanski et al., 2003; Linton et al., 2005).

Patterns of cell surface protein glycosylation are shown to be specific to distinct bacterial strain isotypes, and modification of the related gene sequences is shown to influence host colonisation and biofilm formation capability (Howard et al., 2009). Similarly, post-translational modification of flagellar proteins and S-layer lipooligosaccharide (LOS) are thought to influence immunogenicity, host cell specificity and colonisation, and intracellular survival (Naito et al., 2010; Takeuchi et al., 2003).

Sharing similarities with the splicing basis of the adaptive immune system, the generation of surface structure variation through genetic recombination represents an effective basis for tolerogenic host colonisation. The host immune system then effectively selects the least immunogenic bacterial isotype for proliferation and colonisation. The shed bacteria infect further members of the flock through by faecal-oral (or faecal-wastewater-oral) route and are likely to be good immunological 'fit' for the colonisation of genetically and physiologically similar host animals.

2.7.4 Symptoms and sequelae

Campylobacter has been recognised as a major cause of bacterial enterocolitis since the mid-1980s (Butzler, 2004; FSA, 2015), with the great majority of campylobacteriosis attributed to *Campylobacter jejuni* and *C. coli* (Kamei et al., 2014). Today, an increasing number of *campylobacter* species are considered to represent emerging human pathogens (Bojanić et al., 2016b; Bullman et al., 2013). Less than 500 bacterial cells is enough to cause the illness, with an incubation period of 1 to 7 days post-infection followed by typical enterocolitis symptoms of fever, abdominal cramps and diarrhoea (Schielke et al., 2014a).

Campylobacteriosis is generally self-limiting, but where symptoms do recur the antibiotics, erythromycin and ciprofloxacin are shown to be most effective, although strains resistant to both are beginning to emerge (Jeon and Zhang, 2009). The communication of non-systemic infection between individuals is rare, and usually results from poor hygiene (Olsen et al., 2001). In around 1 case per 100, campylobacteriosis is considered a factor in the development of reactive arthritis (Ajene et al., 2013) and in approximately 1 case in 1000, is associated with the development of Guillain-Barré Syndrome (GBS) (Nachamkin et al., 1998). A form of

autoimmune polyneuropathy, GBS targets the peripheral nervous system and can lead to respiratory failure and death if untreated.

2.7.5 Guillain-Barré Syndrome (GBS) and *Campylobacter* spp. hypervariability

Reflecting the serious nature of the condition, the progression of *Campylobacter* spp. infection is best characterised for *C. jejuni* associated GBS. In a typical case of campylobacteriosis, the immune response prompts proliferation of antibodies specific to specific bacterial cell surface proteins. In GBS however, the antibodies raised against *C. jejuni* cell-surface glycoproteins are cross reactive with the structure of ganglioside glycoproteins in the peripheral nervous system.

In driving localised inflammation, the adaptive immune response enables permeation of the blood-nerve barrier by opsonising antibodies, and the subsequent recruitment of macrophages. The resulting immune cascade targets the ganglioside structure and a de-myelination, or loss of nerve-fibre insulation properties, causes a progressive loss of signalling integrity in the peripheral nervous system (Malik et al., 2014).

The molecular similarity of *C. jejuni* lipo-oligosaccharide and human ganglioside GM1 is acknowledged as the epitope progenitor of auto-antibodies in both GBS and Fisher syndrome (a variant of GBS) (Yuki and Hartung, 2012). Furthermore, a polymorphism in the *C. jejuni* gene coding for sialyltransferase (a transferase that adds sialic acid to the n-linked or O-linked sugar chains of glycoproteins) is key in determining which form of the disease the patient develops. Specific genetic polymorphisms, and presentation of their corresponding lipo-oligosaccharide cell-surface structural elements, may correlate with the development of GBS from campylobacteriosis in the first instance.

A case in point is an outbreak of GBS linked to an outbreak of campylobacteriosis originating in San Luis Rio Colorado, Sonora, Mexico in 2010. The observed frequency of GBS incidence was 13 to 26 times higher than the expected background level, and was considered indicative of a large, but otherwise unreported outbreak of campylobacteriosis (Jackson et al., 2014). Subsequent investigation linked the outbreak to a faulty water disinfection plant. In the absence of data relating the

extent of bacterial enteritis, the increased incidence of GBS relative to background may correlate with a contamination event by a *Campylobacter* population that includes isotypes with patterns of cell surface protein glycosylation with a high level of homology with human ganglioside glycoproteins.

GBS does not result in a percentage of all campylobacteriosis cases, nor does it disproportionately affect a specific group of genetically related individuals. Accordingly, the corresponding immune response may be particular to bacterial cell-surface protein expression characteristics rather than a predisposition specific to the host. Should this be the case, strain or isotype specificity is also likely to correlate with campylobacteriosis associated reactive arthritis.

2.8 In summary

The characterisation of *Campylobacter spp.* presented above is predominantly drawn from validated, culture-based data generated in public health pathogen surveillance and by these same methods applied in a research context. This representation is complimented by an increasingly in-depth categorisation of the *Campylobacter* genus through development of successive molecular analytical techniques to the accepted convention of microbial classification according to conserved sequences within genes coding for the 16s/23s ribosomal subunit.

However, in the evaluation of data generated by contemporary analytical techniques, the limits of detection, identification, and enumeration can easily be overlooked. In understanding microbial species population dynamics, environmental distribution, and interactions therefore, it is essential the microbiologist consider those limitations inherent to any analytical technique applied. The great majority of current biosensor technologies utilise the same molecular interactions as contemporary analytical tools. Accordingly, the mechanisms underlying techniques such as enzyme-linked immunosorbent assays (ELISA), API® strips, and polymerase chain reaction (PCR) are discussed in chapter 3.

Chapter 3

Contemporary molecular techniques for the detection of pathogens

This chapter considers the contemporary molecular microbiology assays routinely applied to the confirmatory identification of microbial species. As analytical tools, the advantages and disadvantages of ELISA, PCR, and enzymatic substrate-based assays are evaluated, in the context of the validation challenges that relegate these techniques to a predominantly confirmatory analytical role.

3.1 Molecular microbiology tools as first-generation biosensors

Molecular biology techniques such as ELISA, PCR, and enzymatic substrate-based assays are routinely applied to confirmatory identification of target organisms as an adjunct to validated culture-based assays. While those challenges inherent to the validation of such methodologies and their transfer between laboratories prevent their application as a primary analytical tool, the biomolecular interactions that underpin these assays are equally suited to use in electrochemical biosensors. Accordingly, the principles behind these techniques warrant consideration.

3.2 Enzyme-linked immunosorbent assay (ELISA)

An ELISA assay for the detection of a specific microbe usually consists of a polystyrene 96 well plate with an antibody specific to the target organism bound to the well surface. Once incubated, any target epitopes – such as bacterial flagella or surface proteins are bound by the antibody while the remainder is rinsed away. To visualize and quantify this interaction, a secondary antibody with a conjugated fluorophore and with specificity to the primary antibody is introduced. When excited using a fluorescence spectrophotometer, the fluorescence measured from the conjugated fluorophore relates directly to the concentration of the target molecule, which can be calculated from a reference standard curve.

ELISA analysis can be challenging from several perspectives. Foremost, the standard is likely to be arbitrary and equate to a known concentration of antibody target, but not necessarily translate to a specific number of organisms. Secondly, as with all antibody-based assays, ELISA tests are highly sensitive to the composition and pH of

the sample matrix. Accordingly, comparison with the standard may not be like-for-like for even slight differences in sample matrices. While these factors effectively prevent method validation, accuracy in ELISA analysis is primarily limited by incomplete distribution of the target molecule within the sample matrix and variability in colourmetric detection as a result of absorbance by the 96 well polystyrene microtiter plate (Hayashi et al., 2004).

A secondary consideration in evaluating the precision of ELISA data is that of microplate spectrophotometer plate reader resolution. Plate readers typically employ 8-bit or 16-bit resolution, although claimed 16-bit resolution can also relate to mathematical interpolation of an 8-bit signal. An 8-bit digital signal therefore relates to the detection of 256 fluorescence levels in the determination of analyte concentration (Krakiwsky et al., 2004; Schulze et al., 2000). Experimental design and can limit analytical error and optimise statistical reliability, and plate layouts typically include standard curves and target samples in triplicate as shown in figure 3.1.

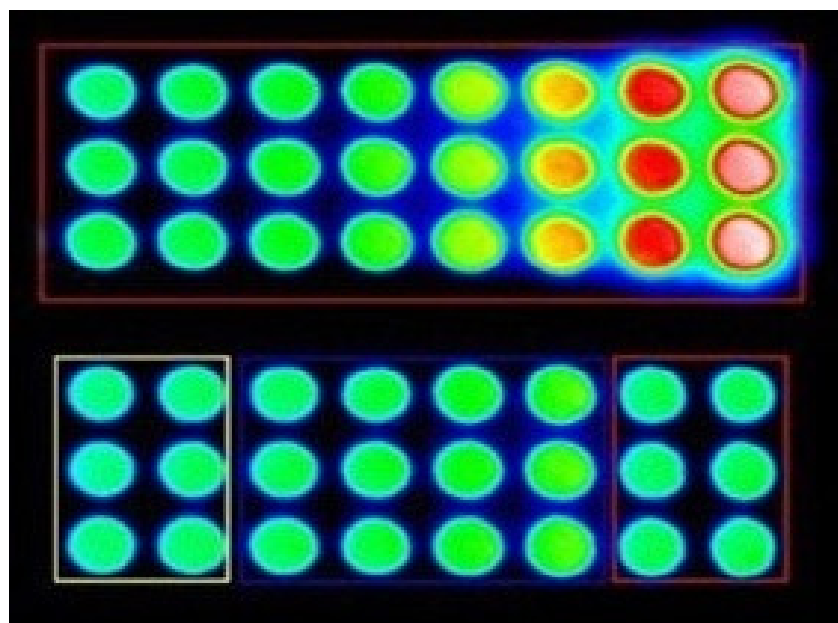


Figure 3.1. Detailing the fluorescence visualisation of reference standard (top, increasing in concentration left to right) and sample inoculations plated in triplicate.

In the great majority of analysis, such intrinsic limitations are insufficient to justify the expense of high-resolution microplate readers. However, exchange the typical 96 well plate for a conducting 96 electrode array and measure the fluorophore signal as a change in current resulting from carbon quenching of the fluorescence, and it becomes a biosensor. Antibody/target binding interactions are now quantified as an analogue electronic signal, and the calculation of detection limits, linear range, and signal resolution is no longer limited by the fluorescence resolution detection range. Accordingly, optimising the detection range prior to processing can greatly increase analytical precision even with an 8-bit analogue to digital converter processor input.

Furthermore, modify the electrode surface with a highly conductive polymer or carbon nano-material, incorporating a high signal to noise ratio, and the detection capabilities are enhanced further. Of course, antibody-based biosensor systems share the same drawbacks of ELISA - sensitivity to sample matrix composition, the influence of sample pH on antibody activity, and arbitrary standard quantification. Equally, method validation and the comparison of results from different labs and even different operators can represent a significant challenge in the absence of well-considered, robust experimental design.

Nonetheless, the progression from ELISA to antibody binding-based biosensors is clear and, other than the transition to electronic reporting techniques, for all intents and purposes, ELISA could be accurately described as a first-generation biosensor. Among molecular analytical assays used to microbiology, ELISA is one of a number of analytical models adopted as detection model in contemporary biosensor systems.

3.3 API®-bioMerieux

API® Campy (API®-bioMerieux SA, Marcy l'Etoile, France), consists of 11 enzymatic substrate tests, 6 assimilation assays, and 3 susceptibility tests, and has been a mainstay of confirmatory *Campylobacter spp.* identification for over 20 years (Gharst et al., 2013; Orenge et al., 2009). Comprehensively characterised in the published literature (Orenge et al., 2009), API® bacterial identification combines principles from chromogenic culture media plates, as shown in figure 3.2, and standard enzymatic substrates tests to identify bacteria according to their metabolic capacity.

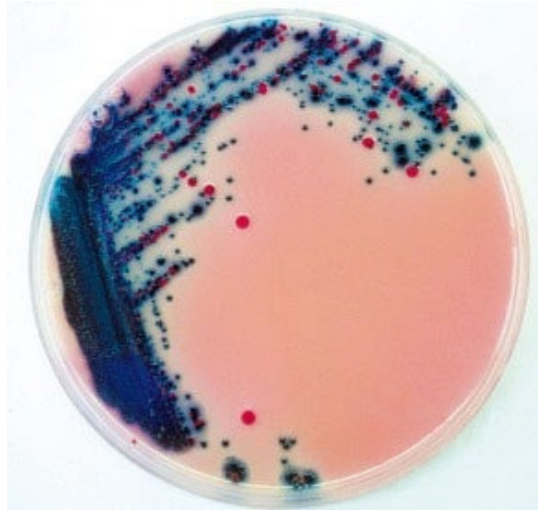


Figure 3.2. Chromogenic medium for Coli differentiation. The bacterial colonies are coloured according to the cleavage of chromogenic substrates. Bacterial production of the enzyme galactosidase (produced by coliforms) results in pink cultures, while glucuronidase production (*E. coli*) cleaves the second substrate and generates teal cultures. Pink and teal gives purple.

Using colour changing reagents to generate simple, unequivocal results as shown in figure 3.3, API® is ideally suited to the automated screening of large sample numbers or analysis by personnel with a non-microbiology background.



Figure 3.3. Typical API® strip, using colorimetric and binary test results to identify microbial species based on largely on their metabolic capacity. The colour indicator system makes API® strips ideal for high throughput automatic analysis.

The major drawback to enzymatic substrate-based identification of microbial target is the analysis timescale. With a combination of bacterial monoculture preparation and then the incubation duration for the enzymatic tests, a positive identification with a high degree of confidence can easily take 96 hours or more (as in the ISO guidelines outlined in section 2.3). Obviously, such long incubation timescales are not suited to biosensor applications. However, electronic detection of glucose concentration is the basis of the most well-known contemporary biosensor – the blood-glucose meter for management of diabetes. Many of these biosensors utilise a microbially derived glucose oxidase enzyme to metabolise the glucose present in a patient blood sample. The enzymatic activity includes an electron flow through the sensor which is measured electronically. This signal corresponds to the level of glucose present in the sample and can be empirically determined through comparison with a signal-glucose concentration reference curve.

Unfortunately, while the principle of enzymatic substrates applied in the API® strip may be applicable to biosensor electronic enumeration, the timescales and necessary incubation conditions involved render it less appealing than near-real-time techniques. Such biosensor arrays may have applications in laboratory based microbial population dynamics, or potentially in the study of DNA exchange in bacterial biofilms, but they have yet to gain traction in microbiology research. On the other hand, as more bacterial species with the capacity to metabolise environmental pollutants are identified, the identification of heavy metal or agrichemical specific metabolic pathways may have potential applications as biosensor recognition elements.

3.4 Polymerase chain reaction (PCR)

Based on the identification of microbial cells by amplification of DNA sequences specific to the target organism, PCR detection of microbial species can be considered comparable, or superior, to enumeration by culture-based techniques (Garcia et al., 2013). As the classification of archaea, bacteria, and fungal species is based on the comparative analysis of highly specific and conserved sequences in the microbial genome, a vast data resource exists to facilitate the identification of sequences specific to a given species, sub-species or strain (Fox et al., 1977; Woese and Fox,

1977). With a vast data resource relating to the sequencing of 16s and 32s ribosomal subunits as a result of such microbial phylogeny, these sequences are commonly used in PCR microbial detection.

PCR is the cyclic copying of a section of DNA and involves a pair of oligonucleotide primers, usually around 25 base-pairs in length, which bind to sequences flanking the gene or identifying sequence of interest. One primer will be specific to one of the DNA strands perhaps the sense strand, binding through complementary base pairing, while the second will be specific to the anti-sense strand. Primer sequences can be selected to amplify a DNA section from a specific target microbe, or to have less specificity, amplifying the 16s coding gene from all the microbial species present in the sample matrix. The exponential nature of PCR amplification is outlined in figure 3.4. When utilised to produce high concentrations of a target sequence for analysis, PCR multiplication can theoretically generate over one million copies from a single template in only 20 multiplication cycles.

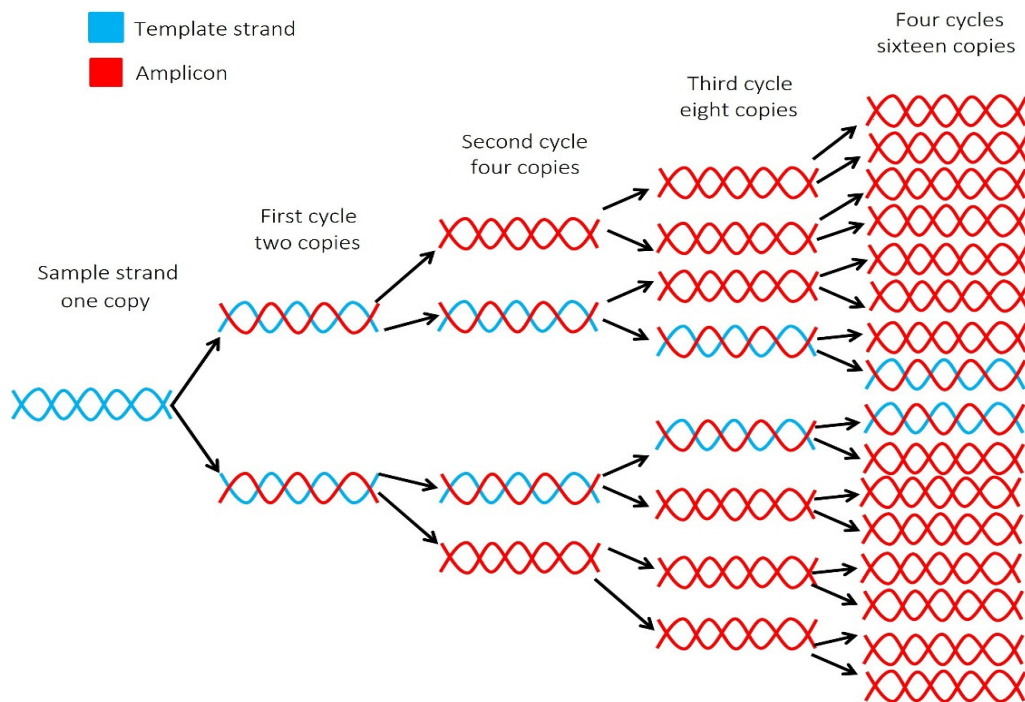


Figure 3.4. PCR multiplication is exponential in nature, following a temperature mediated cycle of DNA synthesis – raised temperature to separate the strands and lowered to allow the primers to bind, engage the DNA polymerase, and replicate the template strand.

Interestingly, the relative composition of microbial species isolated from agricultural watersheds is shown to be influenced by the methods employed. With particular combinations of technique and media resulting in significantly different yields for different species (Khan et al., 2009), the processes involved in preparing DNA samples for PCR warrant consideration.

Before PCR analysis can be carried out, the microbial DNA present in a given sample matrix must be extracted and purified. This may be achieved by ethanol precipitation, phenol-chloroform extraction, or mini-prep kit. Given their simplicity, efficiency, and reliability, mini-prep kits based on silica spin columns are by far the most popular means of sample preparation for PCR. The principles underlying spin column DNA extraction and purification are outlined in figure 3.5.

DNA preparation techniques can demonstrate a limited efficiency in terms of cell lysis efficiency and in nucleic acid recovery. Both lysis buffer-based and mechanical stress-based cell lysis techniques can show varying results according to the target organism membranous, cell wall, or encapsulation structure. While less critical to disruption of cells from a monoculture, inefficient cell lysis can influence the comparative characterisation of microbial populations in an environmental sample.

A further source of bias is found in the efficiency of the subsequent extraction and purification process itself, in terms of both the DNA recovery yield and in its purity – the proportion of associated protein. At times not fully compensated for, such factors can represent a significant source of bias in DNA amplification and can effectively prevent microbial enumeration. In PCR quantification of allergens, a control standard is processed with the sample through extraction and purification to provide a measure of efficiency in the sample preparation methodology.

DNA extraction, purification, hybridisation, and amplification will all have a bearing on the performance of the proposed biosensor platform. However, the principal shortcoming of PCR analysis of microbial populations is the inability to differentiate between DNA sequences from viable cells and those from disrupted, dead cells, or from exogenous DNA expression in biofilm formation.

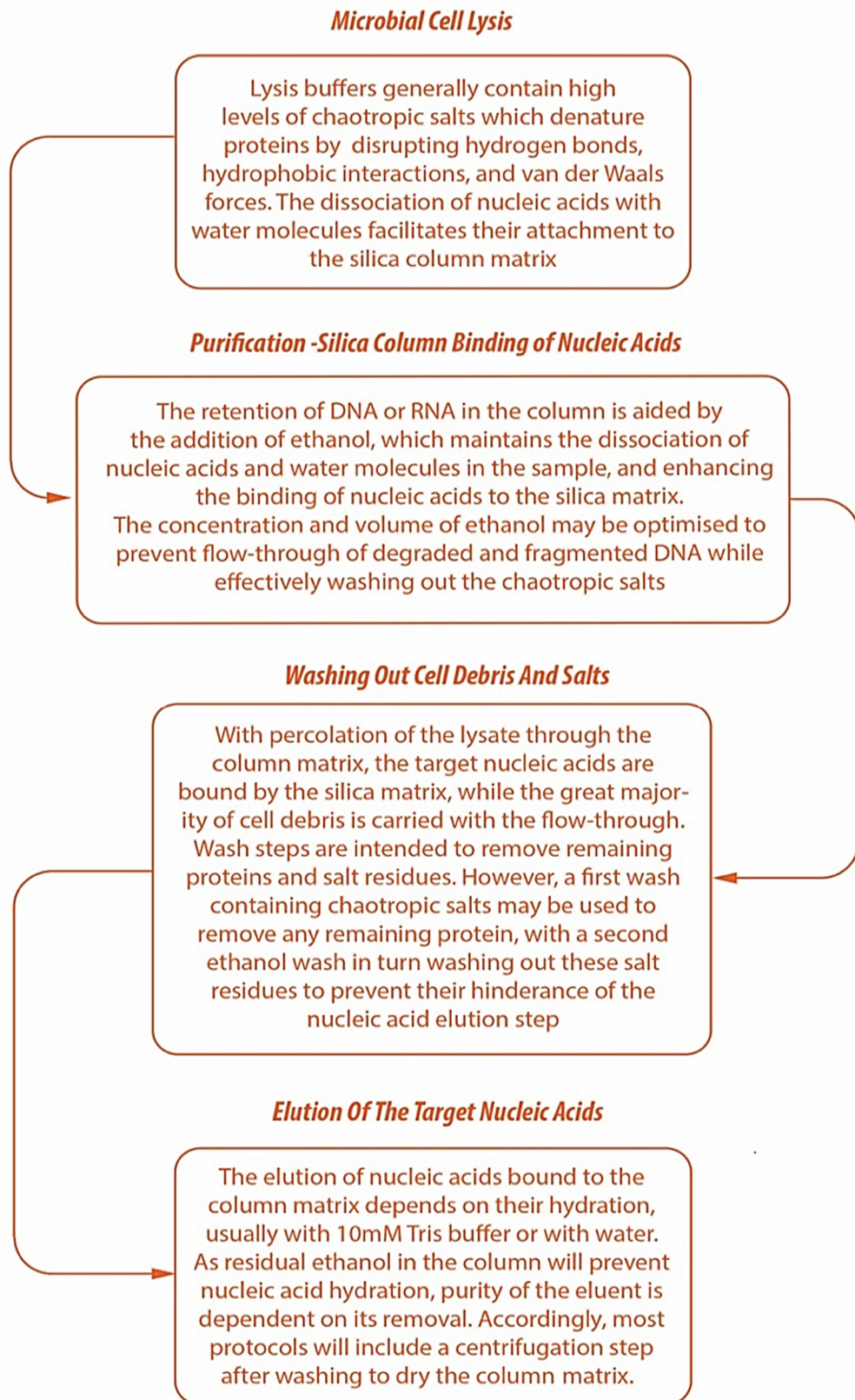


Figure 3.5. Typical mini-prep, or column-based DNA extraction and purification process based on chaotropic salts. DNA is adsorbed to the silica matrix allowing flow-through of cell debris. A low ionic strength buffer allows the DNA to disassociate and be eluted for analysis.

Accordingly, the analyst has no means to determine whether the sample includes viable virulent bacteria or disrupted cell contents. The binding of free DNA from compromised cells prior to the extraction process is proposed as a way to prevent such sequences being part of the analysis as is the co-amplification of mRNA sequences, which degrade quickly following cell lysis and are a reliable indicator of cell viability (Josefsen et al., 2010). While neither technique is routinely applied to confirmatory molecular analysis, both may have application in biosensor-based enumeration of viable microorganisms.

3.5 Data acquisition and sampling rate

In the published literature, the disadvantages of culture-based microbiology are broadly summarised as a necessity for long incubation periods, and a reliance on laboratory-based equipment and processes. Accordingly, significant effort has been applied to the development and validation of rapid molecular protocols for pathogen surveillance applications. However, there can be no doubt that the predominantly laboratory-based nature of microbiology represents an obstacle to the generation of data more quickly and in-the-field, there are fundamental differences between culture-based data and that generated by molecular techniques.

Essentially, culture-based data is dynamic in nature; dependent on viability of the target organism and subsequent proliferation or metabolism of indicator substrates over time. Conversely, molecular techniques such as PCR generate data relating to the presence of structural functional elements, independent of time; a snapshot providing no insight as to the viability or activity of the target. While mRNA characterisation can provide an insight into gene expression, but such analysis is challenging, and is yet to become routine.

Gathering the broadest gamut of data in the characterisation of microbial populations therefore, may depend on conventional and molecular microbiology applied in combination. To propose replacing one with the other does not represent a like-for-like exchange. Electrochemical biosensors certainly fall into the molecular analysis category, generating data of a 'snapshot' perspective, akin to PCR or ELISA. However, where biosensors may have an inherent advantage over contemporary

molecular techniques is in delivery of a near-real-time sampling rate; the capacity to combine multiple datasets to generate a high-resolution, dynamic perspective. Accordingly, biosensors may come to represent a microbiology toolset combining the best characteristics of culture and molecular-based analytical techniques but exceeding the detection capacity and resolution of both.

3.6 Biosensors

Figure 3.6 outlines the commonly accepted biosensor architecture, from the process of analyte driven signal generation, through amplification, to data processing and display; and largely made possible by developments in materials science and the superior electronic qualities of conducting polymers and carbon nanomaterials. Combining high conductivity with low background noise, the utilisation of these materials at the interface between the bioreceptor element makes it possible to quantify the electronic potential of biological interactions; enzymatic REDOX activity, antibody binding, or DNA hybridisation (Velusamy et al., 2009; A. Liu et al., 2017).

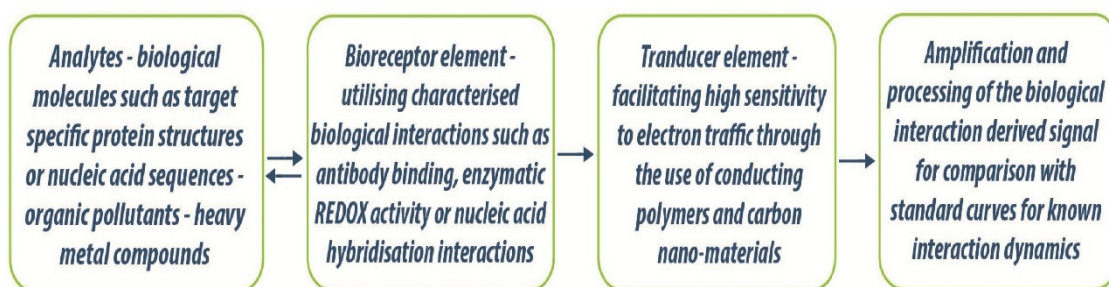


Figure 3.6. Outlining the typical biosensor system architecture and the processing of signals generated by analyte/bioreceptor interaction (Velusamy et al., 2010).

Given the focus of the presented research in the development of a biosensor platform, an insight into what a biosensor is may be overdue. The generally accepted definition of a biosensor is of ‘an analytical device, used for the detection of an analyte, which combines a biological component with a physiochemical detector. The receptor element is a biologically derived material or biomimetic component that interacts (binds or recognises) with the designated target analyte’. The most commonly utilised receptor elements are enzymes, antibodies or nucleic acid

sequences. As argued previously, by this rational, the molecular microbiology techniques previously discussed could be considered biosensor systems, albeit where the physiochemical measurement is one of target associated fluorescence (be it conjugated or intercalating fluorophore molecules).

The published literature outlines a range of biosensor models for the detection of microbial targets based on mass sensitive, optical, and electrochemical transducers, and utilising antibodies, receptor binding proteins, lectins, and immobilised DNA as bioreceptor components (X. Yang et al., 2013). However, many of the discussed techniques are complex and expensive, with limited scope for miniaturisation. Of the remainder, electrochemical biosensors based on conducting polymer or carbon-nanomaterial electrode modification demonstrate appropriate sensitivity, rapid analysis capability, and a potential for low cost miniaturisation (Thirumalraj et al., 2015; T. A. Silva et al., 2017; Lawal, 2016; Y. Lim et al., 2017).

Combining the advantages of electrochemical biosensors with the high specificity of DNA hybridisation interactions represents the logical selection in the design and construction of a biosensor system suited to the detection of food and waterborne pathogens (Liao et al., 2007) and to the characterisation of microbial populations in the environment. Interestingly, the published research outlines hybridisation-based electrochemical biosensors specific to a range of microbial pathogens with a variety of electrode modification materials and techniques.

However, given the universal nature of DNA hybridisation, development of such a biosensor platform in the context of a specific organism or base-pair sequence is to miss the point of DNA as a bioreceptor component. Using angling as an analogy, the biosensor system can be equated to the fishing rod with the lure a target specific DNA probe. The angler may change the lure depending on the type of fish he or she hopes to catch (Lawal, 2016), but the line, rod, and reel remain the same. In short, a DNA hybridisation biosensor can be used to detect any sequence, from any target, there is no difference between DNA from blue green algae or from a blue whale.

Much of the published research relating to DNA hybridisation biosensors is based in material science and electrochemistry, and there is a primary focus on the areas of electrode surface modification and electron transfer optimisation. Given their high sensitivity, low detection limits and rapid action, a great many such biosensor models are based on conducting polymers, carbon nano-materials, or functionalised hybrid compounds utilising precious metals, synthetic polymers, or polysaccharides.

The effectiveness of these biosensor models has been demonstrated in sensitive detection of hybridisation between immobilised DNA probes and sequences specific to a wide range of microorganisms, and in the detection of blood-borne viral targets (Uliana et al., 2014; Velusamy et al., 2009; Liao et al., 2007). With sensitivity superior to that of potentiometric methods, amperometric transduction is most commonly employed in the quantification of electron transfer through the immobilised bioreceptor molecules (Velusamy et al., 2010). The general model of the DNA biosensor presented in the published literature is outlined in figure 3.7 and is based on the hybridisation of synthetic single-stranded DNA (ssDNA) probes with ssDNA target oligonucleotides.

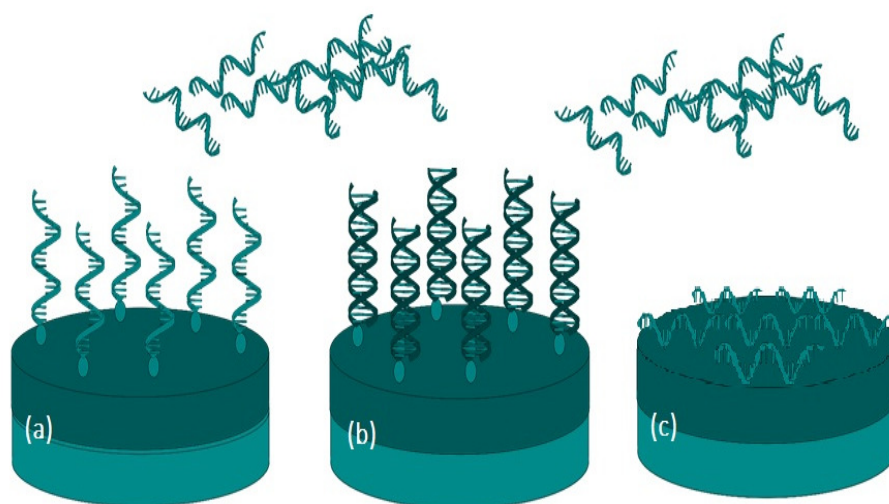


Figure 3.7. Depicts the typical electrochemical DNA hybridisation-based biosensor paradigm: Synthetic ssDNA probe oligonucleotides are immobilised on the modified electrode surface via the amino groups to linker molecules such as thiols, aldehydes, and epoxides, or through biotin-avidin binding (a) and hybridise with complementary ssDNA target sequences (b). Electrochemically Immobilised DNA strands are likely to lie flat on the sensor surface (c).

3.6.1 Biosensor sample DNA preparation

In the development of the proposed DNA biosensor platform therefore, the first consideration is that of sample preparation. Effective analytical performance of the biosensor receptor component will be dependent on delivery of a representative ssDNA sample in an electrolyte solution appropriate to electrochemical analysis. As discussed in the context of PCR, column based chaotropic salt/silica-based DNA extraction is most readily adapted to automated reagent introduction.

DNA within a microbial cell is maintained as a double stranded helix and may have additional quaternary and chromosomal structure in the nucleus of eukaryotic cells. Such double-stranded DNA (dsDNA) is not suited to electrochemical analysis but require denaturing of the tertiary, dsDNA conformation to facilitate the hybridisation of immobilised probe oligonucleotides with their complementary target sequences in the sample. The hybridisation of genomic DNA is fundamental to techniques such as PCR and microarray analysis and in both techniques probe oligonucleotides are able to access their complementary targets through temperature mediated strand separation (Nimse et al., 2014; Kargl et al., 2015; Meyer et al., 2014).

The development of PCR, micro-array and similar analytical techniques has resulted in a comprehensive definition of DNA melt characteristics based on nucleic acid thermodynamics. This accumulated data is equally applicable to the optimisation of temperature driven strand separation and annealing for biosensor probe/target hybridization. Temperature mediated DNA hybridization therefore, represents a comprehensively characterised means by which to direct strand separation, and to optimise the efficiency or duration of a biosensor pathogen detection assay according to analytical requirements.

3.6.2 Biosensor probe oligonucleotide immobilisation

Other than the resolution of the detector, the detection limits, selectivity, and analytical reproducibility of DNA hybridisation biosensors are largely determined by the concentration of probe DNA on the modified electrode surface (Wittmann and

Marquette, 2012). Because of the negative charge of the phosphate groups of the DNA molecule backbone, the upper limit of probe oligonucleotide concentration is effectively limited by the electrostatic repulsion and steric hindrance on the efficiency of DNA hybridisation (Ravan et al., 2014).

Below this optimal concentration non-target sample DNA can adsorb to the sensor surface and erroneously contributing to signal transduction. Blocking proteins are common to ELISA and microarray assays and have been shown effective in inhibiting non-specific binding in biosensors by preventing DNA access to the electrode surface. Nonetheless, uniform distribution of probe oligonucleotides on the modified electrode surface is likely to be fundamental to the optimisation of both hybridization efficiency and immobilisation homogeneity. To this end, techniques such as electromagnetic arrangement of oligonucleotides on the modified electrode surface (Rikken et al., 2014) may have potential in generating homogenous probe dispersal.

3.7 Biosensor platform design criteria

In the delivery of a field-portable, self-contained, simple to use biosensor platform, the research presented must consider four main areas as a starting point for the design and development stage.

3.7.1 DNA extraction

DNA extraction will depend on the design of an integrated sample introduction port, delivery system for multiple reagents, and facility to eliminate DNA residue or waste chemistry as required. The pump mechanism must be robust and provide a consistent laminar flow while not drawing a significant current from the on-board power supply.

3.7.2 DNA conformation

The sample DNA must either be delivered to the analytical cell as ssDNA, or the analytical cell must include a capacity for temperature mediated denaturation prior to or during probe-target DNA hybridisation.

3.7.3 Probe oligonucleotide immobilisation

The immobilisation technique will depend on the electrode modification methodologies used but must generate repeatable result with a high degree of statistical confidence. Non-specific adsorption must be prevented, and stability will be a key requirement.

3.7.4 Potentiostat

All electrochemical biomolecule immobilisation, analysis, and experimentation will be conducted using the desktop EmStat potentiostat (PalmSens, Netherlands) which facilitates linear sweep, differential pulse, and cyclic voltammetry over a voltage range $\pm 3V$ with a potential resolution of 0.1mV and a current range from 1nA to 10mA. All circuitry and operational parameters specific to the onboard electrochemical analysis component and associated microcontroller will be outlined and specified.

3.8 Summary

In reviewing the assays employed in the detection and identification of microbial pathogens, it becomes clear that the techniques used in the development of the great majority of electrochemical biosensors have a basis in contemporary molecular biology. Accordingly, the pros and cons of specific techniques are comprehensively characterised, and extensive data is available in relation to underlying interactions, specificities, and limitations. Chapter 4 outlines the methods and reagents used in development of the DNA extraction and purification component and the adaptation of DNA hybridisation-based techniques to electrochemical analysis.

Chapter 4

Experimental Procedures

4.1 Introduction

This chapter details the experimental reagents, equipment, and techniques used in evaluating the principles to be applied within the biosensor platform, and those employed to generate analytical control and reference data.

4.2 Materials

4.2.1 Analytical reagents

All analytical reagents were supplied through Sigma Aldrich UK.

APTES - (3-Aminopropyl)triethoxysilane (99%)

Graphene Oxide (10 mg/mL, dispersion in NMP)

Guanidine Hydrochloride (GuHCl) (6M)

Magnesium Chloride (MgCl₂)(anhydrous, ≥98%)

Methylene Blue (C₁₆H₁₈ClN³S) (concentrate according to Ehrlich)

PEDOT:PSS - poly(3,4-ethylenedioxythiophene) polystyrene sulfonate
(3.0-4.0% in H₂O, high conductivity)

Potassium Chloride (KCl) (BioXtra, ≥99.0%)

Sodium Acetate (>99%)

Sodium Chloride (NaCl) (BioXtra, ≥99.5%)

Sodium dodecyl sulfate (SDS) (≥99.0%)

Tris-(hydroxymethyl)-amino methane (Tris-HCl) (1M pH 6.5)

4.2.2 Bio-molecules

Campylobacter jejuni oligonucleotides (Integrated DNA Technologies, UK)

Probe – 5' GTG CCT AAT ACA TGC AAG TCG 3'

Target – 5' CGA CTT GCA TGT ATT AGG CAC 3'

Non-comp target 5' ATG GGA CAA GAT ACC GTC 3'

Campylobacter jejuni PCR primers (Thermo Fisher Scientific, UK)

Forward 5' GCA TAT ACA ATG AGA GGC AAT AC

Reverse 5' GCA GAG AAC AAT CCG AAC T

4.2.3 Solutions

Standard electrolyte - (Nitrogen purged), PBS pH 7.2

Activation buffer - PBS pH 5, 5% KCl

Immobilisation buffer – 20mM MgCl₂ 10mM Tris HCl pH 7.2

REDOX buffer – 2mM Methylene Blue in PBS pH 7.2

Silanisation buffer – 1% (3-Aminopropyl)triethoxysilane in ethanol

4.2.4 Consumables

Glassy carbon electrodes (GCE - 5mm diameter)– CH instruments, USA

Screen-printed carbon electrodes (SPCE - 3mm Diameter) Zensor, Taiwan

4.2.5 Apparatus and instrumentation

EmStat 3 (Palm Sens, Netherlands)

Nano-drop 2000 (Thermo Scientific, UK)

Roches 'Lightcycler' (Roche, UK)

4.2.6 Software

PS Trace V4 and V5 (Palm Sens, Netherlands)

Nano-drop 2000 (Thermo Scientific, UK)

Roche Lightcycler 96 (Roche, UK)

4.3 Culture based bacterial enumeration

4.3.1 Microscopy

The viability of *Campylobacter jejuni* ATCC 33291 cultures was determined using hanging drop light microscopy at 100x magnification, with comparison counts made by haemocytometer.

4.3.2 Selective media inoculation

A. C. jejuni culti-loop culture was activated as per Oxoid instructions and incubated in triptone soy broth (TSB) (Oxoid UK, CM0876) for 24 hours at 37°C. Gram staining, oxidase testing, and API®-Campy analysis (API®-biomerieux SA, marcy l'Etoile, France) served to validate aseptic technique and confirm the culture strain as *C. jejuni* ATCC

33291 prior to further inoculation and enumeration. Butzler (Oxoid UK, BR0052) and CCDA (Oxoid UK, SR0155) selective agar (Thermofisher, UK) were inoculated in duplicate with serial dilutions from 10^{-2} to 10^{-6} colony forming units per millilitre (cfu/ml).

4.3.3 Colony counting

Light box colony counts were made from those plates containing closest in number to 300 colonies, and starting concentrations calculated.

4.4 Nucleic acid extraction and purification

4.4.1 CONGEN spin filter kit

Congen Kit F1008 was used as per included guidelines to isolate *Campylobacter Spp.* DNA from inoculant cultures. 1000 μ l of the sample was placed in an Eppendorf tube and centrifuged for 5 minutes at 12,000 rpm to remove the bacterial cells from suspension. After pouring off the supernatant, 400 μ l of the Congen kit lysis buffer was mixed with the pelleted campylobacter cells and incubated at 99°C on an Eppendorf heated agitating plate for 10 minutes, denaturing cell membranes and releasing the bacterial genomic DNA. After a 1-minute centrifuge at 12,000rpm removed the larger cellular debris, the remaining lysate supernatant was pipetted onto a clear spin filter, again supplied with the Congen kit.

After a 1-minute incubation to allow the lysate to permeate, the spin filter was centrifuged for a further minute at 12,000rpm, separating the remaining large cellular debris from the bacterial DNA. The resulting filtrate was mixed with 200 μ l of Congen binding buffer and added to a Congen yellow spin filter. After a short incubation, the yellow filter and receiver tube were centrifuged, again for a minute at 12,000rpm, to spread the bound DNA through the filter media. On discarding this filtrate, any remaining debris associated with the filter-bound DNA was washed out using 550 μ l of wash buffer, and centrifuging at 12,000rpm for 1 minute.

This wash step was repeated, and on the second occasion, the filter was centrifuged for a further 2 minutes at 12,000rpm to remove any remaining wash buffer ethanol. In order to remove the bound DNA from the spin filter, 100µl of preheated elution buffer at 60°C was added to the filter. Allowed to incubate for 3 minutes, the filter was placed in a final receiver tube and centrifuged for 1 minute, releasing the bacterial DNA and culminating in 100ul DNA sample suited to PCR analysis.

4.4.2 Spectrophotometric DNA evaluation

Spectrophotometric DNA quantification and purity evaluation was carried out on the Nano-drop 2000, using the proprietary software. An absorbance analysis a 2µl sample was conducted over a wavelength range 220nm to 350nm.

4.5 Real-time polymerase chain reaction (RT-PCR)

All RT-PCR was carried out using the Roche LightCycler 96 with MIQE quantification calculation.

4.5.1 Sample formulation

The PCR plate was made up with 1µl of each primer, 13µl of Mastermix, and 5µl of purified *C. jejuni* DNA. The sample was serially diluted 1:2 in triplicate prior to inoculation with samples concentrations from 1:1 to 1:2048.

4.5.2 PCR cycle parameters

Table 4.1. Detailing the PCR parameters applied to C. Jejuni 16s amplification using the Roche LightCycler 96.

Initial denaturation	5 mins, 95°C
Cycles	40
Denaturation	15 secs, 95°C
Annealling/extension	30 secs, 65°C
Fluorescence	Sybr Green

4.6 Gel electrophoresis

The NuPage® SDS Page electrophoresis kit was used with the XCell Surelock mini-cell electrophoresis tank and lid (Invitrogen), and the Zoom® Dual Power unit (Invitrogen)

4.6.1 Sample buffer formulation

A sample loading buffer was formulated from the NuPage® kit using 25µl LDS buffer, 10µl 77.5 mg/ml DTT, and 65µl *C. jejuni* sample DNA.

4.6.2 Electrophoresis parameters

A running buffer was prepared from 50ml NuPage® MES made up to 1L with DD water. The preformed gel was loaded, buffer added, and the gel wells loaded with 15µl sample. Lane one was loaded with molecular weight marker (SeeBlue™ Pre-stained Standard, Invitrogen, USA). The Zoon® power unit was set for 200V, 350mA, 100W, and run for 35 minutes.

4.6.3 Visualisation

The completed gels were fixed with a 50ml solution of 50% methanol. 10% acetic acid for a minimum of 60 minutes. Each gel was rinsed with 3 x 50ml double distilled (DD) water and shaking for 5 minutes. The bands were visualised through incubation with 50ml Simply Blue stain for 3 hours. The gel was then washed in DD water on the shaker for a further 3 hours before imaging.

4.7 Electrochemical characterisation and analysis

All analytical electrochemistry was carried out using PS Trace, EmStat 3, and a three-electrode cell as described in Chapter 5.

4.7.1 Electrochemical cell

In order to make best use of the oligonucleotide stock available for analytical purposes, the three-electrode cell was modified to a volume of 1000µl based on a spectrophotometer cuvette and sealed for gas stability using paraffin wax seal. Figure 4.1 shows the cell and associated gas line and electrodes.



Figure 4.1. Cuvette based three-electrode cell using a standard reference and counter electrode with an SPCE and facilitating the analysis of 1000 μ l volumes representative of the biosensor platform analytical cell.

4.7.2 Working electrodes

4.7.2.1 Glassy carbon electrode (GCE) preparation

All analytical experiments based on the modification of a GCE were conducted using the same electrode. Prior to use the electrode surface was polished using alumina paste of 0.3 μ m, followed by 0.05 μ m grain. Once polished the electrode was cleaned by sonication in ethanol for 60 seconds, then in DD water for 60 seconds. Following oven drying at 40 $^{\circ}$ C, the GCE surface was inspected using a 10x eyeglass, and the process repeated if any indication of surface abrasion was detected.

4.7.2.2 Screen printed carbon electrode (SPCE) activation

SPCEs were activated electrochemically by chronoamperometry using a PBS buffer at pH 5 with 5% KCl. An activation voltage of 2V was maintained for 10 minutes.

4.7.2.3 Electrode modification by surface adsorption

Surface adsorption modification was through drop-coating – the simple dropping of the liquid modifying material from a pipette. The drop-coating volume was optimised

as described in chapter 6, and the electrode dried in nitrogen at room temperature or at 40°C depending on the modification material.

4.7.2.4 Electrode surface silanisation

Electrode surface were Silanised by immersion in a solution of 1% APTES in acetone for 5 minutes. The coated electrodes were dried at 120°C for 2 hours and stored with desiccant until ready for use.

4.7.3 Counter and reference electrodes

A platinum wire counter electrode and A silver/silver chloride (Ag/AgCl) reference electrode were used in all analytical electrochemistry over the course of the research.

4.7.4 Electrolytes

Standard electrolyte - (Nitrogen purged), PBS pH 7.2

Activation buffer - PBS pH 5, 5% KCl

Immobilisation buffer – 20mM MgCl₂ 10mM Tris HCl pH 7.2

REDOX buffer – 2mM Methylene Blue in PBS pH 7.2

4.7.5 Cyclic voltammetry

CV was generally conducted over a sweep of -1V to 1V, using a potential step of 0.001V and a scan rate of 0.1 V/S. The sweep range was selected as a range where the REDOX of dissolved oxygen, the indicator molecule methylene blue, and the nucleobases guanine and adenine were characterised for a both glassy carbon and screen-printed carbon electrodes.

4.7.6 Chronoamperometry

CA was used in electrode activation and DNA immobilisation, with a voltage of 2V, and 0.6V respectively and an interval of 0.1seconds over a duration of 600 seconds

4.7.7 Differential pulse voltammetry

DPV was used in the oxidation of monomeric nucleobases and in the oxidation of ssDNA in suspension. A range between 0 and 1.3V was used with a potential step of 0.01V, a potential pulse of 0.025V and a pulse duration of 0.1 seconds.

4.8 DNA immobilisation and hybridisation

4.8.1 DNA immobilisation by UV crosslinking

UV crosslinking of un-modified DNA was carried out according to the method described by Thomas Schuller (Schüler et al., 2009), with probe DNA spotted at 1 μ M concentrations in 8 μ l droplets. The slide surfaces were exposed to UV light at 254nm for 5 minutes and immersed in 0.5% SDS for 10 minute, 20 seconds in DD water, and dried under nitrogen.

4.8.2 DNA immobilisation by electrochemical adsorption

DNA immobilisation by electrochemical adsorption was conducted with a 20mM MgCl₂ 10mM Tris HCl pH 7.2, with the MgCl₂ acting to stabilise the DNA probes. A voltage of 0.6V, below the oxidation voltage of guanine – the most easily oxidised nucleobase – was applied using chronoamperometry over a period of 10 minutes. Loading concentrations between were built up in 1 μ g/ml increments to give an indication of optimal loading densities.

4.8.3 DNA hybridisation incubation

DNA hybridisation characterisation was carried out using the 1000 μ l three-electrode cell on a hotplate at 37°C. No voltage was applied, and an incubation period of 15 minutes was selected. No significant difference was noted for incubation periods over 10 minutes. However, a 15-minute incubation was retained through the experimental characterisation to maintain continuity and to ensure maximal method robustness.

4.9 Surface analysis

4.9.1 Scanning electron microscopy

All samples were gold sputter-coated in an argon, oxygen, and nitrogen atmosphere at a 0.3 Pa pressure. Scanning electron microscopy (SEM) was carried out using a Quanta FEG 650 Electron Microscope with backscatter electron diffraction detection (ThermoFisher, UK).

4.10 Statistical analysis

One-way analysis of variance (ANOVA) is used to determine whether the mean values of three or more groups are statistically different. ANOVA analysis uses F-tests to determine the variance between the mean of each group and are based on the ratio of mean squares. Accordingly, the generated F-value is a measure of the spread of selected sample data around the mean and is the result of the variation between the sample means divided by the variance within the sample groups. Accordingly, larger values correspond to a greater variation between the means of each group.

Statistical analysis of α SPCE stability, the effect of non-specific binding, and the significance of target binding with immobilised probe sequences was calculated using cyclic voltammetry current data generated for over MB peak oxidation range. A one-way ANOVA calculation was performed using SPSS (IBM, USA), with each sample group 'treatment' consisting of 201 current values generated by the voltage input range -0.2V to 0V.

Chapter 5

Design of the field portable analysis platform

This chapter outlines the development of each component within the field portable pathogen detection platform. As an integrated system, this platform is designed to interface with a smartphone app specific to the user's analytical requirements. Such applications might include pathogen surveillance in food production from 'farm-to-fork'; the characterisation of environmental microbial populations as a research tool; or as part of an automated monitoring network, relaying water quality data to a central hub through a Wi-Fi, GPRS, or GSM mobile communications network. At present, no such self-contained analytical platform is available.

5.1 Introduction

As discussed in the introductory section of this thesis, the primary drawback in the detection and identification of microbial species in both pathogen surveillance and research purposes is an almost total reliance on laboratory-based processes and equipment. Accordingly, the foremost consideration in design of the biosensor platform is that it should be field-portable and entirely self-contained with respect to reagents, power supply, and the disposal of all used chemistry. Given that the unit is proposed for use by non-scientific personnel in a production environment or by researchers in the field, the operation of the platform should be simple to use and totally automated in regard to sample preparation, analysis, and data presentation.

For the purposes of validation and auditing within a mandatory pathogen surveillance context, and to facilitate like-for-like laboratory-based analysis, an aliquot of the prepared sample will be subtracted from that to be analysed on-board and stored. All user-adjustable parameters and presentation of analytical data will be tabulated by a task-specific 'app' running on an Android-based smartphone and communicating wirelessly with the platform microprocessor.

In continuation of the research aims of the Velusamy research group, the analytical component of the biosensor platform is based on the electrochemical detection of DNA hybridisation. Electrochemical biosensors represent both a cost effective and

sensitive technique when applied to detection of microbial species. However, while the performance of DNA biosensors is well characterised in relation to synthetic oligonucleotides, it has yet to translate to a self-contained analytical platform. The primary challenge in the achievement of this aim is the development of a model applicable to the extraction and purification of DNA from microbial samples in a conformation suited to electrochemical hybridisation analysis.

5.2 Sample transport - mobile phase

Figure 5.1 outlines the sequence of steps necessary to prepare and analyse a microbial sample and, by extension, the processes which must be automated within the device. As a fundamental part of sample preparation, DNA extraction and purification in the laboratory typically involves significant input from the analyst and equipment such as pipettes, shaker plates, and centrifuge (Section 4.4).

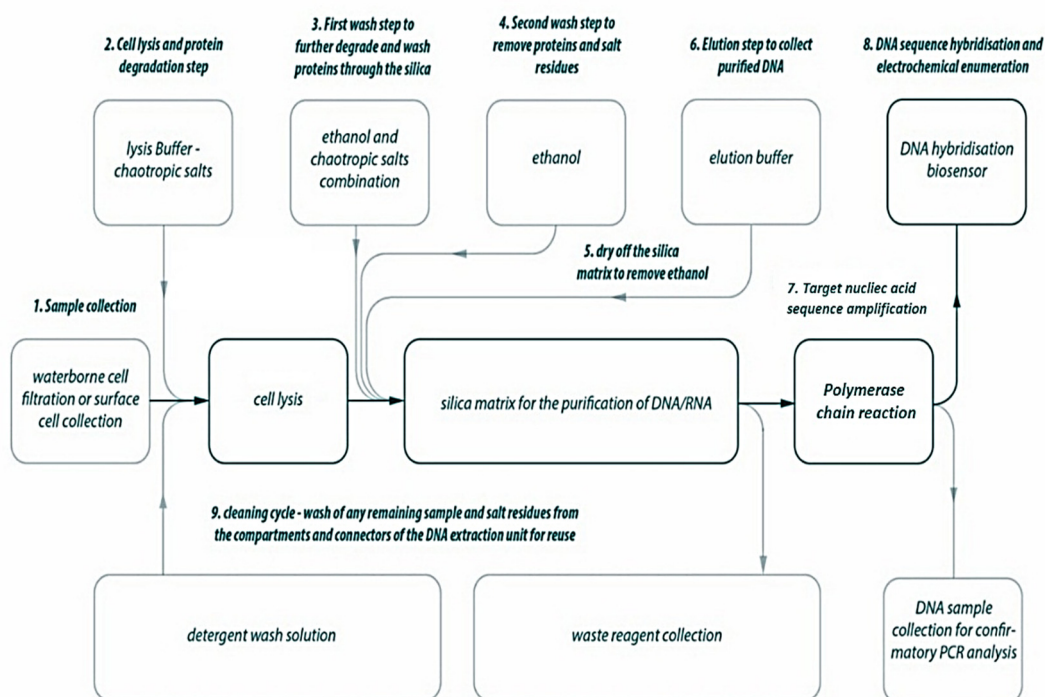


Figure 5.1. Schematic outline of the steps necessary for the extraction and purification of microbial DNA prior to electrochemical analysis of probe-target hybridisation.

The adaptation of this protocol into one that can be easily automated is key to the functionality of the biosensor platform. It also represents the most significant design

challenge in translating the modular microfluidic model outlined in figure 5.2 into a field portable, simple to use biosensor platform.

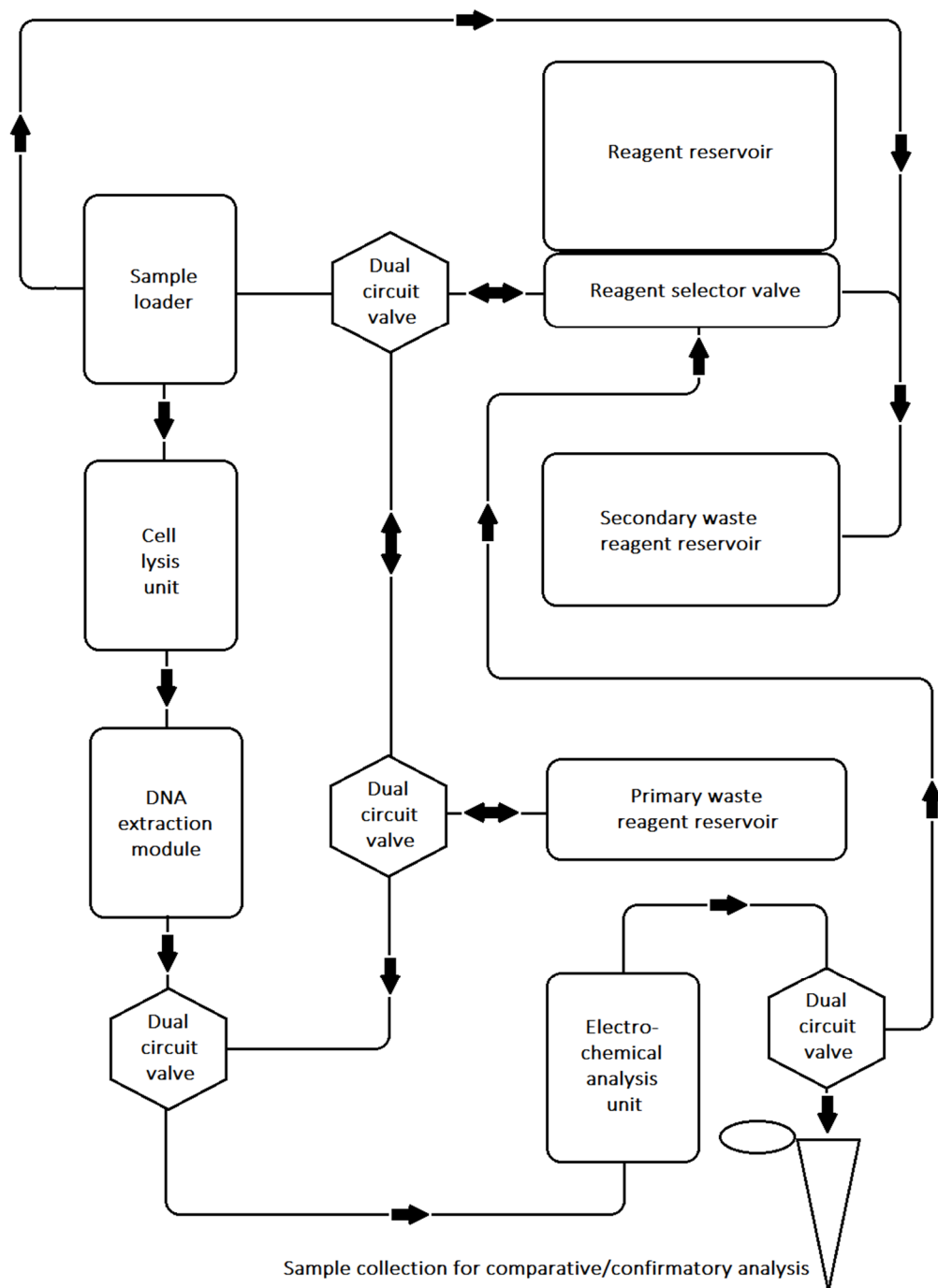


Figure 5.2. Outlining the minimum necessary macro-fluidic architecture to facilitate an entire automation of sample loading, cell lysis, DNA extraction and purification, sample division for confirmatory analysis, electrochemical sample analysis, containment of all used reagents, and utilisation of a self-cleaning cycle for subsequent re-use.

A review of laboratory-based sample handling systems indicates that automation is primarily employed to perform repetitive tasks, such as pipetting small volumes, and to do so with a degree of reproducibility beyond that of their human counterpart. Accordingly, this automated analytical model has been applied to the single-step extraction of DNA in products such as the Chemagic 360 Nucleic Acid Extractor (Perkin Elmer, USA), GX-127 Oligo Purification System (Gilson Inc, USA), QIAcube HT System (Qiagen, Germany) and the MagNa Pure 96 Instrument (Roche Life Science UK). Although such systems are highly effective in reliable and consistent delivery of nucleic acid purification workflow solutions, the repurposing of automated pipette-based techniques for use within a robust, field-portable device faces significant challenges, not least size, complexity, fragility, and associated development and production costs.

Rather than attempting to replicate existing protocols for the extraction and purification of DNA, liquid chromatography (LC) was identified as the analytical technique most analogous to the principles of miniprep-based DNA isolation. LC employs a mobile phase such as water, methanol, or acetonitrile to convey the sample, and a stationary phase matrix such as silica gel, alumina, or a polymer to separate molecular components by adsorption, polar affinity, antibody specificity, or size. Given that the simplest solution is often the best, individual prototype components of the biosensor system were designed to use the reagents specific to each process as a mobile phase medium. Analogous to the mobile phase in LC, the reagents are used to drive the target analyte through each of the sample preparation steps and on to separation, analysis and sample storage.

5.2.1 Reciprocating pumps vs syringe pumps

Given the similarities of the biosensor platform to liquid chromatography, initial brainstorming of design ideas focussed on the adaptation of existing technologies with a proven track record in this discipline. With the key consideration being how to drive the mobile phase through each stage of sample preparation and analysis, the primary focus was that of pumping and sample introduction systems, and reagent management in LC equipment. Reciprocating pumps are common to practically all LC

systems and are used to push the mobile phase through the adsorbent matrix of the separation column – the stationary phase. Piston-based pumps are key to generating the high pressures required to overcome the resistance of the column matrix to mobile phase flow through, and their basic principles are outlined in figure 5.3.

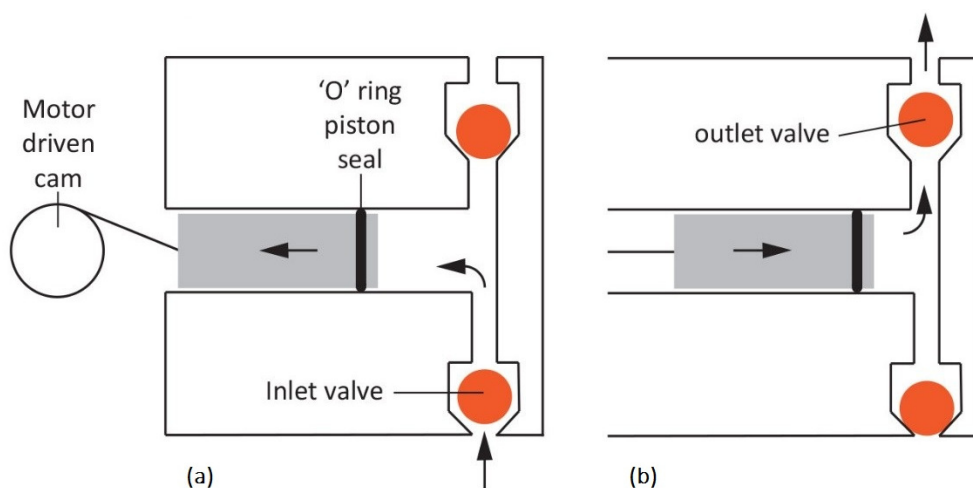


Figure 5.3. Illustrating the operating principle of the reciprocating piston pump typically used to drive the mobile phase in liquid chromatography. Check valves (highlighted orange) act to maintain the liquid flow in one direction through intake (a) and expulsion (b).

While reciprocating pumps are reliable in driving the mobile phase at a user-specified flow rate, there are a number of factors which limit their practical application in the context of a field-portable biosensor platform. Most important of these is the inherent pump cycling as the piston stroke alternates between intake and expulsion. This cycle subjects the mobile phase to a pulse with the same frequency as the pump actuation which can introduce non-laminar flow and may disrupt downstream activities. In LC, mechanical and/or in-line dampers are used to eliminate this pulse, but such measures would both add to the size and weight of the biosensor platform and increase the reagent flow volume of the *macro-fluidic* component.

Furthermore, as piston travel is subject to dwell at each end of the displacement stroke, the relationship between the mobile phase volume being expelled and the rotational position of the cam is non-linear. Accordingly, the delivery of reagents in

volumes other than multiples of the piston displacement requires modelling a first derivative of the position curve according to the specific pump crank throw and piston dimensions. Lastly, operation of the cam, motor, and control electronics are likely to represent a significant draw on the unit power supply.

Used in LC sample injection, the delivery of precise sample or reagent volumes in analytical applications is also achieved using syringe pumps. Figure 5.4 shows a typical infusion pump design for laboratory applications, with a rotating screw controlling travel of the pusher bar and maintaining a constant pressure on the syringe plunger. Withdrawal pumps simply perform this task in reverse, drawing fluid into the syringe as the pusher bar draws the plunger outward, while continuous cycling pumps combine both infusion and withdrawal functionality.

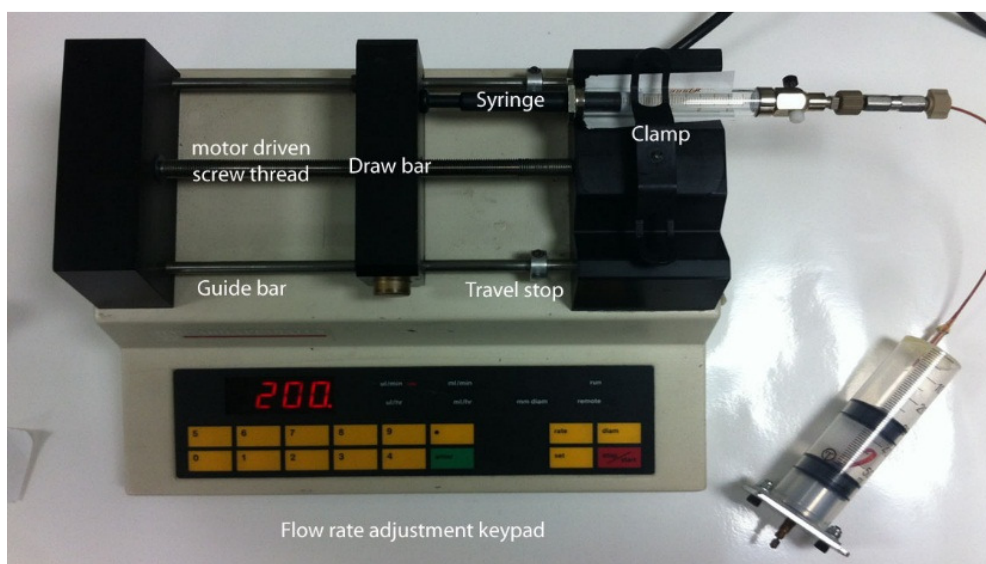


Figure 5.4. Typical twin-channel syringe pump for research applications; rotation of the screw thread causes the drawbar to move along the guide bars and depress the syringe plunger.

Widely employed in analytical, pharmaceutical, and clinical applications, syringe pump designs can vary significantly; from multiple channel analytical units, to wearable infusion systems such as in the dispensing of insulin. Control features typically include adjustable flow rate and back-pressure shut-off, but the key difference between clinical and analytical research pumps is one of step rate. In

analytical research pumps, a geared drive increases the ratio between motor rotation and actuation of the pusher bar. This allows the use of higher motor speeds to be used and effectively eliminates the influence of the motor step rate. As a result, research syringe pumps are able to accurately deliver small volumes of reagent with little or no pulse effect. In contrast, syringe pumps with large step rates are not suited to the continuous delivery of small reagent volumes and exhibit characteristic similar to those of reciprocating piston pumps. As such limitations can be of less importance in drug delivery, wearable dispensing systems are able to take advantage of small-scale stepper motors to drive infusion syringe pumps.

5.2.2 Pressure driven syringe pump design

Of the contemporary delivery systems, a stepper motor driven syringe pump appears most practical. However, given the variety of reagents used in cell lysis and DNA extraction, let alone electrochemical analysis or integral PCR amplification, it is unrealistic to use an infusion pump for each one. Accordingly, initial designs focussed on a bank of reagent syringes driven by pressurised gas from a shared reservoir, and with reagent flow rate controlled by a stepper-motor driven withdrawal pump integral to a primary waste reservoir.

5.2.3 Multichannel pressure driven reagent reservoir

Figure 5.5 shows the initial design drawings for the pressure driven reagent syringe pump unit consisting of 3 component blocks assembled using 4mm stainless-steel through bars, threaded at one end for fastening with an M4 nut. The first of these, (a) the high-pressure block and CO₂ inlet manifold is based loosely on the principle of common rail fuel injection – where the fuel is maintained at pressure and injection to the combustion chamber is controlled by a solenoid/piezo demand valve. In the biosensor platform reagent reservoir, a common rail is charged to operating pressure using a 12g or 16g CO₂ cylinder commonly used in the roadside repair of bicycle tyres or in paint-ball equipment.

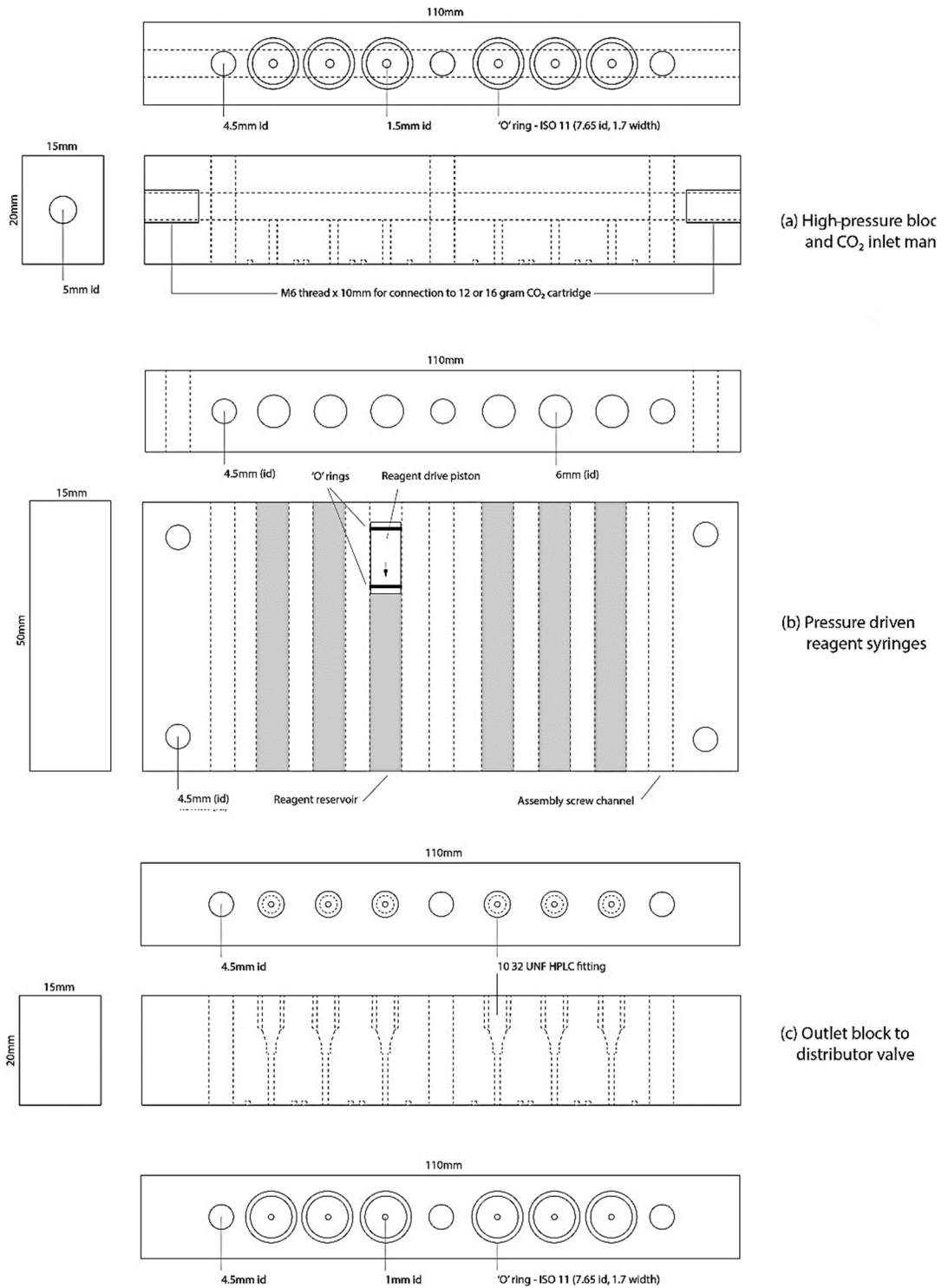


Figure 5.5. Initial drawings for a pressure driven multichannel syringe pump powered by CO₂ cartridges. The high-pressure block (a), reagent reservoirs (b), and outlet block (c), are assembled using threaded 4mm bar in 4.5mm channels and secured with nuts at each end. The outlet block is machined to use standard 10 32 HPLC fittings and 1mm PEEK tubing.

This CO₂ charge maintains a constant and equal pressure on each of 6 drive pistons, in turn acting on each of 6 reagent reservoirs. As the central unit in the assembly of the reagent reservoir, the pressure driven reagent syringe block (b) is designed with mounting points. The length of the reagent reservoir block may be altered according to the reagent volumes required and the practical limitations of the DNA extraction matrix/analytical platform reusability.

The third component of the multichannel reagent reservoir is outlet block (c) which connects the reagent flow to the distributor using standard 10 32 HPLC fittings and 1mm PEEK tubing. Distribution is controlled by a stepper motor controlled radial distribution valve loosely based on a fuel outlet valve and directing reagents through sample preparation and analysis. The reagent flow rate is mediated by a withdrawal syringe pump acting as a primary waste reservoir.

5.2.4 Integrated multichannel reagent reservoir and distributor

In the design process for the subsequent reagent distribution unit, it became immediately apparent that the high-pressure block, the syringe pump reagent reservoir, and the distributor valve could be combined into a single component as shown in figure 5.6. A standardisation of both reagent reservoir and pressure driven plunger dimensions was maintained both to reduce complexity and to allow flexibility within the user interface and the modification of reagent delivery volumes according to the sample matrix and analytical requirements.

The positioning of the outlet port for each reagent reservoir allows for an increase in volume to approximately 50mm without a requirement to change the disc valve dimensions. This enables the same distributor components to be used for a portable biosensor platform with the capacity to carry out a great number of analytical cycles or to facilitate the simultaneous analysis of multiple samples. Equally, an increased reagent reservoir volume may be practical for benchtop laboratory use.

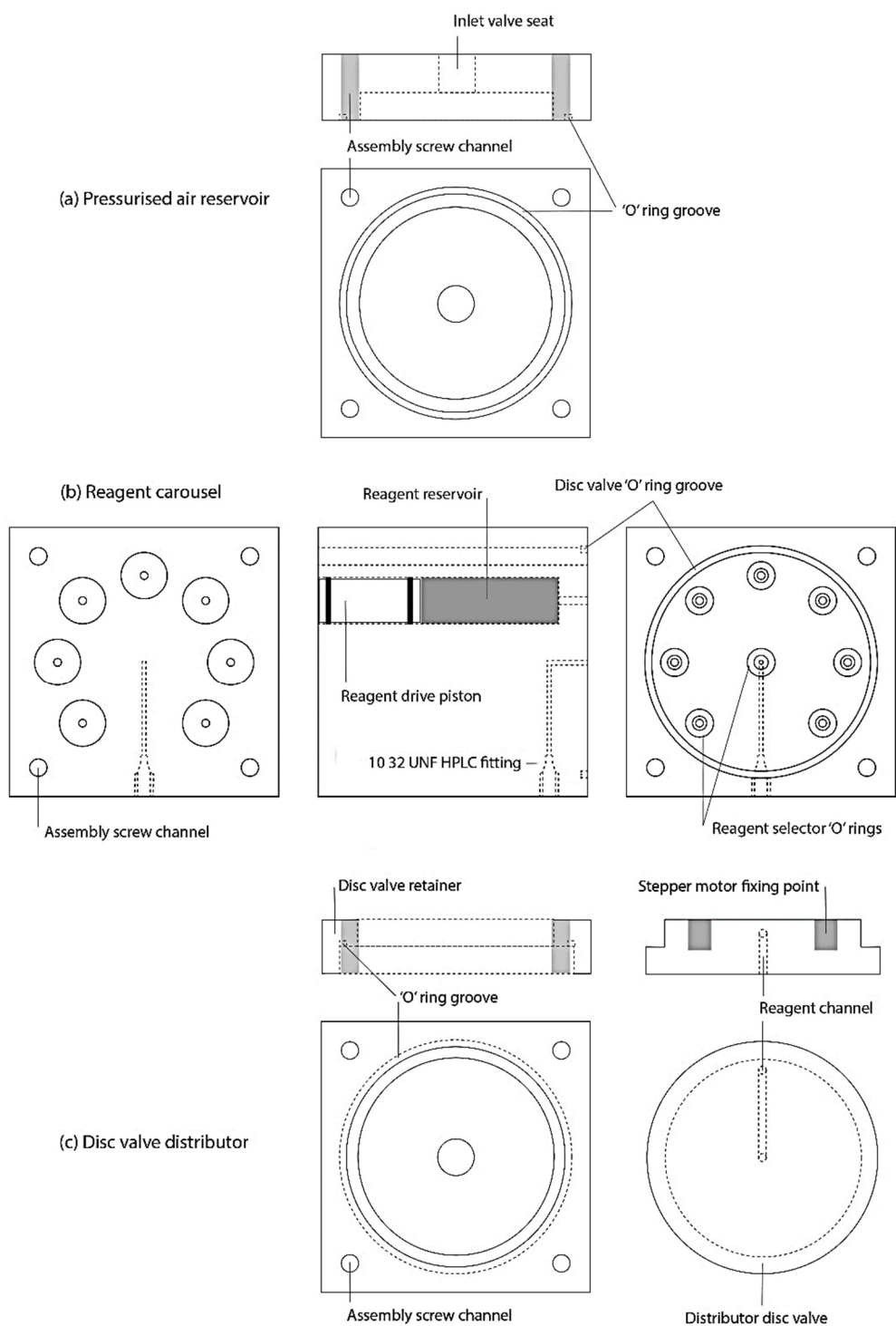


Figure 5.6. Revised drawings for an air pressure driven carousel type multichannel syringe pump. The pressurised air reservoir (a), reagent carousel (b), and stepper motor-controlled rotational disc-valve distributor (c), are again assembled using a through bar system. Reagents from the carousel are supplied to downstream processes by a single 10 32 HPLC fitting.

5.2.5 Reagent air pressure reservoir

In the course of initial testbed experiments, empirical tests showed the CO₂ cartridge pressure reservoir could be replaced by a relatively small air reservoir charged with a hand pump. Accordingly, the air reservoir requirements were calculated using the ideal gas law:

$$Pv = znRt$$

Where P = pressure, v = volume, n = number of moles, R is a constant, and t = temperature (K). For Accordingly, an air reservoir an ideal gas, z is equal to 1 and is discounted. While not an ideal gas, at temperatures from 0°C to 50°C and pressures of 100 to 500 kPa air has a z value between 0.99 and 1.00 and may be discounted.

Accordingly, at a constant temperature, air pressure and volume describe an inverse proportional relationship:

$$Pv = nRt \quad P = \frac{nRt}{v} \quad 300 = \frac{nRt}{50} = 200 = \frac{nRt}{75}$$

An increase in reservoir volume from 50cm³ to 75cm³ though the expulsion of 25ml reagent therefore results in an inversely proportional pressure drop from 300kPa to 200kPa. For a total reagent volume of 5ml per analysis this allows 5 cycles per pressure/reagent fill.

5.2.6 Stepper motor reagent selection

The reagents for each process are delivered in sequence as the sample progresses through each of the preparation and analytical steps. As illustrated in figure 5.6, this is controlled by a single outlet disc valve supported by nitrile O-rings around the circumference and driven directly by a geared stepper motor. The prototype design utilises 7 reagent flow positions from 0° to 315° at intervals of 45° driven by a relatively simple and inexpensive stepper motor.

5.2.7 Stepper motor process control

Rotation of the disc valve and the resulting selection of a reagent or closed position is controlled by an Arduino microcontroller via a servo/motor control board as outlined in section 5.7, as is the power supply by a lithium ion (L-ion) battery pack through a UBEC voltage regulator. Reagent flow rate is controlled using a withdrawal syringe pump regulated by a second stepper motor as outlined in figure 5.7. Rotation of the threaded drive screw (a) moves the plunger (b) from the primary waste reagent reservoir (c), changing the internal volume and regulating the flow of reagent from the carousel via HPLC port (d).

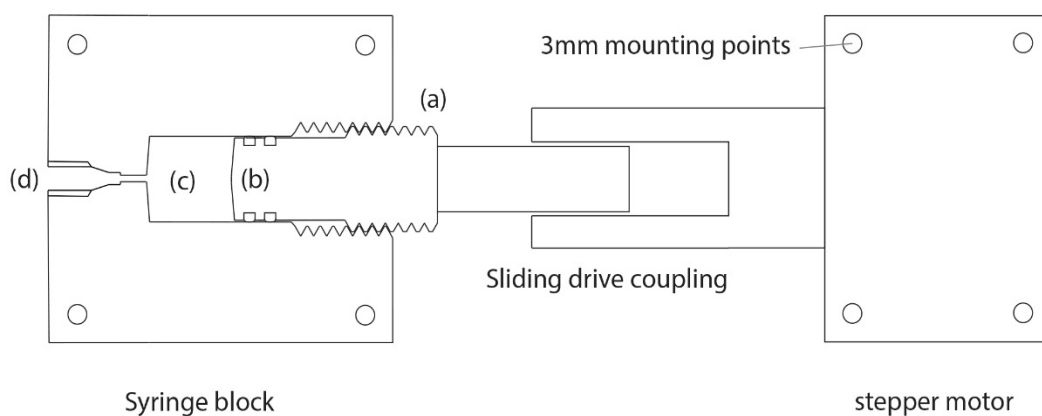


Figure 5.7. Withdrawal/infusion syringe pump design, switchable between the regulation of reagent flow and the expulsion of used reagents to the secondary waste reservoir. Drive screw rotation (a) draws plunger (b) from the primary waste reagent reservoir (c) and regulates carousel reagent outflow, through the microfluidic system to the HPLC port (d).

The thread of the drive screw and its counterpart in the syringe plunger are metric fine 1mm – ensuring that the plunger will travel 1mm for each 360° rotation of the stepper motor. Cyclic pulsing occurring in the reagent flow as a result of using direct drive in the syringe plunger travel is minimised within the programming of the Arduino micro-controller and by the damping effect of the reagent phase flow through the media of the DNA extraction matrix.

5.2.8 Interrupter valves and actuators

In operation of the biosensor platform, processes such as cell lysis or electrochemical DNA analysis should be isolated from the reagent flow to allow cellular degradation or probe/target hybridisation to take place. Accordingly, the rotational valve shown in figure 5.8 was designed to seal reaction chambers and to direct reagent flow.

Each valve housing acts to contain the preceding and superseding reaction chambers and mounts directly to the biosensor platform chassis. The valve actuation travel is controlled by an off-the-shelf TGY-225MG micro-servo with a torque rating of 3.5 kgcm-1. Each valve is powered from the L-ion battery via the UBEC and controlled by the Arduino via the servo/motor control board.

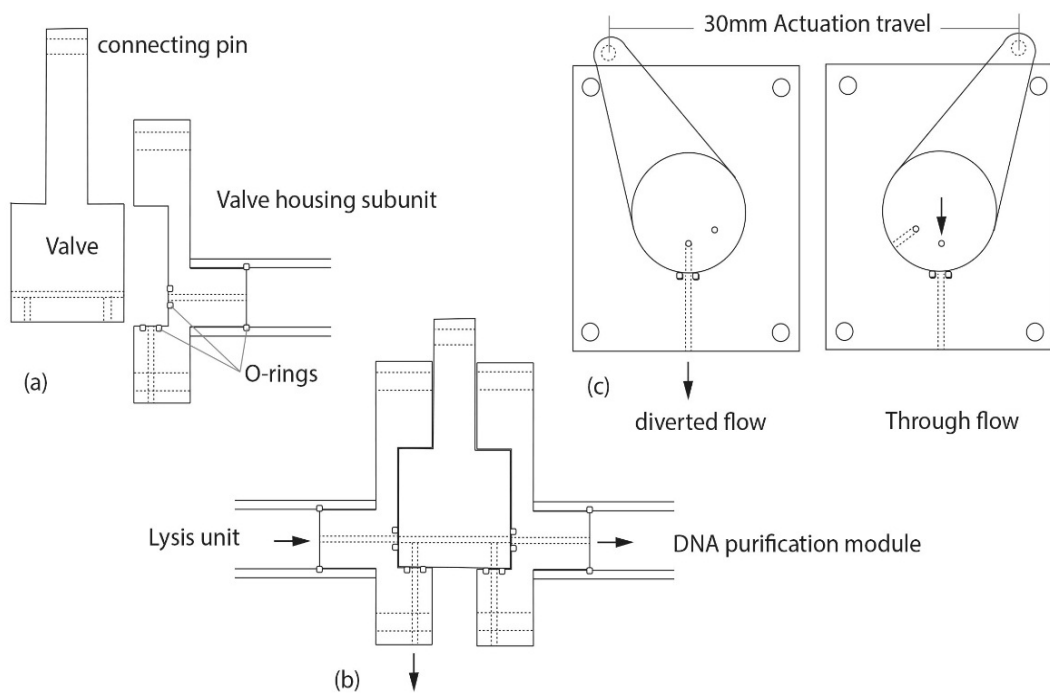


Figure 5.8. Two-way switchable valve to direct reagent flow, waste expulsion, and sterilisation cycle. Paired housings (a) contain the valve cam and fit directly into neighbouring modules (b). Actuation by servo motor allows 30mm travel, with flow closed at 15mm travel (c).

5.3 Sample Introduction

Sample introduction is the only part of the biosensor analytical platform where user input is required. To suit operators without a microbiology or analytical background, sample introduction should be simple and straightforward while the mechanism itself should be robust and reliable. The receiver design must facilitate the wash-through of all sample to ensure precise analysis and should also incorporate a self-cleaning cycle to eliminate overflow and prevent environmental contamination.

5.3.1 Sample volume

Culture-based microbiology typically refers to the enumeration of microbial species as colony-forming units per millilitre (cfu/ml). Similarly, DNA extraction for molecular analysis is typically based on a sample volume of 1ml. Reagent volume relative to the sample must be sufficient to perform their specific task with a degree of method robustness but should also be minimised from the perspective of efficient use of the platform storage volume. As a standard sample volume therefore, 1ml is a large enough volume to minimise variance, but is large enough to maximise the relative volume available for analysis.

5.3.2 Sample receiver design

The sample receiver design is presented in figure 5.9 and consists of a partially threaded sample receiver well and a matching screw-in lid – effectively a hand-driven syringe pump. The screw has an integral groove to receive reagents from the reservoir carousel and direct them through a 10mm (20µm porosity) PTFE frit in the base. The port is sealed by 2 nitrile O-rings situated in grooves along the length of the screw-down lid, and a third at the base of the receiver well. The sample receiver base attaches directly to the top surface of the cell lysis unit, separated by a stainless-steel filter mesh (50µm) and sealed by a nitrile O-ring.

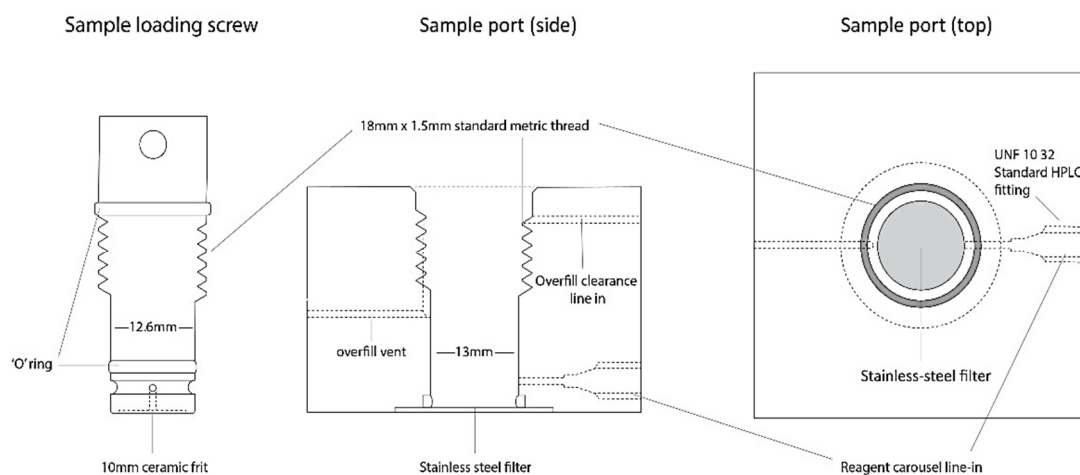


Figure 5.9. The sample receiver consists of a receiver well of base area of 1cm^2 , and a screw down sealed lid. The receiver is connected to the reagent carousel using PEEK tubing and standard HPLC fittings, while the sample well base is attached directly to the cell lysis unit.

5.3.3 Sample loading protocol

Loading of a consistent sample volume has obvious benefits in the generation of reliable and comparable data, and the designed port employs an overflow design to prevent the loading of excess sample volumes. However, underloading represents an equally critical consideration when introducing a sample to the microfluid component using the syringe-pump based screw-lid. Where a sample is less than $1000\mu\text{l}$ in volume, the difference is likely to be made up by trapped air. The introduction of gas bubbles is to be avoided as it has the potential to cause cavitation in the reagent flow and interfere with the downstream processes of cell lysis and DNA purification.

Accordingly, the sample loading protocol specifies a loading volume of $1050\mu\text{l}$, eliminating the potential for underloading while remaining straightforward and within the operating parameters of many commercially available $1000\mu\text{l}$ micropipettes. This sample is placed into the receiver port, the plunger part of the screw-lid engaged with the screw thread, and the lid is screwed home as outlined in figure 5.10. As the lower of the pair of O-rings pair on the screw-lid plunger passes the overfill vent drilling, the volume of the sealed receiver port, and the maximum

sample that can be introduced for analysis, is equal to 1000 μ l. Any sample volume greater in excess of 1000 μ l is expelled via the overflow channel (figure 5.10b). The continued travel of the screw-lid syringe pump initiates the second stage of sample loading and introduction of the sample volume into the lysis chamber (figure 5.10c). As the microfluidic component contains double distilled (DD) water between analyses, an equivalent volume of DD water is displaced into the secondary waste reservoir through the DNA purification unit.

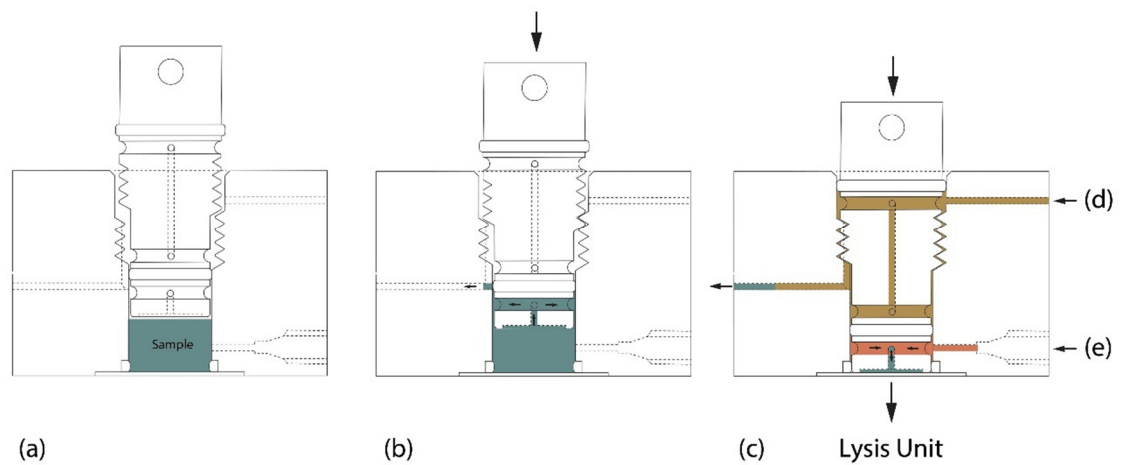


Figure 5.10. The screw down action of the lid (a) expels the excess sample via the overflow vent (b) and delivers 1ml sample to the cell lysis unit (c). Sample overflow is cleared to the secondary waste reagent chamber and the upper screw-lid decontaminated from reagent reservoir 2 (d). Reagents from the carousel are introduced to the receiver via 1mm PEEK tubing and 10 32 HPLC connections, acting as a mobile phase to transfer sample through lysis (e) and DNA purification.

5.3.4 Sample parameters

The great majority of validated protocols for foodborne pathogen surveillance specify sample homogenisation and serial dilution (ISO, 2006) for plating on culture media. The analysis of a sample from an appropriate dilution factor would therefore be relatively straightforward using the developed biosensor system. However, the analysis of water samples presents a greater challenge as the sample volume is typically in the order of litres, given the low microbial numbers present. Accordingly,

the analysis of water sample using the biosensor platform is based on the removal of microbial species from a set volume of water using a sterile membrane filter of area 1cm^2 , and nominal pore size 0.2 or $0.45\mu\text{m}$. On completion of water filtration, the membrane filter is placed sample face down in the receiver well using sterilised tweezers. $1100\mu\text{l}$ of lysis buffer is added, and the loading protocol carried out as above. Pre-coated with a neutralising buffer, the membrane disc may also be used to collect microbial samples from food or food preparation surfaces and processed with a $1100\mu\text{l}$ of lysis buffer as per a filtered sample.

5.3.5 Self-cleaning cycle

As a re-usable platform, it is key that no bacterial cells or nucleic acid residues remain in the sample receiver or surfaces of the screw-lid. To prevent such sample cross-contamination, the receiver design incorporates an integral decontamination process focussing on two specific areas. The first of these, the overflow circuit, covers the volume of the sample receiver contained by the O-rings along the length of the screw lid and includes the overflow vent drillings. The second is the volume below the screw-lid O-ring and is part of the macro-fluidic component.

The overflow circuit is decontaminated using flow-through of a 10% sodium hypochlorite (NaOCl) solution from the carousel reagent reservoir via a servo-motor actuated switch valve. Commonly used in molecular biology laboratories to eliminate nucleic acid residues in analytical areas, 10% NaOCl lyses bacterial cells and degrades proteins, DNA and RNA. To prevent the contamination of subsequent samples, the NaOCl is displaced by a 70% ethyl alcohol solution, cleared using compressed air. That part of the loading port volume within the biosensor platform macro-fluidic component relies on the flow-through of the reagents used in the microbial cell lysis and DNA purification processes to clear any remaining sample, including them in the subsequent analysis. Between each sample run, the entire microfluidic component is sterilised by a 10% NaOCl solution flow through, cleared using 70% ethyl alcohol, and loaded with double distilled water.

5.4 Cell lysis unit

Once the sample has been loaded, the first step toward analysis is breaking open the microbial cells to release the DNA. In a laboratory context, there are a wide range of protocols for the lysis of all types of microbial cells, and these can vary greatly according to the sample matrix. As outlined in the introduction, the detection and identification of microbial pathogens may be best served by characterising the transmission and distribution of both bacterial species and pathogenic genes (such as virulence factors and treatment resistance gene cassettes). Accordingly, in addition to the analysis of sample matrices such as water and food produce, the capacity to detect microbial species or gene cassettes in soils, plant tissue, or plasma would significantly broaden the potential application of the biosensor platform.

The design of the cell lysis unit seeks to exploit chemical, mechanical, and temperature-based methodologies in maximising the effectiveness of the lysis process and in turn the analytical scope of the biosensor platform. To this end, the unit combines detergent-based membrane disruption, mechanical milling, and temperature mediated biomolecule denaturation in breaking down microbial cell-wall and membrane structures. However, as it is unfeasible to attempt a 'one-size-fits-all' solution to cell lysis and DNA extraction, the biosensor platform user interface will facilitate the optimisation of parameters such as lysis duration, temperature, and bead mill oscillation rate.

5.4.1 Lysis buffer

When breaking down microbial cells it is key that the lysis buffer has the capacity to break open as many of those present in the sample matrices as possible but does not degrade or denature the target DNA. The effectiveness of the lysis buffer is largely determined by a detergent component. Accordingly, sodium dodecyl sulphate (SDS), an anionic denaturing surfactant, is widely employed in the lysis of microbial cells, and often in combination with a chaotropic agent (discussed further in section 5.5 in relation to DNA purification) and a salt (NaCl) buffer. The NaCl buffer maintains a pH

and osmolarity appropriate to maintaining the integrity of the sample DNA, while the combined hypotonic buffer and action of the detergent disrupt the cells outer membrane and lead to lysis by plasmolysis. The action of SDS is enhanced by elevated lysis temperatures.

5.4.2 Temperature driven cell lysis

High temperature alone can be sufficient to cause microbial cell lysis by disrupting chemical bonds in the outer membrane of microbial cells. However, in an SDS and salt-based lysis buffer, increased temperatures also cause protein denaturation. In the extraction of nucleic acids, this is useful in denaturing nucleases; enzymes that hydrolyse the phosphodiester bonds between nucleotides and break genomic and plasmid DNA sequences into unreadable fragments or monomers. The platform design uses a fast action Peltier cell to regulate the temperature of the lysis chamber via a copper heatsink.

In consideration of the resistance of DNA to temperature mediated degradation (as opposed to denaturation – separation of the DNA double helix strands) laboratory-based protocols tend to apply temperatures approaching 100°C. Temperatures at or above boiling point can cause phase shift in the reagents, pressurising the container (usually a 1.5ml micro-centrifuge tube) and possibly disrupting interactions between microbial cells, detergents, and chaotropes.

5.4.3 Electromagnetic agitation/bead mill

Key to cell lysis in the laboratory is the employment of a shaker plate to agitate the sample and lysis buffer solution, or a bead mill to exert mechanical shear forces on the microbial cell structure. Both processes are conducted at elevated temperatures. However, given the design criteria for a field-portable biosensor platform and employment of a microfluidic system for sample processing, the incorporation of benchtop shaker-plate or bead mill design principles is unfeasible. In seeking to replicate the bead mill action in a design suited to the biosensor platform design, the prototype device is based on an electromagnetically actuated bead mill prototype.

As initial experiments demonstrated pharmaceutical grade stainless-steel is unsuited to the conduction of an internal electromagnetic field, the testbed lysis unit was lathe-turned from a corrosion resistant 1100 grade aluminium alloy. All experimental protocols were conducted using the unit pictured in figure 5.11, consisting of a two-piece chamber with a nitrile O-ring seal and 3 screw fixings. Sample introduction, reagent flow, and operational pressure are regulated through 1mm internal diameter PEEK tubing and standard 10 32 HPLC fittings.

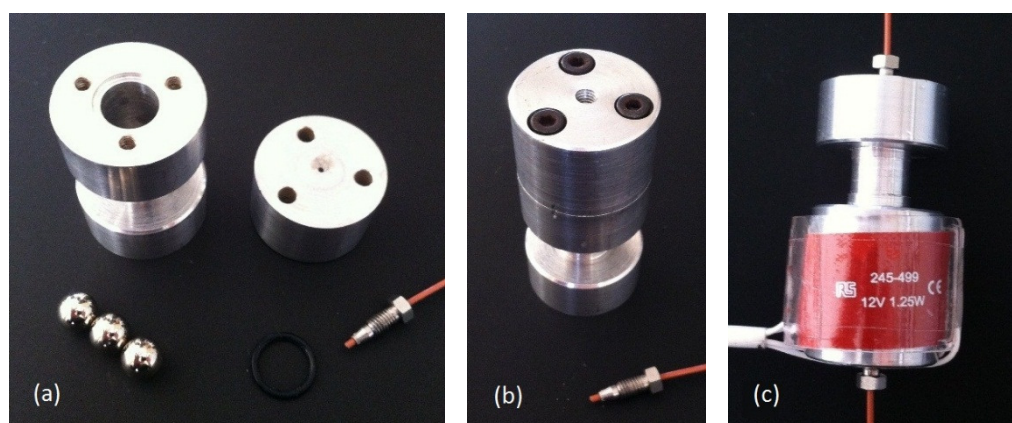


Figure 5.11. Electromagnetic bead mill prototype, detailing the lysis chamber and neodymium chromed ball bearings (a), assembly (b), and heater element (c). 1mm id PEEK tubing and 10 32 HPLC fittings connect the unit for sample/reagent flow through and pressurisation.

A pair of 12 Volt, 1.25-Watt heater elements with a detachable acrylic fixing were used to maintain lysis unit and reagent temperature during analysis. Internal dimensions of 12mm by 28mm give a nominal volume of 3,166 μ l, increased to approximately 3,250 μ l by the concave profile of the cutting tool employed. This internal volume available for the interaction of the sample and lysis buffer solution was adjusted using ball 5mm, 7mm, and 9mm chromed ball bearings of volume 381.7 μ l, 179.6 μ l, and 81.8 μ l respectively. In the emulation of a bead mill process, the lysis unit also contains multiple 1mm ceramic beads which are agitated by the actuation of the chromed ball bearings, but which are unaffected by the electromagnetic field. With a volume of 0.52 μ l each, the inclusion or removal of ceramic beads facilitates fine tuning of the lysis chamber volume.

The initial design proposals for the bead mill were based on a solenoid valve, with 35 SWG enamelled copper wire wound into the recessed part of the lysis chamber body as shown in figure 5.12 (a) and with a wall thickness of 1mm. With the application of current, the induced magnetic field draws ball bearings from the chamber bottom into the upper area. However, with a reliance on gravity to return the ball bearings to rest, the solenoid model does not impart sufficient frequency control, nor does the bearing travel generate sufficient mechanical stresses between the ceramic beads.

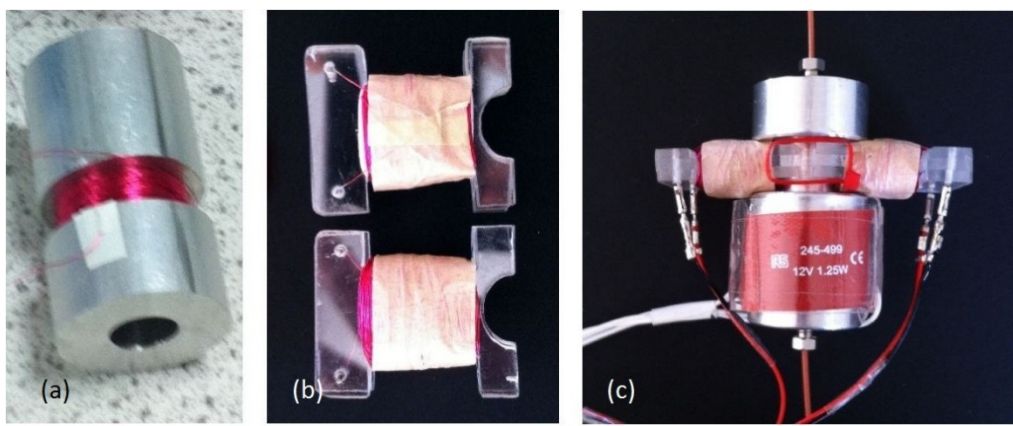


Figure 5.12. Showing the solenoid model actuation bead mill with windings around the top of the lysis chamber (a), acrylic scaffold wound with ~800 windings of 0.2mm/35 SWG (standard wire gauge) poly vinyl acetal coated copper wire, connecting pins, and protective paper wrapping (b), and the electromagnetic scaffolds fitted to the cell lysis unit (c).

Accordingly, a dual circuit electromagnetic model was developed employing a pair of windings (b), 180° apart and perpendicular to the lysis chamber (c). Application of a current to each set of windings in turn causes the ball bearings to oscillate within the lysis chamber, agitating the sample and buffer solution and generating mechanical stresses in contact between ceramic beads, ball bearings and lysis chamber surfaces.

The magnetic principles applied in the design of the electromagnetic component relate to the proportional relationship between the strength of current and the electromagnetic force (Maxwell, 1865). In order to minimise the electromagnetic

force required, and by extension current draw on the power supply, the chrome plated steel ball bearings used in initial experiments were replaced by N42SH (stable to 120°C) neodymium alloy ($\text{Nd}_2\text{Fe}_{14}\text{B}$) permanent magnets.

The electromagnet windings used a 0.2mm/35 SWG (standard wire gauge) polyvinyl acetal coated copper wire, with the windings supported on an acrylic scaffold (b). Acrylic has a magnetic permeability value equivalent to that of free space (μ_0) = 1.256×10^{-6} H/m (Henry's per meter). Magnetic permeability reflects the capacity of a material to be magnetised and describes the proportionality constant between magnetic induction and field intensity. If μ_0 is assumed to be equal to 1, the magnetic permeability of ferrite metals can be as high as 9000 (1.13×10^{-2} H/m), and when used as a winding core, significantly increases the magnetomotive force (*mmf*) generated by the electromagnet.

As the use of neodymium ball bearings minimises the *mmf* required to drive their oscillation within the lysis chamber, the magnetic permeability of the winding core is secondary to dimensions of the coil windings applied. Electromagnet efficiency is dependent on coil diameter, profile, and winding density. The number of windings dictates current draw and *mmf* magnitude according to the relationship:

$$mmf = I \times N$$

Where I = current in Amperes, and N = the number of winding turns - analogous with Ohms law: $V = IR$. In design of the electromagnet component therefore, a key consideration in generating maximum *mmf* is matching current draw to the working parameters of the Arduino servo control board – approximately 200 milliamps. The utilisation of ferrite metal core may be considered as a means to reduce the duration of the oscillation pulse and in turn limit the current draw on the power supply in a 2nd generation biosensor platform prototype.

5.4.4 Pressure driven cell lysis

High pressures are acknowledged to cause cell lysis in bacterial species and their application is the subject of considerable research in the large-scale lysis of microalgae in biofuel refineries. However, the pressures concerned are considerably higher than those employed in the biosensor platform. Many microarray protocols use denaturation temperature in the region of 110°C (Conzone and Pantano, 2004; Nimse et al., 2014) with negligible DNA thermal degradation (breaking of the phosphodiester bonds in DNA phosphate backbone) while PCR protocols generally include an initial prolonged denaturation step at 95°C, again with no significant fragmentation.

However, at pressures between 400kPa and 1MPa thermal degradation of DNA is shown to occur at temperatures greater than 90°C (Karni et al., 2013). There is no reason to suggest that breakage point occurrence is anything other than random and this represents a significant hinderance to gene sequencing or PCR amplification. However, temperature driven gene fragmentation may have utility in the biosensor platform through the generation of shorter nucleotide sequences suited to detection using DNA hybridisation systems.

As the maintenance of the biosensor mobile phase at 200 kPa to 300kPa theoretically increases the boiling point of the double distilled water in the lysis buffer to 133.6°C, the macro-fluidic system has the potential to exploit higher lysis temperatures without gas formation. Conversely, should higher pressures have a negative effect on cell lysis or DNA integrity, mobile phase compression may be reduced as required by unwinding the primary waste reservoir withdrawal syringe pump.

5.5 DNA purification module

Laboratory-based extraction of nucleic acids generally use either a phenol-based protocol, or one based on mini-prep, spin filter kits. In consideration of increased yields and a reduced reliance on organic solvents (Tanaka and Ikeda, 2002;

Montgomery and Sise, 1990; Chowdhury, 1991), the biosensor platform is based on the spin filter or solid phase extraction (SPE) media model. DNA extraction and purification using an SPE media such as silica might best be described as an adjustable filter, the characteristics of which depend on the ionic strength and pH of the mobile phase. A mobile phase of high ionic strength allows denatured proteins and membranes to wash through the silica matrix while nucleic acids stick to its surface. To elute the bound nucleic acids, a mobile phase of low ionic strength reverses this interaction and allows the DNA or RNA to be washed out.

In a miniprep kit (section 4.4), the spin filter acts as the SPE media with the mobile phase driven through the filtration matrix using a mini-centrifuge. However, quite apart from the size, mass and power requirements, the integration of a centrifuge within the macro-fluidics system of the biosensor platform is at best problematic. Instead, the biosensor platform DNA purification unit is based on a stationary phase type column matrix and a mobile phase pressure driven by the reagent carousel syringe pump.

5.5.1 Chaotropic salt-based DNA purification

In the context of molecular biology, the term chaotrope is generally used to describe solutes that act to unwind proteins and destabilise membranes. Chaotropic salts are often referred to in terms of hydrophobicity and hydrophilicity but, as these characteristics can be dependent on solute concentrations or interactions with macromolecules, it is more practical to consider them in the context of disruption of hydrogen binding and van der Waals forces. The structure and functionality of macromolecules such as membranes and enzymes are determined by such dipole and charge interactions with water molecules and the hydration of hydrophobic amino acids.

Where the addition of chaotropic salts increases the chemical polarity of a solvent beyond the capacity of the available water molecules to solvate the salt ions, dipole

interactions between the salt and the hydrogen bonding species are more favourable than those hydrogen bonds acting to maintain protein structure. In the lysis of microbial cells, this chaotropic sequestration of water molecules reduces the hydrophobic effect intrinsic to the structure of the outer membrane, the lipid bilayer integrity is lost, and the cell envelope disintegrates. Exposure to chaotropic salts has much the same effect on tertiary protein folding, including the structural elements responsible for 'packing' Eukaryotic DNA, and causes a loss of protein structural integrity and, by extension, a loss of function.

As neither the structure of DNA nor RNA is dependent on the dipole interactions that are key to protein integrity, they are not denatured by chaotropic salts. However, chaotropes disrupt and disperse the hydration shell that surrounds nucleic acids under normal physiological conditions and act to expose the negatively charged phosphate backbone of the DNA double helix. Although the process is not fully understood, the positive charge saturation of the silica substrate by the chaotropic ions appears to mediate the adsorption of the DNA within this matrix, while allowing the denatured proteins, lipids, and cellular debris to wash through. Utilisation of an elution buffer of low ionic strength negates the charge saturation of the silica matrix and facilitates desorption of the bound nucleic acid within a reformed hydration shell. The elution buffer washed through the silica matrix contains the nucleic acids isolated from the microbial cells of the sample.

All spin filter and miniprep column-based nucleic acid extraction protocols are based on the mediation of cell lysis, protein denaturation, and DNA purification using chaotropic agents. The most commonly used include guanidine hydrochloride (as detailed in figure 5.13) and sodium dodecyl sulphate, but guanidine thiocyanate, ethanol, and magnesium chloride are also used. Applying chaotropic DNA extraction and purification to a flow-through model, the biosensor platform reagents are based on guanidine hydrochloride as a chaotropic salt and sodium dodecyl sulphate as a detergent based on the cost-effectiveness of their application.

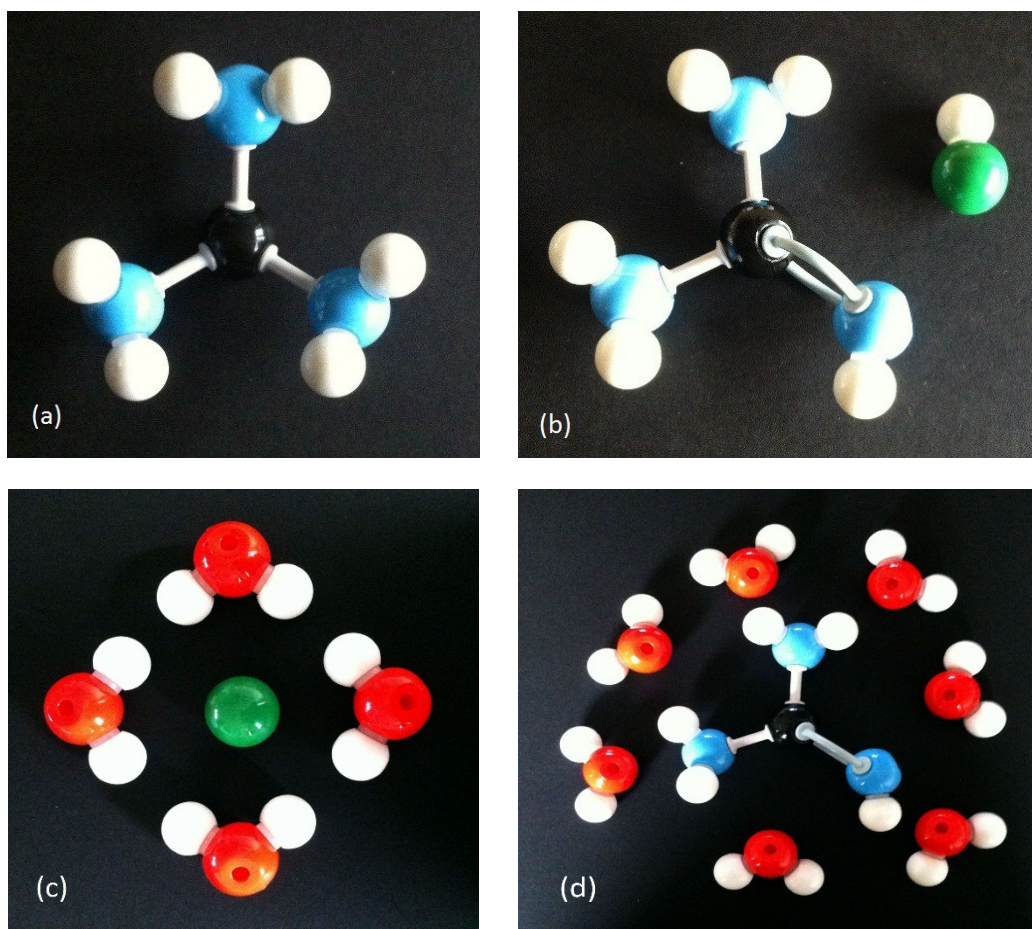


Figure 5.13. Guanidine (Gu) (a), a strong base, and guanidine hydrochloride salt (GuHCl) (b). At high concentrations in solutions, the NH (cation) and Cl (ion) hydrogen bonding interactions with macromolecule hydrogen bonding species and with dipolar water molecules (c and d) disrupt protein hydrophobic regions and the hydration shells of nucleic acid chains.

A pH buffering salt solution is included to maintain the integrity of the target DNA. The initial formulations and their projected roles are outlined in table 5.1 for each stage of the cell lysis and DNA purification process and have a basis in the development of protocols for the extraction of nucleic acids from a range of cell types (Medina-Acosta and Cross, 1993; Boom et al., 1990; F. Yang et al., 1997). Variations of the reagents specified have become standard in protocols for DNA extraction in relation to specific cell types and in general purpose, commercially available DNA extraction and purification kits.

Table 5.1. Reagent formulations for DNA extraction and purification (Medina-Acosta and Cross, 1993; Boom et al., 1990; F. Yang et al., 1997)

Reagent 1. Lysis buffer	High ionic strength buffer: sodium dodecyl sulphate ($\text{CH}_3(\text{CH}_2)_{11}\text{SO}_4\text{Na}$) - a chaotrope and detergent to break down the outer membrane structure of microbial cells, guanidine hydrochloride (GuHCl) – as a chaotrope in cell lysis and protein denaturation and in particular DNases and RNases, and sodium acetate (CH_3OONa) – a buffer suited to stabilising nucleic acids and preventing pH variation from lysed cellular components such as lysosomes. pH 4
Reagent 2. Adsorption buffer	Reduced ionic strength buffer: Guanidine hydrochloride (GuHCl) – to promote the adsorption of nucleic acids to the silica matrices of the purification stationary phase, Tris HCl ($(\text{HOCH}_2)_3\text{CNH}_2$) – pH buffer, and 38% ethanol – prevents hydration of nucleic acids and aids the wash through of cell debris and contaminants. pH 6.5
Reagent 3. Wash buffer	Low ionic strength buffer: low molarity Sodium Chloride (NaCl) – acts to stabilise the DNA, Tris HCl ($(\text{HOCH}_2)_3\text{CNH}_2$) – pH buffer, and ethanol – to wash guanidine salts from the stationary phase matrix. pH 7.5
Reagent 4. Elution buffer	Low ionic strength elution buffer: Tris-HCl – buffer to maintain nucleic acid stability in refrigeration and freezing. pH 8.5

5.5.1 Spin filter silica membrane

In both the commercial and scientific literature, the SPE matrices used in mini-prep, spin filter DNA extraction and purification (section 4.4) are commonly referred to as silica membranes (Moore et al., 2002; Alexander et al., 2007; Roose-Amsaleg et al., 2001; Unterholzner et al., 2017). However, as highlighted by the electron micrograph in figure 5.14, such spin filter membranes consist of filamentous silica with a large surface area to volume ratio for the adsorption of DNA. While this spun matrix has a comparatively dense structure, the pore size is suited to the flow-through of reagents

and degraded cellular components over relatively short periods when subject to the high G-forces generated by a benchtop mini centrifuge.

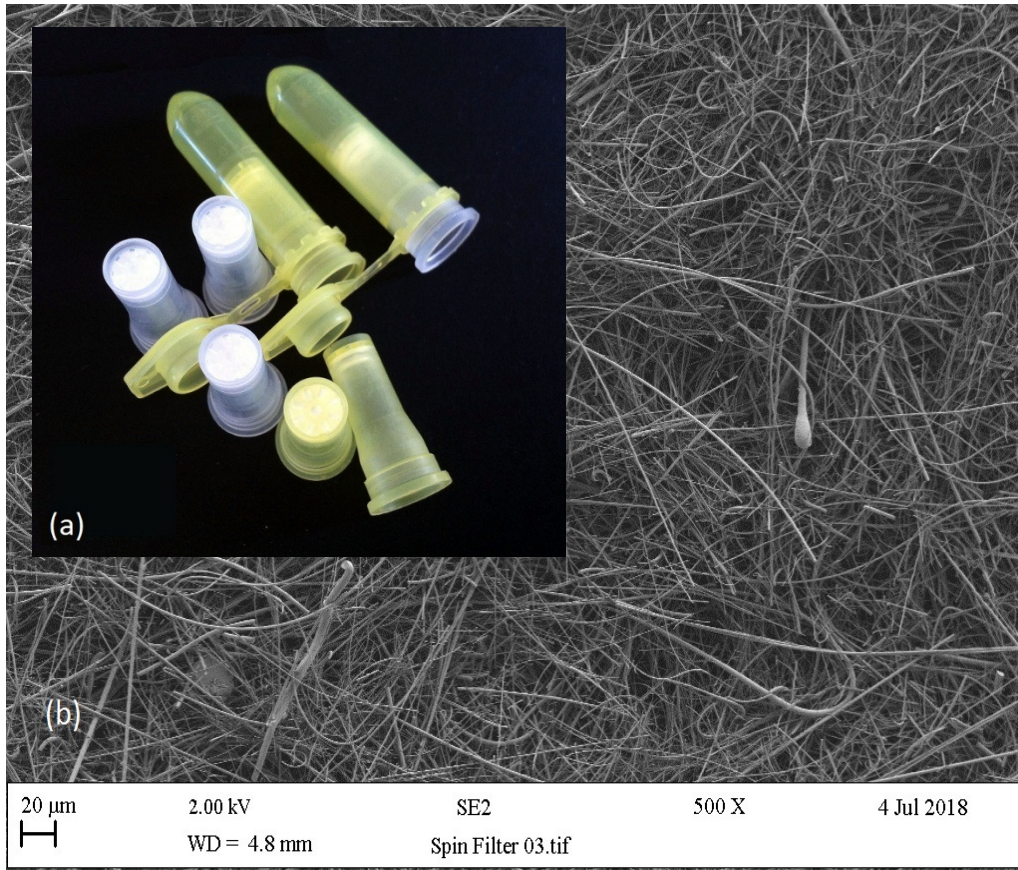


Figure 5.14. (a) Spin filters for bacterial DNA extraction and purification (Congen, Germany). Electron microscopy shows the spun silica matrix (b) – combining a high surface area for nucleic acid adsorption with a relative pore size appropriate to the clearance of cell debris by high speed centrifugation.

5.5.2 DNA purification matrix

As a preliminary testbed, a pair of 0.45μm membrane filters were employed to contain the silica matrix recovered from 5 pristine Congen spin filters within a tube of internal diameter 3.5mm, length 31mm and volume approximately 300μl as per figure 5.15 (a). However, allowing for a packing density with approximately 60% free space, as determined by ethanol saturation and evaporation, the subsequent loading

of adsorption buffer required a pressure approaching 900 kPa to achieve a flow rate exceeding 50 μ l per minute.

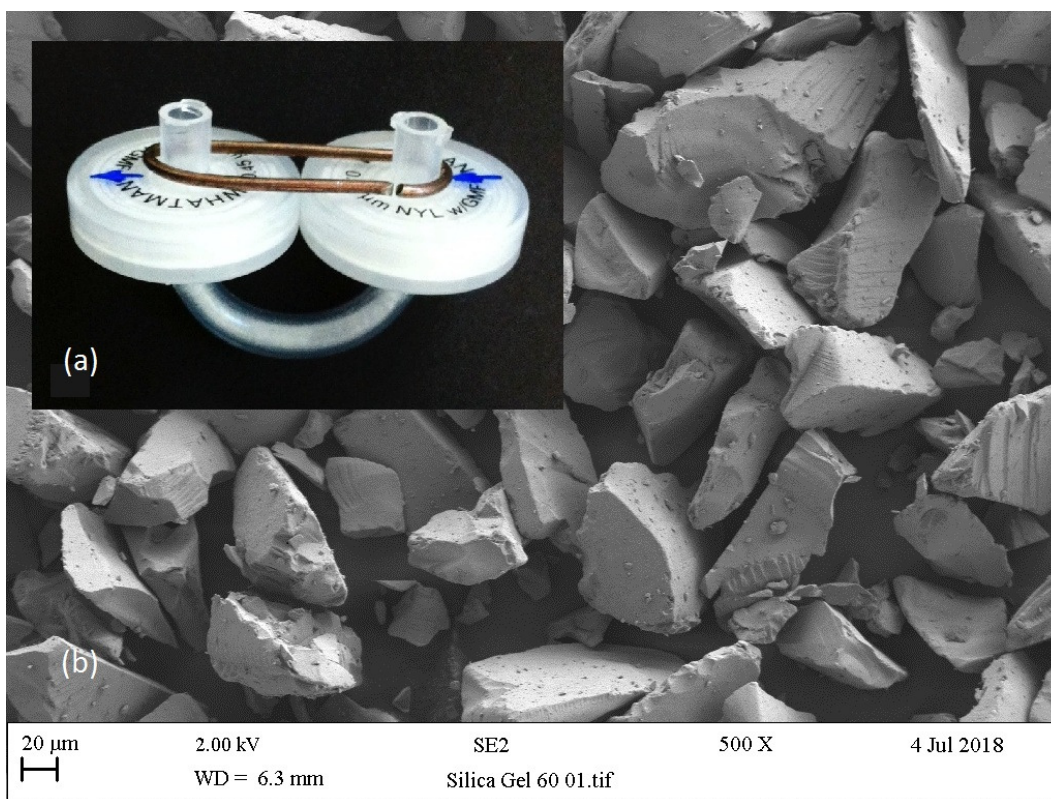


Figure 5.15. Flow-through DNA purification matrix testbed (a), with 0.45 μ m membrane filters acting to retain the chromatography grade silica gel as shown in electron micrograph (b).

Accordingly, silica gel, the most widely utilised stationary phase for LC, was selected as an alternative. Suspended in 70% ethanol, chromatography grade silica gel of particle size 0.063 – 0.2mm as per figure 5.15 (b) was packed into the testbed column. When tested under pressure using a research syringe pump, this column exhibited an acceptable back pressure at flow rates between 100 μ l and 1000 μ l per minute and was selected for initial DNA extraction experiments.

5.5.3 Temperature mediated DNA elution

A significant number of DNA extraction protocols include a heating of the elution buffer, ostensibly to improve DNA desorption from the silica spin filter matrix. However, whether the inclusion of an incubation step employing a heated buffer

results in any significant increase in nucleic acid yields is unclear. As the stationary phase and DNA purification components are heated to 70°C in the elimination of residual ethanol (as detailed in section 6.3.5), and to 95°C in mediation of strand denaturation prior to analysis (Section 5.6.4), the elution of DNA at elevated temperatures is unavoidable. The available data suggests such temperature exposure has no significant detrimental effects on downstream electrochemical analysis or molecular techniques (Jiang et al., 2005; Rossen et al., 1992; Al-Soud and Rådström, 1998).

5.5.4 Deoxyribonucleases and ribonucleases

As discussed briefly in section 5.4.2, deoxyribonucleases and ribonucleases (DNases and RNases) are enzymes that catalyse the hydrolytic splitting of phosphodiester bonds in the DNA sugar-phosphate backbone and preclude sequence-based analysis. The biosensor platform design outlined to this point has a primary focus on the extraction and analysis of DNA. However, the proposed architecture is equally applicable to hybridisation detection of RNA-based viral strains or messenger RNA (mRNA) sequences. For whatever analytical end, the isolation of DNA or RNA components using the proposed mobile phase-based biosensor platform is straightforward. On completion of wash through of denatured proteins, lipids, and cell debris, the silica stationary phase matrix is incubated with a DNase or RNase buffer as appropriate. This nuclease is then washed out, and the target DNA or RNA is eluted as normal.

5.5.5 Sample separation for analytical validation

In order to facilitate laboratory validation of results generated in the field, the eluted DNA sample is divided between the analytical module and a sterile Eppendorf tube loaded by the operator. While the power and weight requirements of refrigeration effectively prohibit the incorporation of a chilled storage unit within the design of the biosensor platform, the vortex system detailed in section 5.6.4 for 'cold-snap' DNA strand separation may have a secondary application in chilling reference samples for cool-box transport.

5.6 Polymerase chain reaction (PCR) amplification module

As outlined in chapter 3, the multiplication of a DNA target sequence through repeated temperature cycling. As both strands of the DNA double helix are duplicated during each round of amplification, multiplication of the target sequence is exponential in nature, and copy numbers increase 1000-fold after 10 cycles, and 1,000,000-fold after 20 cycles. Accordingly, as part of sample preparation within the biosensor platform, PCR amplification represents a means to greatly increase the number of target DNA sequences available for hybridisation and detection.

From the perspective of electrochemical analysis, increased concentration of the target sequence corresponds to an increase in hybridisation signal and, by extension, a greatly enhanced detection limit in the detection of the target microbe. By amplifying DNA sequences relating to specific species or strains in this way, low numbers of a target microbe may be detected and identified with a greatly increased degree of certainty. Furthermore, the multiplication of genes such as those coding for the 16s ribosomal subunit can be used as a non-specific amplification mechanism and facilitate multiplex detection of selected genes using an array of hybridisation biosensors.

5.6.1 'Hotplate' protocol

As outlined in chapter 3, the amplification of specific gene sequences by PCR is a temperature mediated process. While the development of fluorescence detection technologies and the use of intercalating dyes have enabled the analyst to determine the increase in multiplication product cycle-by-cycle, the underlying technique is essentially no different to the most basic PCR methodologies employing a hotplate and a stopwatch. Consequently, the temperature cycling parameters applied to the denaturation, annealing, and extension of 16s coding regions relating to model organism *Campylobacter jejuni* are well defined (De Boer et al., 2015). However, the quantification of microbial species by PCR is often not as clear cut as presented by the literature. Accordingly, the PCR amplification of the *C. jejuni* was evaluated to determine the analytical limitations of the technique from the perspective of biosensor-based microbial enumeration.

5.6.2 Peltier cell temperature modulation

The prototype biosensor platform is designed to utilise a 22mm Peltier cell (Radio Spares, UK) to cycle the heat to the PCR module via a copper heatsink as in the cell lysis unit. Rapid cooling is provided by a 150mm vortex cooler charged from a CO₂ cartridge (as per section 5.6.4). The temperature profile applied will be that used to determine PCR analytical limitations as above – 600 seconds at 95°C (pre-incubation) and cycling between 95°C (strand separation) and 62°C (primer annealing and sequence extension) for 15 and 30 seconds respectively. The number of cycles will be specified through the user interface according to nature of the sample matrix and the probable number of cells present.

5.6.3 Injection system for primers and *master mix*

The chemistry necessary for PCR consists of target specific DNA primers, polymerase enzymes, and nucleotide bases for the multiplication of the target gene sequence, and a salt component (usually MgCl) as a pH buffer and maintain an appropriate DNA structural conformation. This *master mix* is injected into the PCR module using a TGY-225mg micro-servo activated acrylic dispensing pump as shown in figure 5.16.

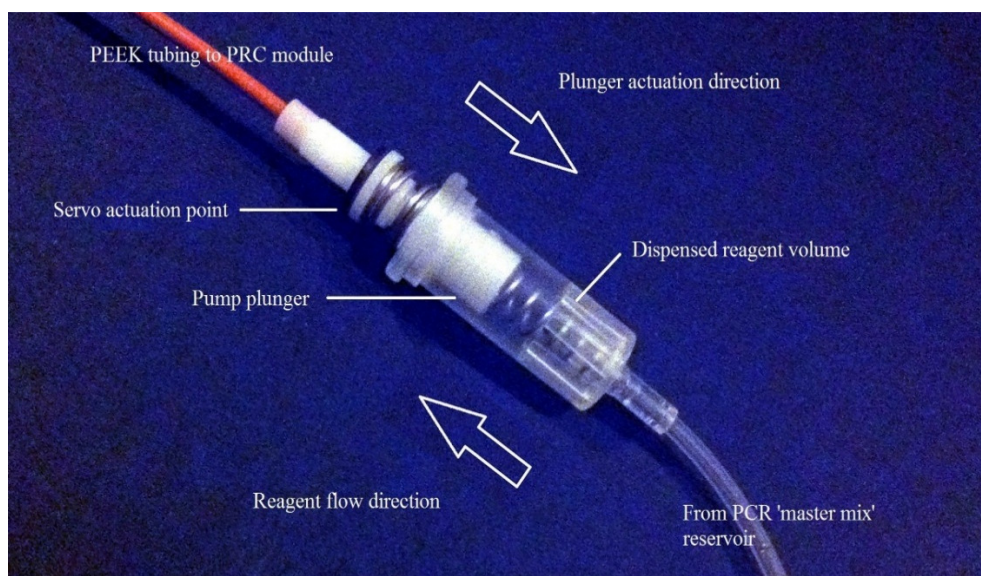


Figure 5.16. Inert acrylic and stainless-steel plunger pump. Injection of PCR components is actuated by an off-the-shelf micro-servo and the pump volume is automatically refilled from the master mix reservoir on return of the spring-loaded plunger.

5.6.4 Vortex *cold-snap* DNA strand denaturation

Hybridisation of the target DNA present in a sample with the probe oligonucleotides present on the biosensor surface is entirely dependent on the target sequence being available in a single stranded conformation. Rapid cooling from 95°C to 0°C removes the energy necessary for the reformation of the DNA double helix, and sample DNA is retained as a single stranded conformation. On return to room temperature, single-stranded target sequences are available to hybridise with probe oligonucleotides immobilised on the biosensor surface. The energetic dynamics dictating the proportionality of double helix reformation versus target-probe binding is not fully understood and may be most usefully determined empirically.

While Peltier cells are widely used to remove heat from electronic components, they are not suited to deliver the cooling necessary to reduce the temperature of reagents in the PCR module rapidly from 95°C to 0°C. Accordingly, the biosensor platform uses a Ranque-Hilsch vortex tube unit (figure 5.17). Effectively a rotor-less turboexpander,

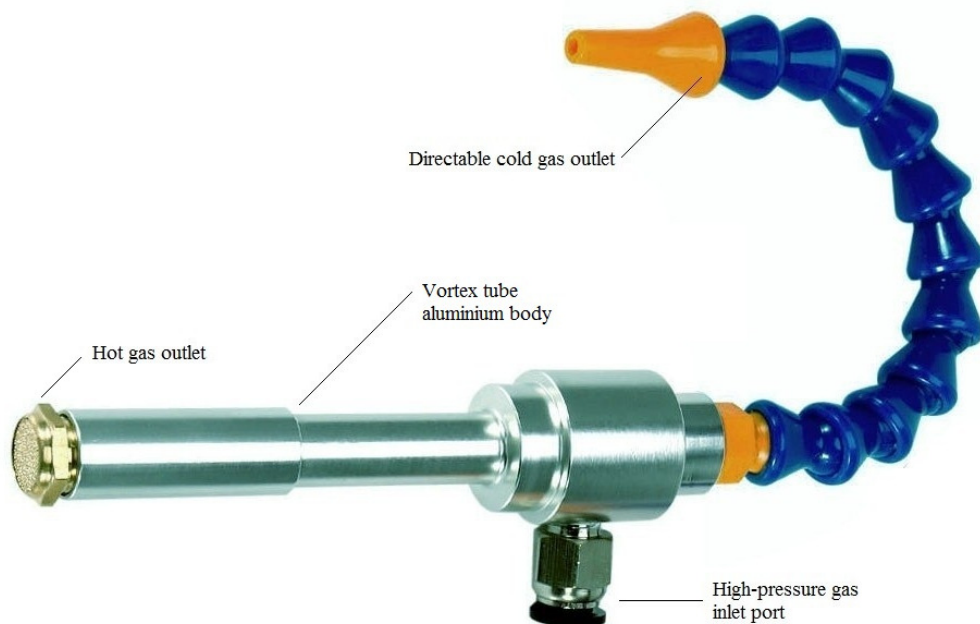


Figure 5.17. 130mm Ranque-Hilsch vortex tube. Integrated within the biosensor platform, the vortex tube provides rapid cooling for temperature mediated DNA denaturation and balances the action of the Peltier cell in cyclic temperature ramping.

the vortex tube utilises a combination of adiabatic gas expansion and centrifugal force to reduce the temperature of a gas flowing along the central axis of the tube. The cold outlet can generate temperatures as low as -50°C , and the hot outlet as high as 200°C .

5.7 Power supply, microprocessor, and electrochemical analysis

As with reagents, the biosensor platform is designed to be self-contained from the perspective of power-supply, process control, and electrochemical analysis. To this end, the prototype is based around an Arduino microprocessor; regulating sample processing and reagent flow via an auxiliary servo board and conducting voltametric analysis through bespoke potentiostat circuitry.

5.7.1 Power supply

Power to the electrical components of the biosensor platform is supplied from a 11.1v lithium polymer (LiPo) battery. Stepper-motors and servo actuation are driven directly from the LiPo at 11.1v, while both the Arduino Uno and the potentiostat circuitry are supplied with 5v by a UBEC voltage regulator.

5.7.2 Arduino micro-controller

Arduino is an electronic platform designed for development of micro-controller systems across a wide range of disciplines. The Arduino platform is open-source platform, with the capacity to drive an output (such as a motor or servo) in response to sensor feedback or according to instructions uploaded from the Arduino PC programming interface. Arduino micro-controllers are inexpensive, easily adapted according to development requirements, and may be extended to connect wirelessly to a smartphone graphic user interface. Specifications for the Arduino Uno are shown in table 5.2 and, as highlighted, the maximum output current is limited to 40/50mA. Accordingly, stepper motor rotation, servo-motor travel, and bead-mill oscillation rates are controlled by a 16 channel 12-bit PWM/servo interface.

Table 5.2. Arduino Uno specifications, highlighting the operating voltage and maximum current draw. 2KB static random-access memory (SRAM) and 1KB electrically erasable programmable read-only memory (EEPROM) allow for process control, potentiostat operation, and Bluetooth data transmission to a smartphone for analysis and presentation.

Microcontroller	<u>ATmega328P</u> 8-bit AVR family microcontroller
Operating Voltage	5V
Recommended Input Voltage	7-12V
Input Voltage Limits	6-20V
Analog Input Pins	6 (A0 – A5)
Digital I/O Pins	14 (6 which provide PWM output)
DC Current on I/O Pins	40 mA
DC Current on 3.3V Pin	50 mA
Flash Memory	32 KB (0.5 KB used by the Bootloader)
SRAM	2 KB
EEPROM	1 KB
Frequency (Clock Speed)	16 MHz

5.7.3 Three-electrode electrochemical cell

The three-electrode cell as illustrated in figure 5.18 forms the basis of the great majority of electrochemical analytical systems and facilitates a characterisation of the interface between the working electrode and the surrounding electrolyte. The surface characteristics of the working electrode (including any surface modification or immobilised biomolecules) and the electrolyte (typically a salt solution) is described by the current generated when a voltage is applied to move the total cell energy away from equilibrium.

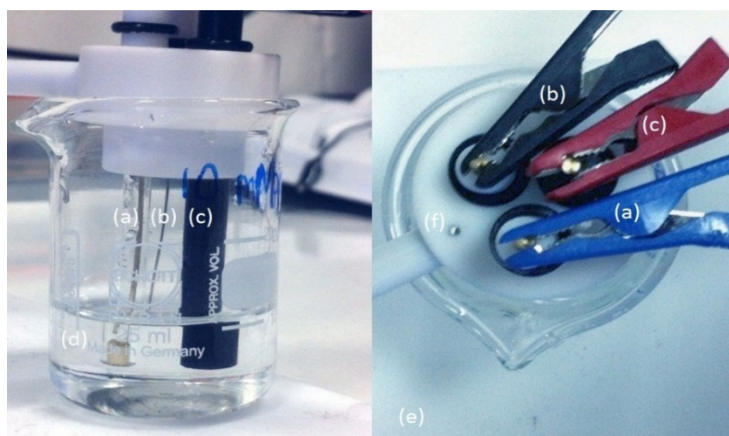


Figure 5.18. A typical research/analytical three-electrode cell comprising reference (a), counter (b), and working (c) electrodes, supported by electrolyte (d). Top view (e) shows the electrode support lid with venting ports to facilitate electrolyte degassing as required (f).

The potential applied through the working electrode is balanced by a fixed-potential counter electrode and is regulated in relation to a reference electrode of known reduction potential. A variety of techniques are employed to drive the three-electrode cell out of equilibrium in a way that generates useful data, but by far the most commonly applied are cyclic voltammetry – the application of a triangular waveform around a zero potential as shown in figure 5.19 – and differential pulse voltammetry – non-cyclic application of the increasing voltage only.

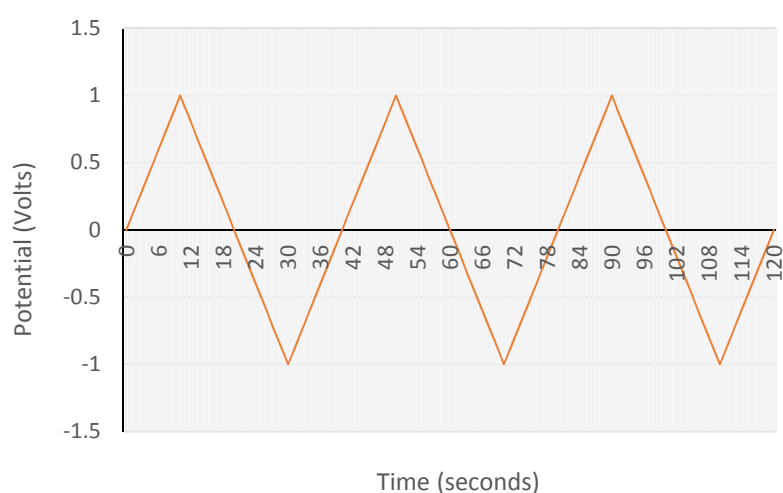


Figure 5.19. Triangular waveform potential as applied in cyclic voltammetry – in this instance diverging from equilibrium by ± 1 Volt with a periodicity of 40 seconds.

The resulting data denotes working electrode properties such as surface charge, capacitance, and conductivity, and electrolyte characteristics such as conductivity and analyte concentration. Figure 5.20 shows a pair of typical cyclic voltammograms with a sweep of ± 0.8 Volts and current generation of approximately $25\mu\text{A}$ to $-30\mu\text{A}$. A decrease in surface capacitance is evident between sweeps as a result of DNA immobilisation on the electrode surface as the nucleic acid molecule acts to regulate the flow of electrons through to the electrode surface. In this instance, the observed paired oxidation and reduction reaction peaks (the REDOX couple) is proportional to a concentration of methylene blue dissolved in the electrolyte solution.

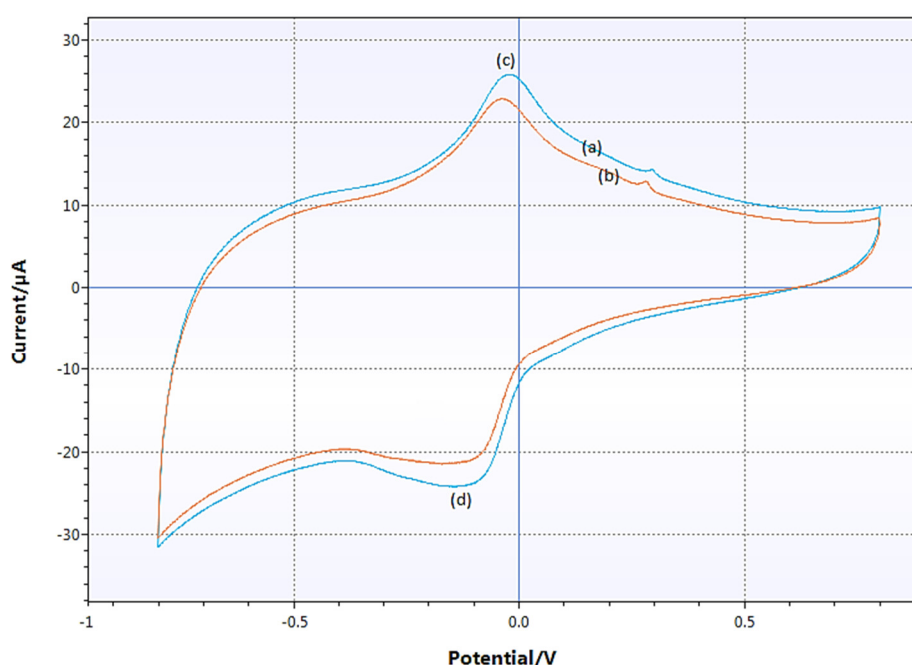


Figure 5.20. Typical cyclic voltammetry traces through a sweep of $\pm 0.8\text{V}$ and showing surface capacitance before (a) and after DNA oligonucleotide immobilisation (b). The REDOX couples (c) and (d) relate to a fixed concentration of the indicator dye methylene blue.

5.7.4 Potentiostat design

In analytical cyclic voltammetry, the generation of a triangular waveform and measurement of the working electrode current are mediated by a potentiostat; a simple circuit that employs operational amplifiers to regulate the potential difference between the working and reference electrodes while the electrical current between

them is recorded. A counter electrode isolates the reference electrode from the charge transfer reaction (Bard et al., 1980). A range of open source coding is available to integrate potentiostat electronics and the Arduino Uno. Figure 5.2.1 outlines the analogue circuitry of the potentiostat and the schematic for integration within the Arduino component of the biosensor platform.

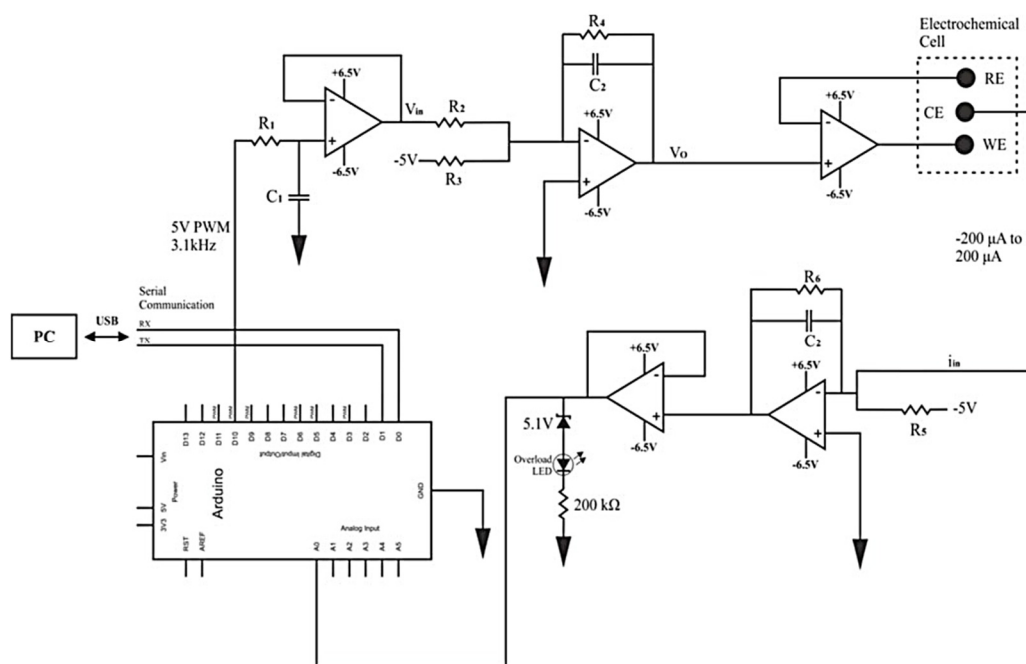


Figure 5.21. Schematic showing the operational-amplifier-based analogue potentiostat circuitry integrated with the Arduino Uno micro-controller through the on-board analogue to digital convertor. The USB interface may be adapted for wireless connection to a smartphone.

5.7.5 Optimisation of electrode characteristics by surface modification

As a consequence of their excellent electronic characteristics and relative low cost, carbon materials are widely exploited as electrode materials in electrochemical analytical applications. However, over the last decades conventional electrode materials such as graphite, glassy carbon, and carbon-based inks have been complemented by electronically superior carbon nanomaterials (W. Yang et al., 2010; Zhu et al., 2012); graphene allotropes (K. S. Novoselov et al., 2004; M. J. Allen et al., 2009), and boron-doped diamonds (Macpherson, 2015; Svítková et al., 2016).

The surface modification of low-cost screen printed, and carbon electrodes enables the electrochemist to control how such electrodes interact with analytes or electrolytes of interest. Accordingly, the modification of conventional electrodes with carbon nano-materials has been the subject of considerable research and has highlighted a wide range of ways in which the exceptional electronic characteristics of such materials may be exploited (Barsan et al., 2015; Sajid et al., 2016; Karimi-Maleh et al., 2015; Velusamy et al., 2011).

In the context of the presented thesis such electrode modification represents a means by which to determine DNA concentrations and levels of DNA hybridisation at lower thresholds and with enhanced detection resolution. This is realised by exploiting the enhanced detection of the oxidation of exposed nitrogenous bases in single stranded DNA, or the catalysis of oxidation and reduction reactions in intercalating/indicator agents such as SYBER-green or methylene blue employing differential pulse or cyclic voltammetry. A combination of excellent conductivity and high biocompatibility mean carbon nanomaterials are ideally suited to this application.

Modifying the active surface of a carbon electrode with nano-material matrix is achieved by adsorption, covalent bonding, or by polymer coating bonding. Adsorption exploits the same types of valence forces involved in the formation of chemical bonds, and the modifying agent is adsorbed as a latticed monolayer. Covalent bonds between a modifying material and an electrode surface generally use agents such as organosilanes (Gayen, 2018; D. Wu et al., 2018) or cyanuric chloride (Yacynych and Kuwana, 1978; El-Moghazy et al., 2018).

Organosilane modification has the advantage of complementing the electronic characteristics of electrode modification materials such as poly(3,4-ethylenedioxythiophene) polystyrene sulfonate (Dąbczyński et al., 2018) (PEDOT). Polymer coating uses chemisorption (S. Wang et al., 2018), physical anchoring in a porous matrix, or electro-polymerisation to fix a polymer film on the electrode surface (Blanco et al., 2018; Velusamy et al., 2011).

Figure 5.22 illustrates the effects of electrode modification by adsorption of 300m²/g graphene platelets to the surface of a glassy carbon electrode (GCE) of surface area 7.07mm², as characterised by cyclic voltammetry. In this instance, 8μl of a 20% graphene platelet suspension in double distilled water was drop coated onto the electrode surface and dried in a nitrogen atmosphere at 40°C. The electrode current generated in response to the applied potential shows a significant increase and can be used to optimise the electrode surface for a specific electrochemical application. Parameters such as film thickness, carrier solvent, adsorption temperature, and drying atmosphere can be adjusted to regulate the electronic and physical characteristics of the modified electrode (Gayen, 2018; Marchena Martín-Francés, 2018).

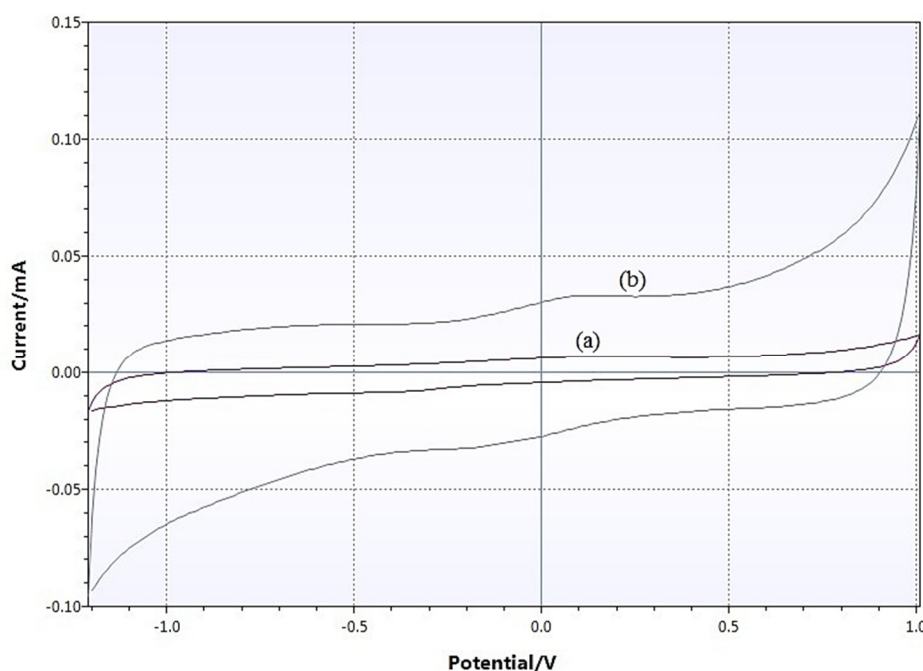


Figure 5.22. Cyclic voltammetry analysis representing the increase in GCE surface capacitance (a) modified by drop-coating 8μl of 20% graphene platelets in DD water and dried in a nitrogen atmosphere at 40°C (b).

A wide range of electrode materials and models have been developed for the detection of DNA hybridisation (Bao et al., 2018; Velusamy et al., 2009; Gooding, 2018; Rajzer, 2017) from wide range of microbial targets. However, with an academic

emphasis on the development of novel materials and techniques, a lesser priority has been given to the refinement, characterisation, and optimisation of contemporary carbon nanomaterials for the routine detection of DNA hybridisation from native DNA samples. While development of the biosensor analytical component builds on the published literature, it has a divergent focus in terms of design criteria.

Unsurprisingly, the electronic characteristics of electrode modification materials is of paramount importance, and consideration be given to their biocompatibility and a capacity to reliably immobilise DNA oligonucleotides with a robustness that prevents their dissociation during sample and reagent flow through. However, the use of low-cost materials such as activated carbons rather than expensive nano-materials has the potential to greatly reduce the production cost of the finished biosensor platform. Equally, both the environmental impact of all materials used, and their recycle-ability represents a production consideration.

The latter is particularly important as the electrode component is likely to be single shot and disposable along with waste reagents requiring that the potential health and environmental impact of electrode nanomaterial disposal must be considered. While relatively limited, the available data indicates a variety of carbon nanomaterial conformations to be hazardous to health and reproductive function (Singh, 2018; Vasyukova et al., 2015; Jia et al., 2005; Hurt et al., 2006). Accordingly, electrochemical surface modification is considered as a way to enhance the electronic characteristics of conventional, inert electrode carbon materials.

5.7.6 Multiplex analysis model

As the basis of microarray and fluorescent in-situ hybridisation analysis (FISH), the surface immobilisation and hybridisation dynamics of DNA oligonucleotides are well characterised in the published literature (Nimse et al., 2014; Flynn et al., 2017; Mannelli et al., 2005). In the detection of hybridisation using intercalating dyes is unchanged by the non-specific adsorption of single stranded DNA to analytical substrates. However, such attachment to the electrode surface has the potential to significantly skew the quantification of probe-target DNA hybridisation when determined through surface capacitance or electron transport in REDOX reactions.

Fundamental to the generation of statistically valid analytical data, the blocking of non-specific DNA adsorption to the electrode surface is also key to facilitating the hybridisation of multiple probe-target DNA combination within a single sample using electrode arrays. When applied to the hybridisation of sequences from several regions within the genome of a specific microbial target, such multiplex targeting has the potential to significantly enhance detection limits and analytical robustness. Alternatively, the targeting of sequences specific to multiple microbial targets may be applied to characterisation of environmental or commensal population dynamics.

5.7.7 Software

All functionality of the biosensor platform is controlled through the Arduino micro-controller. Accordingly, all coding is compiled on the integrated development environment (IDE) interface and uploaded to the Arduino board via a USB connection. The agreed scope of the thesis does not include programming of the user interface, process control, statistical analysis of the potentiostat data, or presentation of the detection results. However, it is useful to outline the role of the Arduino in the context of process control, and to demonstrate the unit's capacity to reproduce the cyclic voltammetry technique applied in the experimental detection of DNA hybridisation presented in chapter 6.

5.7.7.1 Process control

As the biosensor platform is designed to be operated minimal user input beyond the initial setup, all functionality following sample loading is controlled by the Arduino. Analysis of differing cell types or sample matrices will require the operating parameters of the biosensor platform to be modified by the user. Accordingly, a bespoke app running on an Android smartphone will allow the user to select specific sample processing options according to the constraints of the sample matrix. Compiled as a sketch file, this selection is wirelessly uploaded to the on-board Arduino, and functionality of the biosensor platform modified accordingly.

5.7.7.2 Analytical graphic user interface

In outlining the principle underlying the electrochemical analytical techniques of differential pulse and cyclic voltammetry above, the sample analytical plots were generated using highly specialised software designed for electrochemical research applications. However, projected users of the biosensor platform are unlikely to have any use for the great majority of the data presented. Accordingly, the data output from the Arduino-potentiostat must be processed and presented in a simple format. To this end, initial design specifications outlined a simple traffic light system – with red signifying target contamination and so forth.

Building from the Arduino open source code library (Arduino, 2015), a simple cyclic voltammetry Arduino sketch was constructed to run with the potentiostat circuitry outlined in section 5.7.4. The Arduino integrated drive electronics (IDE) interface facilitates both the voltage applied and the corresponding generated current to be viewed as plotter or monitor output as illustrated in figure 5.23. This Arduino monitor output can be wirelessly transmitted to the paired smartphone app as a comma separated value (.csv) file for tabulation and statistical analysis.

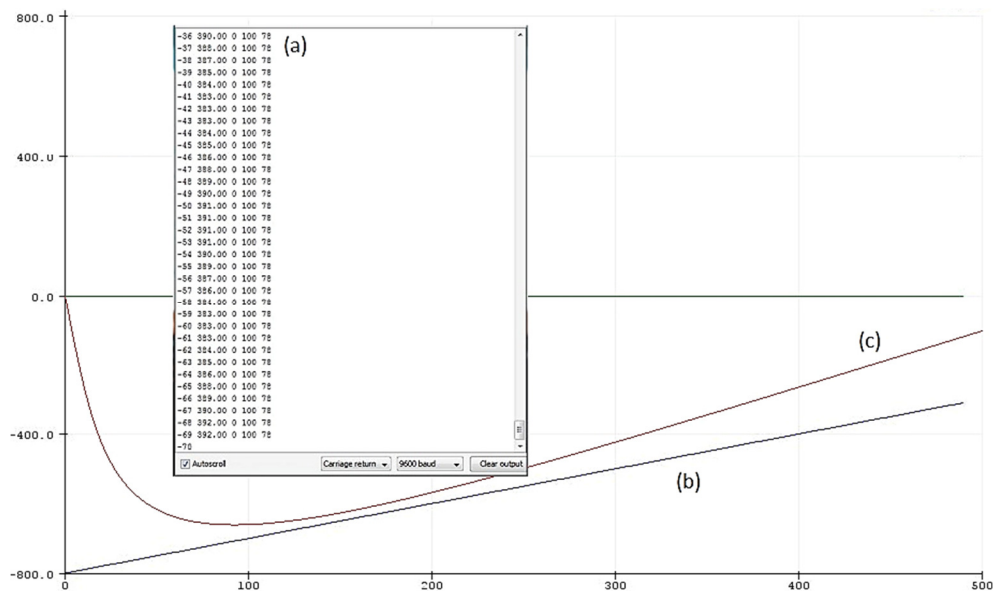


Figure 5.23. Arduino-potentiostat data as a comma separated value monitor output (a) for wireless transmission to the paired smartphone app for statistical analysis, and as a plotter output charting voltage (b) against current (c).

The model for analysis compares electrode values prior to sample introduction (control) with those after hybridisation of target DNA with electrode immobilised probe oligonucleotides (sample). By routinely running 5 or more voltammograms in per analysis, method variance can be considered when comparing control and sample data for statistically significant differences. Alternatively, the data for a given sample may be related to a pre-determined standard curve to generate an approximate number for the microbial cells present in the sample.

5.8 Materials

Components used in the containment or transport of reagents within laboratory and pharmaceutical equipment are typically made from stainless steel of grade 316 or 316L. However, stainless steel is expensive, heavy, and can be very challenging to machine. Accordingly, the effects of long-term exposure to acid and alkali salt solutions must be established for alternative construction and seal materials. Over the course of the developmental process, acrylic sections, nylon pieces, and nitrile O-ring samples were immersed in the biosensor platform adsorption buffer (5M GuHCl, 20mM Tris-HCl, 38% ethanol) and wash buffer (20mM NaCl, 2mM Tris-HCl, 80% ethanol), buffered to pH4.2.

With a relatively high salt and ethanol content combined with a moderately acidic pH, the immersion test was designed to examine the effects of long-term reagent exposure on the materials used in construction of the biosensor macro-fluidic components. The nylon used for high temperature processes and the nitrile O-ring seals used throughout are specified for resistance to high salt concentrations, ethanol containing solutions and reduced pH. However, the reagent carousel, switchable valve parts, analytical cell, and primary waste reagent reservoir/withdrawal syringe are machined from acrylic. Degradation or reconstruction of acrylic surfaces has the potential to be detrimental to the integrity of syringe and valve O-ring seals, permitting cross contamination of reagents and processes. Equally, surface porosity has the potential to entrap DNA molecules and influence the analytical performance of the biosensor.

Figure 5.24 shows electron microscopy of acrylic samples immersed in a combination of adsorption buffer and wash buffer for test durations of 10, 20, 30, 40, and 60 days. At a 10 μ m scale, there is obvious surface reconstruction over the treatment duration. However, a progressive accumulation of salt residue appears from day 20 onward. The salt build-up is easily removed using distilled water and is unlikely to influence the performance of the biosensor. Salt accumulation did not affect syringe pump performance in the prototype biosensor platform.

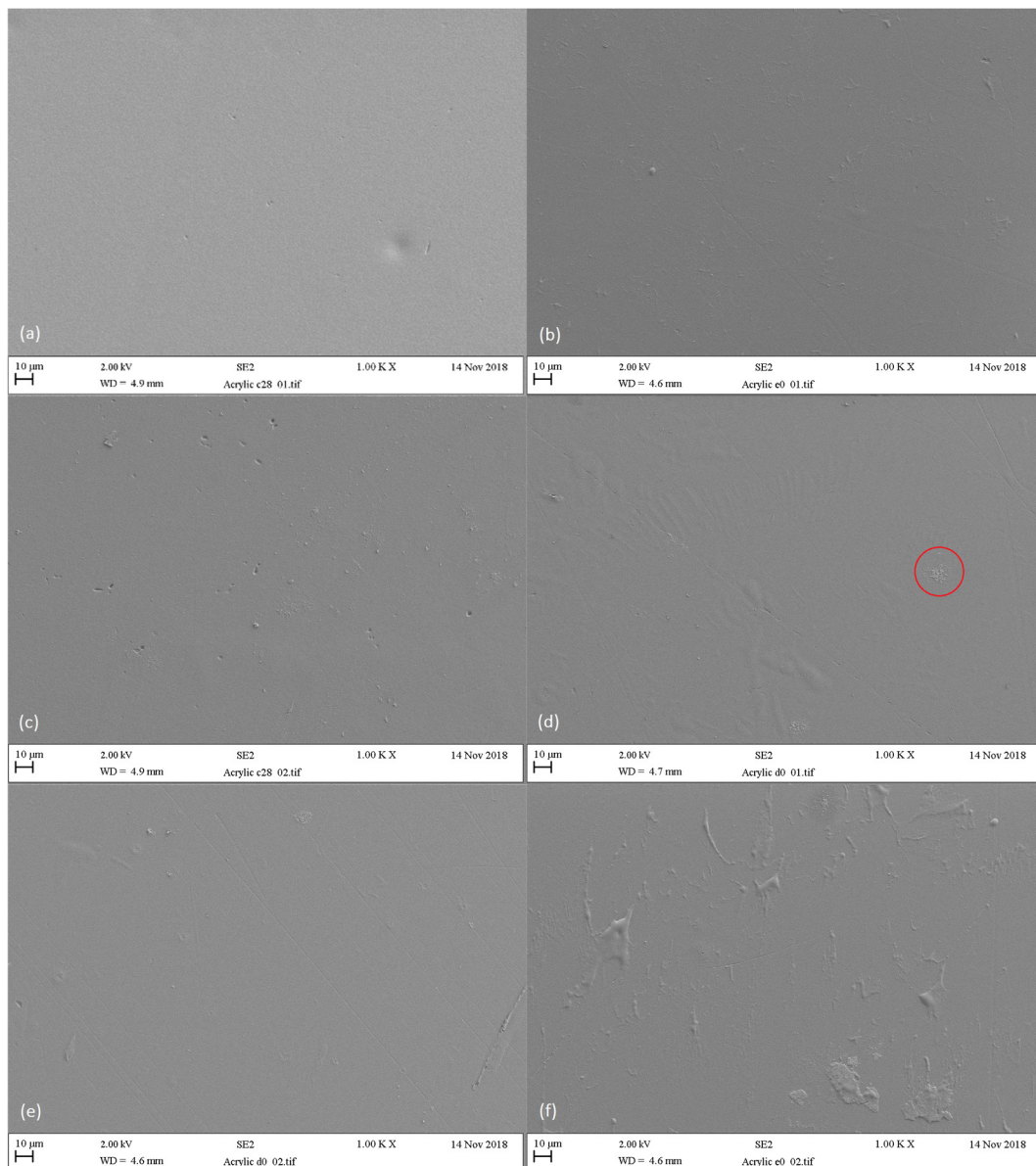


Figure 5.24. Electron microscopy of acrylic surfaces treated with a solution of adsorption buffer and wash buffer at pH4.2, from time (t)=0 (a), t =10 days (b), t =20 days (c), t =30 days (d), t =40 days (e) and t =60 days (f). Salt accumulation is obvious from t =30 days (circled).

Chapter 6.

Results and discussion

6.1 Introduction

Chapter 6 presents the experimental validation of the techniques and principles outlined in the previous section. As in chapter 5, the findings described are presented according to the order in which a sample is processed by the biosensor platform. Accordingly, data is presented in three sections – microbial cell lysis, DNA extraction and purification, and electrochemical analysis of probe-target DNA hybridisation. Where it is relevant, task-specific electronic and engineering solutions are described in the context of their use within the field-portable biosensor platform.

6.2 Microbial cell lysis module

The prototype cell lysis unit as detailed in section 5.4.3 was employed as a test-bed to evaluate the efficacy of the microbial cell disruption techniques proposed for inclusion within the biosensor platform - mechanical stresses, temperature, hydrostatic pressure, detergents, and chaotropic agents. Performance of the module was characterised for the disruption of a 1ml sample of *Campylobacter jejuni* ATCC 33291 containing approximately 3,500 cfu/ml as determined using culture-based methods.

A test-bed version of the reagent syringe pump was constructed from the components shown in figure 6.1 and combined with a pressure regulator as in figure 6.2. With a nominal volume of 50ml (excluding the combined seal and piston volume), the reagent compartment was backfilled with 30ml lysis buffer via the PEEK flow line. A pressure reservoir volume of 20ml was charged to 350kPa. The expulsion of 15ml reagent resulted in a pressure reservoir volume increase to 35ml and a corresponding drop in pressure to approximately 200kPa. The 1ml microbial cell sample was introduced via an in-line HPLC mixer valve at a ratio of 1:1.2 sample to lysis buffer. A research-type withdrawal syringe pump was used to maintain a 500 μ l per minute flow rate by regulating the displacement of Millipore water (acting to maintain hydraulic pressure within the experimental system) via the DNA purification module.

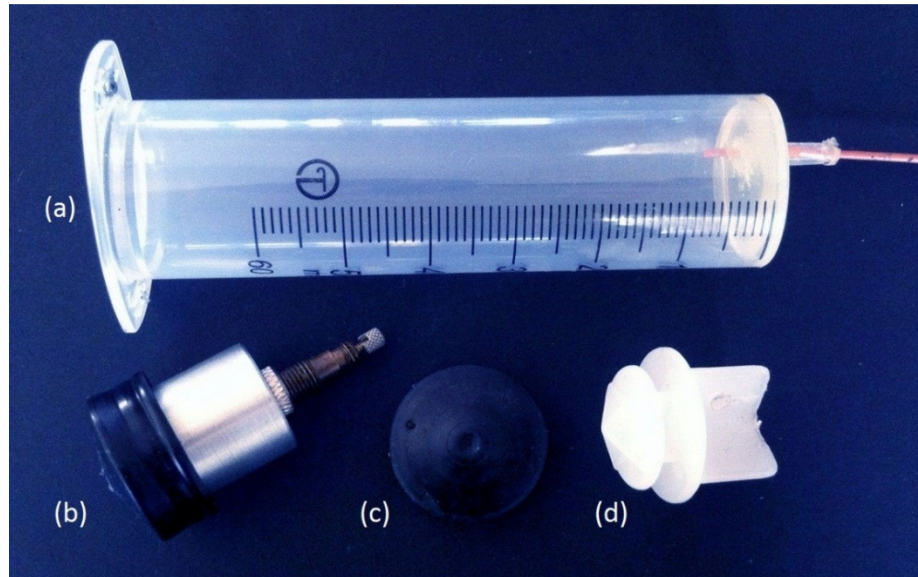


Figure 6.1. Prototype pressure driven syringe pump employed in experimental reagent delivery; with syringe and PEEK flow line (a), sealed valve body (b), seal (c) and piston (d).

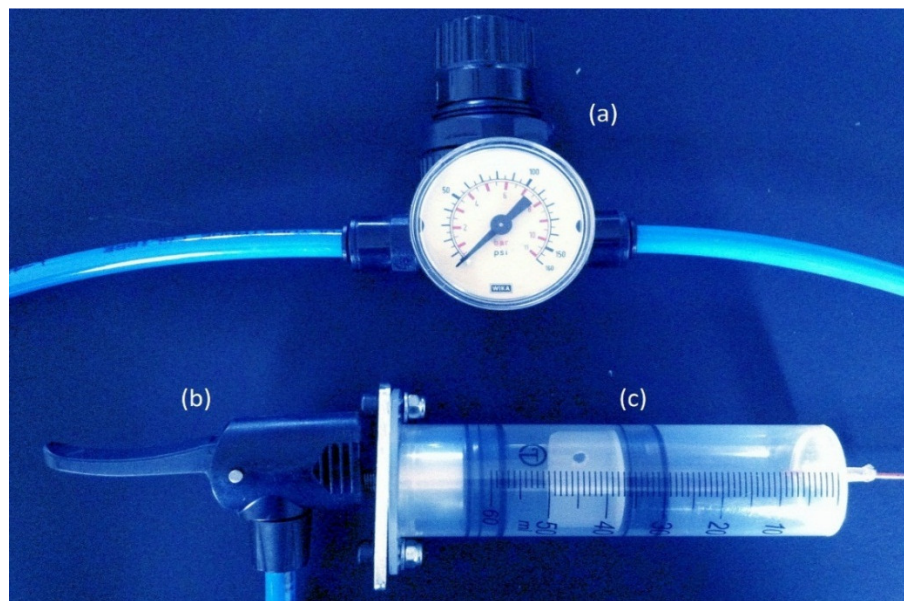


Figure 6.2. Regulator (a) controls the gas pressure from a high-pressure reservoir, via a Presta valve fitting (b) to the syringe reservoir, driving travel of the piston (c) to displace the reagent.

A pair of pressure driven syringe pumps as above were used to deliver reagents through the course of multiple experiments aimed at characterisation of the lysis and DNA purification components of the biosensor platform. Over more than 100 delivery cycles, the constructed test-bed units performed consistently in terms of reagent

displacement and reservoir de-pressurisation and serve to demonstrate the validity of these design principles as a basis for the pressure driven reagent carousel outlined in section 5.2.4.

6.2.1 Robustness in cell lysis and nucleic acid extraction

While deactivation of the great majority of archaea, bacteria, fungi, and protists is relatively straightforward using techniques such as steam autoclave disinfection, the residual cells can be highly resistant to disruption. This resilience stems from the expression of cell wall materials such as peptidoglycan in bacteria or β glucan in yeasts (Perkins, 2012; Erwig and Gow, 2016; Chisti and Moo-Young, 1986) and can vary significantly both within and between microbial species. Furthermore, the encapsulation of dormant and VBNC cells, conferring protection against UV radiation, freeze-thaw cycling, and high salinity, can significantly enhance cell durability (S. Zhang et al., 2015; Besnard et al., 2002b; Handa, 2018).

Detergent/chaotrope-based kits demonstrate a capacity to ensure the disruption of all of the target microbial cells present in a sample by rationalising the lysis of a wide range of potential cell structure variables into a relatively small number of protocol and reagent combinations. Accordingly, a single product may be applicable to cell lysis and DNA extraction across a broad variety of protist, yeast, and bacterial targets.

The wide-ranging specificity of commercial cell lysis and DNA extraction kits is attributable to the relative stability and negative charge intrinsic to nucleic acid polymers. Provided that a pH appropriate to the target DNA is maintained, concentrations of the detergent and chaotropic salt components can be adjusted to maximise the robustness of the lysis buffer and method. The FDA (Food and Drug Administration) regulatory guidelines (Branch, 2005) defines analytical robustness as 'a measure of its capacity to remain unaffected by small, but deliberate variations in method parameters'.

Extending this principle to include the design of detergent/chaotrope-based microbial cell lysis protocols, robustness may usefully be defined as the capacity of a

cell lysis methodology to be unaffected by variation within the sample matrix. Accordingly, a robust lysis buffer/protocol combination should efficiently disrupt all the cells present in a given sample regardless of number of microbial cells present and the expression of environment-specific conformations increasing cellular resilience. This approach is applied very successfully as the basis for a great majority of the commercially available DNA extraction kits.

6.2.2 Lysis buffer

A lysis buffer of 1% sodium dodecyl sulphate (SDS), 4M guanidine hydrochloride, and 0.5M potassium acetate at pH4.2 was employed in the characterisation of the test-bed lysis unit. For the initial experiments, this was combined with an equal cell sample volume of planktonic *C. jejuni* cell at a concentration of approximately 10^6 cfu/ml. No significant difference in subsequent DNA yield was noted in comparison of the experimental lysis buffer performance with that of a Congen bacterial DNA extraction kit (Congen, Germany). This ratio was increased to 1:1.2 (sample: lysis buffer) to further enhance the robustness of the experimental method with no significant effect on DNA extraction yields or fragment size.

6.2.3 Temperature and pressure

In terms of energy consumption and the specification of both heater matrices and construction materials, there are obvious advantages to conducting processes such as cell lysis at the lowest practical temperature. However, both the membrane disruption and protein denaturation characteristics of SDS and GuHCl are considered temperature dependent. Figure 6.3 shows the effect of pressure (~ 300 kPa) and lysis temperature on DNA yield (as determined by spectrophotometry) from *C. jejuni* ($\sim 10^6$ cfu/ml) over the range 20°C to 100°C. Control denotes the DNA extraction yield from the same sample and lysis buffer using a standard protocol. Both standard control samples and those processed using the prototype lysis unit were agitated at 900rpm for 10 minutes.

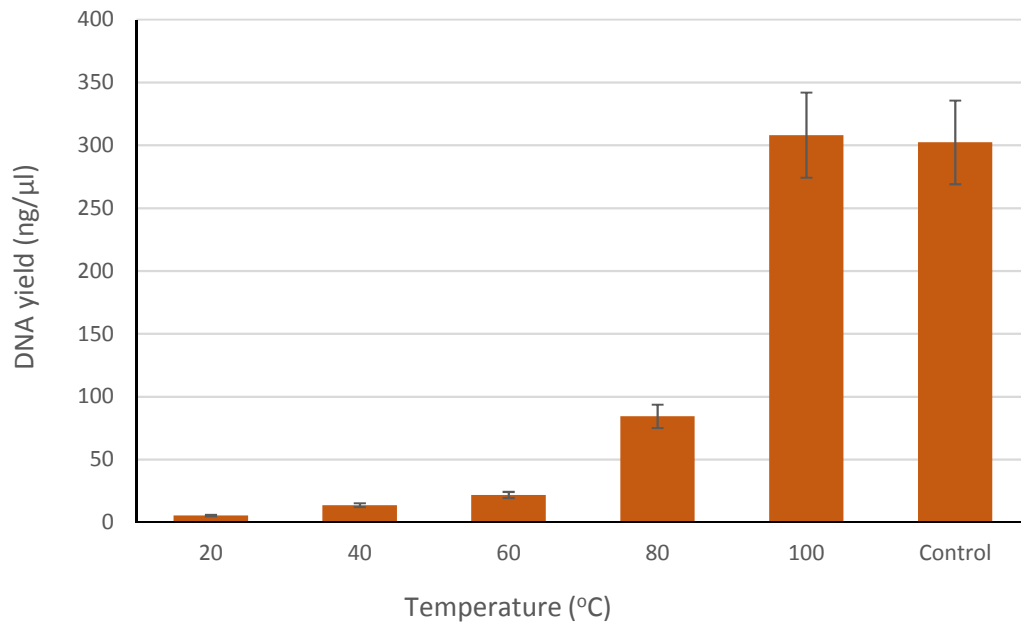


Figure 6.3. Showing the effect of cell lysis temperature on subsequent DNA extraction yield as determined by spectrophotometry for planktonic *C. jejuni* lysis ($\sim 10^6$ cfu/ml) at a pressure of approximately 300kPa. Control sample denotes the DNA yield extracted using a standard protocol. Error bars represent experimental variation as a percentage of the yield value, $n=6$.

Based on comparison of the control group (99°C/ambient pressure) and the 100°C/300kPa lysed sample, pressurisation of the lysis unit appears to have no statistically significant effect on cell lysis and DNA recovery. The relationship between DNA extraction yield and temperature on the other hand, describes a near-exponential association between 100°C and 20°C and is likely to reflect SDS/GuHCl activity in cell lysis and in prevention of target DNA degradation by nucleases. DNA yields at 20°C may correspond to extracellular DNA present in the sample matrix, to low-level SDS and GuHCl activity, or to a combination of both.

Extension of the lysis process duration at 60°C or 80°C is likely to increase DNA yields, possibly to concentrations approaching those of the control samples. However, doing so both prolongs the timescale of the biosensor analytical process and increases the potential degradation of target nucleic acids by constituents of the lysed cell such as lysosomes, nucleases, or other enzymatic proteins. Over a protocol duration of 10 minutes, an increase in lysis chamber temperature from 100°C to 110°C generated

no significant increase in DNA yield (n=2). While such higher lysis temperatures may facilitate shorter protocol durations, the advantages of a reduced process duration may be negated by a corresponding reduction in method robustness.

A consequence of the pressurised reagent delivery model employed in the biosensor platform is an increase in the maximum temperature which may be applied without causing the water-based mobile phase to shift from a liquid to a gas phase. At sea-level atmospheric pressure, 101.3kPa, this phase shift occurs at 100°C and is part of the reason standard lysis protocols are conducted at 99°C; to limit both pressurisation and reagent loss to condensation on the inside of the reaction tube. The biosensor platform macro-fluidic component is designed to operate to a minimum pressure of 200kPa, corresponding to a phase shift temperature in water of 120.2°C. Accordingly, a process temperature of 100°C provides a buffer of +20.2°C below the liquid to gas phase transition point.

However, as field-portable biosensor platform with potential application at low temperatures, it may be appropriate to utilise a process temperature of 105°C. This will allow a $\pm 5^\circ\text{C}$ operating range within which the data indicates a high degree of method robustness but retains a 10°C buffer with the phase transition point. Furthermore, maintaining an operating temperature of $105\pm 5^\circ\text{C}$ represents a lesser challenge than that of $100\pm 1^\circ\text{C}$ or $100\pm 2^\circ\text{C}$, particularly over wide or fluctuating temperature ranges in a food processing, water supply or environmental setting.

6.2.4 Electromagnetic sample agitation

In the context of DNA extraction from the study model organism *C. jejuni*, the prototype lysis unit demonstrates a cell disruption capacity on a par with those commercial, miniprep-based methodologies widely applied in the laboratory. Accordingly, the unit may be considered equally applicable to DNA extraction from pathogens sharing *Campylobacters* Gram-negative cell structure. These include *Escherichia coli*, *Pseudomonas spp.*, *Salmonella spp.*, and *Enterobacter spp.*, and other bacterial species contributing to the transmission of antibiotic resistance within the environment.

It is not uncommon for techniques, protocols, and microfluidic devices specific to DNA-based detection of microbial pathogens to demonstrate a significantly lower sensitivity toward Gram-positive bacteria and yeasts than to Gram-negative species (Morgenthaler and Kostrzewa, 2015; Mahalanabis et al., 2009; Ulrich and Hughes, 2001). Given the universality of DNA and identical techniques used in the genomic analysis of the target species for each study, these differences point to inadequacy in the cell lysis techniques applied to disrupting the more robust peptidoglycan or β glucan cell wall structures in these cells (Brown et al., 2015; Jordan et al., 2008; Pancholi and Chhatwal, 2003; Saha et al., 2013).

In the context of consumer safety or clinical diagnostics such shortcomings could have serious repercussions. Bead milling is considered the most effective way to break down durable cell types (Salonen et al., 2010; Zhou et al., 1996; Shehadul Islam et al., 2017) and, as in the design of temperature or chemical protocols, the degree of mechanical stress applied during the milling process must be balanced against the potential fragmentation of released DNA strands. To this end, and as detailed in chapter 5, the biosensor platform incorporates a novel electromagnetic bead mill.

SDS page electrophoresis was employed to evaluate the performance of the bead mill process and to determine the relative size of DNA fragments by comparing their travel through the SDS gel matrix relative to a standard sizing ladder. Travel is driven by attraction of the negatively charged DNA phosphate backbone from the wells at the top of the gel toward the positively charged anode at the bottom. The rate at which the DNA strand moves through the SDS gel is analogous to the movement of a conga line through a crowded festival square – the longer the DNA strand the more it must thread its way through the gel matrix and the shorter the distance travelled over any given period.

Figure 6.4 shows the SDS electrophoresis of DNA samples from detergent/chaotrope lysed samples without agitation. Lanes 5 -7 were lysed at 100°C/300kPa compared with lane 9, lysed at 99°C and ambient pressure. As with the DNA extraction data

based on spectrophotometric analysis, there appears to be no significant in fragment size because of the difference in lysis pressure. In both the control and the lysis unit samples, the *C. jejuni* DNA forms sharp bands of regular length and indicates DNA fragments of uniform length; suggesting excision of the bacterial genome at regular intervals. Although the band size falls beyond the sizing ladder, the scale described is broadly logarithmic in nature, and indicates a molecular weight of approximately 700kDa equating to DNA fragments approximately 1075 base pairs (bp) in length.

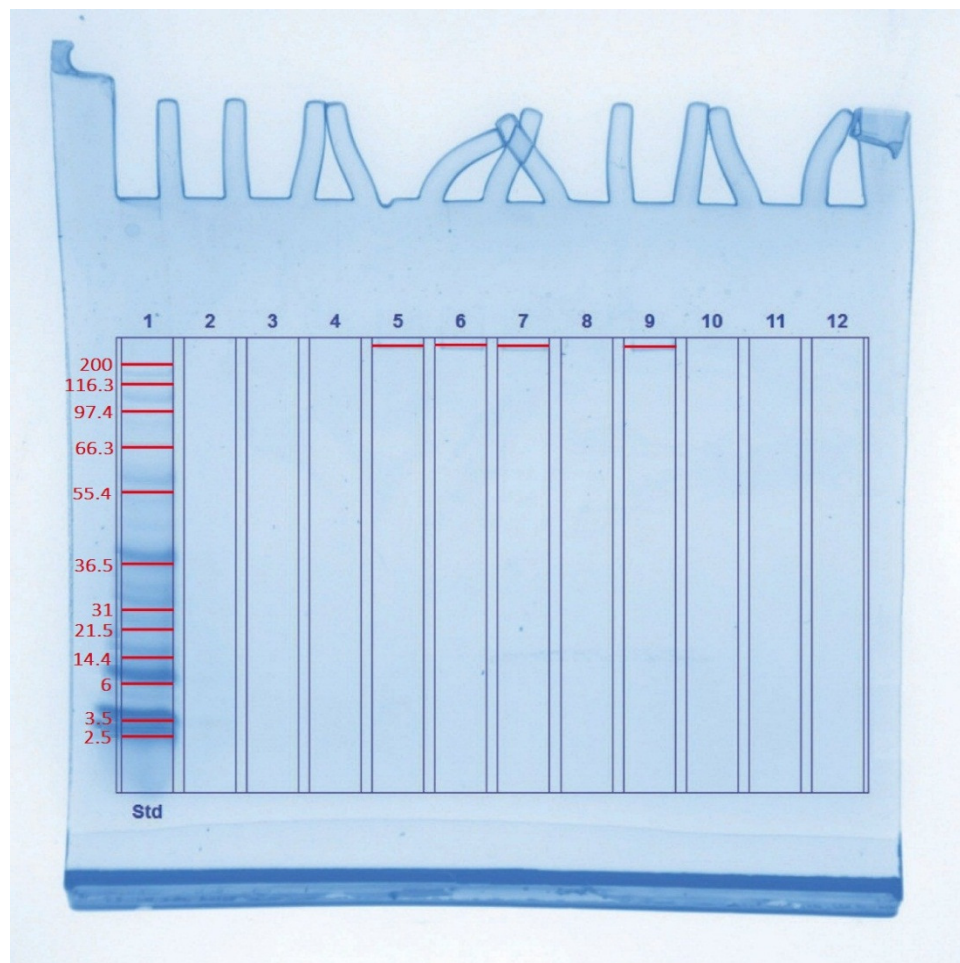


Figure 6.4. Relative size-based separation of *C. jejuni* genomic DNA by SDS page electrophoresis, showing DNA fragmentation from SDS/GuHCl-based *C. jejuni* cell lysis. Lanes 5, 6 & 7 contain samples lysed at 100°C and 300kPa. Control (lane 9) was lysed at 99°C at ambient pressure. No sample agitation was applied during cell lysis. Standard ladder (SeeBlue™ Pre-stained Standard, Invitrogen, USA) relates molecular weight.

Provided the primer regions for amplification of the target sequence fall within the excised section, DNA fragments of this size are well suited to PCR amplification for microbial identification purpose. Amplicons ranging from 200bp to 800bp in length are typically used in multi-locus genotyping and bacterial discrimination at a sub-species level (Klena et al., 2004; Mahendran et al., 2011; van der Graaf-van Bloois et al., 2013). The steric interactions inherent to the interactions of target sequences of this length can generate variation in target-probe hybridisation but can be effectively mitigated through appropriate immobilisation strategies and the use of intermediary REDOX reporter molecules (Ferapontova, 2018; Ozkan-Ariksoysal et al., 2017; Singhal et al., 2017).

Figure 6.5 outlines the effects of shaker plate and electromagnetic bead mill agitation on the fragmentation of DNA from planktonic *C. jejuni* during cell lysis. The samples in lanes 3, 4, and 5 underwent a standard 900rpm shaker-plate protocol at 99°C as per the Congen miniprep kit protocol. In contrast to samples lysed without agitation, each loaded sample lane shows a degree of staining throughout the gel, and between the loading wells and the 200kDa marker (307bp) in particular. The relatively uniform nature of staining across lanes 2, 3, 4, and 5 indicates a background of DNA fragments distributed over the length of each lane and suggests random breakage of the bacterial DNA polymer by shear stresses inherent to the lysis buffer agitation.

Against this background, several distinct bands indicate a more defined separation of the bacterial DNA into three segments, approximately 95kDa/146bp (a) 40kDa/61bp (b) and 21.5/33bp (c) in length, and indicative of genomic or plasmid breakage at sequence specific sites. As a methodology aimed at simulating the shaker-plate action, agitation of the lysis unit at 60rpm mimics both the non-specific liquid shear stress and site-specific genome breakage, albeit with fewer fragments in the order of 61bp (b) or 33bp (c). DNA fragments between 33bp and 146bp are closer in length to oligonucleotides used in DNA hybridisation biosensors in the published literature and typically around 20bp (Jafari et al., 2015; X. Liu et al., 2016; Flynn et al., 2017).

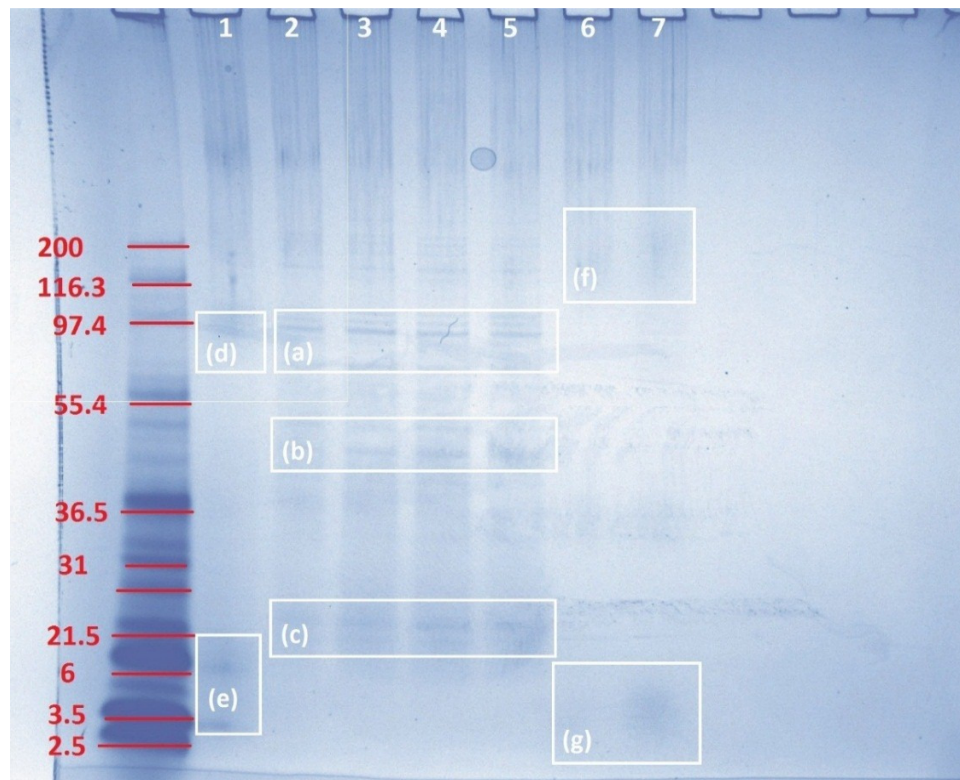


Figure 6.5. Gel electrophoresis separation of *C. jejuni* DNA by standard shaker-plate method at 900 rpm and 99°C (lanes 3, 4 & 5) and utilising the cell lysis unit at 100°C and 300pKa: single 9mm bead - 60 rpm (lane 2), 3 x 9mm beads - 300rpm (lane 1), 4 x 5mm beads - 300rpm (lane 6) and 2 x 5mm beads with 15 x 1mm beads- 300rpm (lane 7). Significant banding patterns are labelled (a) through (g). Standard ladder (SeeBlue™ Pre-stained Standard, Invitrogen, USA) relates molecular weight.

In contrast, lanes 1, 6 and 7 show samples disrupted by electromagnetic bead mill techniques and with the genomic DNA is broken up into less distinct bands and varying in size according to electronic actuation parameters and the milling components employed. In this instance, bead mill cell lysis appears to generate DNA fragments unsuited to electrochemical detection of DNA hybridisation, and indeed may have made a significant contribution to DNA degradation in the process. However, these results support the provision of customisable bead mill options within the biosensor platform setup. Adjusted according to those structural elements present in the outer wall or encapsulation of the target organism, the DNA extraction process can be balanced between providing enough force to lyse the chosen cell types while keeping DNA degradation to a minimum.

6.3 DNA purification module

While the action of the lysis unit mediates the release of nucleic acids from microbial target cells and dictates fragment length, the purification module efficiency determines the yield and purity of the DNA sample available for analysis. The design criteria for a pressure driven flow-through purification matrix highlights four primary variables with an effect on the performance of the purification module:

1. Flow rate – Reagent flow rate through both the lysis unit and the DNA purification column should ideally balance a minimal process duration against the introduction of flow induced shear stresses and the formation of eddies with the potential to aggregate nucleic acids and cellular components. The effects of temperature and sample viscosity must be considered to ensure protocol robustness.
2. DNA binding capacity of the stationary phase material – mediated by chaotrope salt water sequestration and the positive charge saturation of the silica surface.
3. DNA binding surface – smaller stationary phase grain sizes deliver greater surface areas for the same column volume.
4. Column back pressure – smaller grain sizes result in a greater column back pressure directly proportional to the column cross-sectional area.

6.3.1 Silica gel DNA extraction

As determined for a reagent combination of 1ml Bolton broth and 1.2ml lysis buffer, flow rates at and above 180 μ l per minute resulted in non-laminar flow exiting the 1mm PEEK line into a larger fluid reservoir. Accordingly, a provisional flow rate of 120 μ l per minute was applied in all subsequent extraction protocols, allowing a 50% protocol robustness safeguard. Preliminary experiments demonstrated the validity of column-based model DNA extraction using *Fluka* chromatography silica gel (0.063mm to 0.2mm particle size and surface area of 470-530m²/g). Initial DNA recovery in the region of 15% Congen miniprep control samples and an inherent system back pressure limiting reagent flow rate indicated the primary areas to be addressed.

As a means to reduce system pressure, increasing the column cross-sectional area is preferable to increasing the particle size as it does not reduce the surface area available for DNA binding. Consequently, a commercial HPLC column of internal diameter 10mm (cross-sectional area 78.54mm²) was modified using an acrylic insert to allow a stationary phase volume of approximately 340mm³ with a free reagent volume of 200μl for DNA elution (4.2mm depth). As shown in figure 6.6, the stationary phase matrix is contained by 2 x 10μm frits (b), the second fitted after pressure filling the column (c). The lysed sample and subsequent wash-through and elution buffers are driven through the DNA purification module inlet (a) via lysis unit.

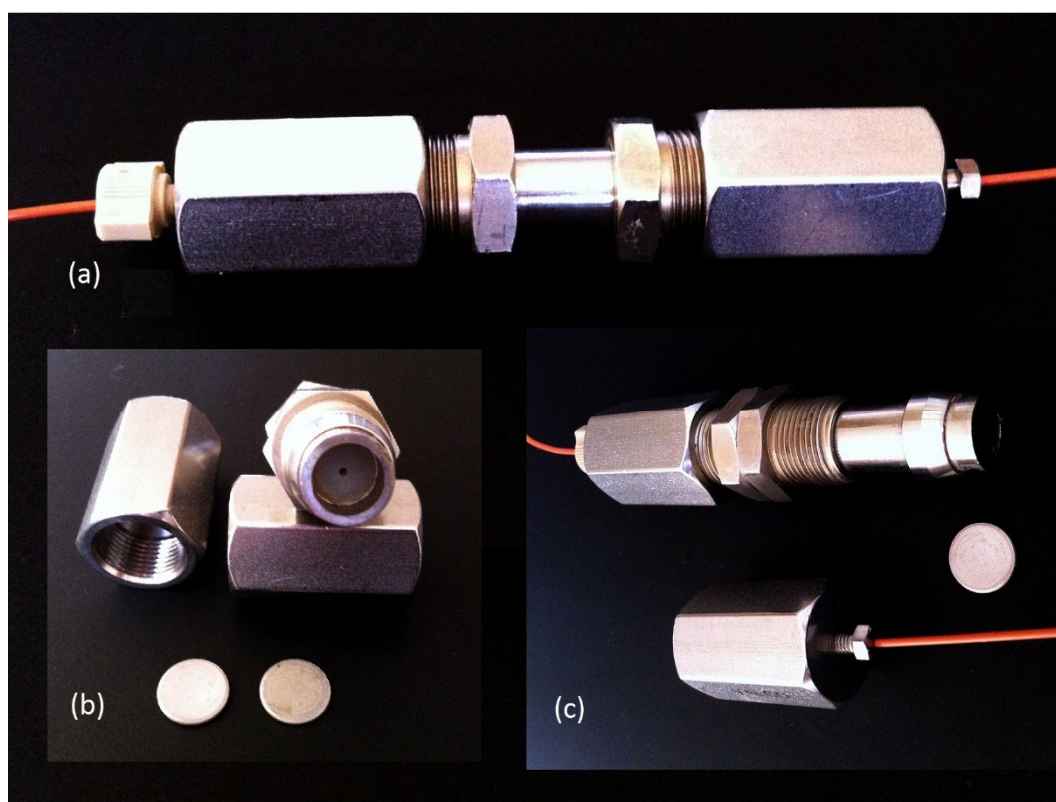


Figure 6.6. Modified 10mm stainless-steel HPLC column, detailing PEEK tubing connected via 10 32 fitting (a) acrylic volume adjustment spacer, pressure fittings, and frits (b); and inlet pressure fitting removed for frit fitment following pump filling of the stationary phase (c).

DNA extraction yields for the *Fluka* silica gel matrix relative to that of the *Congen* miniprep kit (n=5) are presented in Figure 6.7. The modified column (protocols 3 & 4b) shows a significant increase in yield over the high pressure 3mm prototype (protocols

1 & 2) but at levels well below those of the control. This was attributed to ethanol contamination and confirmed when the samples remained liquid when stored at temperatures below freezing.

Residual ethanol from cell debris wash through effectively dilutes elution buffer, prevents rehydration of the matrix-bound DNA and prevents its elution. Flushing the column with compressed air to purge any residual ethanol prior to introduction of the elution buffer resulted in a significantly higher yield (protocol 5 - 500 μ l per minute for 5 minutes, 5b - 1000 μ l per minute for 5 minutes). Investigating alternative materials within the scope of the study, borosilicate glass particles were identified as performing consistently in the extraction of plasmid and genomic DNA (Woodard et al., 1994; Padhye et al., 1997) and the purification of sequences from electrophoresis gels (Vogelstein and Gillespie, 1979).

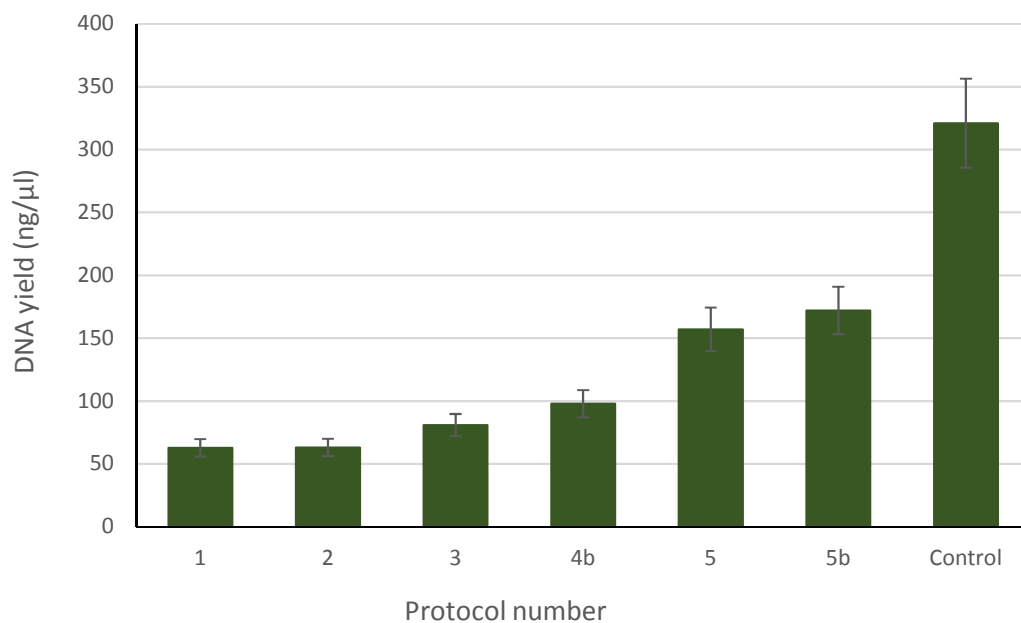


Figure 6.7. Showing DNA recovery over the DNA purification protocol development utilising a 'Fluka' silica gel stationary phase matrix of particle size 63 μ m to 200 μ m with 200 μ l free volume relative to Congen miniprep yield. Error bars indicate variation based on control samples and miniprep extraction protocol, n=5.

6.3.2 Borosilicate glass DNA extraction

Borosilicate (silica and boron trioxide) glass samples were acquired, ground, and Endecott screened to size 0.1mm to 0.125mm. The scanning electron microscopy shown in figure 6.8 highlights the highly granular nature of the resulting matrix and suggests a bias toward smaller particles, possibly attributable to the milling process, as opposed to the more uniform larger particles of the Fluka chromatography silica gel. As a HPLC column stationary phase, the borosilicate demonstrates a performance superior to that of the silica gel and returned significantly higher yields than those achieved using the Congen miniprep kit.

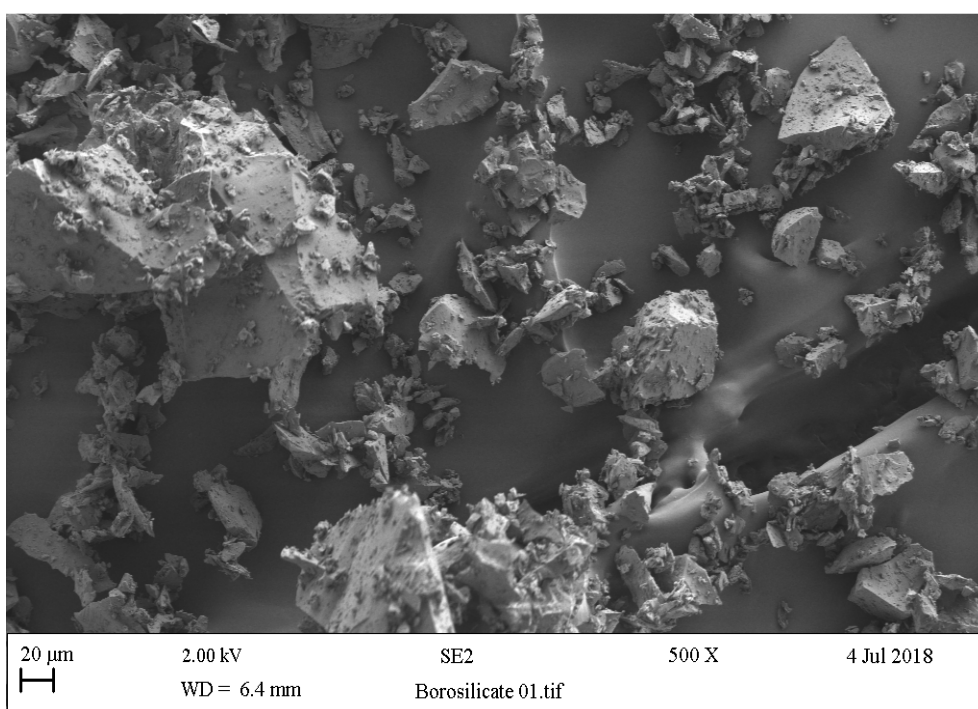


Figure 6.8. Scanning electron microscopy detailing the characteristics of the borosilicate glass stationary phase matrix Endecott filtered to a particle size of to 0.01mm 0.125mm.

Figure 6.9 shows DNA yields from development protocols during optimisation of the cell debris wash-through and residual ethanol elimination process. Nucleic acids are typically quantified by UV spectrophotometry and measurement of sample absorbance at 260nm – the absorbance frequency of single and double stranded DNA and RNA. The absorption of light by a material is described by the Beer-Lambert law,

and the logarithmic relationship that exists between the transmission of light through the DNA suspension and the product of the light path length and absorption coefficients for each nucleic acid base. However, while spectrophotometry represents a precise technique in the determination of pure nucleic acid concentrations, sample contamination with compounds such as GuHCl can lead to DNA over-quantification.

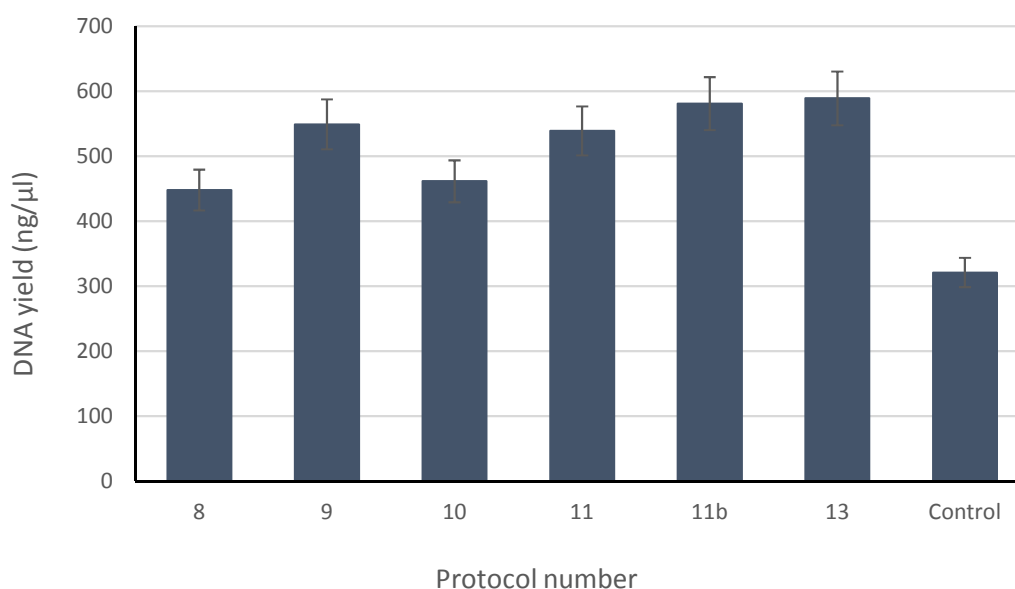


Figure 6.9. Showing DNA recovery over the DNA purification protocol development utilising a borosilicate glass-based stationary phase matrix with 200μl free volume and particle size 0.01mm to 0.125mm. Error bars indicate DNA recovery variation in protocol 13, n=3.

6.3.3 Nucleic acid purity

Accordingly, evaluation of DNA extraction protocols 8 to 13 cannot be based on quantification alone but must also consider sample purity. The principal technique for the determination of DNA sample purity is based on a comparison of nucleic acid absorbance at 260nm (A_{260}) with the absorbance of those protein impurities present absorbing at 280nm (A_{280}). An A_{260}/A_{280} ratio of 1.8 is generally accepted to indicate pure DNA (Held, 2008), while a ratio of 2.0 indicates pure RNA; the absorbance difference relates to the thymine to uracil base substitution in RNA (L. Wang and Stegemann, 2010; Yamaguchi et al., 1992).

The results from DNA quantification presented in figure 6.9 must therefore be considered in the context of sample purity as presented in figure 6.10. As a control, the mean A_{260}/A_{280} ratio of 1.6 is typical of an off-the-shelf general-purpose bacterial DNA extraction kit and reflects a sample matrix appropriate to downstream analytical techniques such as gel electrophoresis or PCR. Conversely, A_{260}/A_{280} ratios over 2.0 for samples from protocols 8 to 10 indicate significant contamination and render the associated DNA quantification unreliable. While still above the pure value of 1.8, mean A_{260}/A_{280} ratios from 2.01 to 1.88 for protocols 11 through 13 indicate decreasing levels of salt contamination corresponding to protocol optimisation.

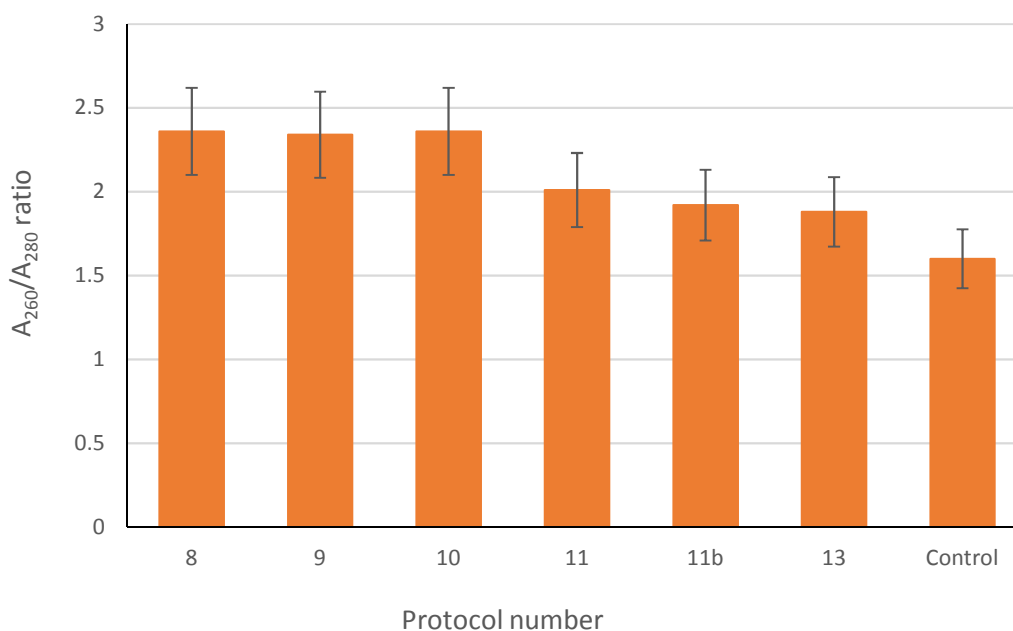


Figure 6.10. Showing DNA purity as determined by the ratio of sample absorbance at 260nm divided by absorbance at 280nm. Values of 2 and above – protocols 8 through 10 – indicate contamination by cell lysis debris and components of the lysis buffer chemistry.

6.3.3.1 Retention of lysis chemistry and cell debris

Investigation of the sample contaminants was based on examination of the sample spectra and comparison of absorbance at 260nm with that at 230nm; corresponding with carbohydrates, phenolate ions, or guanidine hydrochloride retained within the column matrix. Figure 6.11 show a NanoDrop™ spectrum for a protocol 9 sample

purification using 500µl of wash buffer A (5.5M GuHCl, 30mM Tris-HCl pH 6.6, 40% ethyl alcohol) followed by 700µl wash buffer B (25mM NaCl, 2mM Tris-HCl pH 7.7, 75% ethyl alcohol), at a flow rate of 120µl per minute.

In combination, the progressively low ionic strength buffer is designed to stabilise bound nucleic acids while washing cell debris and guanidine salts from the borosilicate column matrix. However, a comparison of absorbance at 260 with absorbance at 230nm - used to determine chaotrope salt retention- yields a value of 0.2 – significantly lower than an A_{260}/A_{230} ratio of 1.5 to 2.0 of clean samples. Of the possible contaminants, the observed spectrum is characteristic of GuHCl column retention, with the shift in peak absorbance value (230nm to 233nm) likely to result from variation in sample pH.

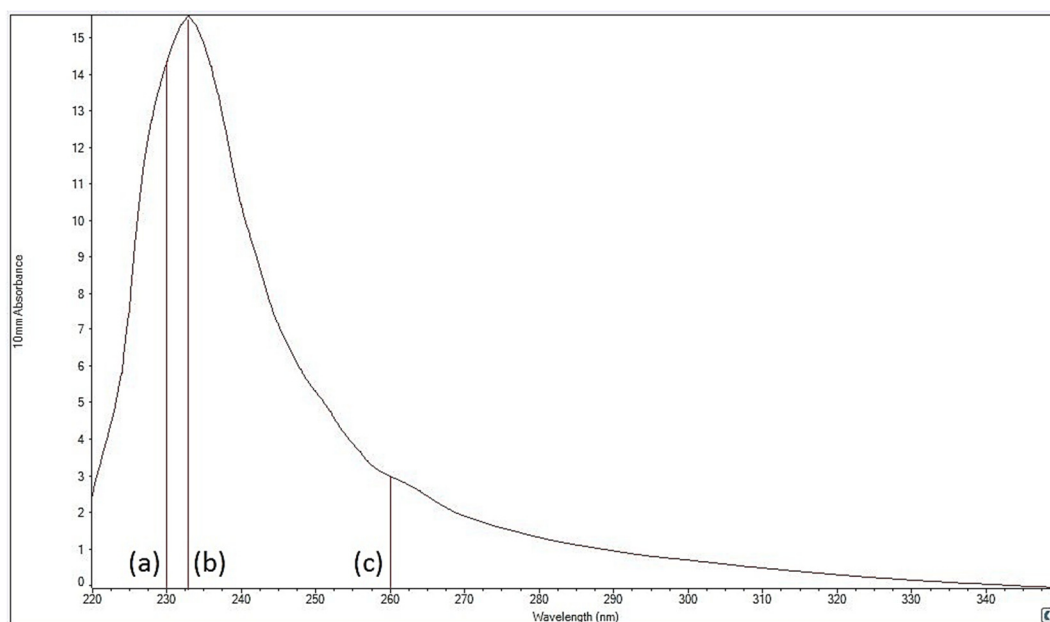


Figure 6.11. UV Spectrum for protocol 9 sample [0.25] showing absorbance of 14.2 absorbance units (AU) at 230nm and 15.6AU at 233nm (b), indicative of GuHCl contamination, and a 3.0AU peak at 260nm associated with nucleic acid absorbance.

Adjustment of the wash buffer volumes was intended to optimise reagent performance while retaining methodology robustness in the context of DNA

recovery. Accordingly, the effects of 50% buffer volume increases were evaluated. A combination of 750µl buffer A: 500µl buffer B (protocol 10) resulted in a reduction of indicated yield at 260nm, an increase in A_{260}/A_{230} ratio to 0.7, no significant change in A_{260}/A_{280} values, and no elimination of GuHCl contamination. Figure 6.12 shows the UV spectrum for a protocol 11 sample with a wash through combination of 500µl buffer A:1150µl buffer B.

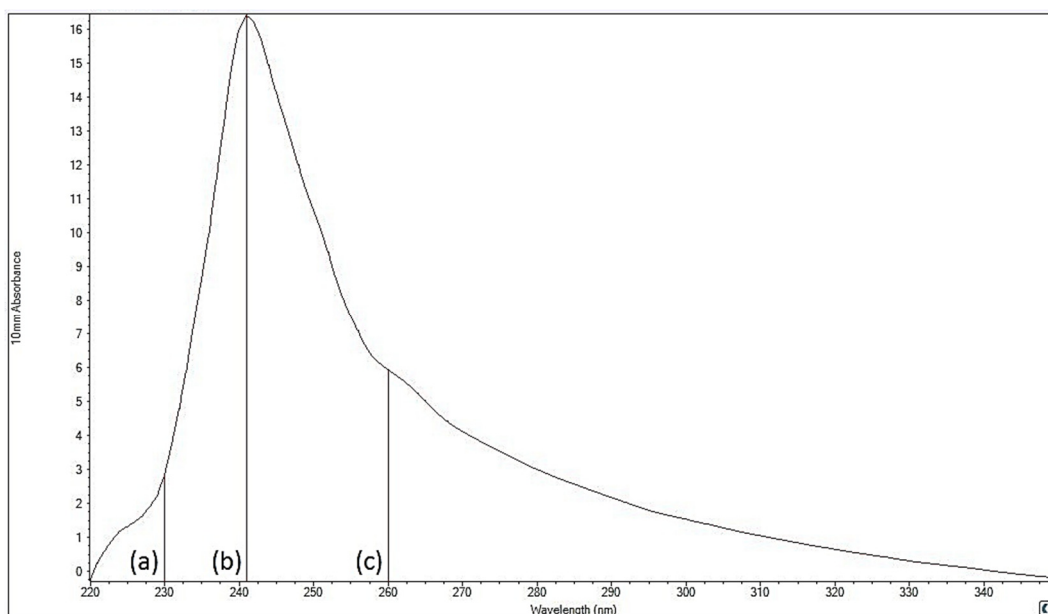


Figure 6.12. UV Spectrum for protocol 11 sample [0.5] showing absorbance of 2.8AU at 230nm (a), peak absorbance of 16.5AU peak at 241.5nm (b), and a 'shoulder' absorbance peak of 5.8AU at 260nm (c) attributable to sample DNA content.

As with protocols 9 and 10, the spectrum describes an absorbance peak significantly greater than that associated with nucleic acid at 260nm, but at 241.5nm in this instance, the peak is above the range expected for GuHCl. The trace describes a 'shoulder' in the absorbance region for DNA/RNA at 260nm and appears to describe an early part of the GuHCl peak in the run up to 230nm before being enveloped by the main peak. An A_{260}/A_{230} ratio of 2.1 implies low level GuHCl elution in the sample, while an A_{260}/A_{280} ratio of 2.01 indicates a significant decrease in protein retention relative to DNA concentration.

6.3.3.2 Ethanol elimination

Alongside chaotropic salts, the most common DNA sample contamination is caused by residual ethanol from the column wash through. In conventional laboratory-based miniprep protocols this ethanol is spun from the filter by micro-centrifuge, and it is straightforward to extend the spin duration to ensure it is entirely removed. However, a through-flow of air to atmosphere at a rate of 1000 μ l per minute over periods of 5, 10 and 15 minutes did not affect the observed absorbance peak at 241.5nm.

To eliminate residual ethanol from the wash out buffers as a source of sample contamination therefore, protocol 11 was modified by heating the stationary phase matrix to 85°C and applying an air flow-through to atmosphere of 1000 μ l per minute for 10 minutes. At 78.2°C the ethanol retained in the column transitions to a gas phase (Haynes, 2014) and is cleared as part of the air flow-through without effecting the bound DNA.

Figure 6.13 shows the effect of temperature mediated ethanol clearance on the absorbance spectrum for protocol 11b and describes a 2.95 AU peak at 260nm to corresponding to nucleic acid absorbance but no peak at 240nm as observed for protocol 11. An A_{260}/A_{280} ratio of 1.92 is higher than indicating a pure sample (Held, 2008) and, taken alone, may indicate a sample containing both DNA and RNA. An A_{260}/A_{230} ratio of 0.92 and absorbance of 3.2AU at 230nm indicates GuHCl retention, also indicated in the comparison of the 11b spectrum with that of control DNA samples extracted using the Congen miniprep kit (Figure 6.14 inset).

Further refinement of the purification protocol may facilitate the generation of 'pure' nucleic acid samples. However, as such residual levels of chaotropic salts appear to have no significant effect on the disruption on the reformation of the DNA hydration shell during elution, they are unlikely to have a significant effect on downstream sequence hybridisation or amplification (section 6.3.4).

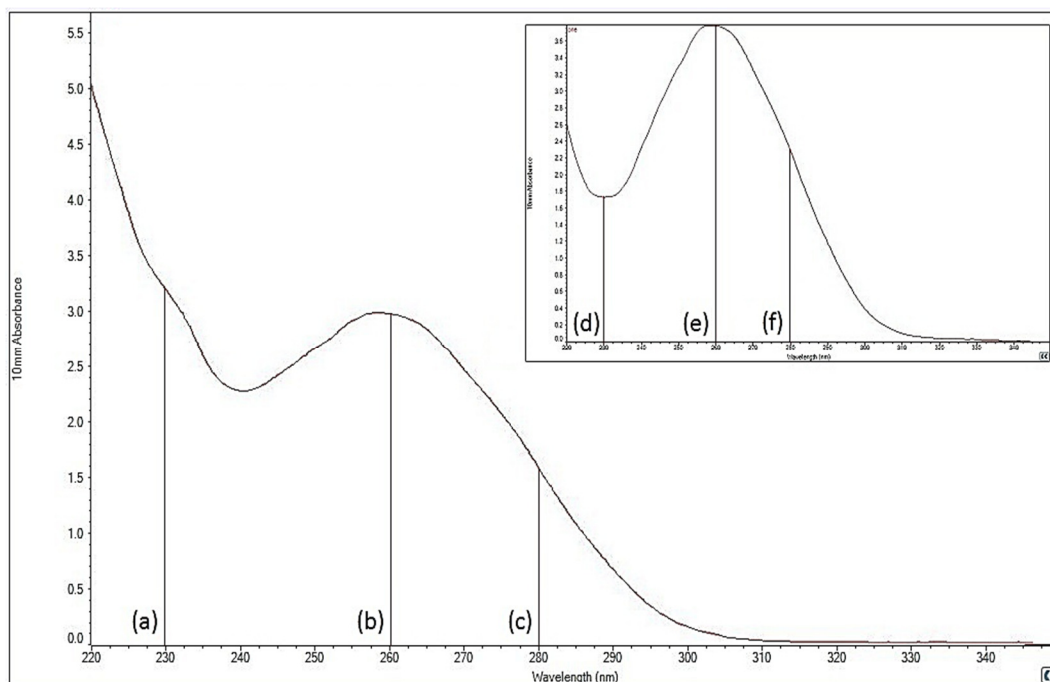


Figure 6.13. UV Spectrum for protocol 11b sample [0.25] with absorbance of 3.2AU at 230nm, a peak absorbance of 2.95 AU at 260nm and absorbance at 280nm of 1.54AU (c). Inset is a corresponding spectrum for the Congen control sample with absorbance values of 1.75AU, 3.6AU, and 2.25AU at 230nm (d), 260nm (e), and 280nm (f) respectively.

6.3.4 DNA elution efficiency

In application of the DNA Elution buffer (10mM Tris HCl pH 8.5) over protocol development, column retention was calculated from spectrophotometry-based DNA quantification from a second 200ul volume elution buffer. As for the standard elution, this buffer was run at 85°C and maintained within the column matrix for a reaction period of 3 minutes. Secondary elution across protocols 8 to 11b generated a mean DNA yield of 3.6ng/μl with a standard deviation of 0.74 (n=6). For protocol 13 (as per protocol 11b but with an increased elution buffer reaction period of 10 minutes), secondary elution generated a mean yield of 4.1ng/μl (n=4) and showed no significant increase as a result of the extended reaction duration. Accordingly, a column retention volume of 5ng DNA should be considered in analytical method robustness.

6.3.5 Stationary phase purge and recycle

Between DNA extraction cycles, the DNA retained within the column matrix is degraded by a 0.7% sodium hypochlorite (NaOCl) solution to prevent contamination of the following sample. The NaOCl is cleared using DD water, which is retained as a 'keeper' solution.

6.3.6 Extraction module flow rate regulation

In the initial design concepts for the biosensor platform, the back pressure generated by the borosilicate stationary phase column matrix was considered to regulate the flow of reagents through the lysis unit and DNA purification module to waste. Figure 6.14 describes the relationship between reagent pressure and flow rate for the prototype column of diameter 10mm, length 4.25mm, and 200 μ l free space within the borosilicate matrix. The selection of a reagent flow rate of 120 μ l in cell lysis and nucleic acid extraction is designed to limit DNA fragmentation to that 'dialled in' for sample preparation purposes. However, as the flow rate of sterilisation and wash solutions are not subject to such limitations, the column matrix represents a simple means to control their flow.

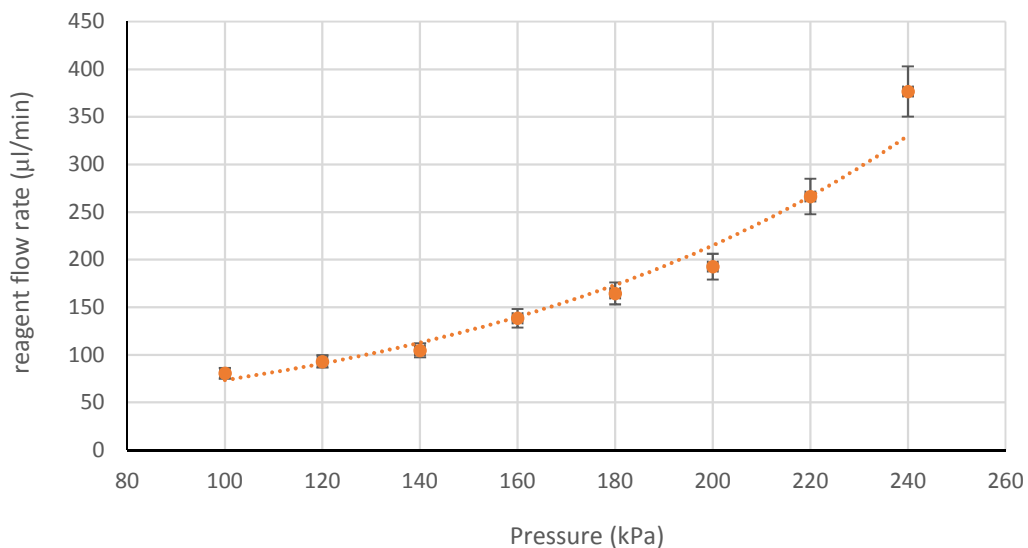


Figure 6.14. Outlining the relationship between reservoir pressure and reagent flow through the 200 μ l free space within the borosilicate glass solid phase extraction matrix of grain size 10 μ m to 125 μ m. Error bars indicate experimental variation, $n=10$.

Rather than complicate the macro-fluidic component further, both the 0.7% NaOCl solution and DD water are contained in a pair syringes of 15ml each, and a shared pressurised air reservoir of volume 60ml. This allows a total fluid displacement of 30ml for a 33% reduction in drive pressure. From an initial charge of 240kPa, the data presented in figure 6.15 indicates a maximum flow rate of approximately 350 μ l per minute, decreasing to a minimum of around 140 μ l per minute over a projected 5 cleaning cycles.

6.4 DNA amplification results

As a way in which to enhance the detection limits of the biosensor platform, there are clear advantages to incorporation of DNA amplification using PCR. By multiplying the number of target sequences available for hybridisation-based electrochemical analysis, biosensor detection sensitivity can be greatly enhanced without any corresponding increase in the background signal. The temperature cycling hardware is straightforward, as is the microprocessor control methodology.

As discussed previously, microbial classification is based on comparative genomics there are extensive data resources and, as discussed previously, regions such as those coding for 16s ribosomal subunits represent unique identifying DNA sequences. Accordingly, in a research or pathogen surveillance setting, the analyst may select primers specific to a unique 16s sequence to amplify only that DNA in a sample specific to a given target species, sub-species, or strain (Haas et al., 2017; Gosselin-Théberge et al., 2016; De Boer et al., 2015). Equally, the analyst may use generic primers to amplify all 16s genes in a sample as a means to classify an entire microbial population (Andrighetto et al., 2016; Garcia-Mazcorro et al., 2017; Parulekar et al., 2017; Raut et al., 2007).

In the characterisation of microbial populations, PCR is also applied quantitatively (Fierer et al., 2005; Lyons et al., 2000; Bach et al., 2002), and with technique

modifications to differentiate between DNA from viable and dead cells (Bae and Wuertz, 2009; Nocker et al., 2006; Chang et al., 2017) in the characterisation of non-culturable populations. However, as the data relating to the use of quantitative PCR has accumulated, the literature indicates a significant degree of variability according to sample processing and the selection of primer sequence (Walker et al., 2015; Law et al., 2015; Suzuki and Giovannoni, 1996). Consequently, it is appropriate to determine the reliability of quantitative derived from the analysis of PCR derived DNA sequences amplified from the product of the cell lysis unit.

The protocol used in the amplification of *C. jejuni* is outlined in chapter 5, However in terms of robustness, both the temperature cycling profile employed and the results generated could be considered representative of sequence amplification from across a wide range of bacterial targets. To evaluate the efficacy of the PCR amplification process, purified *C. jejuni* DNA (disrupted using the biosensor platform lysis unit at 60rpm and purified using the Congen miniprep kit) was serially diluted at a 1 to 2 ratio (1:1 to 1:2048) and plated in triplicate. A 311bp section of the *C. jejuni* genome coding for the 16s ribosomal subunit and bound by the primers: 5' GCATATACAATGA GACGCAATAC and 5' GCAGAGAACAATCCGAACT and 311bp in length was amplified through 50 cycles (95°C for 15secs and 62°C for 30secs).

The resulting triplicate amplicon concentrations are presented in figure 6.15. Given the degree of variation across the selected serial dilution range, the generation of data relating to bacterial enumeration, whether relative or absolute, is unrealistic. This observed variation may reflect inconsistency in pipetting technique and the plating of the serial dilutions. However, in this case, the amplicon concentration of downstream dilutions should not exceed those of any preceding sample. Damage to copies of the template sequence during DNA extraction has the potential to introduce analytical variability. However, the relatively uniform DNA fragmentation evident in gel electrophoresis of *C. jejuni* DNA does not support this premise.

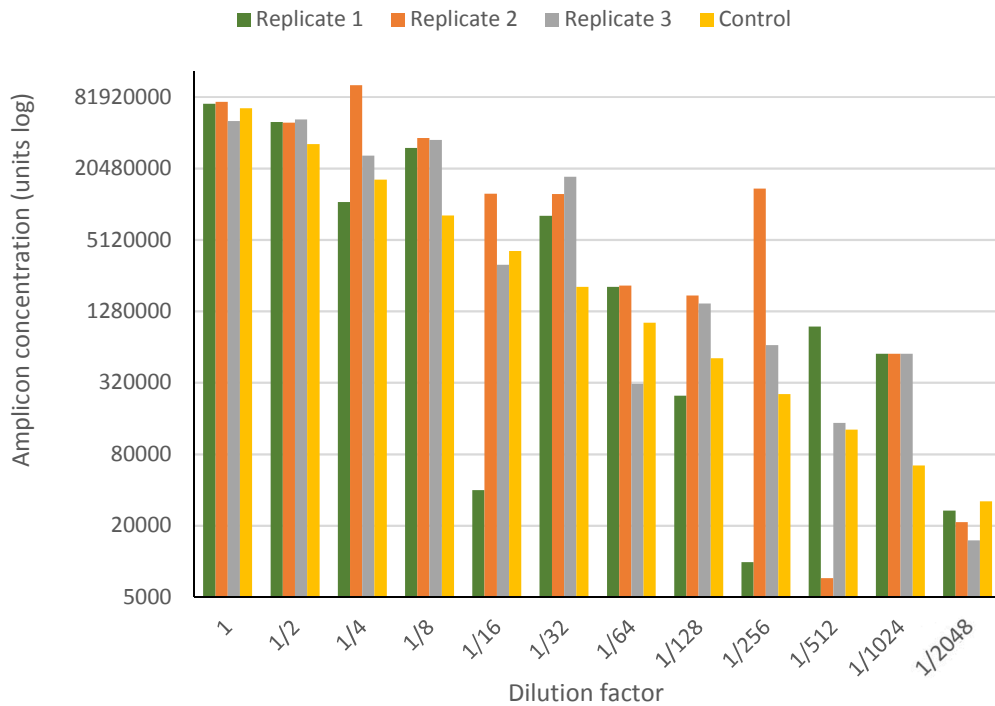


Figure 6.15. Final amplicon concentrations for sample replicates for serial dilutions from 1:1 to 1:2048 following 50 PCR cycles (95°C for 15secs and 62°C for 30secs). Projected control values are presented for comparison.

A scatter plot of the amplification data is presented in figure 6.16 and in describing an R^2 value of 0.63 indicates a relatively limited degree of interdependence between the initial serially diluted replicates and the amplicon concentration at the crossing point cycle number (C_p). This C_p or threshold value denotes the amplification cycle at which the detected fluorescence value shows a statistically significant increase and is inversely proportional to the target sequence copy number in the initial sample (Rodríguez-Lázaro, 2013).

The insights of Henri Poincaré in relation to Science and Method (Poincaré and Maitland, 2003; Davies, 2018) highlight the capacity of small differences present in initial conditions to produce very large differences in final phenomena, and are accepted to have a fundamental effect across a variety of biological systems (Taki et al., 2015; Zajicek, 1991; Faure and Korn, 2001). Accordingly, variation within the initial sample matrix may be amplified exponentially in the polymerase chain reaction

process. The development of sample homogenisation techniques to negate the influence of such variation represents a significant challenge. At this prototype stage therefore, the integration of PCR functionality represents a means by which to enhance the analytical detection limits but not a means by which to quantify microbial populations.

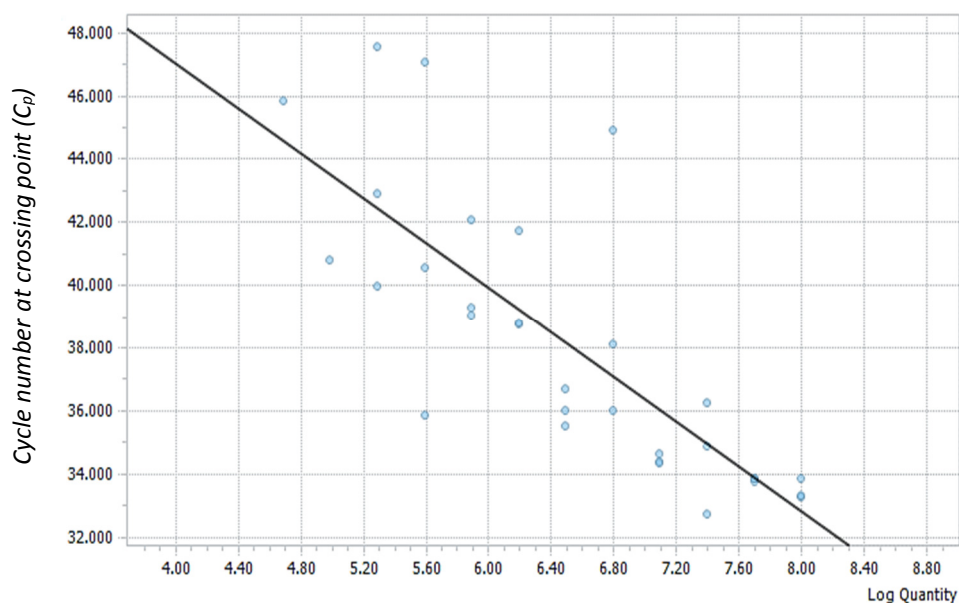


Figure 6.16. Showing the absolute quantification from the *C. jejuni* 1:2 serial dilution with slope -3.5582, efficiency -3.5582, error 1.91, and Y-Intercept 61.25. $R^2=0.63$.

6.5 Electrochemical characterisation of electrode modification

The electronic characteristics of the electrode – electrolyte interface are defined by the atomic structure of the electrode itself; the composition of any adsorbed modifying layer; and elements dispersed within the electrolyte. The aim of this characterisation section is to explore ways in which DNA hybridisation detection may be optimised through electrode modification. The corresponding performance difference is primarily evaluated in terms of electrode surface conductivity, capacitance, and stability, which in turn dictate factors such as detection resolution, sensitivity, and background noise. The data from which this evaluation is drawn was generated using cyclic voltammetry (CV) and differential pulse voltammetry (DPV), using an EmStat potentiostat (Palmsens, Netherlands).

6.5.1 Glassy carbon electrode (GCE), characteristics

Voltammetric characterisation of the GCE represents a baseline against which to measure the effects of surface modification in terms of capacitance, conductivity, and stability of the GCE surface. This data is also useful in the identification of properties specific to the electrolyte and their effects on modified electrode characterisation. When determined from CV data, the capacitance of an electrode material is calculated from that area of the voltammogram *i-E* curve where the Faradaic reaction rate = 0. At this point, the recorded current *ic* is capacitive in nature and is proportional to the CV scan rate.

Where all other variables are equal, the relative capacitance of modified electrodes may also be determined according to their CV peak-to-peak sweep. This comparison technique has the advantage of eliminating any requirement to calculate and subtract any experimental background Faradaic effect. Electrode conductivity is determined as the resistance to electron flow and is calculated from peak voltage difference divided by peak current difference:

$$R = \frac{\Delta V}{\Delta I}$$

Resistance (R) is proportional to the area of the electrode-electrolyte interface, thus differences in electrode surface area must be considered when comparing the performance of electrodes of dissimilar sizes. Any statistically significant variation in electrode surface stability may be determined by one way analysis of variance (ANOVA) or Kruskal-Wallis analysis of two or more voltammogram data sets. On the other hand, any such variation is usually obvious to visual inspection.

Figure 6.17 shows cyclic voltammetry for a GCE for scans of -1v to 1v with a corresponding current range of 0.175mA (-0.085mA to +0.09mA). A degree of surface reconstruction or electrochemical instability is indicated by variation in the current generated for each of the three over the -1V to +1V cyclic voltammetry scans with a drift of approximately 5µA. A stable 3 electrode cell will ideally produce replicate amperometric data for each scan while the parameters remain unchanged. Such

variation may result from electrode surface inconsistencies or from instability in the electrode modification material resulting in surface reconstruction or REDOX associated capacitance. The extent of such baseline variability has a direct bearing on the limit of detection and sensitivity of any associated biosensor system irrespective of the bioreceptor molecule employed.

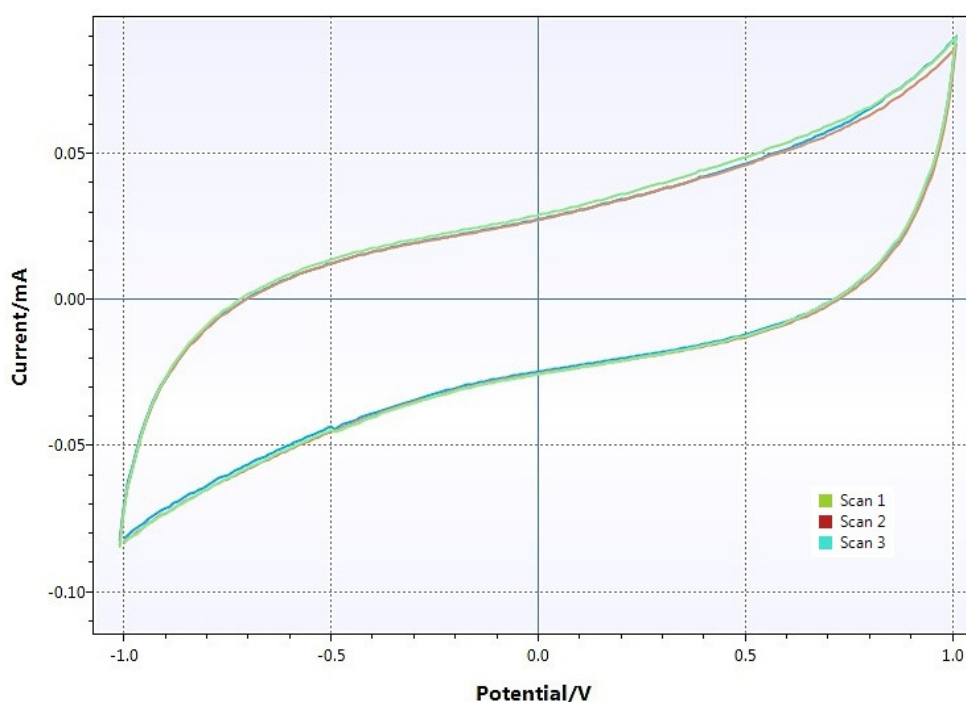


Figure 6.17. Cyclic voltammetry characterisation of a GCE through a 3-cycle sweep of -1V to 1V and the corresponding current range of 0.175mA (-0.085mA to +0.09mA). The variability described over the course of 3 identical voltage scans suggests an instability or reconstruction at the electrode surface. This baseline variation directly limits the sensitivity of the sensor setup regardless of the target affinity of the bioreceptor molecule employed.

Amperometric baseline variation may also result from the electrochemical characteristics of the electrolyte used, and figure 6.18 shows 10 consecutive cyclic voltammetry scans for a polished GCE in phosphate buffered saline (PBS) electrolyte. In this instance, the inverted peak at -0.72V corresponds to the presence of dissolved oxygen in the electrolyte solution. As the oxygen is oxidised with each reverse scan, the peak decreases in size. Easily identified and eliminated by purging the PBS electrolyte with nitrogen, dissolved atmospheric oxygen is not a significant challenge

in electrochemistry. However, the degree of variability in the cyclic voltammetry data does to highlight the fundamental importance of regulating, as much as is possible, the characteristics of the electrode, electrolyte, and the sample matrix containing the target molecule.

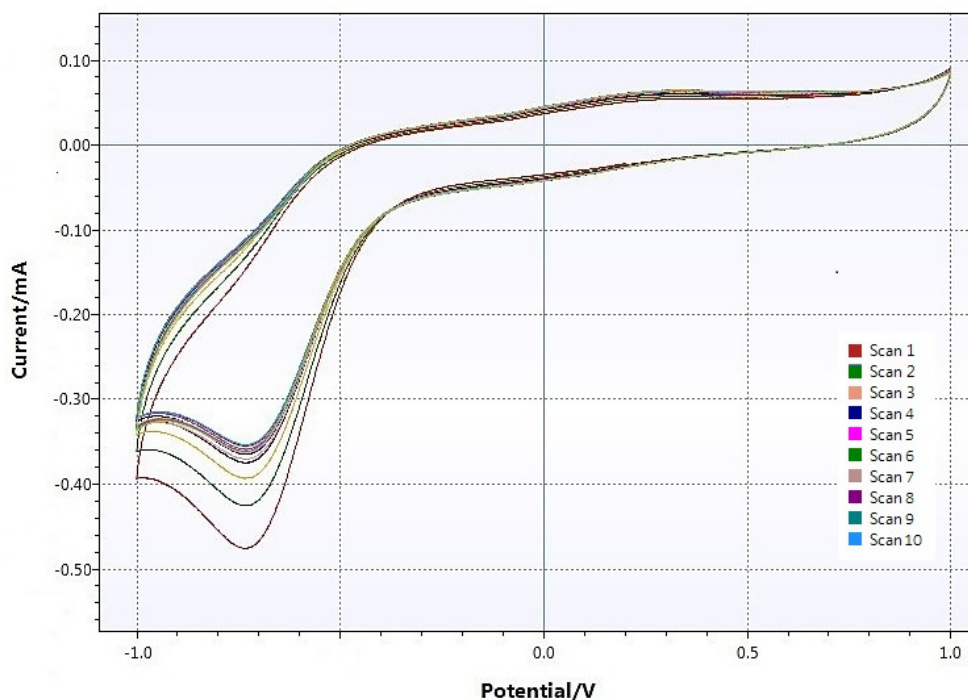


Figure 6.18. Cyclic voltammetry showing forward and reverse scans from -1V to 1V and the corresponding current range for a GCE. The peak at -0.72V denotes the presence of dissolved oxygen in the electrolyte solution and decreases in magnitude as the gas is oxidised by each successive reverse scan.

6.5.2 Graphene oxide (GO)

Since the development of techniques to isolate graphene at the University of Manchester (K. S. Novoselov et al., 2004; K. Novoselov, 2007) a great deal of research energy has focussed on the application of graphene and derivative carbon nano-materials in electrochemistry, and electrode modification in particular (J. Liu et al., 2012; Kim et al., 2010; J.-F. Wu et al., 2010). As a semi-metal material with ultra-high charge mobility, graphene exhibits superior electronic characteristics and a structure suited to functionalisation for detection of biomolecules (Li et al., 2016; D. Chen et al., 2012; Ambrosi et al., 2014).

The advantages to using graphene in electrode modification stem from the inherently reduced resistance of the material, paired with a similarly reduced level of background noise. In the detection of very small changes in charge state associated with biomolecule interactions, electrode modification using graphene materials has generated significant interest, and a variety of DNA hybridisation-based biosensor models are depicted within the published literature (F. Liu et al., 2010; Ambrosi et al., 2014; Pumera, 2011; Hu et al., 2011). Figure 6.19 demonstrates the greater potential for electron flow inherent to graphene materials, with a current range of around one third that of the polished GCE shown above but no associated increase in signal noise.

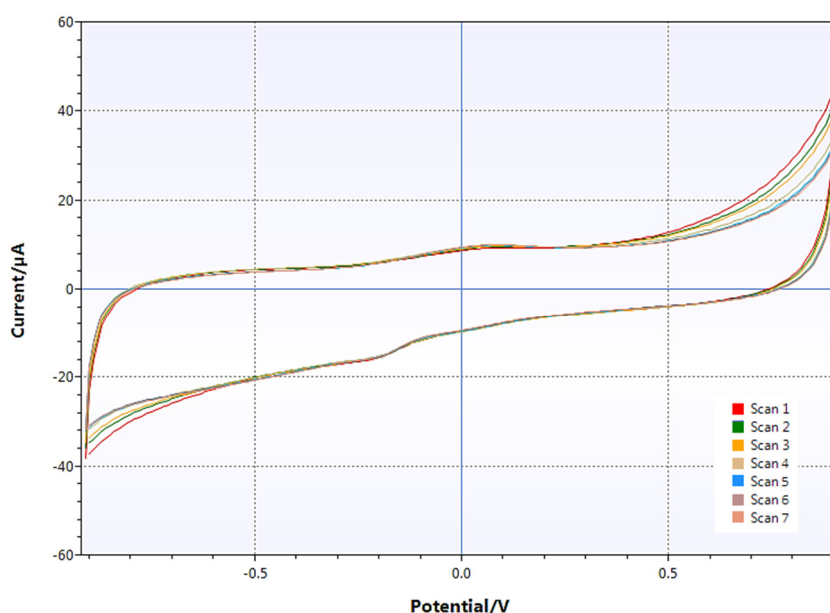


Figure 6.19. Voltammetry depiction of Graphene oxide (GO) modified GCE through a voltage sweep of -1V to 1V. The progressive fall in peak current at maximum voltage application relates the cumulative reduction/oxidation of oxygen containing groups on the GO surface.

While there were obvious advantages to development of a graphene-based DNA-biosensor for integration within the proposed platform, experimental development faced significant obstacles. With a basis in the electrochemical detection of DNA hybridisation, the immobilisation of probe oligonucleotides on the electrode surface is key to the functionality of the biosensor platform analytical component. However, as a result of oxygen molecules (**C-O**, **C-OOH**, **C=O**, and **C-OH**) on the surface structure

Graphene materials exhibit a net negative charge. Similarly, the DNA molecules has a net negative charge from its phosphate backbone structure. The immobilisation of DNA probe sequences therefore must overcome the electronic repulsion of the graphene coated electrode surface. Eliminating the oxygen containing groups, and so the electronegative charge of the Graphene oxide layer, represented the most practicable way to achieve this, and both chemical and electrochemical reduction techniques were evaluated in their restoration of the GO modified electrode surface.

6.5.3 Reduced graphene oxide (rGO)

Cyclic voltammetry-based electrochemical reduction of GO modified GCEs was performed using a sweep of -1V to 0.2V, while further GCEs were modified using commercially sourced rGO. The obstacles to the removal of all oxygen containing groups within the GO matrix are well documented in the literature (W.-J. Ong et al., 2015; Yuan et al., 2016), and attempts to circumvent these and restore the GO layer to a completely neutral surface charge were unsuccessful. Neither chemically nor electrochemically rGO modified electrodes demonstrated an immobilisation of probe oligonucleotide sequences appropriate to DNA hybridisation-based biosensing applications.

As an alternative to the detection of species or treatment resistant genes through the detection of probe-target DNA hybridisation interactions, the detection of elevated DNA concentrations in water samples was considered as a basic marker indicating microbial contamination. The experimental evaluation of rGO in detection of purine and pyrimidine nucleobases is presented in figure 6.20. The DPV peaks highlighted show the oxidation of guanine at 0.8V (a), adenine at 0.98V (b), and thymine at 1.16V (c). The corresponding signal demonstrates a concentration dependent response in the 1 μ A region and a very low signal to noise ratio. As a general purpose, routine surveillance sensor, this technique has potential applications in the first line detection of microbial contamination in areas such as water supply or food processing. However, while demonstrating the sensitivity of reduced Graphene oxide electrode modification, it lacks the specificity required for the biosensor platform.

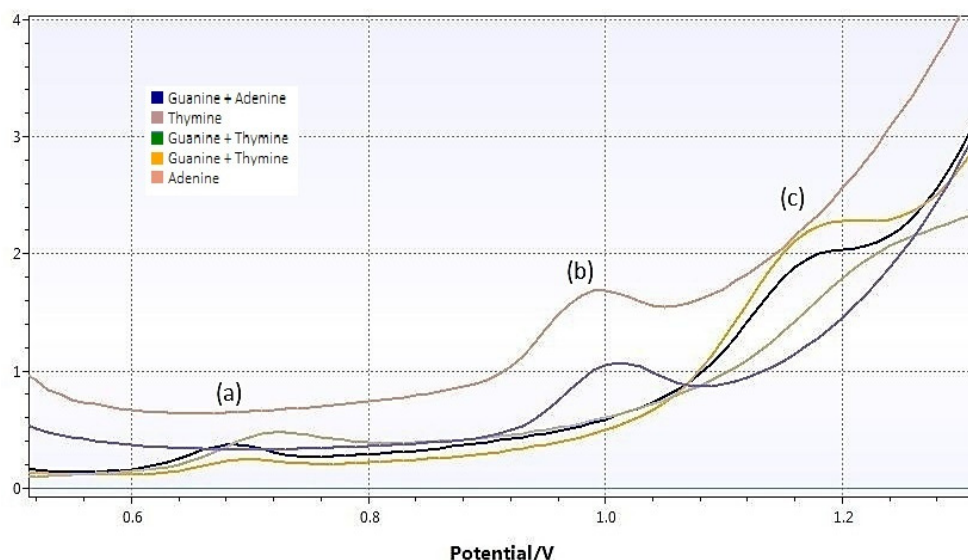


Figure 6.20. Differential pulse voltammetry (DPV) scans showing the oxidation of guanine (a), adenine (b), and thymine (c) at 100 μ M concentrations employing a reduced Graphene oxide modified GCE.

6.5.4 Graphene oxide and cellulose microfibrils

In the context of the Velusamy laboratory's work with GO and cellulose microfibre (CMF) electrode modification in the detection of biomolecules and environmental pollutants (Velusamy et al., 2017; Velusamy et al., 2019; Palanisamy et al., 2017; Palanisamy et al., 2019), the application of these materials in a hybridisation-based sensor was considered. Figure 6.21 demonstrates the improvement in detection of a 10 μ M dopamine concentration resulting from the modification of a screen-printed carbon electrode (SPCE) with CMF, graphite, and a graphite-CMF composite.

While the graphite-CMF SPCE demonstrates excellent characteristics for the immobilisation of enzymes and detection of dopamine, attempts to electrochemically adsorb DNA probe sequences were unsuccessful. As with GO, the poor retention of DNA oligonucleotides is likely to correspond to the presence of abundant oxygen functional groups (**C-O**, **C-OOH**, **C=O**, and **C-OH**) associated with edge plane defects on the surface of the exfoliated graphite and a net electronegative surface charge. As shown in figure 6.22, the similar abundance of oxygen functional groups within GO-CMF composites require prolonged cyclic oxidation and reduction to become electronically stable and appear equally unsuited to DNA immobilisation.

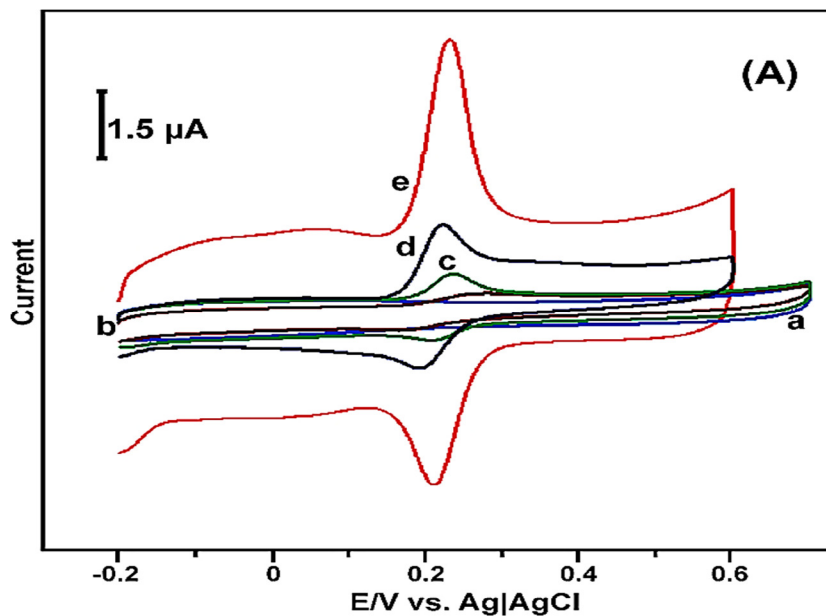


Figure 6.21. Highlights the change in cyclic voltammetry response sensitivity for the detection of a $10\mu\text{M}$ dopamine concentration using a bare (a), graphite (b), cellulose microfiber (CMF) (c), CMF coated graphite (d), and graphite-CMF composite (e) modified screen printed electrode.

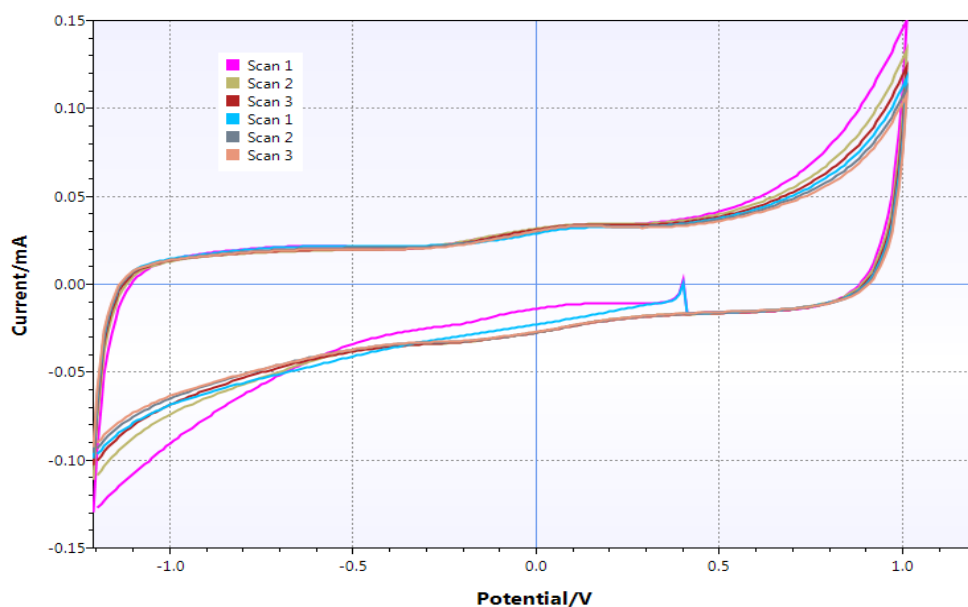


Figure 6.22. Cyclic voltammetry REDOX stabilisation of a Graphene oxide (GO)-cellulose microfiber modified electrode (2 sets of 3 scans). The abundant oxygen functional groups associated with the GO require prolonged oxidation and reduction cycling to acquire levels of electronic stability suited to analytical electrochemistry techniques.

Adjusting the thickness of the electrode modification layer was considered as a mechanism to regulate the electro-negativity of the GO-CMF layer. As both the oxidation of DA and the electronegativity of the electrode surface correlate with the availability of oxygen functional groups and edge plane defects in the graphite-CMF coating, the characterisation of DA oxidation in relation to the volume of graphite-CNF applied as a drop-coated electrode modification layer was used as a starting point. Figure 6.23 describes the relationship between the volume of graphite-CMF composite applied to the electrode surface and the resulting oxidation of DA. While experimentation with GO-CMF and DNA immobilisation/hybridisation proved unsuccessful, this simple and efficient drop coating methodology was adopted for all subsequent electrode modification with conducting polymer coatings.

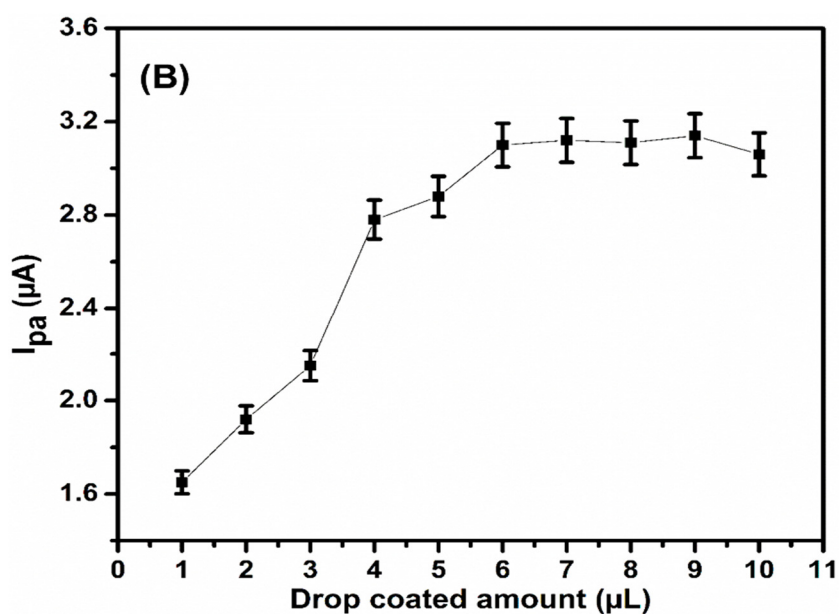


Figure 6.23. Describes the relationship between the volume of graphite-CMF used to drop-coat the electrode surface and the resulting levels of dopamine oxidation. The peak height increases significantly with an increase in volume from 1µl to 6µl and indicates an optimal electrode modification volume between layer thickness at 6µl and 9µl.

6.5.5 Graphene oxide, cellulose microfibrils, and Nafion™

Nafion™ copolymer consists of a tetrafluoroethylene backbone with sidechains of perfluoro-3,6-dioxo-4-methyl-7-octene-sulfonic acid. These sulfonic acid terminal

groups confer H₂O and OH group binding properties and Nafion™ is used as a carbon nano-material dispersal agent and coating media, and as a spacer and stabilising matrix, reducing resistance in electrode surface modification (S. H. Lim et al., 2005; J. Wang et al., 2003; Zohourtalab and Razmi, 2018). Figure 6.24 highlights the sub-1 μ A current range of a GO-CMF-Nafion™ modified electrode, ideally suited to detection and quantification of DNA hybridisation events. However, over a range of amalgamation ratios from 1:5 to 1:1 - GO-CMF to Nafion™, no significant retention of immobilised DNA sequences was detected.

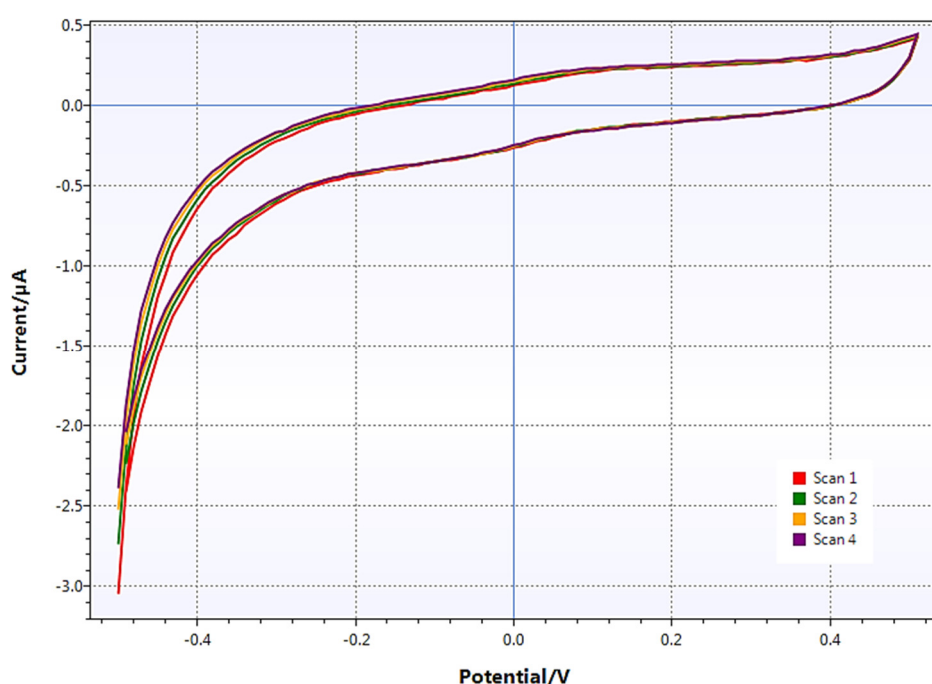


Figure 6.24. Consecutive cyclic voltammetry scans highlighting the current range of a GO-CMF-Nafion™ modified electrode surface in the region of 1 μ A.

6.5.6 Poly(3,4-ethylenedioxythiophene)- polystyrene sulfonate (PEDOT:PSS)

In considering alternatives to GO-based electrode modification, PEDOT:PSS was identified as a potential alternative with applications in both screen printed electrode manufacture and in electrode modification for biomolecule immobilisation and electrochemical sensing (R. K. Pal et al., 2017; García-Hernández et al., 2016; Wisitsoraat et al., 2013). A polyanion doped polythiophene, PEDOT:PSS is a conducting polymer with high electrical conductivity and a low REDOX potential. The

PEDOT component is a positively charged conjugated polymer, while deprotonated sulfonate groups in the PSS carry a negative charge, and together form the PEDOT:PSS macromolecular salt with no net neutral surface charge. As a relatively low cost, thin-film coating demonstrating potential DNA immobilisation compatibility, PEDOT:PSS was evaluated as an electrode modification material for biosensor platform use.

6.5.7 PEDOT - (3-Aminopropyltriethoxysilane (APTES))

As an adjunct to PEDOT:PSS, APTES was considered as a way to improve surface retention of the immobilised DNA probe sequences. A silane coupling reagent with an aminopropyl group on one end and an amine and silane reactive component on the other, APTES is widely used in glass surface functionalisation in microfluidics and molecular biology (Gunda et al., 2014; Mishra et al., 2014). In the context of DNA immobilisation, silane-based nucleic acid immobilisation techniques developed in microarray, immuno-assays, and fluorescent in-situ hybridisation (FISH) (Z. Zhang et al., 2016; Roy et al., 2016; Coombs et al., 2018) have been adapted for use in electrochemical biosensors in the detection and quantification of biomolecular targets and DNA sequences associated with bacterial species and viral agents (Adam et al., 2018; MN et al., 2016; Rajapaksha et al., 2017; Roshila et al., 2017).

In DNA functionalisation of a glass surface, the APTES silane reactive component links to the silica substrate while the aminopropyl group is available to link with the DNA sugar-phosphate backbone. UV light provides the energy for NH₂-DNA crosslinking, and reaction pH dictates the specificity of the bond linkage (North et al., 2018). The silica surface must be pristine and entirely free of organics and typical silanisation protocols involve immersing the glass slides in a 1% dilution of APTES in acetone for 10 minutes followed by vacuum drying. In electrode modification, APTES coating may similarly be achieved by an immersion protocol, or through co-polymerisation during spin-coating, drop-coating, or electro-polymerisation.

6.5.8 Activated screen-printed carbon electrode (α SPCE)

Building on the experience gained through the characterisation of bare GCEs and modifications using GO, the second stage of electrode modification aimed to consider

in more detail the inherent constraints on electrode design for the biosensor system. With both relative cost and functional flexibility as primary considerations, PEDOT:PSS modification of SPCEs was evaluated in combination with APTES as a crosslinker both for DNA immobilisation and for binding the PEDOT:PSS film to the SPCE surface. The electronic characteristics of SPCEs are not of the order of those demonstrated by a GCE. However, their conductivity may be improved significantly by electrochemical reconstruction of the surface layer in a process described as electrode activation (Thirumalraj et al., 2015; Kumar et al., 2010; Palanisamy et al., 2015). Figure 6.25 shows electron microscopy of the 'as printed' SPCE surface and shows a rough and porous morphology compared to that of the GCE (inset).

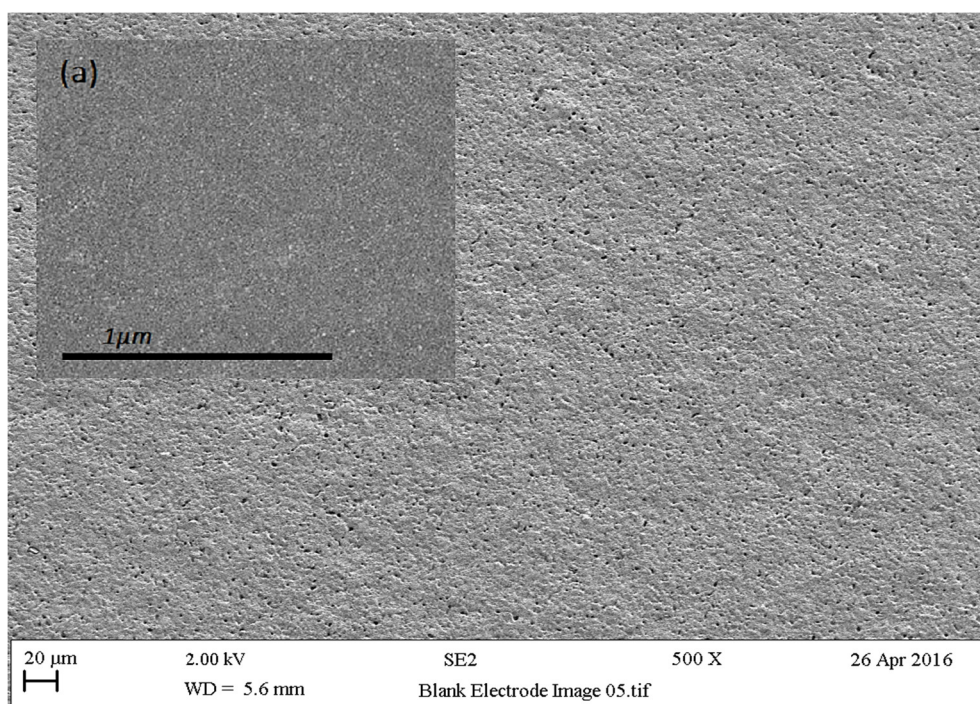


Figure 6.25. Scanning electron microscopy (500X) detailing the SPCE surface morphology prior to electrochemical activation. In comparison to the smooth and relatively uniform surface of the GCE (a) inset, the SPCE surface exhibits minor surface undulation and granularity, along with a high degree of porosity.

Electrochemical activation of SPCE is mediated using chronoamperometry and the application 2V over 600 seconds in a moderately acid electrolyte (pH5). The decrease in current associated with reconstruction of the electrode surface is presented in

figure 6.26 and corresponds to increased surface area as a result of electrochemical 'etching'. The etching process may be moderated by variation in the electrolyte pH and ionic strength, the voltage applied, and the chronoamperometry timing.

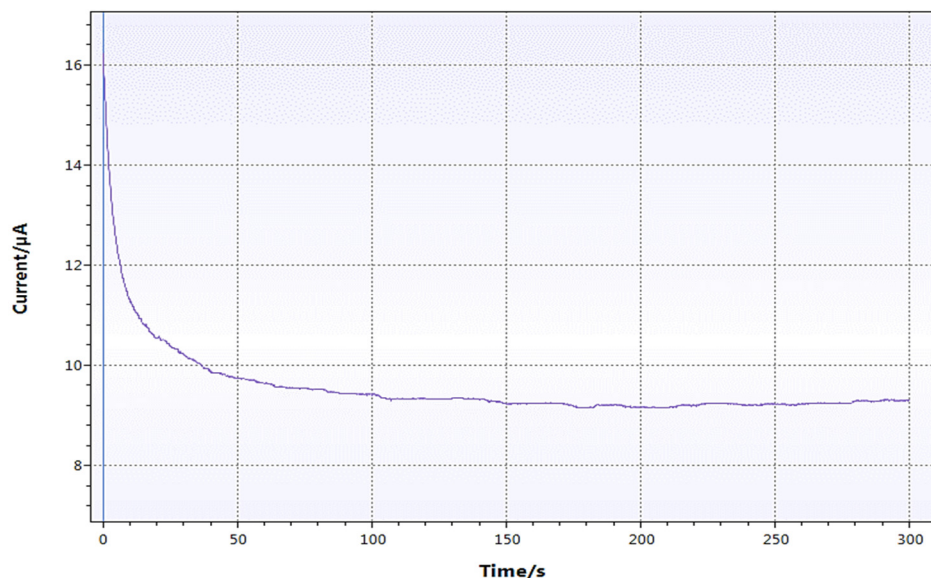


Figure 6.26. Chronoamperometry scan the effect on current flow on the activation of an SPCE at 2.0V for 300s. The decrease in current corresponds with an increase in SPCE surface area during electrochemical 'etching'. The observed variability may be attributed to gas bubble formation on the electrode surface and to localised temperature fluctuation.

The change in surface morphology associated with SPCE activation morphology is evident in the electron micrographs shown in figure 6.29 and highlights a significant increase in surface area. The surface exhibits a greater degree of 3-dimensional structure and extensive fracturing of the graphite carbon layer to expose edge flake morphology. Activated SPCEs (α SPCEs) are acknowledged to show significantly greater levels of surface defect and a significantly increased capacity for electron transfer when compared to non-activated SPCEs (Prasad et al., 2008; Karuppiah et al., 2014).

In terms of electronic characteristics, figure 6.28 shows cyclic voltammetry for both an 'as printed' SPCE and the same electrode following activation. While both the SPCE and α SPCE generate a similar current range for the voltage applied, the α SPCE scan describes the generation of higher current for a greater part of the scan (b) than that

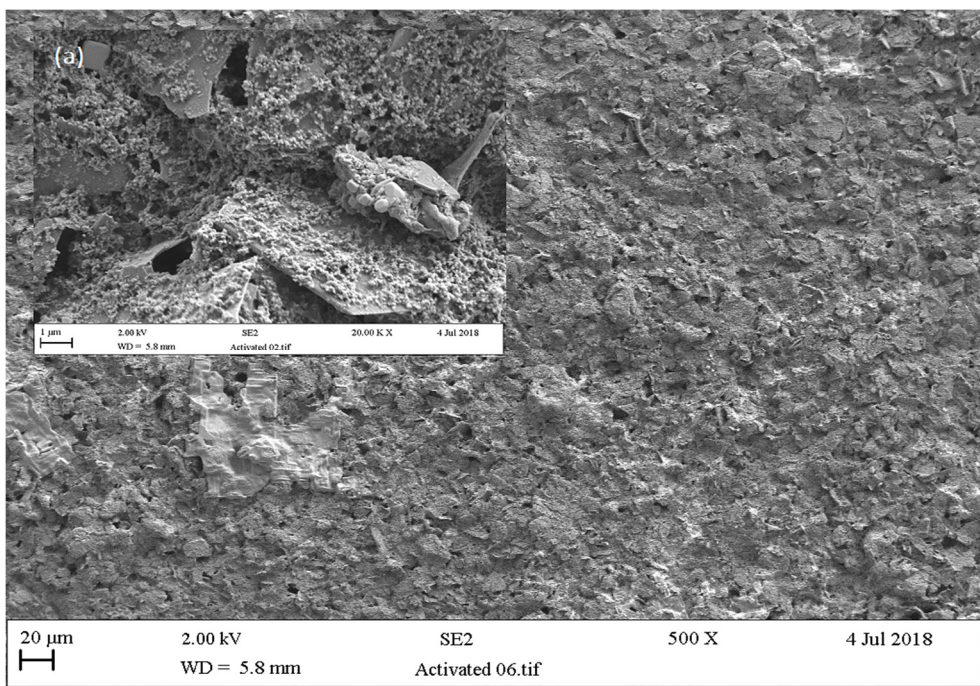


Figure 6.27. Scanning electron microscopy (500X) detailing the activated screen-printed carbon electrode (α SPCE) surface morphology and fractured edge flake morphology, inset (a).

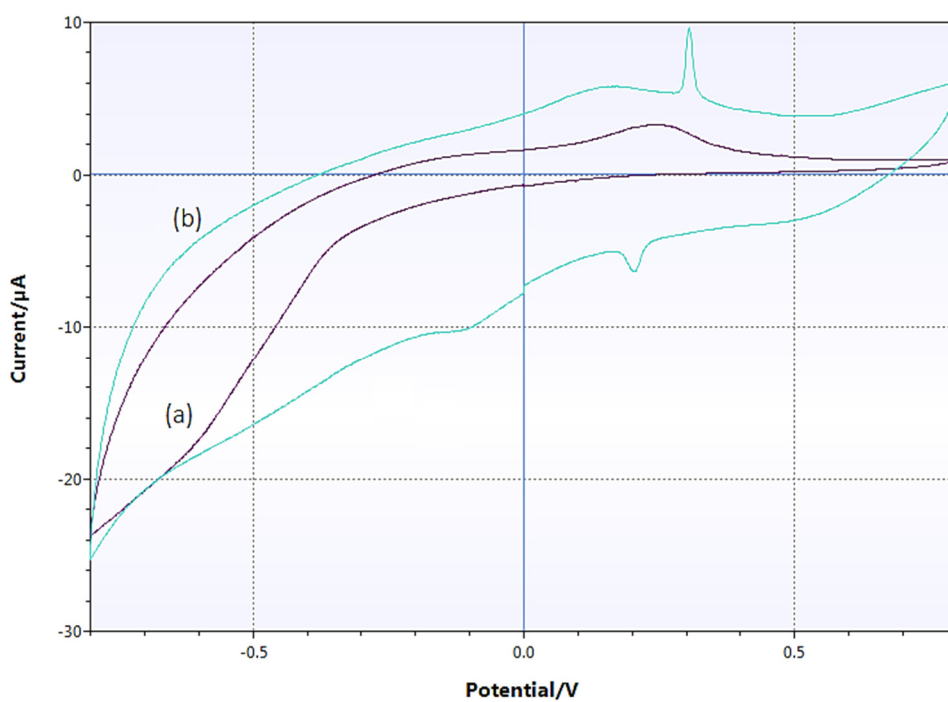


Figure 6.28. Cyclic voltammetry for the SPCE (a) and α SPCE (b) showing a significant increase in surface capacitance, and a characteristic REDOX pair at 0.3V and 0.22V on the forward and reverse scans respectively.

of the untreated SPCE (a). The differing shape, and specifically the increased area within the scan plot, described by the α SPCE reflects both a significantly increased surface capacitance and increased electron conductivity. Accordingly, α SPCEs exhibit greater sensitivity in the detection of REDOX reactions or electronic variation resulting from biomolecular interaction such as DNA oligonucleotide hybridisation than the 'as printed' counterpart. Interestingly, the α SPCE demonstrates a REDOX couple at 0.3V on the forward scan, and around 0.22V on the reverse. This anomaly was observed in every activated *Zensor* SPCE and demonstrated relatively consistent peak current values in the current range generated over forward and reverse scans.

6.5.9 α SPCE and PEDOT

As an indicator of surface conductivity and capacitance, the REDOX couple represents a convenient means to evaluate, visually and mathematically, the efficiency of drop coating electrode modification, DNA probe immobilisation, and non-specific blocking protein layer deposition. Figure 6.29 demonstrates a decrease in peak REDOX current between the bare α SPCE before and after electrochemical PEDOT:PS deposition.

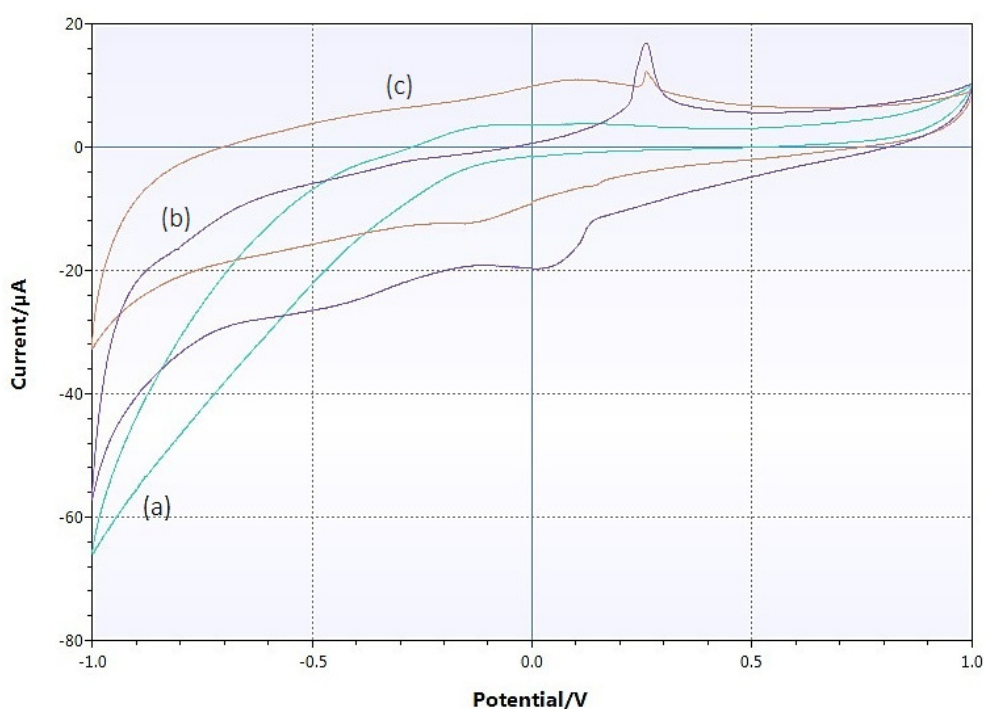


Figure 6.29. Describing the change in surface capacitance and peak REDOX current for an 'as printed' SPCE (a), and the α SPCE (b) pre and post electrochemical PEDOT:PSS deposition (c).

6.5.10 Silanised α SPCE

The co-polymerisation of PEDOT:PSS and APTES was intended to act as an anchor to immobilise probe oligonucleotides and stabilise the SPCE-PEDOT:PSS interface. With functionality similar to that of Nafion in the organisation of GO-CMF, crosslinking PEDOT:PSS with APTES in electrode modification was proposed to introduce an equivalent gain in electron transfer capacity. The evaluation of APTES-PEDOT:PSS modified α SPCEs was based on the detection of a standard concentration curve for the nucleobase guanine and the detection of single stranded DNA sequences by DPV.

The data generated is discussed below, but the fundamental obstacle to the use of APTES-PEDOT:PSS modified α SPCE was the dissociation of electrode modification layer from the α SPCE surface. The scanning electron microscopy presented in figure 6.30 highlights the uniform and even structure of the APTES-PEDOT:PSS surface prior to electrochemical analysis. Despite extended curing periods, frequent cracking of the APTES-PEDOT:PSS layer limited the application of the modified electrode.

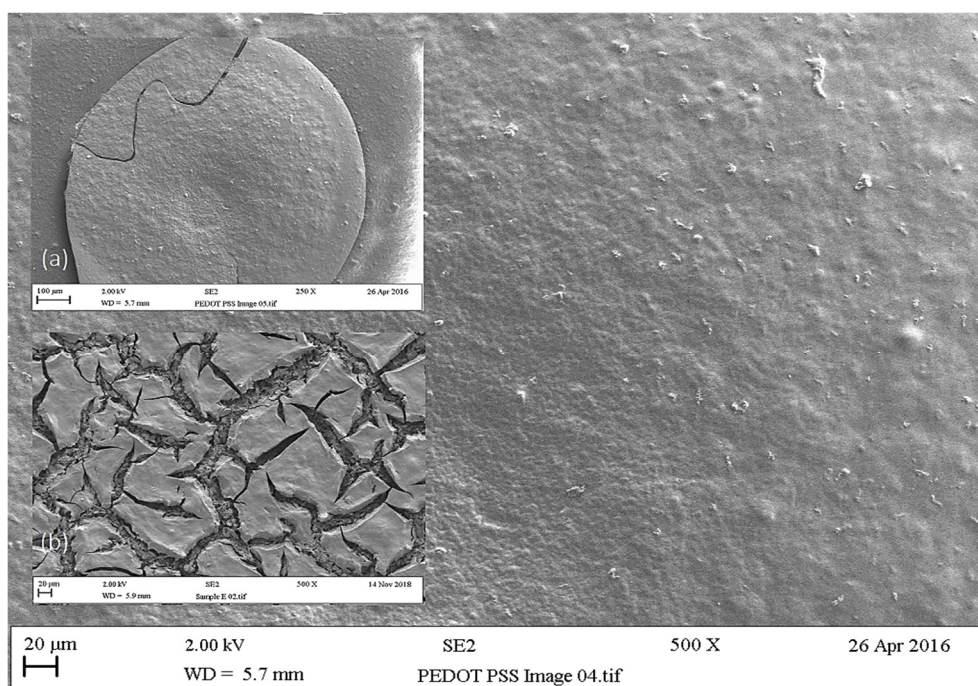


Figure 6.30. Scanning electron microscopy showing the morphology of a PEDOT:PSS:APTES modified α SPCE. Inset shows fracturing of the modification layer during curing (a) and surface fragmenting as a result of DPV electrochemical analysis (b).

While it seems logical that the loss of structural integrity during electrochemical analysis would originate from instabilities introduced during the curing process, electron microscopy shows a more widespread deterioration of the APTES-PEDOT:PSS layer than might be expected in this context. Alteration of the APTES-PEDOT:PSS ratios, variation of the electrode modification layer thickness and adjustment of the drop-coating curing conditions achieved no significant change in the rate of modified electrode failure. Accordingly, the electronic performance of PEDOT:PSS without silanisation co-polymerisation was considered, as was potential applications for the modified electrode within these constraints. (García-Hernández et al., 2016)

6.6 PEDOT:PSS- α SPCE detection of guanine

While neither the detection of DNA bases nor the non-specific detection of DNA falls within the design criteria of a 'biosensor for the detection and identification of microbial pathogens' the detection and quantification the total DNA in a microbial sample was considered to have equivalence with total carbon assays employed in water contamination testing. By this principle, any DNA concentration present in a water supply above a preordained limit could be considered indicative of microbial contamination. A dual approach was proposed to meet this end –detection of DNA nucleobases (a representative sample) and detection of single-stranded DNA.

Figure 6.31 shows the DPV oxidation of guanine at 2.5 to 25 picomolar concentrations in the electrolyte solution as detected using the PEDOT:PSS modified α SPCE. In describing a proportional relationship between the concentration of nucleobases in the electrolyte and the area under the corresponding DPV peak, peak, this technique is appropriate to the detection of threshold level microbial contamination in water of the order of 100,000 copies of a microbial genome. Depolymerisation of microbial sample DNA to a nucleobase level is within the capacity of the biosensor platform cell lysis unit and may be optimised through the addition of digestion enzymes. Alternatively, the platform may be specific to the detection of extracellular DNA sequestered from larger water volumes or flow-through filtration units.

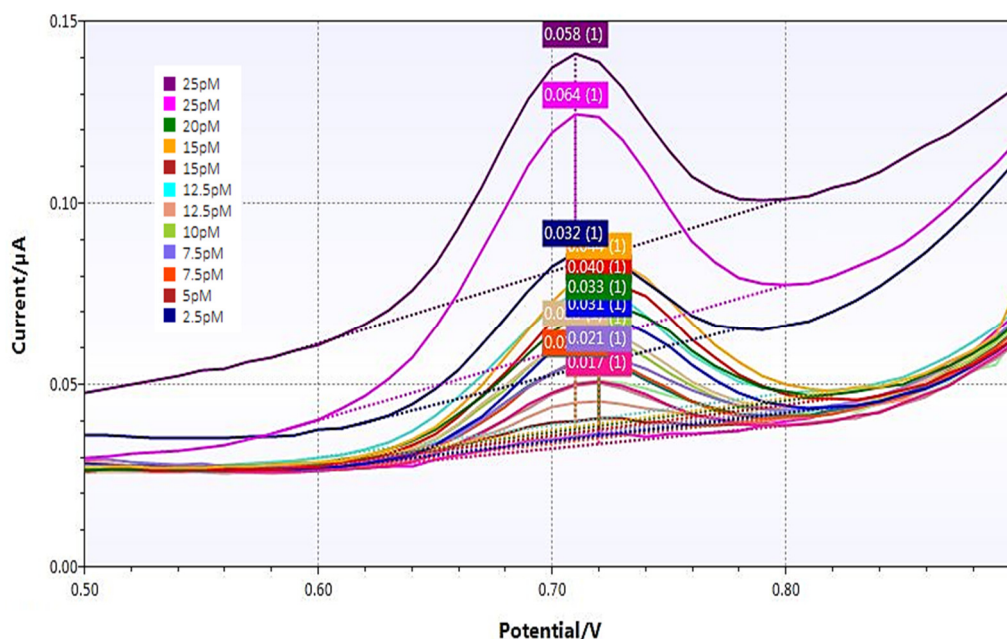


Figure 6.31. DPV oxidation of 2.5 to 25 picomolar concentrations of guanine. In comparative DPV analysis, the analyte concentration present in the electrolyte is directly proportional to the area under the corresponding oxidation curve.

6.7 PEDOT:PSS- α SPCE detection of single-stranded DNA

The non-specific detection and quantification of microbial contamination in water samples may also be determined by measuring the DNA present and referencing this value against a standard curve relating DNA concentration to microbial cell numbers for typical target organisms. For instance, the *Campylobacter jejuni* genome consists of 1,481,641 nucleic acid base pairs, relatively small by bacterial standards. The mean weight of a single base pair is 679 Daltons, equating to a molecular mass of 679g/mol, and a single *C. jejuni* cell weighs 1.006×10^6 kDa or 1.67fg (Gruss and Sauer, 1975; Knox et al., 2017). Accordingly, the DNA from 400 *C. jejuni* cells will have a mass of approximately 0.7pg and a corresponding molarity of 1pM in 1ml of electrolyte.

The validity of this approach is demonstrated in figure 6.32 and figure 6.33; showing the oxidation of native *C. jejuni* single stranded DNA (ssDNA) at concentrations of 1pM to 5pM (~400 to ~20,000 cells) and 5pM to 25pM (~20,000 to ~100,000 cells) respectively. As the DNA double helix conformation prevents the electrochemical

oxidation of paired nucleobases, temperature mediated strand separation was applied prior to analysis, and reannealing prevented by sample flash freezing.

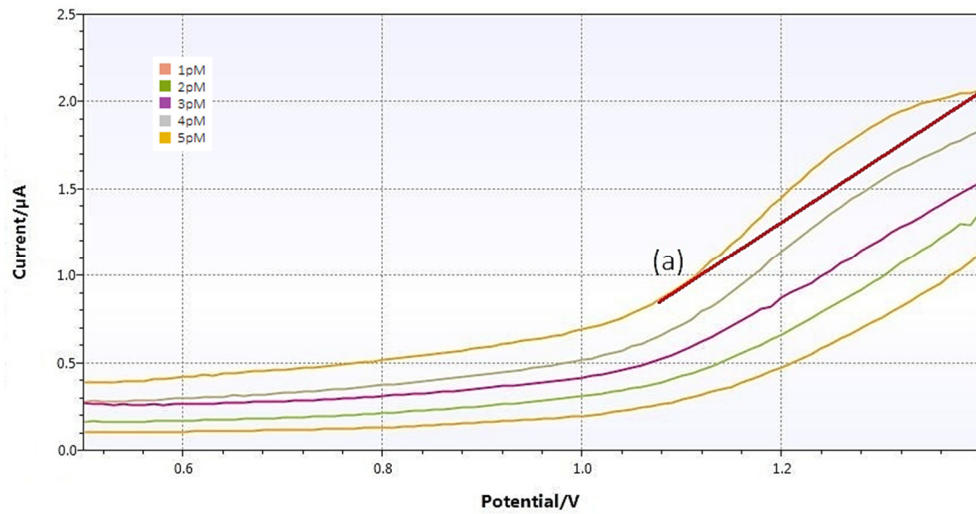


Figure 6.32. DPV quantification of 1 to 5 pM concentrations of *C. jejuni* single-stranded DNA (ssDNA) showing significant peak volume over the analytical baseline (a) at [5pM].

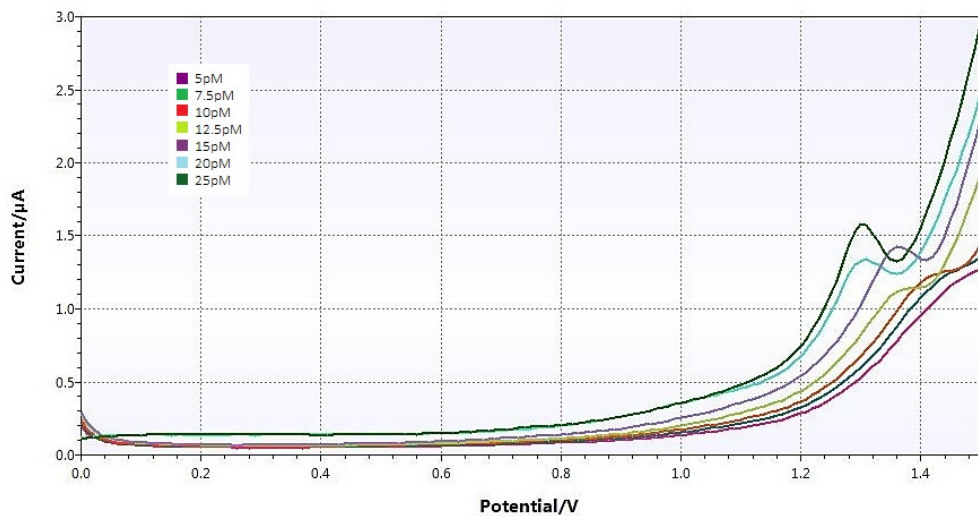


Figure 6.33. DPV nucleobase oxidation detection for *C. jejuni* ssDNA concentrations from 5pM to 25pM as an increase in peak size at 1.2V to 1.5V.

While demonstrating an analytical capacity appropriate to the detection of food and waterborne microbial pathogens, the techniques explored above were not considered to deliver on the design specification of the biosensor platform in terms of microbial pathogen identification. However, the development of the analytical

protocol presented an opportunity to further evaluate and consider the implications of deterioration and failure in PEDOT:PSS and APTES-PEDOT:PSS modified electrodes. Over the course of this experimental development, electrode failure was preceded by appearance of a significant peak at 0.3V as shown in figure 6.34; a consequence of the separation of the modification layer from the α SPCE carbon base. However, this loss of integrity was not reflected in a corresponding decrease in REDOX peak values.

6.8 α SPCE characterisation

Given that the high failure rate in PEDOT:PSS-modified α SPCEs significantly hindered the development of a DNA hybridisation-based detection model, bare α SPCEs were considered as a substrate for direct DNA probe immobilisation. Expanding on the cyclic voltammetry presented in relation to the electronic characteristics of the α SPCE, figure 6.34 also highlights the relative stability of the activated carbon surface, particularly in the positive voltage range applicable to the oxidation of nucleobases and ssDNA. The progressive drift observed in the negative voltage range is likely to correspond to the oxidation-reduction of oxygen groups on the α SPCE surface.

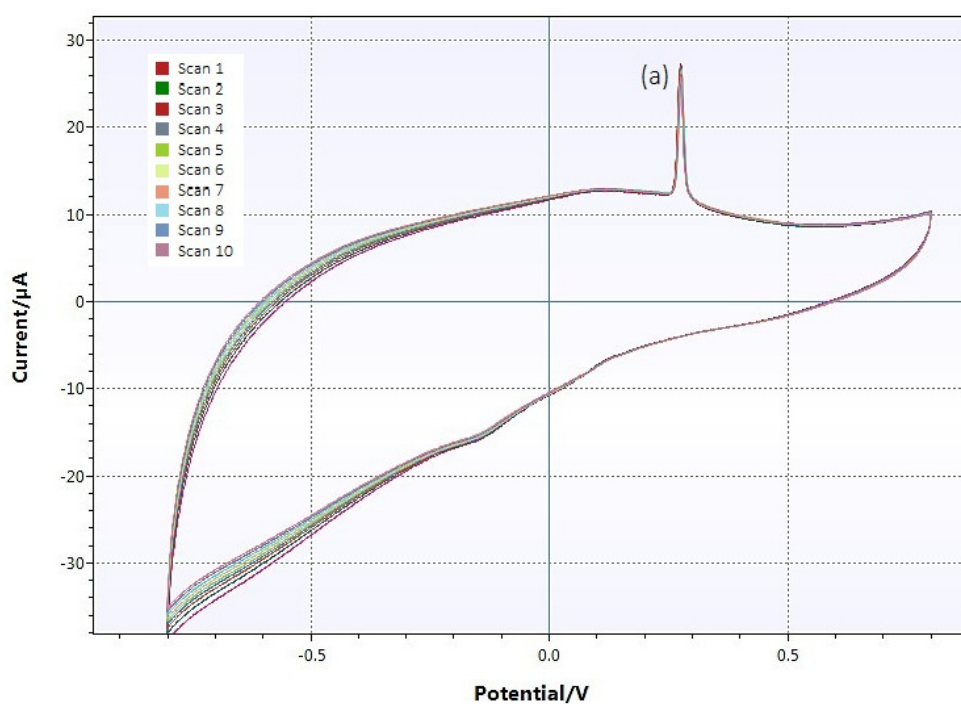


Figure 6.34. Cyclic voltammetry characterisation of α SPCE stability highlighting the characteristic peak at 0.3V (a) and oxygen group REDOX activity between 0V and -0.8V.

6.9 Single-stranded DNA probe immobilisation

The inclusion of APTES in the experimental research was prompted by use of the molecule as a crosslinker in the immobilisation of both dsDNA and ssDNA on silica surfaces (Nyati et al., 2011; Conzone and Pantano, 2004; S. Taylor et al., 2003). By way of an alternative, UV crosslinking was considered for the immobilisation of DNA directly onto the α SPCE surface. as was chronoamperometry - extensively applied in biomolecule immobilisation for electrochemical analysis (Velusamy et al., 2009; Millan et al., 1992; Rasheed et al., 2017).

6.9.1 UV-crosslinking

UV-crosslinking was considered the preferential technique in DNA immobilisation as it avoids potential deformation of the DNA conformation by the currents applied in chronoamperometry and, by extension, any knock-on effect on probe-target binding affinities. However, neither UV immobilised DNA on glass nor on electrode surfaces could be detected electrochemically or using fluorescence markers. In glass-APTES-DNA probe immobilisation, both the array dot size and the probe length were at the detection limit for the LICOR unit used and data generated had no practical application. In the UV-crosslinking of DNA directly to the α SPCE surface, techniques to counter or compensate for carbon quenching of the energy required for stable crosslinked bond formation warrants further consideration.

6.9.2 Electrochemical immobilisation

Chronoamperometric DNA immobilisation yielded best results, showing significant changes in surface electronegativity proportional to the quantity of probe bound to the α SPCE surface. Figure 6.35 shows cyclic voltammetry for the α SPCE before and after the immobilisation of 2 μ g DNA probe. As discussed previously, the characteristic peak at .03V shows a reduction in size after DNA immobilisation which is likely to be proportional to effective surface coverage. The stability of the electrode through washing with DD water indicated a robust mechanism of α SPCE-DNA binding.

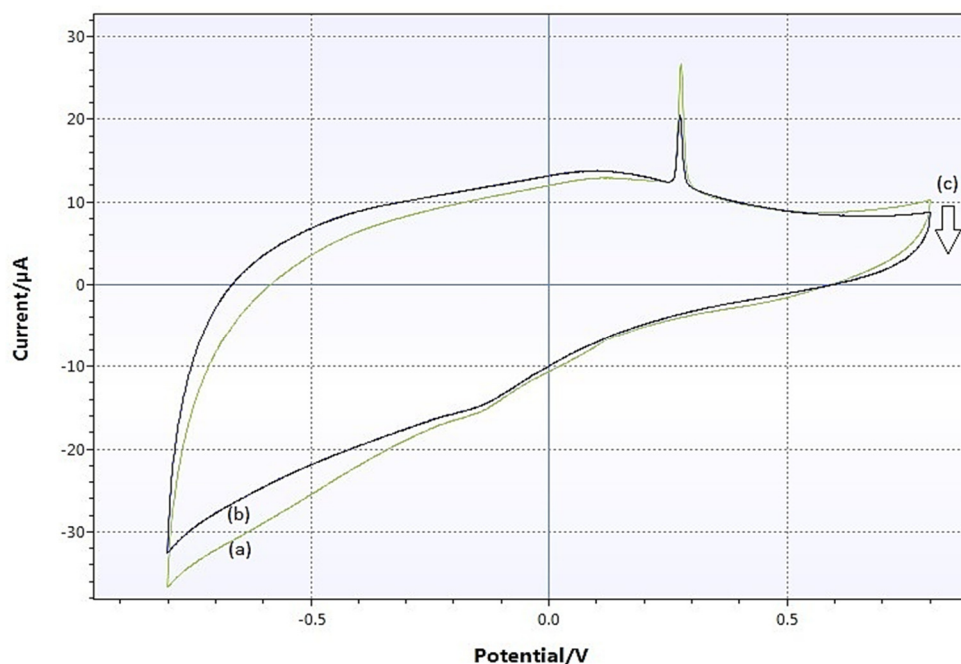


Figure 6.35. Cyclic voltammetry showing activated electrode (a), 2ug DNA immobilisation (b), and associated increase in surface negativity (c).

6.10 Co-factor detection of DNA hybridisation using Methylene blue

To enhance the detection of DNA hybridisation events, methylene blue (MB) was employed as a REDOX cofactor. The principle is similar to that of oxidation of ssDNA in solution in that the MB REDOX reaction is facilitated through the DNA nucleobases. For a fixed concentration of electrolyte MB therefore, the factor limiting peak size is the surface area of the electrode available to the REDOX reaction. Binding of target DNA from the sample with immobilised probe sequences forms prevents MB REDOX through the exposed nucleobases, with the reduction in peak height being proportional to the extent of target-probe hybridisation.

Figure 6.36 shows the REDOX peaks for a PBS/10mM MB electrolyte as mediated through an α SPCE with approximately 50% DNA overlay. Again, the reduction of the characteristic α SPCE peak at 0.3V is likely to reflect MB surface saturation and represents a convenient indicator of the electrode surface characteristics. The characterisation of a significant peak in this instance suggesting a requirement to employ a higher MB concentration in the electrolyte or extend the incubation period.

As discussed previously, the peak height at 0.3V on trace (a) indicates a partial DNA coverage which may be countered by increasing the surface probe concentration or blocking the exposed α SCE surface to prevent both surface MB REDOX and the binding of non-target sample sequences.

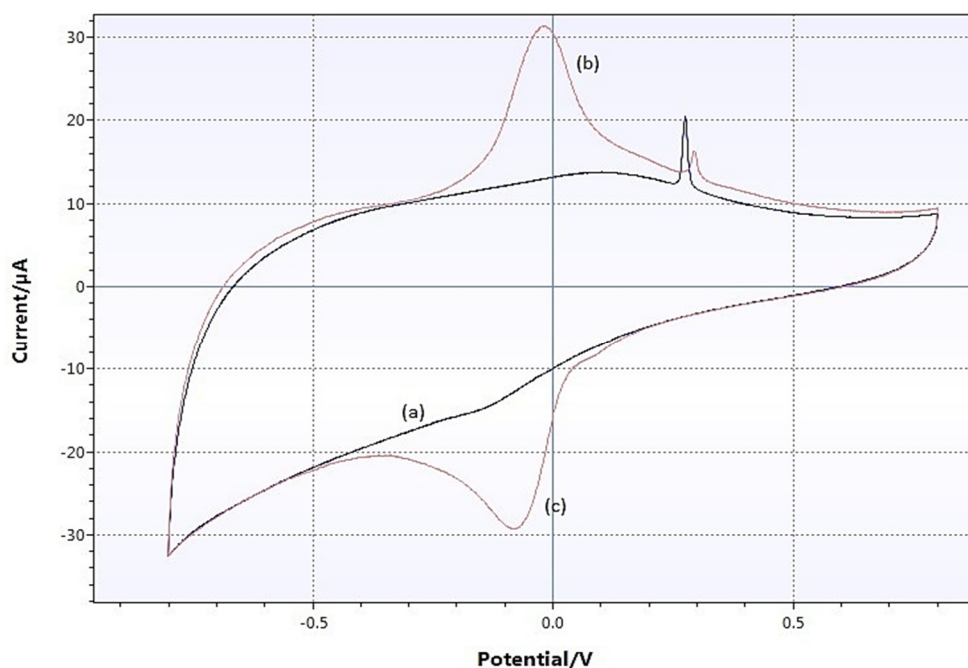


Figure 6.36. Cyclic voltammetry characterisation of immobilised DNA (a) and electrode/DNA with associated oxidation (b) and reduction (c) peaks for 10 mM methylene blue (MB).

6.11 Bovine serum albumin (BSA) – blocking non-specific binding

In the great majority of biomolecular assays, bovine serum albumin (BSA) is the primary means to prevent non-target molecules present in the sample matrix from binding to analytical surfaces. The role of BSA in this instance is the same – preventing both non-target DNA sequences and MB from binding to the electrode surface and erroneously influencing the quantification of probe-target hybridisation. Figure 6.37 demonstrates the blocking effect of BSA, and the peak sizes resulting from MB REDOX reactions occurring only through the ssDNA probe oligonucleotides. The stability of the BSA-DNA combination highlighted in figure 6.38 represents an analytical baseline against which subsequent changes in the MB REDOX couple can be compared for statistical significance and, where appropriate, relative quantification.

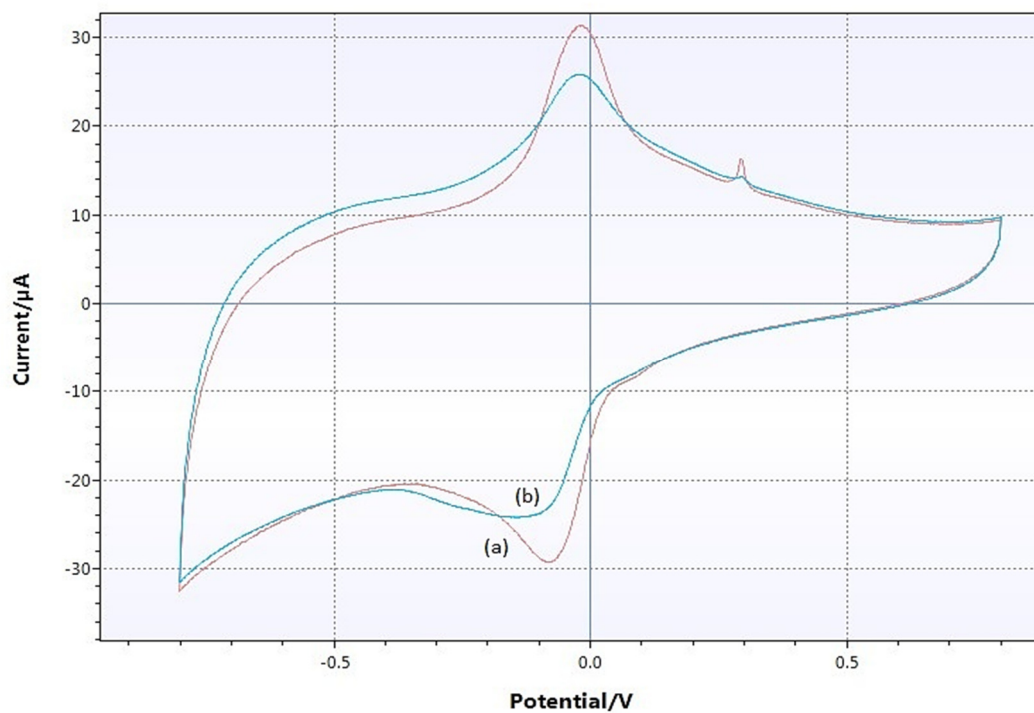


Figure 6.37. Voltammogram highlighting the blocking effect of BSA in restricting methylene blue oxidation and reduction (a) via the immobilised ssDNA sequences only (b).

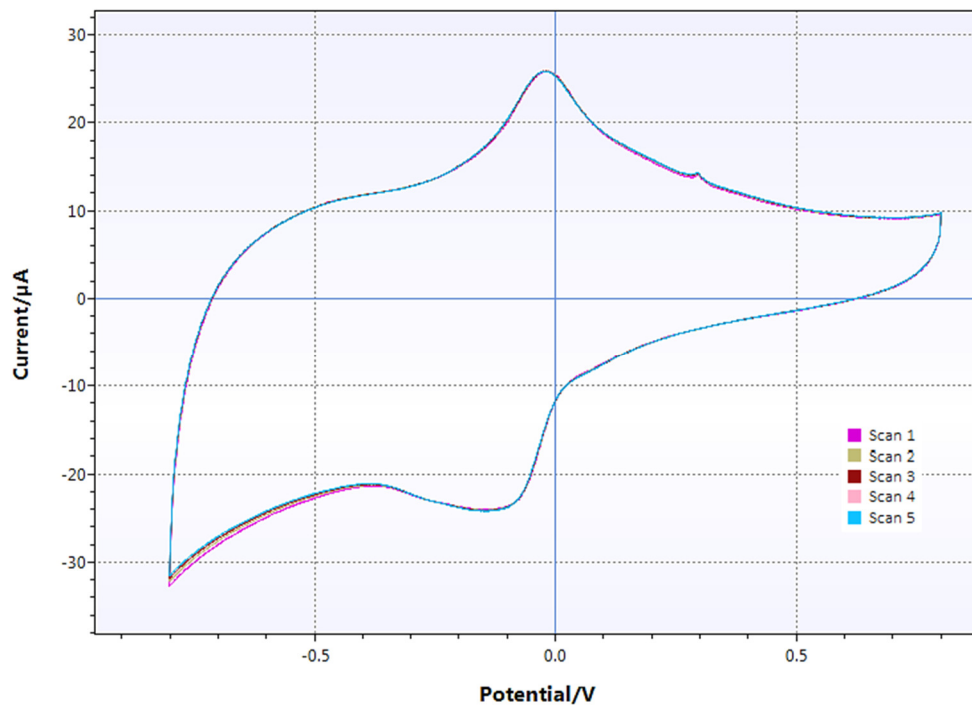


Figure 6.38. Highlighting the stability of the immobilised DNA/BSA blocking protein combination through 5 voltammetry scans -0.8V to 0.8V.

Figure 6.39 highlights both the effectiveness of BSA in preventing non-complementary target sequences from binding to the electrode surface, and the specificity of the probe-target hybridisation event. However, despite no statistically significant change in the MB redox couple values, the characteristic α SPCE peak at 0.3V shows a degree of flattening post-incubation. The presence of the peak despite BSA blocking indicates a need to further refine the BSA blocking protocol. During development of the electrode blocking protocol a 1%BSA solution negatively affected the stability of the BSA-BDA- α SPCE combination. Accordingly, a 0.5% BSA blocking solution was employed for electrode blocking in the presented data. The endurance of the characteristic α SPCE peak indicates the need for a higher concentration blocking solution or an extension of the incubation duration.

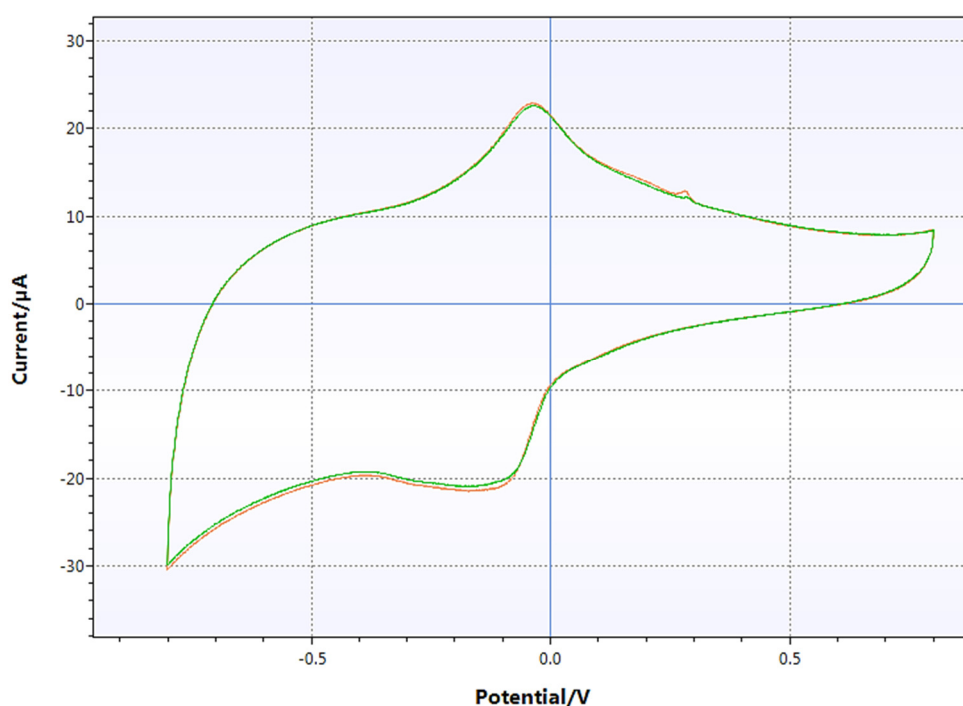


Figure 6.39. Cyclic voltammetry showing the MB REDOX couple before (red) and after (green) electrode incubation with $2\mu\text{g/ml}$ non-complementary target sequences for 15 minutes.

6.12 Electrochemical detection of DNA hybridisation

The statistically significant reduction in REDOX couple peak size following electrode incubation with target sequences complementary to the immobilised probes is shown in figure 6.40. This observed difference reflects the reduced number of ssDNA

oligonucleotides available for BM REDOX interactions as a result of probe-target hybridisation. The data presented also highlights the robustness of the α SPCE-DNA immobilisation as the electrode was rinsed gently in DD water for 5 minutes to remove residual MB prior to each 'challenge' or analytical step. Interestingly, the characteristic α SPCE peak at 0.3V is present on both traces rather than flattening as a result of non-specific binding of the complementary fragments. This absence of non-specific binding suggests a high degree of binding efficiency in target-probe hybridisation and warrants in-depth characterisation.

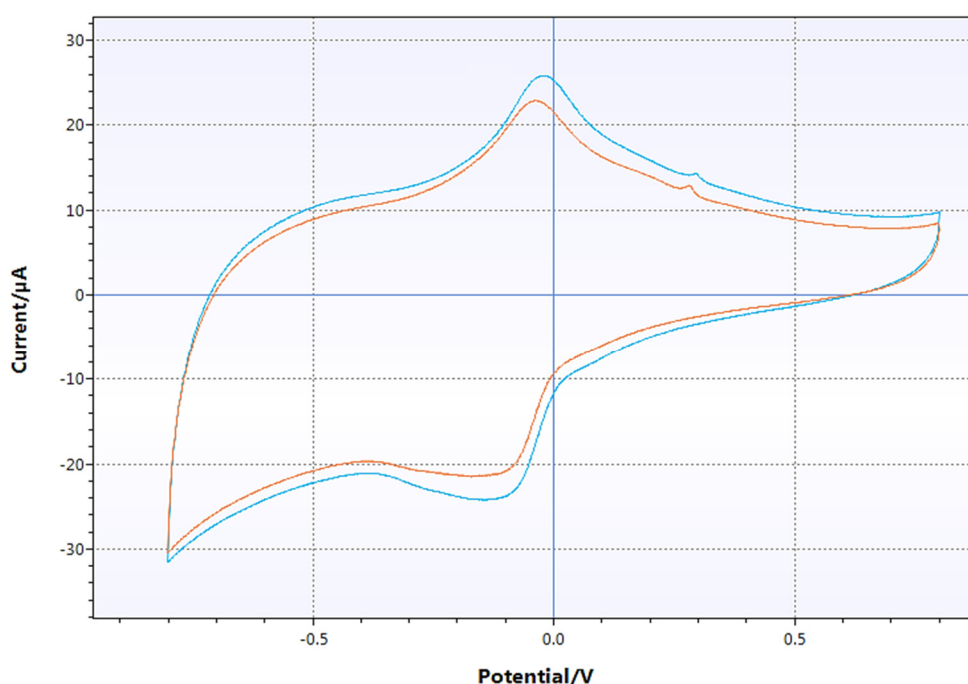


Figure 6.40. Cyclic voltammetry showing the MB REDOX couple before (blue) and after (red) electrode incubation with $2\mu\text{g/ml}$ complementary target sequences for 15 minutes.

α SPCE-based probe-target hybridisation detection was evaluated in the detection of both *C. jejuni* PCR product, and for native *C. jejuni* DNA sequences generated using the biosensor platform lysis unit and DNA purification module. MB REDOX peak values generated by cyclic voltammetry indicates a concentration dependent correlation between electron transfer rates and the hybridisation of immobilised probe oligonucleotides with both PCR amplicons and native DNA samples. Expanding this relationship to a practical scale suited to the relative enumeration of *C. jejuni* is entirely dependent on the incorporation of a DNA amplification capability.

To put the challenges in perspective, in each microgram of probe oligonucleotide immobilised or hybridised in the presented research, there are approximately 4.34×10^{13} separate copies of the 21bp sequence specific to the *C. jejuni* 16s coding region. To detect 500 cells therefore, a number acknowledged as sufficient to cause disease (Schielke et al., 2014c), the biosensor would have to have the capacity to detect the change in REDOX activity resulting from the hybridisation of only 500 of the 1.74×10^{14} probe sequences coating the electrode surface.

However, with PCR amplification of the sample DNA the challenge of statistically significant differentiation becomes practical. In 35 amplification cycles (~35 minutes) 500 target sequences are potentially multiplied to around 17.2 trillion sequences, with the capacity to hybridise $1/10^{\text{th}}$ of the immobilised probes on the α SPCE surface. While the precision of this process is contingent on a robust PCR protocol, figure 6.41 demonstrates a clear decrease in MB REDOX activity in response to the cumulative introduction of $7.4\mu\text{g}$ aliquots of PCR amplicon, each containing $0.5\mu\text{g}$ of target DNA.

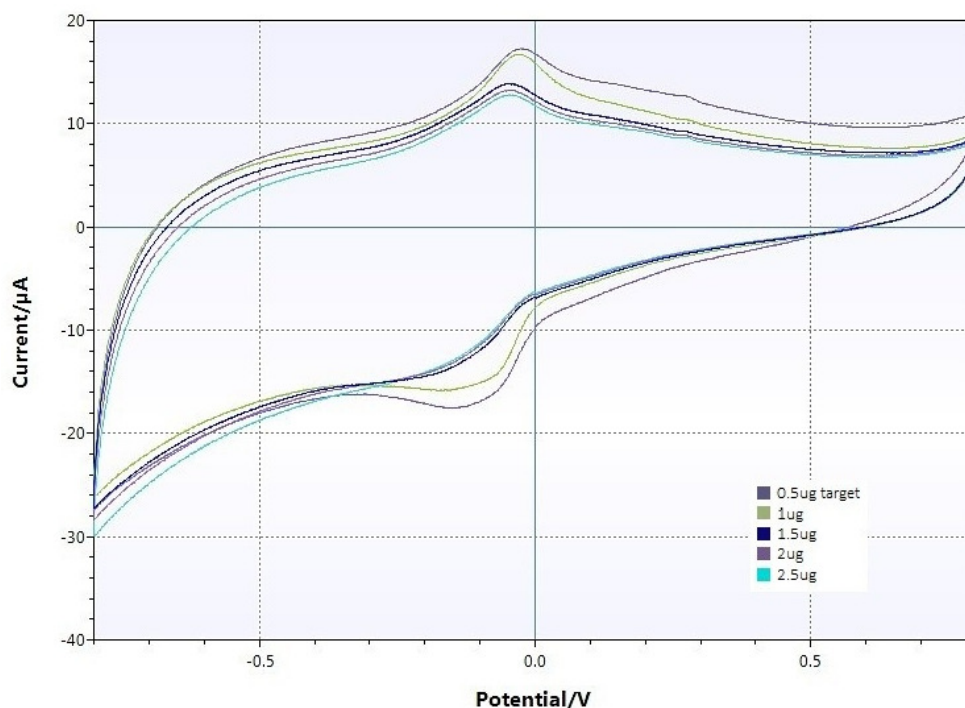


Figure 6.41. Cyclic voltammetry data outlining the decrease in MB REDOX couple activity resulting from the cumulative addition of PCR amplicon aliquots of $0.5\mu\text{g}$ of target DNA.

6.13 Statistical analysis of cyclic voltammetry data

Each addition of 0.5 μ g target DNA equates to the identifying sequences of approximately 625 *C. jejuni* cells prior to PCR amplification. To identify statistically significant differences in probe-target hybridisation, a one-way analysis of variance (ANOVA) test was conducted using data points from the cyclic voltammetry relating current values in the MB oxidation peak between -0.2V and zero shown in figure 6.42.

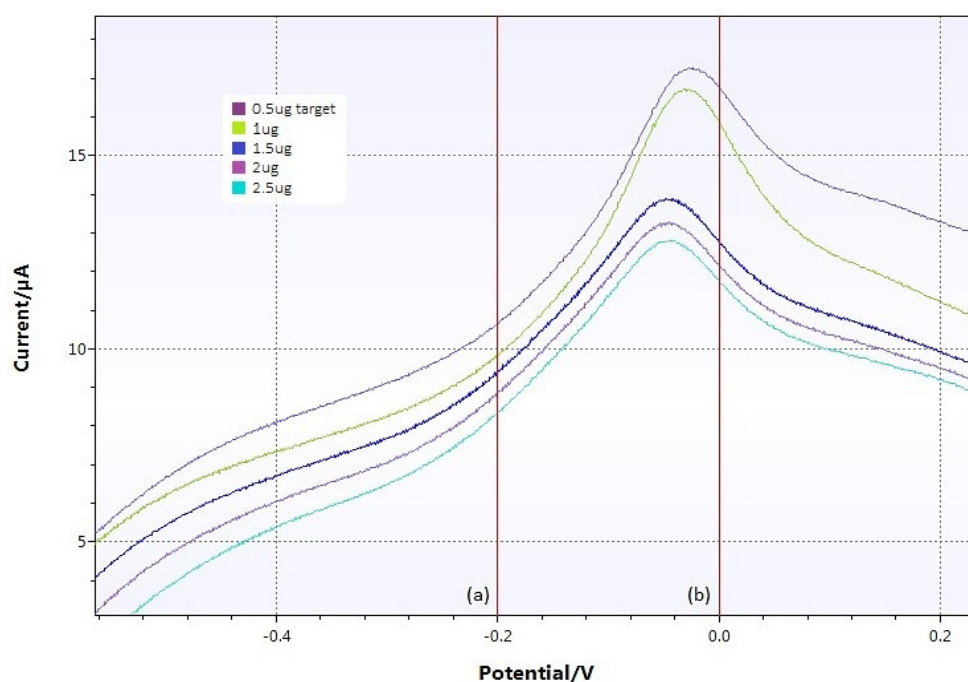


Figure 6.42. Detailing the cyclic voltammetry data range selected -0.2V (a) to 0V (b) to test the hypothesis: cumulative addition of 0.5 μ g of target sequence DNA has no statistically significant effect on MB REDOX electron transfer levels.

The resulting analysis presented in figure 6.43 indicates a statistically significant difference between the area under the curve as described by the current generated by each reduction in MB oxidation peak corresponding to incremental probe-target hybridisation ($F=102.1$). As tested, the α SPCE-DNA biosensor shows a statistically significant limit of detection of approximately 0.5 μ g/ml (7.2×10^{-14} M) target DNA. As demonstrated in figure 6.44, the data describes a linear relationship between target DNA hybridisation and peak MB oxidation electron transfer. An R^2 value of 0.9 indicates a strong goodness-of-fit and supports the ANOVA analysis.

Summary of Data						
	Treatments					
	1	2	3	4	5	Total
N	202	202	202	202	202	1010
ΣX	2856.4911	2722.3987	2230.7389	2325.5526	2440.9874	12576.1688
Mean	14.141	13.4772	11.0433	11.5126	12.0841	12.452
ΣX^2	41443.6415	37831.329	25049.0756	27178.0234	29920.5325	161422.602
Std.Dev.	2.2854	2.3825	1.4359	1.4191	1.4514	2.1876

Source	SS	df	MS	
Between-treatments	1395.0627	4	348.7657	$F = 102.0864$
Within-treatments	3433.4592	1005	3.4164	
Total	4828.5219	1009		

The F -ratio value is 102.0864. The p -value is $< .00001$. The result is significant at $p < .05$.

Figure 6.43. Summary of the statistical evaluation of changes in DNA MB REDOX activity levels resulting from cumulative additions of 0.5 μ g aliquots of target sequence. Treatments 1 to 5 refer to for current values generated by voltages between -0.2V and 0V and corresponding to the incremental addition of 0, 0.5 μ g, 1 μ g, 1.5 μ g and 2 μ g of target DNA.

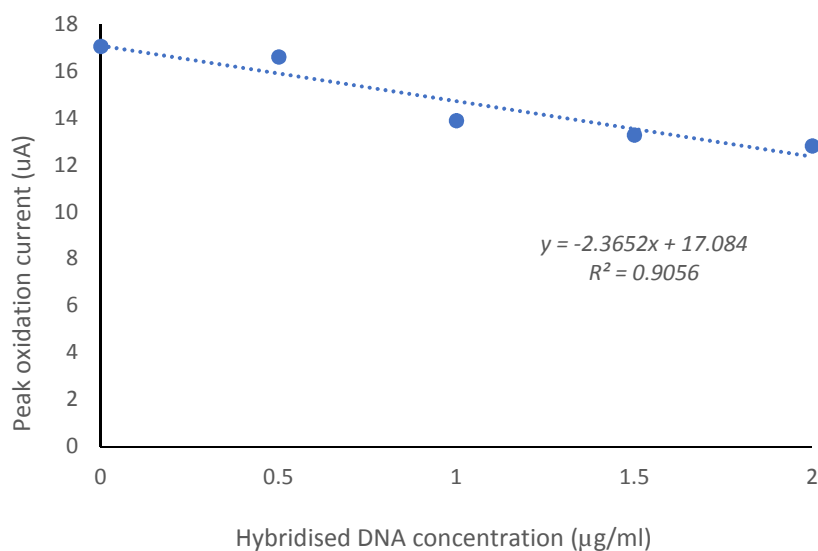


Figure 6.44. Describes the linear relationship between peak methylene blue oxidation current and the cumulative hybridisation of 0.5 μ g to 2.0 μ g target with immobilised probe DNA.

ANOVA analysis was used throughout the sensor development process to determine the stability of as-prepared electrodes. Figure 6.45 shows the data summary relating the stability of the α SPCE following DNA immobilisation and BSA blocking. With an F-value of 0.31, the as-prepared electrode shows no statistically significant difference between cyclic voltammetry scans over the voltage range -0.2V to 0V. An F-value of 3.32 was calculated for the incubation of non-complementary DNA sequences with the prepared electrode, indicating a degree of non-specific DNA binding, but at a level low enough to compensate for in subsequent data analysis and presentation.

Summary of Data						
	Treatments					
	1	2	3	4	5	Total
N	201	201	201	201	201	1005
ΣX	4209.938	4242.0346	4278.0618	4340.6996	4316.4228	21387.1568
Mean	20.945	21.1046	21.2839	21.5955	21.4747	21.281
ΣX^2	96992.4748	98643.1446	100607.5986	102769.5497	102196.6293	501209.397
Std.Dev.	6.6391	6.7515	6.9115	6.7193	6.893	6.7743

Result Details				
Source	SS	df	MS	
Between-treatments	56.3775	4	14.0944	$F = 0.30628$
Within-treatments	46018.2175	1000	46.0182	
Total	46074.595	1004		

The F -ratio value is 0.30628. The p -value is .873868. The result is *not* significant at $p < .05$.

Figure 6.45. Summary of the statistical evaluation of DNA immobilised and BSA blocked α SPCE prior to incremental hybridisation with target sequence aliquots. Treatments 1 to 5 refer to cyclic voltammetry generated current data for the voltage range -0.2V and 0V.

DNA hybridisation-based biosensors are pushing into the atto-molar (10^{-18} M) range (Z. Wu et al., 2017; Rahman et al., 2017), the α SPCE-DNA biosensor demonstrates a

detection sensitivity in the same region as hybridisation based methodologies described as ultrasensitive (Shariati et al., 2019; Lin et al., 2015; Shahrokhian and Salimian, 2018). Accordingly, in the context of label-free DNA biosensors, the α SPCE-DNA developed demonstrates the potential to rival methods using much more complex nano-materials and elaborate construction techniques. The detection resolution and statistically significant demarcation of sample concentrations from a focus on real-world applications and the delivery of accurate, reliable, repeatable results with a high level of statistical certainty.

In consideration of the potential interfering influence of residual chemistry from the RT-PCR process the amplicon samples were isolated using a Monarch nucleic acid purification kit. RT-PCR master mix typically contains *Taq* polymerase, MgCl₂ buffering salts, dNTPs – (the DNA building blocks) and SYBER Green (an intercalating dye for the fluorescent visualisation of dsDNA). The comparison of electrochemical analysis data generated by the MB α SPCE-DNA biosensor showed no significant difference in the characterisation of as-found *C. jejuni* PCR amplicons and those purified using the Monarch system and indicates no steric or electronic interference from RT-PCR master mix components.

Chapter 7

Conclusions and future direction

7.1 Introduction

The measurable outcomes generated by the presented research stem from the novel design and process execution in the biosensor platform, and the primary objective of re-imagining the basis of each step in the processing and analysis of microbial sample to allow their integration within a simple to use, field-portable device. Accordingly, the prototype device is self-contained, each process is executed automatically, and user input is limited to sample loading and the selection of analytical parameters specific to the microbial sample. Currently, this prototype is unique in incorporating portable DNA extraction, PCR target amplification, and electrochemical analysis in a single, simple, field-portable device. The design represents a high-resolution, low-cost solution to microbial detection and has no requirement for laboratory-based resources or processes. The platform is suited to a wide range of analytical roles from microbial pathogen surveillance and food and water supply, to clinical diagnostics and the characterisation of antimicrobial resistance vectors.

7.2 Equivalent portable technologies

While a plethora of biosensor systems and portable PCR platforms are described in the published literature, systems which have made the transition to commercial viability are relatively few in number. Of these, a large proportion are antibody-based and so do not take advantage of the superior resolution of nucleic acid-based analysis, while those that do have a primary focus on viral targets due to a lack of field-portable cell lysis and DNA purification techniques.

In part a result of its demonstration on the International Space Station, the portable molecular analytical platform that has received far and away the greatest attention in the scientific press is the Minion gene sequencer from Oxford Nanopore. However, while offering high-resolution analysis, Oxford Nanopore do not supply a portable DNA extraction and purification solution. The Minion is single use, requires a skilled and trained operator, and is relatively expensive. DNA hybridisation-based analysis

has formed the basis of early sequencing and gene expression characterisation in fluorescent in-situ hybridisation arrays (FISH) and microarray techniques and is the technology most similar in principle to the electrochemical DNA hybridisation-based biosensor. The portable application of fluorescence technologies is at present limited to spectrophotometry platforms such as the Promega QuantiFluor®, designed to determine the quantity and purity of DNA in a sample. Such devices could be re-tasked for the detection and identification of a specific amplified DNA target, but their resolution is limited compared to electrochemical techniques.

7.3 Laboratory-based applications

The extensive variation in laboratory-based cell lysis and DNA purification protocols can represent a challenge in the comparison of results, and even different operators can affect the data produced. Accordingly, the cell lysis and DNA extraction module of the biosensor platform may have potential benchtop applications. The reliability and repeatability inherent to the automated DNA purification process represents an advantage in the generation of samples for microarray, gene sequencing, and PCR – and particularly quantitative PCR. A redesign of the automated biosensor system for multi-channel or high throughput laboratory applications could make a valuable contribution to molecular biology method validation, and the transfer of analytical protocols between laboratory facilities; areas that present a significant challenge in biopharmaceutical development and manufacture.

7.4 Suggested further research

The detection limit and specificity demonstrated by the biosensor is comparable with that of contemporary, laboratory-based, DNA hybridisation detection techniques described in the literature. However, the optimisation of factors such as the electrode surface area, electrolyte composition and the selection of REDOX reporter molecule, the analytical component of the biosensor platform have the potential to generate statistically reliable DNA sequences in the attomolar range. Adjustment of the operational parameters of the platform components means such enhancement could be used to deliver highly sensitive detections, or to reduce the time taken for less critical measurements.

The preliminary results presented demonstrate the validity of the biosensor platform design and support the development of a portable molecular biology platform with the capacity to process and characterise multiple samples simultaneously. Among the greatest advantages of the α SPCE-DNA biosensor is one of high electronic stability that translates to repeatability, reliability, and statistical validity in practical use. The experimental data relating to probe specificity in relation to target and non-complementary DNA indicates appropriate differentiation for multiplex DNA detection. With electrode optimisation and miniaturisation, the next design aim is the construction of an electrode array such as that outlined in figure 7.1, applicable to the characterisation of multiple microbial targets within a single sample.

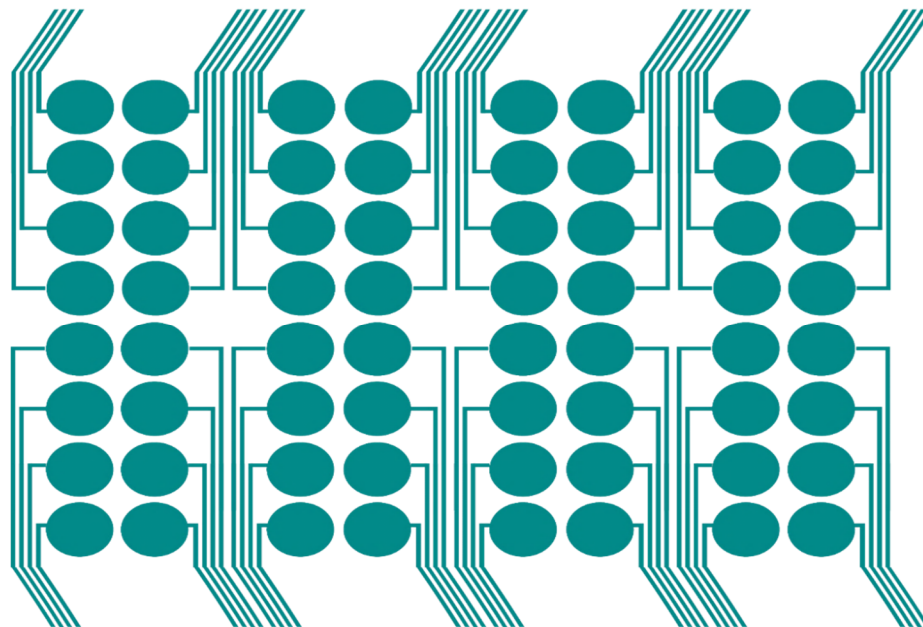


Figure 7.1. Biosensor array design, facilitating the detection of multiple DNA sequences simultaneously with applications in the characterisation of microbial population dynamics, for clinical genotyping, or in antibiotic resistance characterisation.

Biosensor arrays may be tasked to hybridise multiple DNA sequences within a single sample, delivering analytical redundancy and increasing the statistical confidence in detection and identification of specific genes. In clinical diagnostics, immobilisation of multiple antibiotic resistance indicator genes in an array could allow the clinician to

select an effective therapeutic antibiotic based on a single, near-real-time, analysis. In a research context, the electrochemical biosensor array has the potential to rival multiplex PCR and to carry out multi-locus genotyping.

7.4.1 The development of user specific interface 'apps'

In laboratory based molecular biology, the specificity of an analysis is determined by the protocol followed by the analyst. However, for the biosensor platform, all such sample preparation and analytical parameters will be executed through a dedicated graphic user interface (GUI) in the form of a smart phone app. Although the scope of the research extended only to statistical analysis and process control using Arduino, the app GUI is anticipated to add or remove access to analytical features according to the user. This could be a 'single button' analysis for routine pathogen surveillance through to a fully customisable platform for use in a research or education setting.

7.5 In summary

At the current prototype stage, the biosensor platform demonstrates an analytical capability that is simply not otherwise available in a self-contained, field-portable analytical device operating in near-real-time. The presented single channel design is fully automated, from cell lysis and DNA purification to target sequence amplification and hybridisation-based electrochemical detection. Demonstrating the capacity to detect and identify as few as 500 *Campylobacter* cells, the analytical resolution is favourably comparable with much more expensive and time-consuming laboratory-based techniques. Furthermore, in sample processing and preparation, the reliability and repeatability demonstrated has potential applications in benchtop DNA extraction where operator variability is a significant obstacle to method validation.

In the detection of microbial pathogens, the biosensor platform has demonstrated its validity for development as a practical tool for use in food and water supply, in agriculture, and in environmental research. However, with the allocation of research resources, development, and optimisation the system could also have potential roles

in clinical diagnostics and personalised medicine. Where access to laboratory resources are limited or unavailable, be it in developing countries or out-of-hours accident and emergency rooms, a biosensor platform based on the presented research has the potential to meet the pressing requirement for a low-cost, portable device to expedite diagnosis of sepsis, meningitis, or the identification of treatment resistant pathogens.

References

Adam, T., Mohammed, A. M., Dhahi, T. S., Azua, N. F. N., Azizah, N., Hashim, U. and Gopinath, S. C. (2018) 'Semiconductor Nanowires Biosensors for Highly Selective and Multiplexed Detection of Biomolecules.' *Journal of Telecommunication, Electronic and Computer Engineering (JTEC)*, 10(2-8) pp. 155-158.

Agunos, A., Waddell, L., Léger, D. and Taboada, E. (2014) 'A systematic review characterizing on-farm sources of *Campylobacter* spp. for broiler chickens.' *PLoS One*, 9(8) p. e104905.

Ajene, A. N., Fischer Walker, C. L. and Black, R. E. (2013) 'Enteric pathogens and reactive arthritis: a systematic review of *Campylobacter*, *Salmonella* and *Shigella*-associated reactive arthritis.' *J. Health Popul. Nutr.*, 31(3) pp. 299-307.

Al-Soud, W. A. and Rådström, P. (1998) 'Capacity of nine thermostable DNA polymerases to mediate DNA amplification in the presence of PCR-inhibiting samples.' *Applied and environmental microbiology*, 64(10) pp. 3748-3753.

Alexander, P. J., Rajanikanth, G., Bacon, C. D. and Bailey, C. D. (2007) 'Recovery of plant DNA using a reciprocating saw and silica-based columns.' *Molecular Ecology Notes*, 7(1) pp. 5-9.

Allen, M. J., Tung, V. C. and Kaner, R. B. (2009) 'Honeycomb carbon: a review of graphene.' *Chemical reviews*, 110(1) pp. 132-145.

Allen, V., Bull, S., Corry, J., Domingue, G., Jørgensen, F., Frost, J., Whyte, R., Gonzalez, A., et al. (2007) 'Campylobacter spp. contamination of chicken carcasses during processing in relation to flock colonisation.' *Int. J. Food Microbiol.*, 113(1) pp. 54-61.

Ambrosi, A., Chua, C. K., Bonanni, A. and Pumera, M. (2014) 'Electrochemistry of graphene and related materials.' *Chemical reviews*, 114(14) pp. 7150-7188.

Andrighetto, C., Dalmaso, A., Lombardi, A., Civera, T. and Bottero, M. T. (2016) 'Isolation and characterisation of lactic acid bacteria from donkey milk.' *Journal of Dairy Research*, 83(3) pp. 383-386.

Arduino, S. A. (2015) 'Arduino.' *Arduino LLC*,

Ayrapetyan, M., Williams, T. C. and Oliver, J. D. (2015) 'Bridging the gap between viable but non-culturable and antibiotic persistent bacteria.' *Trends in microbiology*, 23(1) pp. 7-13.

Bach, H.-J., Tomanova, J., Schloter, M. and Munch, J. (2002) 'Enumeration of total bacteria and bacteria with genes for proteolytic activity in pure cultures and in

environmental samples by quantitative PCR mediated amplification.' *Journal of microbiological methods*, 49(3) pp. 235-245.

Bae, S. and Wuertz, S. (2009) 'Discrimination of viable and dead fecal Bacteroidales bacteria by quantitative PCR with propidium monoazide.' *Applied and environmental microbiology*, 75(9) pp. 2940-2944.

Baker-Austin, C., Trinanes, J., Gonzalez-Escalona, N. and Martinez-Urtaza, J. (2017) 'Non-cholera vibrios: the microbial barometer of climate change.' *Trends in microbiology*, 25(1) pp. 76-84.

Bao, J., Hou, C., Zhao, Y., Geng, X., Samalo, M., Yang, H., Bian, M. and Huo, D. (2018) 'An enzyme-free sensitive electrochemical microRNA-16 biosensor by applying a multiple signal amplification strategy based on Au/PPy-rGO nanocomposite as a substrate.' *Talanta*,

Bard, A. J., Faulkner, L. R., Leddy, J. and Zoski, C. G. (1980) *Electrochemical methods: fundamentals and applications*. Vol. 2. Wiley New York.

Barsan, M. M., Ghica, M. E. and Brett, C. M. (2015) 'Electrochemical sensors and biosensors based on redox polymer/carbon nanotube modified electrodes: a review.' *Analytica chimica acta*, 881 pp. 1-23.

Battersby, T., Whyte, P. and Bolton, D. (2016a) 'Protecting broilers against *Campylobacter* infection by preventing direct contact between farm staff and broilers.' *Food Cont.*, 69 pp. 346-351.

Battersby, T., Whyte, P. and Bolton, D. (2016b) 'Protecting broilers against *Campylobacter* infection by preventing direct contact between farm staff and broilers.' *Food Control*, 69 pp. 346-351.

Battersby, T., Whyte, P. and Bolton, D. (2016c) 'The pattern of *Campylobacter* contamination on broiler farms; external and internal sources.' *J. Appl. Microbiol.*,

Beery, J., Hugdahl, M. and Doyle, M. (1988) 'Colonization of gastrointestinal tracts of chicks by *Campylobacter jejuni*.' *Appl. Environ. Microbiol.*, 54(10) pp. 2365-2370.

Berendonk, T. U., Manaia, C. M., Merlin, C., Fatta-Kassinos, D., Cytryn, E., Walsh, F., Bürgmann, H., Sørum, H., et al. (2015) 'Tackling antibiotic resistance: the environmental framework.' *Nature Reviews Microbiology*, 13(5) p. 310.

Berrang, M., Buhr, R., Cason, J. and Dickens, J. (2001) 'Broiler carcass contamination with *Campylobacter* from feces during defeathering.' *J. Food Prot.*, 64(12) pp. 2063-2066.

- Besnard, V., Federighi, M., Declercq, E., Jugiau, F. and Cappelier, J.-M. (2002a) 'Environmental and physico-chemical factors induce VBNC state in *Listeria monocytogenes*.' *Vet. Res.*, 33(4) pp. 359-370.
- Besnard, V., Federighi, M., Declercq, E., Jugiau, F. and Cappelier, J.-M. (2002b) 'Environmental and physico-chemical factors induce VBNC state in *Listeria monocytogenes*.' *Veterinary research*, 33(4) pp. 359-370.
- Blanco, M., Pinzon, C. B. and Vergara, S. G. (2018) *Synthesis and characterization of polypyrrole-TiO₂ coatings on AISI 304 stainless steel*. Vol. 1119: IOP Publishing.
- Bojanić, K., Midwinter, A. C., Marshall, J. C., Rogers, L. E., Biggs, P. J. and Acke, E. (2016a) 'Variation in the limit-of-detection of the ProSpecT *Campylobacter* microplate enzyme immunoassay in stools spiked with emerging *Campylobacter* species.' *Journal of Microbiological Methods*, 127 pp. 236-241.
- Bojanić, K., Midwinter, A. C., Marshall, J. C., Rogers, L. E., Biggs, P. J. and Acke, E. (2016b) 'Variation in the limit-of-detection of the ProSpecT *Campylobacter* microplate enzyme immunoassay in stools spiked with emerging *Campylobacter* species.' *J. Microbiol. Methods*, 127 pp. 236-241.
- Bolton, F. and Robertson, L. (1982) 'A selective medium for isolating *Campylobacter jejuni/coli*.' *Journal of Clinical Pathology*, 35(4) pp. 462-467.
- Bolton, F., Coates, D., Hutchinson, D. and Godfree, A. (1987) 'A study of thermophilic *Campylobacter* in a river system.' *Journal of Applied Bacteriology*, 62(2) pp. 167-176.
- Bondarczuk, K., Markowicz, A. and Piotrowska-Seget, Z. (2016) 'The urgent need for risk assessment on the antibiotic resistance spread via sewage sludge land application.' *Environment international*, 87 pp. 49-55.
- Boom, R., Sol, C., Salimans, M., Jansen, C., Wertheim-van Dillen, P. and Van der Noordaa, J. (1990) 'Rapid and simple method for purification of nucleic acids.' *Journal of clinical microbiology*, 28(3) pp. 495-503.
- Boulton, C. and Quain, D. (2008) *Brewing yeast and fermentation*. John Wiley & Sons.
- Branch, S. K. J. J. o. p. a. b. a. (2005) 'Guidelines from the international conference on harmonisation (ICH).' 38(5) pp. 798-805.
- Bronowski, C., James, C. E. and Winstanley, C. (2014) 'Role of environmental survival in transmission of *Campylobacter jejuni*.' *FEMS Microbiol. Lett.*, 356(1) pp. 8-19.

- Brown, L., Wolf, J. M., Prados-Rosales, R. and Casadevall, A. (2015) 'Through the wall: extracellular vesicles in Gram-positive bacteria, mycobacteria and fungi.' *Nature Reviews Microbiology*, 13(10) p. 620.
- Brüssow, H. (2015) 'Growth promotion and gut microbiota: insights from antibiotic use.' *Environ. Microbiol.*, 17(7) pp. 2216-2227.
- Bullman, S., Lucid, A., Corcoran, D., Sleator, R. D. and Lucey, B. (2013) 'Genomic investigation into strain heterogeneity and pathogenic potential of the emerging gastrointestinal pathogen *Campylobacter ureolyticus*.' *PloS one*, 8(8) p. e71515.
- Butzler, J. P. (2004) 'Campylobacter, from obscurity to celebrity.' *Clin. Microbiol. Infec.*, 10(10) pp. 868-876.
- Casadevall, A. and Pirofski, L.-a. (1999) 'Host-pathogen interactions: redefining the basic concepts of virulence and pathogenicity.' *Infection and immunity*, 67(8) pp. 3703-3713.
- Chang, C.-W., Hung, N.-T. and Chen, N.-T. (2017) 'Optimization and application of propidium monoazide-quantitative PCR method for viable bacterial bioaerosols.' *Journal of Aerosol Science*, 104 pp. 90-99.
- Chaveerach, P., Ter Huurne, A., Lipman, L. and Van Knapen, F. (2003) 'Survival and resuscitation of ten strains of *Campylobacter jejuni* and *Campylobacter coli* under acid conditions.' *Applied and environmental microbiology*, 69(1) pp. 711-714.
- Chen, D., Feng, H. and Li, J. (2012) 'Graphene oxide: preparation, functionalization, and electrochemical applications.' *Chemical reviews*, 112(11) pp. 6027-6053.
- Chen, L., Yang, J., Yu, J., Yao, Z., Sun, L., Shen, Y. and Jin, Q. (2005) 'VFDB: a reference database for bacterial virulence factors.' *Nucleic acids research*, 33(suppl_1) pp. D325-D328.
- Chen, Q., An, X., Li, H., Su, J., Ma, Y. and Zhu, Y.-G. (2016) 'Long-term field application of sewage sludge increases the abundance of antibiotic resistance genes in soil.' *Environment international*, 92 pp. 1-10.
- Chernov, T., Tkhakakhova, A., Ivanova, E., Kutovaya, O. and Turusov, V. (2015) 'Seasonal dynamics of the microbiome of chernozems of the long-term agrochemical experiment in Kamennaya Steppe.' *Eurasian soil science*, 48(12) pp. 1349-1353.
- Chisti, Y. and Moo-Young, M. (1986) 'Disruption of microbial cells for intracellular products.' *Enzyme and Microbial Technology*, 8(4) pp. 194-204.
- Chowdhury, K. (1991) 'One step' miniprep' method for the isolation of plasmid DNA.' *Nucleic acids research*, 19(10) p. 2792.

Conzone, S. D. and Pantano, C. G. (2004) 'Glass slides to DNA microarrays.' *Materials Today*, 7(3) pp. 20-26.

Cook, K. and Bolster, C. (2007) 'Survival of *Campylobacter jejuni* and *Escherichia coli* in groundwater during prolonged starvation at low temperatures.' *J. Appl. Microbiol.*, 103(3) pp. 573-583.

Coombs, S. G., Khodjaniyazova, S. and Bright, F. V. (2018) 'Exploiting the 3-Aminopropyltriethoxysilane (APTES) autocatalytic nature to create bioconjugated microarrays on hydrogen-passivated porous silicon.' *Talanta*, 177 pp. 26-33.

Corry, J. and Atabay, H. (2001) 'Poultry as a source of *Campylobacter* and related organisms.' *J. Appl. Microbiol.*, 90(S6)

Coward, C., van Diemen, P. M., Conlan, A. J., Gog, J. R., Stevens, M. P., Jones, M. A. and Maskell, D. J. (2008) 'Competing isogenic *Campylobacter* strains exhibit variable population structures in vivo.' *Appl. Environ. Microbiol.*, 74(12) pp. 3857-3867.

Cox, N., Richardson, L. and Harrison, M. (2015) 'Efficiency of Several Cultural Methods and a Chick Bioassay to Recover Dry-Stressed *Campylobacter*.' *Journal of Food Safety*, 35(1) pp. 91-101.

D'Odorico, P., Yoo, J. C. and Jaeger, S. (2002) 'Changing seasons: an effect of the North Atlantic Oscillation?' *Journal of climate*, 15(4) pp. 435-445.

Dale, E. L., Nolan, S. P., Berghaus, R. D. and Hofacre, C. L. (2015) 'On farm prevention of *Campylobacter* and *Salmonella*: lessons learned from basic biosecurity interventions.' *J. Appl. Poultry Res.*, p. pfv016.

Davies, B. (2018) *Exploring chaos: Theory and experiment*. CRC Press.

Dąbczyński, P., Marzec, M. M., Pięta, Ł., Fijałkowski, K., Raczowska, J., Bernasik, A., Budkowski, A. and Rysz, J. (2018) 'Engineering a Poly (3, 4-ethylenedioxythiophene):(Polystyrene Sulfonate) Surface Using Self-Assembling Molecules • A Chemical Library Approach.' *ACS Omega*, 3(4) pp. 3631-3639.

De Boer, P., Rahaoui, H., Leer, R., Montijn, R. and Van der Vossen, J. (2015) 'Real-time PCR detection of *Campylobacter* spp.: A comparison to classic culturing and enrichment.' *Food microbiology*, 51 pp. 96-100.

de Zoete, M. R., van Putten, J. P. and Wagenaar, J. A. (2007) 'Vaccination of chickens against *Campylobacter*.' *Vaccine*, 25(30) pp. 5548-5557.

Devane, M., Nicol, C., Ball, A., Klena, J., Scholes, P., Hudson, J., Baker, M., Gilpin, B., et al. (2005) 'The occurrence of *Campylobacter* subtypes in environmental

reservoirs and potential transmission routes.' *Journal of Applied Microbiology*, 98(4) pp. 980-990.

Djennad, A., Nichols, G., Loiacono, G., Fleming, L., Kessel, A., Kovats, S., Lake, I., Sarran, C., et al. (2017) 'The seasonality and effects of temperature and rainfall on campylobacter infections.' *International Journal of Population Data Science*, 1(1)

Donalies, U. E., Nguyen, H. T., Stahl, U. and Nevoigt, E. (2008) 'Improvement of *Saccharomyces* yeast strains used in brewing, wine making and baking.' *In Food Biotechnology*. Springer, pp. 67-98.

Du, M., Chen, J., Zhang, X., Li, A., Li, Y. and Wang, Y. (2007) 'Retention of virulence in a viable but nonculturable *Edwardsiella tarda* isolate.' *Appl. Environ. Microbiol.*, 73(4) pp. 1349-1354.

Ducret, A., Chabaliere, M. and Dukan, S. (2014) 'Characterization and resuscitation of 'non-culturable' cells of *Legionella pneumophila*.' *BMC Microbiol.*, 14(1) p. 1.

El-Moghazy, A. Y., Zhao, C., Istamboulie, G., Amaly, N., Si, Y., Noguer, T. and Sun, G. (2018) 'Ultrasensitive label-free electrochemical immunosensor based on PVA-co-PE nanofibrous membrane for the detection of chloramphenicol residues in milk.' *Biosensors and Bioelectronics*, 117 pp. 838-844.

Elmi, A., Nasher, F., Jagatia, H., Gundogdu, O., Bajaj-Elliott, M., Wren, B. and Dorrell, N. (2015) 'Campylobacter jejuni outer membrane vesicle-associated proteolytic activity promotes bacterial invasion by mediating cleavage of intestinal epithelial cell E-cadherin and occludin.' *Cell. Microbiol.*,

Erwig, L. P. and Gow, N. A. (2016) 'Interactions of fungal pathogens with phagocytes.' *Nature Reviews Microbiology*, 14(3) p. 163.

Evans, M. R., Ribeiro, C. D. and Salmon, R. L. (2003) 'Hazards of healthy living: bottled water and salad vegetables as risk factors for *Campylobacter* infection.' *Emerg. Infect. Dis.*, 9(10) pp. 1219-1225.

Faure, P. and Korn, H. (2001) 'Is there chaos in the brain? I. Concepts of nonlinear dynamics and methods of investigation.' *Comptes Rendus de l'Académie des Sciences-Series III-Sciences de la Vie*, 324(9) pp. 773-793.

Ferapontova, E. E. (2018) 'DNA electrochemistry and electrochemical sensors for nucleic acids.' *Annual Review of Analytical Chemistry*, 11 pp. 197-218.

Fierer, N., Jackson, J. A., Vilgalys, R. and Jackson, R. B. (2005) 'Assessment of soil microbial community structure by use of taxon-specific quantitative PCR assays.' *Applied and environmental microbiology*, 71(7) pp. 4117-4120.

- Findlater, A. and Bogoch, I. I. (2018) 'Human mobility and the global spread of infectious diseases: a focus on air travel.' *Trends in parasitology*,
- Flynn, S., Monaghan, R., Bogan, J., McKenna, M., Cowley, A., Daniels, S., Hughes, G. and Kelleher, S. (2017) 'Controlling wettability of PECVD-deposited dual organosilicon/carboxylic acid films to influence DNA hybridisation assay efficiency.' *Journal of Materials Chemistry B*, 5(42) pp. 8378-8388.
- Fox, G. E., Magrum, L. J., Balch, W. E., Wolfe, R. S. and Woese, C. R. (1977) 'Classification of methanogenic bacteria by 16S ribosomal RNA characterization.' *Proceedings of the National Academy of Sciences*, 74(10) pp. 4537-4541.
- Frossard, A., Donhauser, J., Mestrot, A., Gygax, S., Bååth, E. and Frey, B. (2018) 'Long-and short-term effects of mercury pollution on the soil microbiome.' *Soil Biology and Biochemistry*, 120 pp. 191-199.
- FSA, U. (2015) 'A Microbiological survey of Campylobacter contamination in fresh whole UK produced chilled chickens at retail sale – interim report to cover Quarters 1 – 3. <https://www.food.gov.uk/sites/default/files/campylobacter-survey-q2-report.pdf>.' [Online] [Accessed
- Garcia, A. B., Kamara, J. N., Vigre, H., Hoorfar, J. and Josefsen, M. H. (2013) 'Direct quantification of Campylobacter jejuni in chicken fecal samples using real-time PCR: evaluation of six rapid DNA extraction methods.' *Food Analytical Methods*, 6(6) pp. 1728-1738.
- Garcia-Mazcorro, J. F., Castillo-Carranza, S. A., Guard, B., Gomez-Vazquez, J. P., Dowd, S. E. and Brighthsmith, D. J. (2017) 'Comprehensive molecular characterization of bacterial communities in feces of pet birds using 16S marker sequencing.' *Microbial ecology*, 73(1) pp. 224-235.
- García-Hernández, C., García-Cabezón, C., Martín-Pedrosa, F., De Saja, J. A. and Rodríguez-Méndez, M. L. (2016) 'Layered composites of PEDOT/PSS/nanoparticles and PEDOT/PSS/phthalocyanines as electron mediators for sensors and biosensors.' *Beilstein journal of nanotechnology*, 7 p. 1948.
- Gayen, P. (2018) *Surface Modification of Electrode Surfaces for Water Treatment and Sensing Applications*.
- Gharst, G., Oyarzabal, O. A. and Hussain, S. K. (2013) 'Review of current methodologies to isolate and identify Campylobacter spp. from foods.' *Journal of microbiological methods*, 95(1) pp. 84-92.
- Giovannoni, S. J., Tripp, H. J., Givan, S., Podar, M., Vergin, K. L., Baptista, D., Bibbs, L., Eads, J., et al. (2005) 'Genome streamlining in a cosmopolitan oceanic bacterium.' *science*, 309(5738) pp. 1242-1245.

- Glick, B. R. (2015) 'Introduction to plant growth-promoting bacteria.' *In Beneficial Plant-Bacterial Interactions*. Springer, pp. 1-28.
- Gomes, A. M. and Malcata, F. X. (1999) 'Bifidobacterium spp. and Lactobacillus acidophilus: biological, biochemical, technological and therapeutical properties relevant for use as probiotics.' *Trends in Food Science & Technology*, 10(4-5) pp. 139-157.
- Gooding, J. J. (2018) Remembering Some of the Giants of Biosensing. ACS Publications.
- Goodwin, C. S., ARMSTRONG, J. A., CHILVERS, T., PETERS, M., COLLINS, M. D., SLY, L., McCONNELL, W. and HARPER, W. E. (1989) 'Transfer of *Campylobacter pylori* and *Campylobacter mustelae* to *Helicobacter* gen. nov. as *Helicobacter pylori* comb. nov. and *Helicobacter mustelae* comb. nov., respectively.' *International Journal of Systematic and Evolutionary Microbiology*, 39(4) pp. 397-405.
- Gosselin-Théberge, M., Taboada, E. and Guy, R. A. (2016) 'Evaluation of real-time PCR assays and standard curve optimisation for enhanced accuracy in quantification of *Campylobacter* environmental water isolates.' *Journal of microbiological methods*, 129 pp. 70-77.
- Gregg, W. W., Rousseaux, C. S. and Franz, B. A. (2017) 'Global trends in ocean phytoplankton: a new assessment using revised ocean colour data.' *Remote Sensing Letters*, 8(12) pp. 1102-1111.
- Gruss, P. and Sauer, G. (1975) 'Repetitive primate DNA containing the recognition sequences for two restriction endonucleases which generate cohesive ends.' *FEBS letters*, 60(1) pp. 85-88.
- Gunda, N. S. K., Singh, M., Norman, L., Kaur, K. and Mitra, S. K. (2014) 'Optimization and characterization of biomolecule immobilization on silicon substrates using (3-aminopropyl) triethoxysilane (APTES) and glutaraldehyde linker.' *Applied Surface Science*, 305 pp. 522-530.
- Guévremont, E., Lamoureux, L., Loubier, C. B., Villeneuve, S. and Dubuc, J. (2014) 'Detection and characterization of *Campylobacter* spp. from 40 dairy cattle herds in Quebec, Canada.' *Foodborne pathogens and disease*, 11(5) pp. 388-394.
- Haas, K., Overesch, G. and Kuhnert, P. (2017) 'A Quantitative Real-Time PCR Approach for Assessing *Campylobacter jejuni* and *Campylobacter coli* Colonization in Broiler Herds.' *Journal of food protection*, 80(4) pp. 604-608.
- Habib, I., Uyttendaele, M. and De Zutter, L. (2011) 'Evaluation of ISO 10272: 2006 standard versus alternative enrichment and plating combinations for enumeration and detection of *Campylobacter* in chicken meat.' *Food microbiology*, 28(6) pp. 1117-1123.

Handa, K. (2018) *Effects of low temperatures, freeze-thaw cycles, salinity and humic acids on the survivability of Salmonella typhimurium and its transport behavior in model subsurface granular media*. McGill University.

Hanning, I., Jarquin, R. and Slavik, M. (2008) 'Campylobacter jejuni as a secondary colonizer of poultry biofilms.' *J. Appl. Microbiol.*, 105(4) pp. 1199-1208.

Hansson, I., Engvall, E. O., Vågsholm, I. and Nyman, A. (2010) 'Risk factors associated with the presence of Campylobacter-positive broiler flocks in Sweden.' *Preventive veterinary medicine*, 96(1-2) pp. 114-121.

Hayashi, Y., Matsuda, R., Maitani, T., Imai, K., Nishimura, W., Ito, K. and Maeda, M. (2004) 'Precision, limit of detection and range of quantitation in competitive ELISA.' *Analytical chemistry*, 76(5) pp. 1295-1301.

Haynes, W. M. (2014) *CRC handbook of chemistry and physics*. CRC press.

Held, P. (2008) 'Measure Your Purity.' *GIT Laboratory Journal*, 5 pp. 9-11.

Hendrixson, D. R. and DiRita, V. J. (2004) 'Identification of Campylobacter jejuni genes involved in commensal colonization of the chick gastrointestinal tract.' *Mol. Microbiol.*, 52(2) pp. 471-484.

Hermans, D., Pasmans, F., Heyndrickx, M., Van Immerseel, F., Martel, A., Van Deun, K. and Haesebrouck, F. (2012) 'A tolerogenic mucosal immune response leads to persistent Campylobacter jejuni colonization in the chicken gut.' *Crit. Rev. Microbiol.*, 38(1) pp. 17-29.

Hermans, D., Van Deun, K., Martel, A., Van Immerseel, F., Messens, W., Heyndrickx, M., Haesebrouck, F. and Pasmans, F. (2011) 'Colonization factors of Campylobacter jejuni in the chicken gut.' *Vet. Res.*, 42(1) p. 1.

Hermans, D., Van Steendam, K., Verbrugghe, E., Verlinden, M., Martel, A., Seliwiorstow, T., Heyndrickx, M., Haesebrouck, F., et al. (2014) 'Passive immunization to reduce Campylobacter jejuni colonization and transmission in broiler chickens.' *Vet. Res.*, 45 p. 27.

Hernroth, B. E. and Baden, S. P. (2018) 'Alteration of host-pathogen interactions in the wake of climate change—Increasing risk for shellfish associated infections?' *Environmental research*, 161 pp. 425-438.

Herrera, P., Aydin, M., Park, S., Khatiwara, A. and Ahn, S. (2013) 'Utility of egg yolk antibodies for detection and control of foodborne Salmonella.' *Agric. Food Anal. Bacteriol.*, 3 pp. 195-217.

- Hiett, K., Cox, N. and Rothrock, M. (2013) 'Polymerase chain reaction detection of naturally occurring *Campylobacter* in commercial broiler chicken embryos.' *Poultry Sci.*, 92(4) pp. 1134-1137.
- Hiett, K. L. (2017) 'Campylobacter jejuni Isolation/Enumeration from Environmental Samples.' *Campylobacter jejuni: Methods and Protocols*, pp. 1-8.
- Hoseinzade, H., Ardakani, M., Shahdi, A., Rahmani, H. A., Noormohammadi, G. and Miransari, M. (2016) 'Rice (*Oryza sativa* L.) nutrient management using mycorrhizal fungi and endophytic *Herbaspirillum seropedicae*.' *Journal of integrative agriculture*, 15(6) pp. 1385-1394.
- Howard, S. L., Jagannathan, A., Soo, E. C., Hui, J. P., Aubry, A. J., Ahmed, I., Karlyshev, A., Kelly, J. F., et al. (2009) 'Campylobacter jejuni glycosylation island important in cell charge, legionaminic acid biosynthesis, and colonization of chickens.' *Infect. Immun.*, 77(6) pp. 2544-2556.
- Hu, Y., Hua, S., Li, F., Jiang, Y., Bai, X., Li, D. and Niu, L. (2011) 'Green-synthesized gold nanoparticles decorated graphene sheets for label-free electrochemical impedance DNA hybridization biosensing.' *Biosensors and Bioelectronics*, 26(11) pp. 4355-4361.
- Humphrey, T., O'Brien, S. and Madsen, M. (2007) 'Campylobacters as zoonotic pathogens: a food production perspective.' *International journal of food microbiology*, 117(3) pp. 237-257.
- Hurt, R. H., Monthieux, M. and Kane, A. (2006) 'Toxicology of carbon nanomaterials: status, trends, and perspectives on the special issue.' *Carbon*, 44(6) pp. 1028-1033.
- Ica, T., Caner, V., Istanbulu, O., Nguyen, H. D., Ahmed, B., Call, D. R. and Beyenal, H. (2012) 'Characterization of mono- and mixed-culture *Campylobacter jejuni* biofilms.' *Appl. Environ. Microbiol.*, 78(4) pp. 1033-1038.
- ISO. (2006) 'International Organisation for Standardization (ISO). 2006a. ISO 10272-1 Microbiology of Food and Animal Feeding Stuffs - Horizontal Method for Detection and Enumeration of *Campylobacter* spp - Part 2: Enumeration Method. ISO, Geneva, Switzerland.'
- ISO, E. (2006) '10272-1: 2006 Microbiology of food and animal feeding stuff—Horizontal method for detection and enumeration of *Campylobacter* spp.' *International Organization for Standardization, Geneva, Switzerland*,
- Jackson, B., ZEGARRA, J. A., Lopez-Gatell, H., Sejvar, J., Arzate, F., Waterman, S., NÚÑEZ, A. S., Lopez, B., et al. (2014) 'Binational outbreak of Guillain–Barré syndrome associated with *Campylobacter jejuni* infection, Mexico and USA, 2011.' *Epidemiology and infection*, 142(05) pp. 1089-1099.

Jafari, S., Faridbod, F., Norouzi, P., Dezfuli, A. S., Ajloo, D., Mohammadipanah, F. and Ganjali, M. R. (2015) 'Detection of *Aeromonas hydrophila* DNA oligonucleotide sequence using a biosensor design based on Ceria nanoparticles decorated reduced graphene oxide and Fast Fourier transform square wave voltammetry.' *Analytica chimica acta*, 895 pp. 80-88.

Jeon, B. and Zhang, Q. (2009) 'Sensitization of *Campylobacter jejuni* to fluoroquinolone and macrolide antibiotics by antisense inhibition of the CmeABC multidrug efflux transporter.' *J. Antimicrob. Chemoth.*, 63(5) pp. 946-948.

Jia, G., Wang, H., Yan, L., Wang, X., Pei, R., Yan, T., Zhao, Y. and Guo, X. (2005) 'Cytotoxicity of carbon nanomaterials: single-wall nanotube, multi-wall nanotube, and fullerene.' *Environmental science & technology*, 39(5) pp. 1378-1383.

Jiang, J., Alderisio, K. A., Singh, A. and Xiao, L. (2005) 'Development of procedures for direct extraction of *Cryptosporidium* DNA from water concentrates and for relief of PCR inhibitors.' *Applied and environmental microbiology*, 71(3) pp. 1135-1141.

Jordan, S., Hutchings, M. I. and Mascher, T. (2008) 'Cell envelope stress response in Gram-positive bacteria.' *FEMS microbiology reviews*, 32(1) pp. 107-146.

Josefsen, M. H., Löfström, C., Hansen, T. B., Christensen, L. S., Olsen, J. E. and Hoorfar, J. (2010) 'Rapid quantification of viable *Campylobacter* bacteria on chicken carcasses, using real-time PCR and propidium monoazide treatment, as a tool for quantitative risk assessment.' *Applied and environmental microbiology*, 76(15) pp. 5097-5104.

Kalmokoff, M., Lanthier, P., Tremblay, T.-L., Foss, M., Lau, P. C., Sanders, G., Austin, J., Kelly, J., et al. (2006) 'Proteomic analysis of *Campylobacter jejuni* 11168 biofilms reveals a role for the motility complex in biofilm formation.' *J. Bacteriol.*, 188(12) pp. 4312-4320.

Kamei, K., Asakura, M., Somroop, S., Hatanaka, N., Hinenoya, A., Nagita, A., Misawa, N., Matsuda, M., et al. (2014) 'A PCR-RFLP assay for the detection and differentiation of *Campylobacter jejuni*, *C. coli*, *C. fetus*, *C. hyointestinalis*, *C. lari*, *C. helveticus* and *C. upsaliensis*.' *Journal of medical microbiology*, 63(5) pp. 659-666.

Kargl, R., Vorraber, V., Ribitsch, V., Köstler, S., Stana-Kleinschek, K. and Mohan, T. (2015) 'Selective immobilization and detection of DNA on biopolymer supports for the design of microarrays.' *Biosensors and Bioelectronics*, 68 pp. 437-441.

Karimi-Maleh, H., Tahernejad-Javazmi, F., Atar, N., Yola, M. L. t., Gupta, V. K. and Ensafi, A. A. (2015) 'A novel DNA biosensor based on a pencil graphite electrode modified with polypyrrole/functionalized multiwalled carbon nanotubes for determination of 6-mercaptopurine anticancer drug.' *Industrial & Engineering Chemistry Research*, 54(14) pp. 3634-3639.

Karni, M., Zidon, D., Polak, P., Zalevsky, Z. and Shefi, O. (2013) 'Thermal degradation of DNA.' *DNA and cell biology*, 32(6) pp. 298-301.

Karuppiyah, C., Palanisamy, S., Chen, S.-M., Ramaraj, S. K. and Periakaruppan, P. (2014) 'A novel and sensitive amperometric hydrazine sensor based on gold nanoparticles decorated graphite nanosheets modified screen printed carbon electrode.' *Electrochimica Acta*, 139 pp. 157-164.

Keener, K., Bashor, M., Curtis, P., Sheldon, B. and Kathariou, S. (2004) 'Comprehensive review of Campylobacter and poultry processing.' *Comp. Rev. Food Sci. F.*, 3(2) pp. 105-116.

Khan, I. U., Gannon, V., Loughborough, A., Jokinen, C., Kent, R., Koning, W., Lapen, D. R., Medeiros, D., et al. (2009) 'A methods comparison for the isolation and detection of thermophilic Campylobacter in agricultural watersheds.' *Journal of microbiological methods*, 79(3) pp. 307-313.

Khan, I. U., Gannon, V., Jokinen, C. C., Kent, R., Koning, W., Lapen, D. R., Medeiros, D., Miller, J., et al. (2014) 'A national investigation of the prevalence and diversity of thermophilic Campylobacter species in agricultural watersheds in Canada.' *Water Res.*, 61 pp. 243-252.

Kim, Y.-R., Bong, S., Kang, Y.-J., Yang, Y., Mahajan, R. K., Kim, J. S. and Kim, H. (2010) 'Electrochemical detection of dopamine in the presence of ascorbic acid using graphene modified electrodes.' *Biosensors and Bioelectronics*, 25(10) pp. 2366-2369.

Kirk, M. D., Pires, S. M., Black, R. E., Caipo, M., Crump, J. A., Devleeschauwer, B., Döpfer, D., Fazil, A., et al. (2015) 'World Health Organization estimates of the global and regional disease burden of 22 foodborne bacterial, protozoal, and viral diseases, 2010: a data synthesis.' *PLoS medicine*, 12(12) p. e1001921.

Klena, J. D., Parker, C. T., Knibb, K., Ibbitt, J. C., Devane, P. M., Horn, S. T., Miller, W. G. and Konkkel, M. E. (2004) 'Differentiation of Campylobacter coli, Campylobacter jejuni, Campylobacter lari, and Campylobacter upsaliensis by a multiplex PCR developed from the nucleotide sequence of the lipid A gene lpxA.' *Journal of Clinical Microbiology*, 42(12) pp. 5549-5557.

Knox, M. A., Andriuzzi, W. S., Buelow, H. N., Takacs-Vesbach, C., Adams, B. J. and Wall, D. H. (2017) 'Decoupled responses of soil bacteria and their invertebrate consumer to warming, but not freeze-thaw cycles, in the Antarctic Dry Valleys.' *Ecology letters*, 20(10) pp. 1242-1249.

Koenraad, P., Rombouts, F. and Notermans, S. (1997) 'Epidemiological aspects of thermophilic Campylobacter in water-related environments: a review.' *Water environment research*, 69(1) pp. 52-63.

- Kong, X., Jin, D., Jin, S., Wang, Z., Yin, H., Xu, M. and Deng, Y. (2018) 'Responses of bacterial community to dibutyl phthalate pollution in a soil-vegetable ecosystem.' *Journal of hazardous materials*, 353 pp. 142-150.
- Krakiwsky, S. E., Turner, L. E. and Okoniewski, M. M. (2004) *Graphics processor unit (GPU) acceleration of finite-difference time-domain (FDTD) algorithm*. Vol. 5: IEEE.
- Kumar, A. S., Sornambikai, S., Gayathri, P. and Zen, J.-M. (2010) 'Selective covalent immobilization of catechol on activated carbon electrodes.' *Journal of Electroanalytical Chemistry*, 641(1-2) pp. 131-135.
- Lake, I., Gillespie, I., Bentham, G., Nichols, G., Lane, C., Adak, G. and Threlfall, E. (2009) 'A re-evaluation of the impact of temperature and climate change on foodborne illness.' *Epidemiology & Infection*, 137(11) pp. 1538-1547.
- Lake, I. R., Hooper, L., Abdelhamid, A., Bentham, G., Boxall, A. B., Draper, A., Fairweather-Tait, S., Hulme, M., et al. (2012) 'Climate change and food security: health impacts in developed countries.' *Environmental Health Perspectives*, 120(11) pp. 1520-1526.
- Law, J. W.-F., Ab Mutalib, N.-S., Chan, K.-G. and Lee, L.-H. (2015) 'Rapid methods for the detection of foodborne bacterial pathogens: principles, applications, advantages and limitations.' *Frontiers in microbiology*, 5 p. 770.
- Lawal, A. T. (2016) 'Synthesis and utilization of carbon nanotubes for fabrication of electrochemical biosensors.' *Materials Research Bulletin*, 73 pp. 308-350.
- Le, M., Porcelli, I., Weight, C., Gaskin, D., Carding, S. and van Vliet, A. (2012) 'Acid-shock of *Campylobacter jejuni* induces flagellar gene expression and host cell invasion.' *Eur. J. Microbiol. Immunol.*, 2(1) pp. 12-19.
- Lertsethtakarn, P., Ottemann, K. M. and Hendrixson, D. R. (2011) 'Motility and chemotaxis in *Campylobacter* and *Helicobacter*.' *Ann. Rev. Microbiol.*, 65 pp. 389-410.
- Li, D., Zhang, W., Yu, X., Wang, Z., Su, Z. and Wei, G. (2016) 'When biomolecules meet graphene: from molecular level interactions to material design and applications.' *Nanoscale*, 8(47) pp. 19491-19509.
- Li, L., Mendis, N., Trigui, H., Oliver, J. D. and Faucher, S. P. (2014) 'The importance of the viable but non-culturable state in human bacterial pathogens.' *Frontiers in microbiology*, 5 p. 258.
- Li, S.-H., Jin, Y., Cheng, J., Park, D.-J., Kim, C.-J., Hozzein, W. N., Wadaan, M. A., Shu, W.-S., et al. (2014) '*Gordonia jinhuaensis* sp. nov., a novel actinobacterium, isolated from a VBNC (viable but non-culturable) state in pharmaceutical wastewater.' *Anton. Leeuw.*, 106(2) pp. 347-356.

- Liao, J. C., Mastali, M., Li, Y., Gau, V., Suchard, M. A., Babbitt, J., Gornbein, J., Landaw, E. M., et al. (2007) 'Development of an advanced electrochemical DNA biosensor for bacterial pathogen detection.' *The Journal of Molecular Diagnostics*, 9(2) pp. 158-168.
- Lim, S. H., Wei, J., Lin, J., Li, Q. and KuaYou, J. (2005) 'A glucose biosensor based on electrodeposition of palladium nanoparticles and glucose oxidase onto Nafion-solubilized carbon nanotube electrode.' *Biosensors and Bioelectronics*, 20(11) pp. 2341-2346.
- Lim, Y., Sharma, D. and Shin, H. (2017) *Development of patternable nanoporous carbon electrodes for use as biosensors based on redox cycling effect*. IEEE.
- Lin, M., Wang, J., Zhou, G., Wang, J., Wu, N., Lu, J., Gao, J., Chen, X., et al. (2015) 'Programmable engineering of a biosensing interface with tetrahedral DNA nanostructures for ultrasensitive DNA detection.' *Angewandte Chemie International Edition*, 54(7) pp. 2151-2155.
- Lindmark, H., Boqvist, S., Ljungström, M., Ågren, P., Björkholm, B. and Engstrand, L. (2009) 'Risk factors for campylobacteriosis: an epidemiological surveillance study of patients and retail poultry.' *Journal of clinical microbiology*, 47(8) pp. 2616-2619.
- Linton, D., Dorrell, N., Hitchen, P. G., Amber, S., Karlyshev, A. V., Morris, H. R., Dell, A., Valvano, M. A., et al. (2005) 'Functional analysis of the Campylobacter jejuni N-linked protein glycosylation pathway.' *Mol. Microbiol.*, 55(6) pp. 1695-1703.
- Liu, A., Lang, Q., Liang, B. and Shi, J. (2017) 'Sensitive detection of maltose and glucose based on dual enzyme-displayed bacteria electrochemical biosensor.' *Biosensors and Bioelectronics*, 87 pp. 25-30.
- Liu, F., Choi, J. Y. and Seo, T. S. (2010) 'Graphene oxide arrays for detecting specific DNA hybridization by fluorescence resonance energy transfer.' *Biosensors and Bioelectronics*, 25(10) pp. 2361-2365.
- Liu, J., Tang, J. and Gooding, J. J. (2012) 'Strategies for chemical modification of graphene and applications of chemically modified graphene.' *Journal of Materials Chemistry*, 22(25) pp. 12435-12452.
- Liu, X., Shuai, H.-L., Liu, Y.-J. and Huang, K.-J. (2016) 'An electrochemical biosensor for DNA detection based on tungsten disulfide/multi-walled carbon nanotube composites and hybridization chain reaction amplification.' *Sensors and Actuators B: Chemical*, 235 pp. 603-613.
- Lloyd-Price, J., Abu-Ali, G. and Huttenhower, C. (2016) 'The healthy human microbiome.' *Genome medicine*, 8(1) p. 51.

- Logue, J. B., Stedmon, C. A., Kellerman, A. M., Nielsen, N. J., Andersson, A. F., Laudon, H., Lindström, E. S. and Kritzberg, E. S. (2016) 'Experimental insights into the importance of aquatic bacterial community composition to the degradation of dissolved organic matter.' *The ISME journal*, 10(3) p. 533.
- Lok, C. (2015) 'Mining the microbial dark matter.' *Nature*, 522(7556) p. 270.
- Lugert, R., Groß, U. and Zautner, A. E. (2015) 'Campylobacter jejuni: Components for adherence to and invasion of eukaryotic cells.' *Berl. Münch. Tierärztl.*, 128(3/4) pp. 10-17.
- Lund, M., Wedderkopp, A., Wainø, M., Nordentoft, S., Bang, D. D., Pedersen, K. and Madsen, M. (2003) 'Evaluation of PCR for detection of Campylobacter in a national broiler surveillance programme in Denmark.' *Journal of applied microbiology*, 94(5) pp. 929-935.
- Luo, H., Thompson, L. R., Stingl, U. and Hughes, A. L. (2015) 'Selection maintains low genomic GC content in marine SAR11 lineages.' *Molecular biology and evolution*, p. msv149.
- Lyons, S. R., Griffen, A. L. and Leys, E. J. (2000) 'Quantitative real-time PCR for Porphyromonas gingivalis and total bacteria.' *Journal of Clinical Microbiology*, 38(6) pp. 2362-2365.
- Macpherson, J. V. (2015) 'A practical guide to using boron doped diamond in electrochemical research.' *Physical Chemistry Chemical Physics*, 17(5) pp. 2935-2949.
- Mahalanabis, M., Al-Muayad, H., Kulinski, M. D., Altman, D. and Klapperich, C. M. (2009) 'Cell lysis and DNA extraction of gram-positive and gram-negative bacteria from whole blood in a disposable microfluidic chip.' *Lab on a Chip*, 9(19) pp. 2811-2817.
- Mahendran, V., Riordan, S. M., Grimm, M. C., Tran, T. A. T., Major, J., Kaakoush, N. O., Mitchell, H. and Zhang, L. (2011) 'Prevalence of Campylobacter species in adult Crohn's disease and the preferential colonization sites of Campylobacter species in the human intestine.' *PLoS One*, 6(9) p. e25417.
- Malik, A., Gadsden, B., Sharma, D., Dybas, L. A. and Mansfield, L. (2014) 'Janus-faced immunity to an enteric pathogen: how Campylobacter mediates colitis and autoimmunity (MUC2P. 820).' *J. Immunol.*, 192(1 Supplement) pp. 68.64-68.64.
- Man, S. M. (2011) 'The clinical importance of emerging Campylobacter species.' *Nature Reviews Gastroenterology and Hepatology*, 8(12) pp. 669-685.

- Mannelli, I., Minunni, M., Tombelli, S., Wang, R., Spiriti, M. M. and Mascini, M. (2005) 'Direct immobilisation of DNA probes for the development of affinity biosensors.' *Bioelectrochemistry*, 66(1-2) pp. 129-138.
- Marchena Martín-Francés, M. (2018) 'Scalable techniques for graphene on glass.'
- Marin, C., Peñaranda, D. S., Ingresa-Capaccioni, S., Vega, S. and Marco-Jiménez, F. (2015) 'Molecular Detection of *Campylobacter* spp in Day-Old Chick Demonstrate Vertical Transmission in Poultry Production.' *Journal of Animal and Veterinary Sciences*, 2(4) pp. 32-36.
- Marmur, J. and Doty, P. (1962) 'Determination of the base composition of deoxyribonucleic acid from its thermal denaturation temperature.' *Journal of molecular biology*, 5(1) pp. 109-118.
- Marshall, B. and Warren, J. R. (1984) 'Unidentified curved bacilli in the stomach of patients with gastritis and peptic ulceration.' *The Lancet*, 323(8390) pp. 1311-1315.
- Maxwell, J. C. (1865) 'VIII. A dynamical theory of the electromagnetic field.' *Philosophical transactions of the Royal Society of London*, 155 pp. 459-512.
- McArthur, A. G., Waglechner, N., Nizam, F., Yan, A., Azad, M. A., Baylay, A. J., Bhullar, K., Canova, M. J., et al. (2013) 'The comprehensive antibiotic resistance database.' *Antimicrobial agents and chemotherapy*, pp. AAC. 00419-00413.
- McCrackin, M., Helke, K. L., Galloway, A. M., Poole, A. Z., Salgado, C. D. and Marriott, B. p. (2016) 'Effect of antimicrobial use in agricultural animals on drug-resistant foodborne campylobacteriosis in humans: a systematic literature review.' *Critical reviews in food science and nutrition*, 56(13) pp. 2115-2132.
- Medina-Acosta, E. and Cross, G. A. (1993) 'Rapid isolation of DNA from trypanosomatid protozoa using a simple 'mini-prep' procedure.' *Molecular and biochemical parasitology*, 59(2) pp. 327-329.
- Meldrum, R., Griffiths, J., Smith, R. and Evans, M. R. (2005a) 'The seasonality of human campylobacter infection and *Campylobacter* isolates from fresh, retail chicken in Wales.' *Epidemiology and Infection*, 133(01) pp. 49-52.
- Meldrum, R., Griffiths, J., Smith, R. and Evans, M. R. (2005b) 'The seasonality of human campylobacter infection and *Campylobacter* isolates from fresh, retail chicken in Wales.' *Epidemiol. Infect.*, 133(01) pp. 49-52.
- Membré, J.-M., Laroche, M. and Magras, C. (2013) 'Meta-analysis of *Campylobacter* spp. Survival Data within a Temperature Range of 0 to 42° C.' *J. Food Protect.*, 76(10) pp. 1726-1732.

Meunier, M., Guyard-Nicodème, M., Hirschaud, E., Parra, A., Chemaly, M. and Dory, D. (2016) 'Identification of Novel Vaccine Candidates against *Campylobacter* through Reverse Vaccinology.' *J. Immunol. Res.*, 2016

Meyer, R., Giselbrecht, S., Rapp, B. E., Hirtz, M. and Niemeyer, C. M. (2014) 'Advances in DNA-directed immobilization.' *Current opinion in chemical biology*, 18 pp. 8-15.

Mifflin, J., Templeton, J. and More, S. (2001) *Epidemiological studies of Campylobacter colonisation of broiler. f locks in south east Queensland*. Vol. 13:

Millan, K. M., Spurmanis, A. J. and Mikkelsen, S. R. (1992) 'Covalent immobilization of DNA onto glassy carbon electrodes.' *Electroanalysis*, 4(10) pp. 929-932.

Mishra, S. K., Srivastava, A. K. and Kumar, D. (2014) 'Bio-functionalized Pt nanoparticles based electrochemical impedance immunosensor for human cardiac myoglobin.' *RSC Advances*, 4(41) pp. 21267-21276.

MN, M. N., Hashim, U., Arshad, M. M., Kasjoo, S., Rahman, S., Ruslinda, A., Fathil, M., Adzhri, R., et al. (2016) 'Electrical detection of dengue virus (DENV) DNA oligomer using silicon nanowire biosensor with novel molecular gate control.' *Biosensors and Bioelectronics*, 83 pp. 106-114.

Montgomery, G. and Sise, J. (1990) 'Extraction of DNA from sheep white blood cells.' *New Zealand Journal of Agricultural Research*, 33(3) pp. 437-441.

Moore, D., Dowhan, D., Chory, J. and Ribaud, R. K. (2002) 'Isolation and purification of large DNA restriction fragments from agarose gels.' *Current protocols in molecular biology*, 59(1) pp. 2.6. 1-2.6. 12.

Morgenthaler, N. G. and Kostrzewa, M. (2015) 'Rapid identification of pathogens in positive blood culture of patients with sepsis: review and meta-analysis of the performance of the sepsityper kit.' *International journal of microbiology*, 2015

Muela, A., Seco, C., Camafeita, E., Arana, I., Orruño, M., López, J. A. and Barcina, I. (2008) 'Changes in *Escherichia coli* outer membrane subproteome under environmental conditions inducing the viable but nonculturable state.' *FEMS Microbiol. Ecol.*, 64(1) pp. 28-36.

Müller, D., Krasemann, H., Brewin, R. J., Brockmann, C., Deschamps, P.-Y., Doerffer, R., Fomferra, N., Franz, B. A., et al. (2015) 'The Ocean Colour Climate Change Initiative: II. Spatial and temporal homogeneity of satellite data retrieval due to systematic effects in atmospheric correction processors.' *Remote Sensing of Environment*, 162 pp. 257-270.

Nachamkin, I., Allos, B. M. and Ho, T. (1998) 'Campylobacter species and Guillain-Barre syndrome.' *Clin. Microbiol. Rev.*, 11(3) pp. 555-567.

Naito, M., Frirdich, E., Fields, J. A., Pryjma, M., Li, J., Cameron, A., Gilbert, M., Thompson, S. A., et al. (2010) 'Effects of sequential *Campylobacter jejuni* 81-176 lipooligosaccharide core truncations on biofilm formation, stress survival, and pathogenesis.' *J. Bacteriol.*, 192(8) pp. 2182-2192.

Newell, D. and Fearnley, C. (2003) 'Sources of *Campylobacter* colonization in broiler chickens.' *Applied and environmental microbiology*, 69(8) pp. 4343-4351.

Nimse, S. B., Song, K., Sonawane, M. D., Sayyed, D. R. and Kim, T. (2014) 'Immobilization techniques for microarray: challenges and applications.' *Sensors*, 14(12) pp. 22208-22229.

Nocker, A., Cheung, C.-Y. and Camper, A. K. (2006) 'Comparison of propidium monoazide with ethidium monoazide for differentiation of live vs. dead bacteria by selective removal of DNA from dead cells.' *Journal of microbiological methods*, 67(2) pp. 310-320.

North, S. H., Lock, E. H., Walton, S. G. and Taitt, C. R. (2018) Processing microtitre plates for covalent immobilization chemistries. Google Patents.

Novoselov, K. (2007) 'Graphene: Mind the gap.' *Nature materials*, 6(10) p. 720.

Novoselov, K. S., Geim, A. K., Morozov, S. V., Jiang, D., Zhang, Y., Dubonos, S. V., Grigorieva, I. V. and Firsov, A. A. (2004) 'Electric field effect in atomically thin carbon films.' *science*, 306(5696) pp. 666-669.

Nyati, K. K., Prasad, K. N., Rizwan, A., Verma, A. and Paliwal, V. K. (2011) 'TH1 and TH2 response to *Campylobacter jejuni* antigen in Guillain-Barre syndrome.' *Archives of neurology*, 68(4) pp. 445-452.

Nylen, G., Dunstan, F., Palmer, S., Andersson, Y., Bager, F., Cowden, J., Feierl, G., Galloway, Y., et al. (2002) 'The seasonal distribution of campylobacter infection in nine European countries and New Zealand.' *Epidemiology and Infection*, 128(03) pp. 383-390.

Oliver, J. D. (2005a) 'The viable but nonculturable state in bacteria.' *J Microbiol*, 43(1) pp. 93-100.

Oliver, J. D. (2005b) 'The viable but nonculturable state in bacteria.' *J. Microbiol.* , 43(1) pp. 93-100.

Oliver, J. D. (2005c) 'The viable but nonculturable state in bacteria.' *J. Microbiol.*, 43(1) pp. 93-100.

Olsen, S. J., Hansen, G. R., Bartlett, L., Fitzgerald, C., Sonder, A., Manjrekar, R., Riggs, T., Kim, J., et al. (2001) 'An outbreak of *Campylobacter jejuni* infections associated

with food handler contamination: the use of pulsed-field gel electrophoresis.' *J. Infect. Dis.*, 183(1) pp. 164-167.

On, S. L. (2013) 'Isolation, identification and subtyping of *Campylobacter*: Where to from here?' *Journal of microbiological methods*, 95(1) pp. 3-7.

Ong, P. Y. and Leung, D. Y. (2016) 'Bacterial and viral infections in atopic dermatitis: a comprehensive review.' *Clinical reviews in allergy & immunology*, 51(3) pp. 329-337.

Ong, W.-J., Tan, L.-L., Chai, S.-P., Yong, S.-T. and Mohamed, A. R. (2015) 'Surface charge modification via protonation of graphitic carbon nitride (g-C₃N₄) for electrostatic self-assembly construction of 2D/2D reduced graphene oxide (rGO)/g-C₃N₄ nanostructures toward enhanced photocatalytic reduction of carbon dioxide to methane.' *Nano Energy*, 13 pp. 757-770.

Orenga, S., James, A. L., Manafi, M., Perry, J. D. and Pincus, D. H. (2009) 'Enzymatic substrates in microbiology.' *Journal of Microbiological Methods*, 79(2) pp. 139-155.

Ozkan-Ariksoysal, D., Kayran, Y. U., Yilmaz, F. F., Ciucu, A. A., David, I. G., David, V., Hosgor-Limoncu, M. and Ozsoz, M. (2017) 'DNA-wrapped multi-walled carbon nanotube modified electrochemical biosensor for the detection of *Escherichia coli* from real samples.' *Talanta*, 166 pp. 27-35.

Padhye, V. V., York, C. and Burkiewicz, A. (1997) Nucleic acid purification on silica gel and glass mixtures. Google Patents.

Pal, C., Bengtsson-Palme, J., Kristiansson, E. and Larsson, D. J. (2016) 'The structure and diversity of human, animal and environmental resistomes.' *Microbiome*, 4(1) p. 54.

Pal, R. K., Kundu, S. C. and Yadavalli, V. K. (2017) 'Biosensing using photolithographically micropatterned electrodes of PEDOT: PSS on ITO substrates.' *Sensors and Actuators B: Chemical*, 242 pp. 140-147.

Palanisamy, S., Thirumalraj, B., Chen, S.-M., Ali, M. A. and Al-Hemaid, F. M. (2015) 'Palladium nanoparticles decorated on activated fullerene modified screen printed carbon electrode for enhanced electrochemical sensing of dopamine.' *Journal of colloid and interface science*, 448 pp. 251-256.

Palanisamy, S., Velusamy, V., Chen, S.-W., Yang, T. C., Balu, S. and Banks, C. E. (2019) 'Enhanced reversible redox activity of hemin on cellulose microfiber integrated reduced graphene oxide for H₂O₂ biosensor applications.' *Carbohydrate polymers*, 204 pp. 152-160.

Palanisamy, S., Ramaraj, S. K., Chen, S.-M., Yang, T. C., Yi-Fan, P., Chen, T.-W., Velusamy, V. and Selvam, S. (2017) 'A novel laccase biosensor based on laccase

immobilized graphene-cellulose microfiber composite modified screen-printed carbon electrode for sensitive determination of catechol.' *Scientific reports*, 7 p. 41214.

Pancholi, V. and Chhatwal, G. S. (2003) 'Housekeeping enzymes as virulence factors for pathogens.' *International Journal of Medical Microbiology*, 293(6) pp. 391-401.

Parker, M., Gunning, P., Macedo, A., Malcata, F. and Brocklehurst, T. (1998) 'The microstructure and distribution of micro-organisms within mature Serra cheese.' *Journal of applied microbiology*, 84(4) pp. 523-530.

Parkhill, J., Wren, B., Mungall, K., Ketley, J., Churcher, C., Basham, D., Chillingworth, T., Davies, R., et al. (2000) 'The genome sequence of the food-borne pathogen *Campylobacter jejuni* reveals hypervariable sequences.' *Nature*, 403(6770) pp. 665-668.

Parulekar, N. N., Kolekar, P., Jenkins, A., Kleiven, S., Utkilen, H., Johansen, A., Sawant, S., Kulkarni-Kale, U., et al. (2017) 'Characterization of bacterial community associated with phytoplankton bloom in a eutrophic lake in South Norway using 16S rRNA gene amplicon sequence analysis.' *PloS one*, 12(3) p. e0173408.

Patrick, M. E., Christiansen, L. E., Wainø, M., Ethelberg, S., Madsen, H. and Wegener, H. C. (2004) 'Effects of climate on incidence of *Campylobacter* spp. in humans and prevalence in broiler flocks in Denmark.' *Appl. Environ. Microbiol.*, 70(12) pp. 7474-7480.

Pedrós-Alió, C. and Manrubia, S. (2016) 'The vast unknown microbial biosphere.' *Proceedings of the National Academy of Sciences*, p. 201606105.

Perkins, H. (2012) *Microbial cell walls and membranes*. Springer Science & Business Media.

Pitkänen, T. (2013a) 'Review of *Campylobacter* spp. in drinking and environmental waters.' *Journal of microbiological methods*, 95(1) pp. 39-47.

Pitkänen, T. (2013b) 'Review of *Campylobacter* spp. in drinking and environmental waters.' *J. Microbiol. Methods*, 95(1) pp. 39-47.

Poincaré, H. and Maitland, F. (2003) *Science and method*. Courier Corporation.

Prasad, K. S., Muthuraman, G. and Zen, J.-M. (2008) 'The role of oxygen functionalities and edge plane sites on screen-printed carbon electrodes for simultaneous determination of dopamine, uric acid and ascorbic acid.' *Electrochemistry Communications*, 10(4) pp. 559-563.

Pumera, M. (2011) 'Graphene in biosensing.' *Materials today*, 14(7-8) pp. 308-315.

Rahman, M., Heng, L. Y., Futra, D., Chiang, C. P., Rashid, Z. A. and Ling, T. L. (2017) 'A Highly Sensitive Electrochemical DNA Biosensor from Acrylic-Gold Nano-composite for the Determination of Arowana Fish Gender.' *Nanoscale research letters*, 12(1) p. 484.

Rahube, T. O., Marti, R., Scott, A., Tien, Y.-C., Murray, R., Sabourin, L., Zhang, Y., Duenk, P., et al. (2014) 'Impact of fertilizing with raw or anaerobically digested sewage sludge on the abundance of antibiotic-resistant coliforms, antibiotic resistance genes, and pathogenic bacteria in soil and on vegetables at harvest.' *Applied and environmental microbiology*, 80(22) pp. 6898-6907.

Rajapaksha, R., Hashim, U., Uda, M. A., Fernando, C. and De Silva, S. (2017) 'Target ssDNA detection of E. coli O157: H7 through electrical based DNA biosensor.' *Microsystem Technologies*, 23(12) pp. 5771-5780.

Rajzer, M. S. (2017) *Fast detection of bacterial pathogens like Yersinia pestis or Bacillus anthracis with electrochemical detection systems*. Zakład Mikrobiologii.

Ramamurthy, T., Ghosh, A., Pazhani, G. P. and Shinoda, S. (2014) 'Current perspectives on viable but non-culturable (VBNC) pathogenic bacteria.' *Frontiers in public health*, 2 p. 103.

Rasheed, P. A., Radhakrishnan, T., Nambiar, S. R., Thomas, R. T. and Sandhyarani, N. (2017) 'Graphitic carbon nitride as immobilization platform for ssDNA in a genosensor.' *Sensors and Actuators B: Chemical*, 250 pp. 162-168.

Raut, A. D., Kapadnis, B. P., Shashidhar, R., Bandekar, J. R., Vaishampayan, P. and Shouche, Y. S. (2007) 'Nonspecific PCR amplification of the 16S rRNA gene segment in different bacteria by use of primers specific for Campylobacter, Arcobacter, and Helicobacter spp.' *Journal of clinical microbiology*, 45(4) pp. 1376-1377.

Ravan, H., Kashanian, S., Sanadgol, N., Badoei-Dalfard, A. and Karami, Z. (2014) 'Strategies for optimizing DNA hybridization on surfaces.' *Analytical biochemistry*, 444 pp. 41-46.

Resistance, R. o. A. (2016) *Tackling drug-resistant infections globally: final report and recommendations*. Review on Antimicrobial Resistance.

Reuter, M., Mallett, A., Pearson, B. M. and van Vliet, A. H. (2010) 'Biofilm formation by Campylobacter jejuni is increased under aerobic conditions.' *Appl. Environ. Microbiol.*, 76(7) pp. 2122-2128.

Rikken, R. S., Nolte, R. J., Maan, J. C., van Hest, J. C., Wilson, D. A. and Christianen, P. C. (2014) 'Manipulation of micro-and nanostructure motion with magnetic fields.' *Soft Matter*, 10(9) pp. 1295-1308.

- Roca, I., Akova, M., Baquero, F., Carlet, J., Cavaleri, M., Coenen, S., Cohen, J., Findlay, D., et al. (2015) 'The global threat of antimicrobial resistance: science for intervention.' *New microbes and new infections*, 6 pp. 22-29.
- Rodríguez-Lázaro, D. (2013) *Real-time PCR in food science: current technology and applications*. Horizon Scientific Press.
- Roose-Amsaleg, C., Garnier-Sillam, E. and Harry, M. (2001) 'Extraction and purification of microbial DNA from soil and sediment samples.' *Applied Soil Ecology*, 18(1) pp. 47-60.
- Rosenquist, H., Sommer, H. M., Nielsen, N. L. and Christensen, B. B. (2006) 'The effect of slaughter operations on the contamination of chicken carcasses with thermotolerant *Campylobacter*.' *Int. J. Food Microbiol.*, 108(2) pp. 226-232.
- Roshila, M., Hashim, U., Azizah, N., Nadzirah, S., Arshad, M. M., Ruslinda, A. and Gopinath, S. C. (2017) *Effect of different concentration of HPV DNA probe immobilization for cervical cancer detection based IDE biosensor*. Vol. 1808: AIP Publishing.
- Rossen, L., Nørskov, P., Holmstrøm, K. and Rasmussen, O. F. (1992) 'Inhibition of PCR by components of food samples, microbial diagnostic assays and DNA-extraction solutions.' *International journal of food microbiology*, 17(1) pp. 37-45.
- Rowan, D. D. and Popay, A. J. (2017) 'Endophytic fungi as mediators of plant-insect interactions.' *In Insect-Plant Interactions (1993)*. CRC Press, pp. 99-120.
- Roy, S., Soh, J. H. and Ying, J. Y. (2016) 'A microarray platform for detecting disease-specific circulating miRNA in human serum.' *Biosensors and Bioelectronics*, 75 pp. 238-246.
- SacristAN, S. and GARCÍA-ARENAL, F. (2008) 'The evolution of virulence and pathogenicity in plant pathogen populations.' *Molecular plant pathology*, 9(3) pp. 369-384.
- Saha, R., Saha, N., Donofrio, R. S. and Bestervelt, L. L. (2013) 'Microbial siderophores: a mini review.' *Journal of basic microbiology*, 53(4) pp. 303-317.
- Sahin, O., Zhang, Q., Meitzler, J. C., Harr, B. S., Morishita, T. Y. and Mohan, R. (2001) 'Prevalence, antigenic specificity, and bactericidal activity of poultry anti-*Campylobacter* maternal antibodies.' *Applied and environmental microbiology*, 67(9) pp. 3951-3957.
- Sajid, M., Nazal, M. K., Mansha, M., Alsharaa, A., Jillani, S. M. S. and Basheer, C. (2016) 'Chemically modified electrodes for electrochemical detection of dopamine in the presence of uric acid and ascorbic acid: a review.' *TrAC Trends in Analytical Chemistry*, 76 pp. 15-29.

- Salmonová, H. and Bunešová, V. (2017) 'Methods of Studying Diversity of Bacterial Communities: A Review.' *Scientia Agriculturae Bohemica*, 48(3) pp. 154-165.
- Salonen, A., Nikkilä, J., Jalanka-Tuovinen, J., Immonen, O., Rajilić-Stojanović, M., Kekkonen, R. A., Palva, A. and de Vos, W. M. (2010) 'Comparative analysis of fecal DNA extraction methods with phylogenetic microarray: effective recovery of bacterial and archaeal DNA using mechanical cell lysis.' *Journal of microbiological methods*, 81(2) pp. 127-134.
- Sathyendranath, S., Brewin, R. J., Jackson, T., Mélin, F. and Platt, T. (2017) 'Ocean-colour products for climate-change studies: What are their ideal characteristics?' *Remote Sensing of Environment*, 203 pp. 125-138.
- Savory, A. and Duncan, T. (2016) 'Regenerating Agriculture to Sustain Civilization.' *In Land Restoration*. Elsevier, pp. 289-309.
- Schielke, A., Rosner, B. M. and Stark, K. (2014a) 'Epidemiology of campylobacteriosis in Germany—insights from 10 years of surveillance.' *BMC Infect. Dis.*, 14(1) p. 1.
- Schielke, A., Rosner, B. M. and Stark, K. (2014b) 'Epidemiology of campylobacteriosis in Germany—insights from 10 years of surveillance.' *BMC infectious diseases*, 14(1) p. 30.
- Schielke, A., Rosner, B. M. and Stark, K. (2014c) 'Epidemiology of campylobacteriosis in Germany—insights from 10 years of surveillance.' *BMC infectious diseases*, 14(1) p. 1.
- Schneitz, C. and Hakkinen, M. (2016) 'The efficacy of a commercial competitive exclusion product on *Campylobacter* colonization in broiler chickens in a 5-week pilot-scale study.' *Poultry Sci.*, 95(5) pp. 1125-1128.
- Schulze, R., Krummenauer, F., Schalldach, F. and d'Hoedt, B. (2000) 'Precision and accuracy of measurements in digital panoramic radiography.' *Dentomaxillofacial Radiology*, 29(1) pp. 52-56.
- Schüler, T., Nykytenko, A., Csaki, A., Möller, R., Fritzsche, W. and Popp, J. (2009) 'UV cross-linking of unmodified DNA on glass surfaces.' *Analytical and bioanalytical chemistry*, 395(4) pp. 1097-1105.
- Seliwiorstow, T., De Zutter, L., Houf, K., Botteldoorn, N., Baré, J. and Van Damme, I. (2016) 'Comparative performance of isolation methods using Preston broth, Bolton broth and their modifications for the detection of *Campylobacter* spp. from naturally contaminated fresh and frozen raw poultry meat.' *International Journal of Food Microbiology*, 234 pp. 60-64.

- Shahrokhian, S. and Salimian, R. (2018) 'Ultrasensitive detection of cancer biomarkers using conducting polymer/electrochemically reduced graphene oxide-based biosensor: Application toward BRCA1 sensing.' *Sensors and Actuators B: Chemical*, 266 pp. 160-169.
- Shariati, M., Ghorbani, M., Sasanpour, P. and Karimizefreh, A. (2019) 'An ultrasensitive label free human papilloma virus DNA biosensor using gold nanotubes based on nanoporous polycarbonate in electrical alignment.' *Analytica chimica acta*, 1048 pp. 31-41.
- Shehadul Islam, M., Aryasomayajula, A. and Selvaganapathy, P. (2017) 'A review on macroscale and microscale cell lysis methods.' *Micromachines*, 8(3) p. 83.
- Sheppard, S. K., Dallas, J. F., Wilson, D. J., Strachan, N. J., McCarthy, N. D., Jolley, K. A., Colles, F. M., Rotariu, O., et al. (2010) 'Evolution of an agriculture-associated disease causing *Campylobacter coli* clade: evidence from national surveillance data in Scotland.' *PLoS One*, 5(12) p. e15708.
- Shoaf-Sweeney, K. D., Larson, C. L., Tang, X. and Konkel, M. E. (2008) 'Identification of *Campylobacter jejuni* proteins recognized by maternal antibodies of chickens.' *Applied and environmental microbiology*, 74(22) pp. 6867-6875.
- Silva, J. and Teixeira, P. (2015) 'Tackling *Campylobacter*: a Review.' *American Journal of Advanced Food Science and Technology*, 3(2) pp. 107-124.
- Silva, T. A., Moraes, F. C., Janegitz, B. C. and Fatibello-Filho, O. (2017) 'Electrochemical Biosensors Based on Nanostructured Carbon Black: A Review.' *Journal of Nanomaterials*, 2017
- Singh, D. (2018) *Thermal Decomposition of Nano-Enabled Products: Potential Environmental Health and Safety Implications*.
- Singhal, C., Ingle, A., Chakraborty, D., Pundir, C. and Narang, J. (2017) 'Impedimetric genosensor for detection of hepatitis C virus (HCV1) DNA using viral probe on methylene blue doped silica nanoparticles.' *International journal of biological macromolecules*, 98 pp. 84-93.
- Smith, S., Messam, L. L. M., Meade, J., Gibbons, J., McGill, K., Bolton, D. and Whyte, P. (2016) 'The impact of biosecurity and partial depopulation on *Campylobacter* prevalence in Irish broiler flocks with differing levels of hygiene and economic performance.' *Infect. Ecol Epidemiol.*, 6
- Snyder, E., Kampanya, N., Lu, J., Nordberg, E. K., Karur, H., Shukla, M., Soneja, J., Tian, Y., et al. (2006) 'PATRIC: the VBI pathosystems resource integration center.' *Nucleic acids research*, 35(suppl_1) pp. D401-D406.

Sockett, P., Cowden, J., Le, S. B., Ross, D., Adak, G. and Evans, H. (1993) 'Foodborne disease surveillance in England and Wales: 1989-1991.' *Communicable disease report. CDR review*, 3(12) pp. R159-173.

Sterk, A., de Man, H., Schijven, J. F., de Nijs, T. and de Roda Husman, A. M. (2016) 'Climate change impact on infection risks during bathing downstream of sewage emissions from CSOs or WWTPs.' *Water research*, 105 pp. 11-21.

Stern, N., Cox, N., Bailey, J., Berrang, M. and Musgrove, M. (2001) 'Comparison of mucosal competitive exclusion and competitive exclusion treatment to reduce Salmonella and Campylobacter spp. colonization in broiler chickens.' *Poultry Sci.*, 80(2) pp. 156-160.

Stiborova, H., Wolfram, J., Demnerova, K., Macek, T. and Uhlik, O. (2015) 'Bacterial community structure in treated sewage sludge with mesophilic and thermophilic anaerobic digestion.' *Folia microbiologica*, 60(6) pp. 531-539.

Suzuki, M. T. and Giovannoni, S. J. (1996) 'Bias caused by template annealing in the amplification of mixtures of 16S rRNA genes by PCR.' *Applied and environmental microbiology*, 62(2) pp. 625-630.

Svensson, S. L., Pryjma, M. and Gaynor, E. C. (2014) 'Flagella-mediated adhesion and extracellular DNA release contribute to biofilm formation and stress tolerance of Campylobacter jejuni.' *PloS one*, 9(8) p. e106063.

Svítková, J., Ignat, T., Švorc, L., Labuda, J. and Barek, J. (2016) 'Chemical modification of boron-doped diamond electrodes for applications to biosensors and biosensing.' *Critical reviews in analytical chemistry*, 46(3) pp. 248-256.

Sweden-EPA. (2006) *Wastewater treatment in Sweden. ISBN 978-91-620-8416-5.*

Szymanski, C. M., Logan, S. M., Linton, D. and Wren, B. W. (2003) 'Campylobacter—a tale of two protein glycosylation systems.' *Trends Microbiol.*, 11(5) pp. 233-238.

Takeuchi, K., Taguchi, F., Inagaki, Y., Toyoda, K., Shiraishi, T. and Ichinose, Y. (2003) 'Flagellin glycosylation island in Pseudomonas syringae pv. glycinea and its role in host specificity.' *J. Bacteriol*, 185(22) pp. 6658-6665.

Taki, F. A., Pan, X. and Zhang, B. (2015) 'Revisiting Chaos Theorem to Understand the Nature of miRNAs in Response to Drugs of Abuse.' *Journal of cellular physiology*, 230(12) pp. 2857-2868.

Tanaka, J. and Ikeda, S. (2002) 'Rapid and efficient DNA extraction method from various plant species using diatomaceous earth and a spin filter.' *Breeding science*, 52(2) pp. 151-155.

- Taylor, E. V., Herman, K. M., Ailes, E., Fitzgerald, C., Yoder, J., Mahon, B. and Tauxe, R. (2013a) 'Common source outbreaks of Campylobacter infection in the USA, 1997–2008.' *Epidemiol. Infect.*, 141(05) pp. 987-996.
- Taylor, E. V., Herman, K. M., Ailes, E., Fitzgerald, C., Yoder, J., Mahon, B. and Tauxe, R. (2013b) 'Common source outbreaks of Campylobacter infection in the USA, 1997–2008.' *Epidemiology and infection*, 141(05) pp. 987-996.
- Taylor, S., Smith, S., Windle, B. and Guiseppi-Elie, A. (2003) 'Impact of surface chemistry and blocking strategies on DNA microarrays.' *Nucleic acids research*, 31(16) pp. e87-e87.
- Teh, K. H., Flint, S. and French, N. (2010) 'Biofilm formation by Campylobacter jejuni in controlled mixed-microbial populations.' *Int. J. Food Microbiol*, 143(3) pp. 118-124.
- Thirumalraj, B., Palanisamy, S. and Chen, S.-M. (2015) 'An amperometric nitrobenzene electrochemical sensor based on electrochemically activated graphite modified screen printed carbon electrode.' *Int. J. Electrochem. Sci*, 10 pp. 4173-4182.
- Thomas, C., Hill, D. and Mabey, M. (2002) 'Culturability, injury and morphological dynamics of thermophilic Campylobacter spp. within a laboratory-based aquatic model system.' *J. Appl. Microbiol*, 92(3) pp. 433-442.
- Turonova, H., Briandet, R., Rodrigues, R., Hernould, M., Hayek, N., Stintzi, A., Pazlarova, J. and Tresse, O. (2015) 'Biofilm spatial organization by the emerging pathogen Campylobacter jejuni: comparison between NCTC 11168 and 81-176 strains under microaerobic and oxygen-enriched conditions.' *Front. Microbiol.*, 6
- Uliana, C. V., Riccardi, C. S. and Yamanaka, H. (2014) 'Diagnostic tests for hepatitis C: recent trends in electrochemical immunosensor and genosensor analysis.' *World Journal of Gastroenterology: WJG*, 20(42) p. 15476.
- Ulrich, R. and Hughes, T. (2001) 'A rapid procedure for isolating chromosomal DNA from Lactobacillus species and other Gram-positive bacteria.' *Letters in applied microbiology*, 32(1) pp. 52-56.
- Unterholzner, S. J., Rozhon, W. and Poppenberger, B. (2017) 'Analysis of In Vitro DNA Interactions of Brassinosteroid-Controlled Transcription Factors Using Electrophoretic Mobility Shift Assay.' *In Brassinosteroids*. Springer, pp. 133-144.
- Ursell, L. K., Metcalf, J. L., Parfrey, L. W. and Knight, R. (2012) 'Defining the human microbiome.' *Nutrition reviews*, 70(suppl_1) pp. S38-S44.
- van der Graaf-van Bloois, L., van Bergen, M. A., van der Wal, F. J., de Boer, A. G., Duim, B., Schmidt, T. and Wagenaar, J. A. (2013) 'Evaluation of molecular assays for

identification *Campylobacter fetus* species and subspecies and development of a *C. fetus* specific real-time PCR assay.' *Journal of microbiological methods*, 95(1) pp. 93-97.

Vasyukova, I., Gusev, A. and Tkachev, A. (2015) *Reproductive toxicity of carbon nanomaterials: a review*. Vol. 98: IOP Publishing.

Velusamy, V., Arshak, K., Korostynska, O., Oliwa, K. and Adley, C. (2009) *Design of a real time biorecognition system to detect foodborne pathogens-DNA Biosensor*. IEEE.

Velusamy, V., Arshak, K., Korostynska, O., Oliwa, K. and Adley, C. (2010) 'An overview of foodborne pathogen detection: In the perspective of biosensors.' *Biotechnology advances*, 28(2) pp. 232-254.

Velusamy, V., Arshak, K., Yang, C. F., Yu, L., Korostynska, O. and Adley, C. (2011) 'Comparison between DNA immobilization techniques on a redox polymer matrix.' *American Journal of Analytical Chemistry*, 2(03) p. 392.

Velusamy, V., Palanisamy, S., Chen, S.-W., Balu, S., Yang, T. C. and Banks, C. E. (2019) 'Novel electrochemical synthesis of cellulose microfiber entrapped reduced graphene oxide: A sensitive electrochemical assay for detection of fenitrothion organophosphorus pesticide.' *Talanta*, 192 pp. 471-477.

Velusamy, V., Palanisamy, S., Chen, S.-M., Chen, T.-W., Selvam, S., Ramaraj, S. K. and Lou, B.-S. (2017) 'Graphene dispersed cellulose microfibers composite for efficient immobilization of hemoglobin and selective biosensor for detection of hydrogen peroxide.' *Sensors and Actuators B: Chemical*, 252 pp. 175-182.

Vereen, E., Lowrance, R. R., Jenkins, M. B., Adams, P., Rajeev, S. and Lipp, E. K. (2013) 'Landscape and seasonal factors influence *Salmonella* and *Campylobacter* prevalence in a rural mixed use watershed.' *Water Res.*, 47(16) pp. 6075-6085.

Vergani, L., Mapelli, F., Marasco, R., Crotti, E., Fusi, M., Di Guardo, A., Armiraglio, S., Daffonchio, D., et al. (2017) 'Bacteria associated to plants naturally selected in a historical PCB polluted soil show potential to sustain natural attenuation.' *Frontiers in microbiology*, 8 p. 1385.

Verma, S. K., Gond, S. K., Mishra, A., Sharma, V. K., Kumar, J., Singh, D. K., Kumar, A. and Kharwar, R. N. (2017) 'Fungal Endophytes Representing Diverse Habitats and Their Role in Plant Protection.' *In Developments in Fungal Biology and Applied Mycology*. Springer, pp. 135-157.

Vogelstein, B. and Gillespie, D. (1979) 'Preparative and analytical purification of DNA from agarose.' *Proceedings of the National Academy of Sciences*, 76(2) pp. 615-619.

- Vogtmann, E. and Goedert, J. J. (2016) 'Epidemiologic studies of the human microbiome and cancer.' *British journal of cancer*, 114(3) p. 237.
- Véron, M. and Chatelain, R. (1973) 'Taxonomic study of the genus *Campylobacter* Sebald and Véron and designation of the neotype strain for the type species, *Campylobacter fetus* (Smith and Taylor) Sebald and Véron.' *International Journal of Systematic and Evolutionary Microbiology*, 23(2) pp. 122-134.
- Walker, A. W., Martin, J. C., Scott, P., Parkhill, J., Flint, H. J. and Scott, K. P. (2015) '16S rRNA gene-based profiling of the human infant gut microbiota is strongly influenced by sample processing and PCR primer choice.' *Microbiome*, 3(1) p. 26.
- Wang, J., Musameh, M. and Lin, Y. (2003) 'Solubilization of carbon nanotubes by Nafion toward the preparation of amperometric biosensors.' *Journal of the American Chemical Society*, 125(9) pp. 2408-2409.
- Wang, L. and Stegemann, J. P. (2010) 'Extraction of high quality RNA from polysaccharide matrices using cetyltrimethylammonium bromide.' *Biomaterials*, 31(7) pp. 1612-1618.
- Wang, P., Goggins, W. B. and Chan, E. Y. (2018) 'A time-series study of the association of rainfall, relative humidity and ambient temperature with hospitalizations for rotavirus and norovirus infection among children in Hong Kong.' *Science of The Total Environment*, 643 pp. 414-422.
- Wang, S., Zhang, X., Huang, J. and Chen, J. (2018) 'High-performance non-enzymatic catalysts based on 3D hierarchical hollow porous Co₃O₄ nanododecahedras in situ decorated on carbon nanotubes for glucose detection and biofuel cell application.' *Analytical and bioanalytical chemistry*, 410(7) pp. 2019-2029.
- Whiley, H., van den Akker, B., Giglio, S. and Bentham, R. (2013) 'The role of environmental reservoirs in human campylobacteriosis.' *Int. J. Environ. Res. Pub. Heal.*, 10(11) pp. 5886-5907.
- Wilkins, L. G., Fumagalli, L. and Wedekind, C. (2016) 'Effects of host genetics and environment on egg-associated microbiotas in brown trout (*Salmo trutta*).' *Molecular Ecology*, 25(19) pp. 4930-4945.
- Wilkins, L. G., Rogivue, A., Fumagalli, L. and Wedekind, C. (2015) 'Declining diversity of egg-associated bacteria during development of naturally spawned whitefish embryos (*Coregonus*.' *Aquatic Sciences*, 77(3) pp. 481-497.
- Wilson, D. J., Gabriel, E., Leatherbarrow, A. J., Cheesbrough, J., Gee, S., Bolton, E., Fox, A., Hart, C. A., et al. (2009) 'Rapid evolution and the importance of recombination to the gastroenteric pathogen *Campylobacter jejuni*.' *Mol. Bio. Evol.*, 26(2) pp. 385-397.

- Wisitsoraat, A., Pakapongpan, S., Sriprachuabwong, C., Phokharatkul, D., Sritongkham, P., Lomas, T. and Tuantranont, A. (2013) 'Graphene–PEDOT: PSS on screen printed carbon electrode for enzymatic biosensing.' *Journal of Electroanalytical Chemistry*, 704 pp. 208-213.
- Wittmann, C. and Marquette, C. (2012) 'DNA Immobilization.' *Encyclopedia of Analytical Chemistry*,
- Woese, C. R. and Fox, G. E. (1977) 'Phylogenetic structure of the prokaryotic domain: the primary kingdoms.' *Proceedings of the National Academy of Sciences*, 74(11) pp. 5088-5090.
- Wong, Y. Y. (2017) *Identifying Potential Fungi Species Through Molecular Approach and Its Biosurfactants Production*. INTI INTERNATIONAL UNIVERSITY.
- Woodard, D. L., Howard, A. J. and Down, J. A. (1994) Process for purifying DNA on hydrated silica. Google Patents.
- Wu, D., Liu, Y., Wu, Y., Tan, B. and Xie, Z. (2018) 'Microporous carbons derived from organosilica-containing carbon dots with outstanding supercapacitance.' *Dalton Transactions*, 47(17) pp. 5961-5967.
- Wu, J.-F., Xu, M.-Q. and Zhao, G.-C. (2010) 'Graphene-based modified electrode for the direct electron transfer of cytochrome c and biosensing.' *Electrochemistry Communications*, 12(1) pp. 175-177.
- Wu, Z., Yang, R., Zu, D. and Sun, S. (2017) 'Microscopic Differentiation of Plasmonic Nanoparticles for the Ratiometric Read-out of Target DNA.' *Scientific reports*, 7(1) p. 14742.
- Xu, H.-S., Roberts, N., Singleton, F. L., Attwell, R. W., Grimes, D. J. and Colwell, R. R. (1982) 'Survival and viability of nonculturable *Escherichia coli* and *Vibrio cholerae* in the estuarine and marine environment.' *Microbial Ecol.*, 8(4) pp. 313-323.
- Yacynych, A. M. and Kuwana, T. (1978) 'Cyanuric chloride as a general linking agent for modified electrodes: Attachment of redox groups to pyrolytic graphite.' *Analytical Chemistry*, 50(4) pp. 640-645.
- Yamaguchi, M., Dieffenbach, C., Connolly, R., Cruess, D., Baur, W. and Sharefkin, J. (1992) 'Effect of different laboratory techniques for guanidinium-phenol-chloroform RNA extraction on A260/A280 and on accuracy of mRNA quantitation by reverse transcriptase-PCR.' *Genome Research*, 1(4) pp. 286-290.
- Yang, F., Wang, W., Chen, R. and Xu, X. (1997) 'A simple and efficient method for purification of prawn baculovirus DNA.' *Journal of virological methods*, 67(1) pp. 1-4.

- Yang, W., Ratinac, K. R., Ringer, S. P., Thordarson, P., Gooding, J. J. and Braet, F. (2010) 'Carbon nanomaterials in biosensors: should you use nanotubes or graphene?' *Angewandte Chemie International Edition*, 49(12) pp. 2114-2138.
- Yang, X., Kirsch, J. and Simonian, A. (2013) 'Campylobacter spp. detection in the 21st century: A review of the recent achievements in biosensor development.' *Journal of microbiological methods*, 95(1) pp. 48-56.
- Yuan, T., Jiang, Y., Sun, W., Xiang, B., Li, Y., Yan, M., Xu, B. and Dou, S. (2016) 'Ever-Increasing Pseudocapacitance in RGO–MnO–RGO Sandwich Nanostructures for Ultrahigh-Rate Lithium Storage.' *Advanced Functional Materials*, 26(13) pp. 2198-2206.
- Yuki, N. and Hartung, H.-P. (2012) 'Guillain–Barré syndrome.' *New England Journal of Medicine*, 366(24) pp. 2294-2304.
- Zajicek, G. (1991) 'Chaos and biology.' *Methods of information in medicine*, 30(01) pp. 01-03.
- Zhang, S., Ye, C., Lin, H., Lv, L. and Yu, X. (2015) 'UV disinfection induces a VBNC state in Escherichia coli and Pseudomonas aeruginosa.' *Environmental science & technology*, 49(3) pp. 1721-1728.
- Zhang, Z., Hu, W., Zhang, Q., Li, P. and Li, C. (2016) 'Competitive Immunoassays Using Antigen Microarrays.' *In Microarray Technology*. Springer, pp. 237-247.
- Zhou, J., Bruns, M. A. and Tiedje, J. M. (1996) 'DNA recovery from soils of diverse composition.' *Applied and environmental microbiology*, 62(2) pp. 316-322.
- Zhu, Z., Garcia-Gancedo, L., Flewitt, A. J., Xie, H., Moussy, F. and Milne, W. I. (2012) 'A critical review of glucose biosensors based on carbon nanomaterials: carbon nanotubes and graphene.' *Sensors*, 12(5) pp. 5996-6022.
- Zohourtalab, A. and Razmi, H. (2018) 'Selective Determination of Glucose in Blood Plasma by Using an Amperometric Glucose Biosensor Based on Glucose Oxidase and a Chitosan/Nafion/IL/Ferrocene Composite Film.' *Iranian Journal of Analytical Chemistry*, 5(1) pp. 9-16.

Appendix A – Acronyms

μA	Micro Ampere
μV	Micro Volt
APTES	(3-Aminopropyl)triethoxysilane
CA	Chronoamperometry
CMF	Cellulose microfibre
crGO	Chemically reduced Graphene oxide
CV	Cyclic voltammetry
DD	Double distilled
DNA	Deoxy-ribonucleic acid
DPV	Differential pulse voltammetry
dsDNA	Double-stranded DNA
EEPROM	Electronically erasable programable read-only memory
ELISA	Enzyme-linked immunosorbent assay
erGO	Electronically reduced Graphene oxide
FISH	Fluorescent in-situ hybridisation
GCE	Glassy carbon electrode
GO	Graphene oxide
GPRS	General packet radio service
GSM	Global System for Mobile communications
HPLC	High-pressure liquid chromatography
IDE	Integrated development environment
LC	Liquid chromatography
mRNA	Messenger RNA
PBS	Phosphate buffered saline
PCR	Polymerase chain reaction
PEDOT:PSS	Poly(3,4-ethylenedioxythiophene) polystyrene sulfonate
PEEK	Polyether ether ketone

PWM	Pulse-width modulation
REDOX	Reduction–oxidation reaction
rGO	Reduced Graphene oxide
RNA	Ribonucleic acid
SDS	Sodium dodecyl sulfate
siRNA	Small interfering messenger RNA
SPCE	Screen printed carbon electrode
SRAM	Static random-access memory
ssDNA	Single-stranded DNA
tRNA	Transfer RNA
UBEC	Ultimate Battery Eliminator Circuit
αSPCE	Activated Screen printed carbon electrode

Appendix B - List of publication and conferences

Characterization of *Campylobacter jejuni* population dynamics during storage at different temperatures and packaging regimes.

James Hall, Daniel M. Anang, Vijayalakshmi Velusamy and Brijesh Tiwaric

Food Packaging and Shelf Life – publication pending.

Hydrothermal Synthesis of Cr₂Se₃ Hexagons for Sensitive and Low-level Detection of 4-Nitrophenol in Water

Sukanya Ramaraj, Sakthivel Mani, Shen-Ming Chen, Selvakumar Palanisamy,

Vijayalakshmi Velusamy, James M. Hall, Tse-Wei Chen & Tien-Wen Tseng

Scientific Reports volume 8, Article number: 4839 (2018)

Selective Colorimetric Detection of Nitrite in Water using Chitosan Stabilized Gold Nanoparticles Decorated Reduced Graphene oxide

Baishnisha Amanulla, Selvakumar Palanisamy, Shen-Ming Chen, Te-Wei Chiu,

Vijayalakshmi Velusamy, James M. Hall, Tse-Wei Chen & Sayee Kannan Ramaraj

Scientific Reports volume 7, Article number: 14182 (2017)

Facile preparation of a cellulose microfibrils–exfoliated graphite composite: a robust sensor for determining dopamine in biological samples

Selvakumar Palanisamy, Pan Yi-Fan, Shen-Ming Chen, Vijayalakshmi Velusamy &

James M. Hall

Cellulose October 2017, Volume 24, Issue 10, pp 4291–4302

A robust nitrobenzene electrochemical sensor based on chitin hydrogel entrapped graphite composite

Rajalakshmi Sakthivel, Selvakumar Palanisamy, Shen-Ming Chen, Sukanya Ramaraj,

Vijayalakshmi Velusamy, Pan Yi-Fan, James M. Hall, Sayee Kannan Ramaraj

Journal of the Taiwan Institute of Chemical Engineers, Volume 80, November 2017,

Pages 663-668

Functional NanoMaterials: From Spectroscopy to Bioimaging

14th -16th December 2017

IISER Kolkata, British council and Royal Society of Chemistry

Nano-Biomaterials for water purification

12th -16th December 2016

Mahatma Gandhi University, British council and Royal Society of Chemistry

Manchester Biomaterials Conference

15th June 2016

University of Manchester